Greenhouse gas emissions from channels draining intact and degraded tropical peat swamp forest

Thesis

Greenhouse gas emissions from channels draining intact and degraded tropical peat swamp forest

Matthew S. Kent

B.Sc. (Hons.) Bangor University, Wales

A thesis submitted to the Open University, in accordance with the requirements for the degree of Doctor of Philosophy in Biogeochemistry

Submitted April 2018

Abstract

Degradation of tropical peat swamp forest (PSF) can destabilise the ecosystem carbon balance with significant amounts of carbon lost via drainage channels. Peat-draining channels are typically supersaturated with greenhouse gases and can constitute evasive hotspots within catchments, but losses by fluvial emissions have not yet been quantified for intact and degraded PSF. These fluvial emissions are presented in this study, which considers differences between land-use classes, across both wet and dry seasons, and how fluvial greenhouse gas fluxes were affected by a strong El Niño.

Wet season CO_2 emissions were $\leq 2-$times higher than dry season emissions, for both land classes, with normal seasonal ranges of $3.36-4.67$ and $2.58-3.13$ g$\cdot CO_2$-C$\cdot m^{-2}\cdot d^{-1}$ for the intact and degraded land classes, respectively. When scaled up, the intact and degraded PSF channels contributed less than a millionth, and $<1\%$, of total CO_2 flux, respectively, to landscape-scale ecosystem emissions. Radiocarbon dating of channel CO_2 found that it was recently photosynthesised for the intact PSF, but the age of the degraded PSF CO_2-C was $341-1655$ BP, indicating that carbon from deep peat layers was being degraded.

Diffusive CH_4 fluxes from channels were $\leq 9-$times higher in degraded PSF than in intact PSF, the ranges being $9.47-16.8$ and $1.25-2.16$ mg$\cdot CH_4$-C$\cdot m^{-2}\cdot d^{-1}$, respectively. The El Niño event caused an anomalous water table drawdown which resulted in a state shift in the intact PSF whereby channels produced quantities of CH_4 comparable to the degraded PSF; however, CH_4 fluxes returned to normal afterwards, demonstrating ecosystem resilience. The El Niño also promoted the lowest and highest fluxes of CO_2 and CH_4, respectively, at both land classes. Channel emissions made a negligible contribution to total CH_4 fluxes at the intact PSF, but channels at the degraded PSF, which cover 0.5% of the landscape, may have contributed $\leq 68\%$ of the total landscape CH_4 flux when ebullition estimates are included.

Acknowledgements

I am extremely grateful to Vincent Gauci (Open University) for giving me the opportunity to work on this project. Thank you for your guidance and patience, and I extend this gratitude to my other supervisors, Sue Page (University of Leicester), Chris Evans (Centre for Ecology and Hydrology) and, particularly, Mark Brandon (Open University). This research was made possible by funding from the AXA Research Fund, the Natural Environment Research Council (NERC) and the Open University − thank you.

This thesis was made possible by my incredible field guides. Words can not express my gratitude for your hard work, positive attitudes and friendship; Idrus, Hanafi and Sandy. I am grateful also to Ibu Siska, Pak Kitso and Pak Suwido (RIP) from the University of Palangkaraya, and all of the Borneo Nature Foundation, particularly Bernat Ripoll and Karen Jeffers. Thank you to David Bastviken (University of Linköping) for teaching me the floating chamber method, Mark Garnett (NERC Radiocarbon Facility in East Kilbride) for analysing my samples, and Dusan Materić (Utrecht University) for a great collaborative project using my samples.

Several staff have helped me in supportive roles: Liz Lomas, thank you for your tireless support for the students; Mike Peacock, Patrick Rafferty and Emily Sear, for everything you've done to help me, and Sunitha Pangala for getting me started on the analyser and writing the NERC grant proposal.

I wouldn't have made it without the wonderful support and friendship of the students and staff in the department. It's been fun and thanks for the memories of wild swimming, bivi adventures, cycle rides, climbing, slacklining, boardgames and pub trips; John, Adele, Nick, Bertie, Eleni, Laura, Matt, Ginny, Carla, Carrie, Stacy, Clare, Sam, Wes, Tom, and everyone else.

Lastly: my housemates, Rob, Joanna and Carme; my wonderful family; Dad, Beki, Leafy, Gen, Graham, Jim and Martin; and Naomi, thank you all for your love and support, for always being there, and making my life so special.

Contents

List of Figures

List of Tables

Chapter 1

Introduction

1.1 Peatlands and their role in the carbon cycle

Peatlands play a significant role in the carbon (C) cycle in that they are highly concentrated soil stores of historic C (Limpens et al., 2008). They form at latitudes that feature a wet climate (see Fig. 1.1) and where the decomposition of the dead remains of plants that inhabit an area is impeded due to low oxygen levels (Freeman et al., 2001), thereby facilitating the build-up of partially decayed organic matter.

Since high rainfall can cause inundation, and water can act as a barrier to the ingress of oxygen to soils, a water table that is close to or at the peat surface for most of the year creates anoxic conditions, greatly limiting aerobic degradation of plant material (Rydin and Jeglum, 2006). If the plant material contains large amounts of phenolic acids, these can act to further inhibit the enzymes responsible for organic matter degradation (Freeman et al., 2001). The partially decayed organic carbon in peatlands has sometimes accumulated to considerable depths (5-10 m) over many millennia (Limpens et al., 2008).

As peatland ecosystems typically accumulate more C than they lose, they are considered 'carbon sinks' (Limpens et al., 2008). Figure 1.1 shows the largest peatlands and that the largest proportion of global peatland C is found in the northern hemisphere. Here, peatlands formed as a result of natural climatic change since the end of the last glacial period, and where the retreating glaciers left topographical features suited to water retention and peat formation (Gorham, 1991). As such, most of these peatlands formed during the Holocene are less than 10,000 years old.

In the tropics, whilst some peatlands were forming during the glacial period and can be over

25,000 years old, most formed during the Holocene as a result of post-glacial changes in sea level (Page et al., 2004). Whenever they were formed, during the Holocene, tropical peatlands underwent rapid rates of peat accumulation and are typically significantly deeper than northern peatlands. Deeper tropical peats, therefore, have a larger soil C volume-to-area ratio than northern hemisphere peatlands (Page et al., 2011).

The atmosphere contains ~750 Pg·C (Sundquist, 1993; 1 Pg = 1×10^{15} g, or one gigatonne) which is similar to the amount held in peat soils; northern hemisphere, tropical and southern hemisphere peatlands are respectively estimated to contain 500 ± 100 Pg·C (Yu, 2012), 69.6−129.8 Pg·C (Page et al., 2011; Dargie et al., 2017), and 15 Pg·C (Yu et al., 2010), totalling between 484.6 and 744.8 Pg·C. Tropical peats therefore contain between 14−17 % of the total amount of C held in peats, globally.

Peatlands in the northern hemisphere have been the subject of much research, but it has only been in the last two decades that the global importance of tropical peatlands has been appreciated. Like their equivalents in the northern hemisphere they perform numerous ecosystem services, such as flood mitigation and providing habitat for organisms that are specialised to live in waterlogged, nutrient-poor environments (Rydin and Jeglum, 2006; Yule, 2010). They can also be substantial sinks and sources of carbon dioxide (CO_2; Page et al., 2002; Page et al., 2009b; Couwenberg et al., 2010; Hirano et al., 2012) and also methane (CH_4; Jauhiainen et al., 2008; Couwenberg et al., 2010). Given that both CO_2 and CH_4 are atmospheric greenhouse gases there is a need for tropical peatlands to be better understood so that their influence over global change can be quantified.

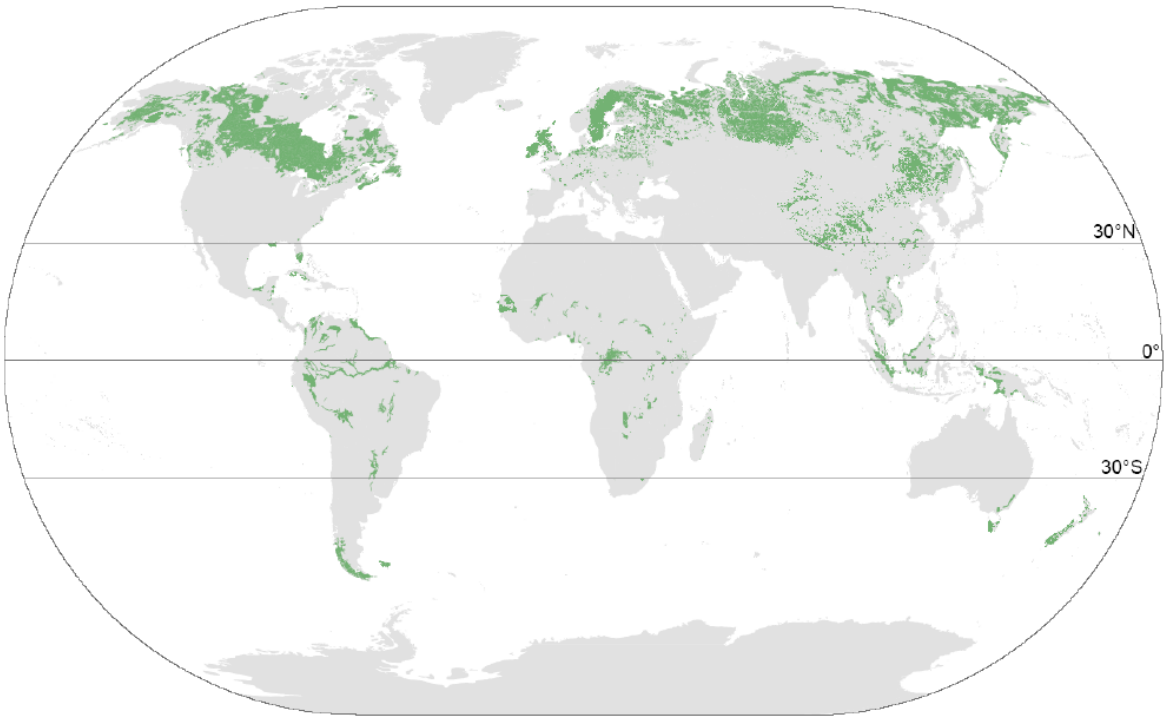

Figure 1.1: Global distribution of peatlands (Source: Yu et al., 2010). Peatlands occur in climatically wet areas: mostly where the polar and mid-latitude atmospheric circulation cells meet around 60° north and south, respectively, and; at the equator where the north and south Hadley atmospheric circulation cells meet.

1.1.1 Peat swamp forests and threats to their carbon store

Tropical peatlands occupy ~11 % of global peatland area, with about 50 % of this occurring in Southeast Asia (see Fig. 1.2). In this region the most extensive peatlands are 'ombrotrophic' (i.e. rain-fed systems). Some peat domes can exceed 20 m in depth and so a large amount of peat C can be stored per unit area, with respect to northern peats (Page et al., 2004; Posa et al., 2011).

Tropical peatlands differ significantly from northern peatlands in that they are predominantly forested ecosystems as opposed to moss and shrub-dominated ecosystems.

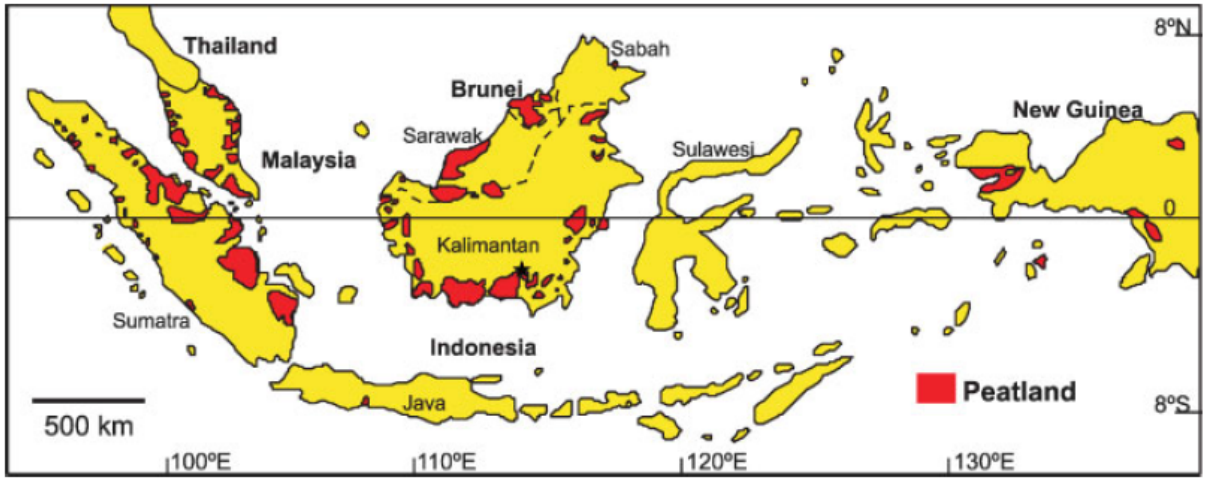

Figure 1.2: Map of the Indonesian archipelago and surrounding nations (Source: Page et al., 2004). Borneo is the largest island in the centre which is made up of Brunei, the Malaysian provinces of Sabah and Sarawak, and the Indonesian provices that make up Kalimantan. The provincial capital of Central Kalimantan, Palangkaraya, is marked by a black star. The horizontal line marks the equator. Most of Southeast Asia's peatlands are found in coastal or sub-coastal locations.

Southeast Asia holds ˜69 Pg·C in its peatlands, or ˜66 % of the total amount of tropical peatland C. Indonesia alone contains ˜ 54 % (57 Pg) of total tropical peatland C, making it the most tropical peat C-dense country in the world (Page et al., 2011; Dargie et al., 2017). The natural vegetation cover of the peatlands in this region are known as peat swamp forests. In terms of the countries with the greatest peatland area in Southeast Asia, Indonesia has the most (20.7 Mha), whereas the next highest, Malaysia, has considerably less (2.6 Mha; Page et al., 2011). Maintaining a forest and a high water table has been recognised as being important in maintaining peats and the long-term peat swamp forest C sink ecosystem service they provide (Page et al., 1999; Page and Baird, 2016).

Indonesia is a developing country and is one of the world's emerging economies that has one of the fastest economic growth rates (Anderson et al., 2015). One of the driving forces of this growth has been the large-scale exploitation of its extensive natural resources, including its peat swamp forests, in recent decades (Miettinen et al., 2012).

In the decade between 2000 and 2010, considerable amounts of forest and peatland cover were lost to land use change in Malaysia and Indonesia; Miettinen et al. (2011) estimated that they deforested 2.3 Mha and 8.8 Mha of their forests and converted 0.56 Mha (55 %) and 2.20 Mha (17.3%) of their peatlands, respectively, to other uses, such as agriculture (see Fig. 1.3). Indonesia's peatlands are particularly C-dense and have been estimated to contain 3,350±110 Mg·C·ha^{-1} (Tonks et al., 2017), but land-use

change, including deforestation and conversion to large-scale plantations and small-holder farms, has caused very substantial (˜4−7×) losses of peat C and C storage capacity per unit area (Tonks et al., 2017).

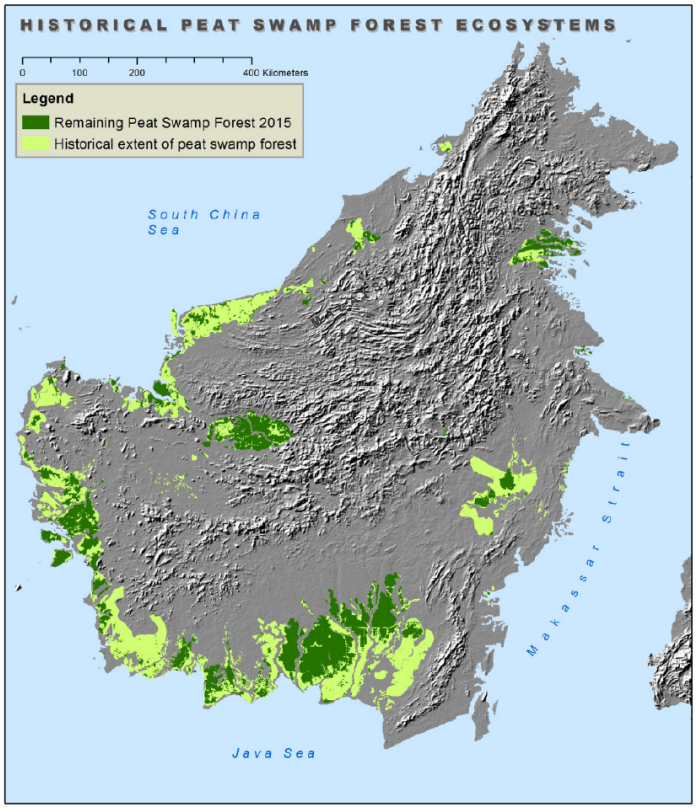

Figure 1.3: Map of past and current peat swamp forest cover on Borneo (Source: Wulffraat et al., 2016). Peat swamp forest is now at 42 % of historical cover, the vast majority of that being lost since 1990 (Miettinen et al., 2017).

Tropical peat swamp forest is dependent on comparatively high levels of rainfall, which is the sole source of water into the ecosystem; they are normally wet environments, where the water table is near or at the peat surface for most of the year (Page and Baird, 2016). Peat swamp forest is generally given little social value and may even be seen by some as a nuisance (Meijaard et al., 2013); its swamp-like nature means that access is very difficult and, up until recently, the land was considered unsuitable for many kinds of agriculture. Initially, the swamp forests were exploited for their timber but more recently, and particularly since the 1990s, the land has been drained to allow conversion to agricultural land or plantations for the oil palm and paper pulp industries (Koh et al., 2011). Due to its various land uses, peat swamp forest in southeast Asia exists as a broad spectrum of conditions; peat swamp forest can be pristine or undisturbed, lightly or heavily impacted by disturbance and then subsequently abandoned, or converted partially or entirely for agriculture.

Many classifications, reflecting the many land uses of peat swamp forest have been devised. These

classifications have included: pristine peat swamp forest, whereby there is no obvious anthropogenic impacts (Miettinen et al., 2016); intact peat swamp forest, whereby selective logging or channel construction may have taken place yet the maintains e.g. typical floras and ecosystem services associated with pristine peat swamp forest (Jauhiainen et al., 2011; Moore et al., 2013); degraded peat swamp forests, which have been deforested and had larger channels constructed and may have been abandoned (Sundari et al., 2012; Moore et al., 2013); oil palm plantations, whereby the vegetation are replaced with *Elaeis* spp. (Miettinen et al., 2012); paper pulp plantations, whereby *Acacia* spp. replaces the peat swamp vegetation (Evans et al., 2019). These land use types are selected as the more researched representatives from the peat swamp forest land use spectrum to demonstrate their differing characteristics in Fig. 1.4 and Table 1.1. However, there are many more definitions and states of peat swamp forest: oil palm plantations can be on a range of rotation lengths (Warren et al., 2017), and may represent young or mature plantations (Cooper et al., 2019); forest plantations may consist of other commercial tree species where a range of management practices may be employed (Evans et al., 2019); peat swamp forest can be used for other agricultural uses such as growing pineapples, coconuts, rice, sago palm, rubber, and others on smallholder or industrial scales (Miettinen et al., 2016; Evans et al., 2019); and newly establishing pioneer peat swamp forest (Cole et al., 2015), however the quality of this peat swamp forest may be affected by the disturbance history of the peat dome.

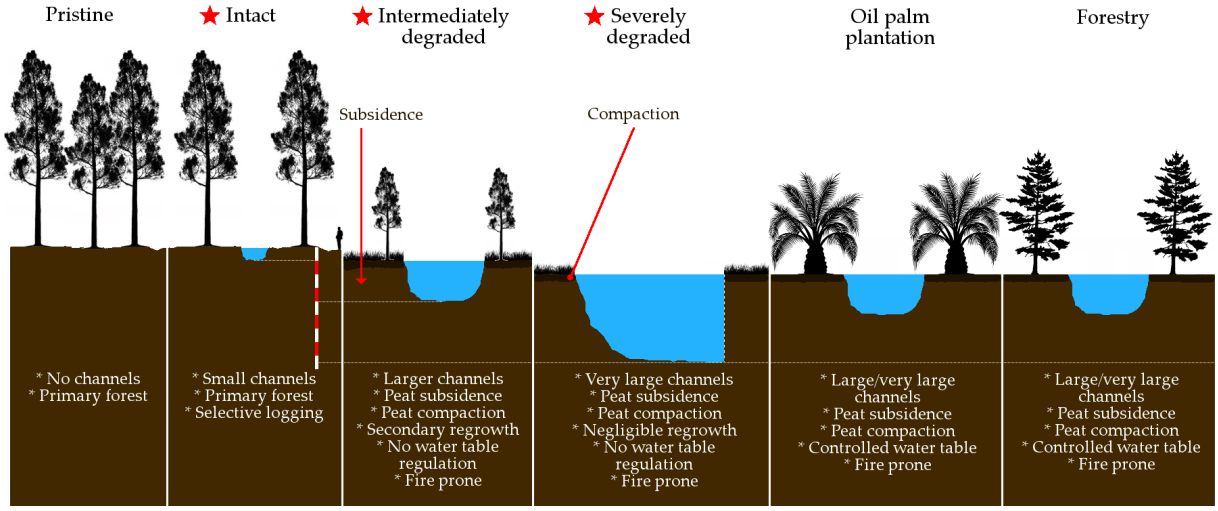

Figure 1.4: Representative intact, degraded and converted peat swamp forest types demostrating some types of land uses, and characteristics and vulnerabilities of the peat resulting from those land uses. The land class types investigated in this thesis are marked with red stars. A red and white scale bar represent depth in metres to demonstrate the depth of the channels typically associated with disturbed/converted peat swamp forest.

Ideally, to investigate the impacts of land use change on peat swamp forest, studies would compare a disturbed or converted peatland to its intact analogue, a pristine peat swamp forest. However, a study by Miettinen et al. (2016) of Penisular Malaysia, Sumatra and Borneo showed that 93.6 % of swamp forests had been impacted by humans since 1990. Pristine forest is therefore scarce, 66 % of which is in Brunei (Miettinen et al., 2016). As a result, the virtually all published studies assessing the impacts of land use change on peat swamp forest have used intact, lightly disturbed forest for comparison as it maintains, for example, the typical floras and ecosystem services associated with pristine peat swamp forest (Hirano et al., 2007; Jauhiainen et al., 2011; Moore, 2011; Moore et al., 2013).

Degraded and converted peatlands, such as those in Fig. 1.4, are typified by having been heavily logged or deforested, and by the presence of large channels that drain water from the surrounding catchments. Deforestation impacts biodiversity, and the structure and stability of the peat (Baird et al., 2017; Evans et al., 2019), and the channels significantly alter water table amplitude and lower mean annual water table depth, with respect to intact peat swamp forest (Sundari et al., 2012). Therefore, the ecosystem characteristics, and hydrological and biogeochemical functioning of degraded and/or converted peatland can be fundamentally different to intact peat swamp forest (see Table 1.1).

Table 1.1: Characteristic ecological, geochemical and environmental data for comparison of PSF land use types. Where sources present values from multiple studies, values presented are means of the all studies, with the number of studies in parentheses. More detailed information on typical vegetation across the types can be found in e.g. Page et al., 1999, Harrison et al., 2010, Moore, 2011 and Cole et al., 2015. Land cover estimates span Peninsular Malaysia, Sumatra and Borneo.

	Pristine PSF	Intact PSF	Intermediately degraded PSF	Severely degraded PSF	Oil palm plantation	Forestry (*Acacia* plantation)	Source
Vegetation type	Primary forest	Primary forest missing some economic spp.	Secondary forest Tall scrub	Ferns Low scrub Bare peat	*Elaeis* spp.	*Acacia* spp.	1
Land cover (%)	6.4	22.8	11.1	5.4		(49.8)	1
Mean water table (cm)		-25.6 (5)			-56.0 (5)	-70.0 (2)	2
		6.0	-14.0		-39—21		3
		-18.3	-39.6	-55.5	-65.5	-78.6	4
Organic matter (%)		94.1	88.8			86.1—77.3	3
Moisture content (%)		82.3	46.3			33.9—56.6	3
Pore water pH		3.4	3.7		3.7—3.9		3
Air temperature (°C)		26.3	26.0	26.0	31.7	32.3	4
Peat temperature (°C)		26.3	28.8	29.5	27.5	30.5	4
Subsidence ($cm \cdot yr^{-1}$)		-2.1 (5)			-3.4 (7)	-4.8 (2)	2
CO_2 emissions ($Tg \cdot C \cdot yr^{-1}$)		9.45	9.20	13.6	34.2	22.6	5
Net CO_2 balance ($Mg \cdot C \cdot ha^{-1} \cdot yr^{-1}$)		-1.4	5.3	11.2	8.2	19.6	4
CH_4 emissions ($kg \cdot C \cdot ha^{-1} \cdot yr^{-1}$)		28.6	3.7	5.2	-0.2	2.0	4

Sources used: 1) Miettinen et al., 2016; 2) Evans et al., 2019; 3) Cooper et al., 2019; 4) Hergoulac'h and Verchot, 2014; 5) Miettinen et al., 2017.

A lowered water table resulting from the channels dug when changing land use is generally regarded as the driver of significant changes in peat biogeochemistry. The most impacted sites are considered to be those with the lowest water tables; lower water tables make it harder for peat swamp vegetation to survive and peat oxidation and compaction are promoted (Evans et al., 2019). Oxidation results in a drop in organic matter content, and as soil moisture reduces it becomes more prone to peat fires during dry seasons (Page et al., 2001). Environmental changes also take place as a result of defor-

estation and drainage of peat swamp forest, for example, pH and air and peat temperatures generally increase as the water table becomes lower. The emission of greenhouse gases such as CO_2 and CH_4 are also affected and, importantly, degraded and converted peatlands typically switch from CO_2 sinks to becoming CO_2 sources (Hergoulac'h and Verchot, 2014; Miettinen et al., 2017).

1.1.2 Peat swamp forest degradation in Central Kalimantan

Central Kalimantan in Indonesia is probably the most researched region in terms of comparisons of intact and degraded peat swamp forests; extant there are both large areas of intact peat swamp forest, and intermediately and severely degraded peatlands that are separated only by a major river, the Sabangau River. Being in such close proximity, numerous studies have reported on the peatlands' respective biogeochemistries, carbon balances and greenhouse gas fluxes, with some of these data being collected simultaneously (Hirano et al., 2012, Sundari et al., 2012; Moore et al., 2013).

Table 1.2 highlights some significant environmental and biogeochemical differences between intact, intermediately degraded and severely degraded in Central Kalimantan. Temperatures are typically hotter, and rainfall and water tables lower, at the degraded land use types than intact peat swamp forest. Ecosystem respiration and gross primary productivity are highest at intact peat swamp forest, and decrease as the severity degradation increases across the land use classes. There is a much more significant reduction in gross primary productivity in the degraded land land use classes and therefore their respective net ecosystem exchanges of carbon (dioxide) are ˜2 to 3−times higher than intact peat swamp forest (Hirano et al., 2012).

Research pertaining to the channels draining intact and degraded peat swamp forest are very scarce, and therefore understanding of these small fluvial systems is currently limited; Table 1.2 includes the two existing studies regarding carbon fluxes from the channels, and some environmental data from a study of fish populations in the Sabangau Forest (Thornton et al., 2018). Therefore, many data presented in this thesis represent newly acquired, previously unavailable data. Data from rivers will be discussed later in this chapter, but these data are limited in terms of interpreting differences between land use types as the rivers can drain a mix of intact and degraded catchments and therefore, taking a geochemical perspective, the signals are mixed and do not yield direct information on the effects of land use change. Moore et al. (2013) was the first study to compare differences between intact peat swamp

Table 1.2: Environmental and biogeochemical data for catchments and channels in intact and degraded PSF in Central Kalimantan. Air temperatures were recorded ~30 m from the ground by flux towers, and therefore do not represent temperatures beneath the canopy in intact PSF. §The intermediately degraded sites in Hirano et al. (2012) were drained but not deforested.

	Intact	Intermediately degraded	Severely degraded	Source
Catchment data				
Air temperature (°C)	26.3†		25.9−26.8*	†Hirano et al., 2007 *Sundari et al., 2012
Soil temperature (°C)	24.3−27.4		25.1−28.5	Sundari et al., 2012
Rainfall ($mm \cdot yr^{-1}$)	2,744	2,356	2,225	Moore, 2011
Mean water table (cm)	0.26−−0.72		−0.10−−1.26	Sundari et al., 2012
Ecosystem respiration ($g \cdot C \cdot m^{-2} \cdot yr^{-1}$)	3,642	3,519§	1,787	Hirano et al., 2012
Gross primary productivity ($g \cdot C \cdot m^{-2} \cdot yr^{-1}$)	3,468	3,191§	1,289	Hirano et al., 2012
Net ecosystem exchange ($g \cdot C \cdot m^{-2} \cdot yr^{-1}$)	174	328§	499	Hirano et al., 2012
Channel data				
Channel width (m)	<3	3−6	10−25	Moore, 2011
Channel depth (m)	~1	2−3	1−7	Moore, 2011
Dissolved O_2 ($mg \cdot L^{-1}$)	1.2−1.7			Thornton et al., 2018
Water temperature (°C)	25.4−26.4			Thornton et al., 2018
pH	3.4−4.3			Thornton et al., 2018
Mean annual DOC ($mg \cdot L^{-1}$)	68.0	55.0	48.3	Moore et al., 2013
DO^{14}C age (yrs before present)	Modern	188−735	1,308−1,760	Moore et al., 2013
TOC loss ($g \cdot C \cdot m^{-2} \cdot yr^{-1}$)	63	88	105	Moore et al., 2013
CO_2 emissions ($g \cdot m^{-2} \cdot d^{-1}$)			9.0	Jauhiainen and Silvennoinen, 2012
CH_4 emissions ($mg \cdot m^{-2} \cdot d^{-1}$)			164	Jauhiainen and Silvennoinen, 2012

forest and its intermediately and severely degraded counterparts. Like the terrestrial study of Hirano et al. (2012), Moore et al. found that there were significant differences of carbon cycling and export between the three land use types; intact peat swamp forest exported 63 $mg \cdot L^{-1}$ of recently photosynthesised carbon to its channels, whereas as the level of degradation increased, the peatlands released less carbon (48.3−55 $mg \cdot L^{-1} \cdot$TOC) but was 188−1,760 years-old in age (see Table 1.2). From the data presented, it is clear that land use change of peat swamp forest is having an effect on carbon losses from previously stable stores, but there are other symptoms of peatland degradation in terms of the compromising the ecological resilience of peat swamp forest and the ecosystem losing carbon.

One example of large-scale agricultural development on peatland was the Mega Rice Project in Central Kalimantan, which started in 1995 and abruptly ended in 1999 (Moore, 2011). Rice is the staple

food in Indonesia, and although some rice is grown in the country it continues to be a net-importer. The Mega Rice Project was intended to bring about Indonesian self-sufficiency in rice production (Boehm and Siegert, 2001; Moore, 2011) through deforestation and drainage of >1 Mha of peat swamp forest and conversion to rice fields. This involved cutting >4,000 km of channels to drain the peatland and subsequently to provide water table control that would enable wet rice production (de Vries, 2003). The channels were not cut correctly and the land was drained excessively and the peat became too dry to grow rice (Boehm and Siegert, 2001).

Dry peats can become combustible, and during the 1997−98 El Niño severe fires swept across much of the Mega Rice Project and other areas of degraded peatland (Boehm and Siegert, 2001; Page et al., 2002). The project was abandoned by the Indonesian Government in 1999, having failed to produce an economic rice crop. Since then, the uncontrolled nature of the drainage means that the land is subject to seasonal floods during the wet season and fires during the dry season, creating a very challenging environment for peat swamp forest vegetation to re-establish, and also exacerbating C loss from the peat (Page et al., 2009a).

Fires constitute a major C loss pathway from degraded peatlands (Page et al., 2002), but it is frequently used as a cheap and effective method to clear land of unwanted vegetation and debris. Burning is often carried out during the dry season in an attempt to clear degraded peatlands but the low rainfall during this time can allow the fires to spread. However, drier years, such as those exacerbated by El Niño, mean that there may be negligible or no rain for protracted periods and fires can get very large and, consequently, may burn completely out of control (Koplitz et al., 2016).

Fires during El Niño years have released globally significant amounts of C to the atmosphere in periods of a few months; Page et al. (2002) estimated that 0.95 Pg·C was released during extensive peatland fires in 1997, while fires occurring during years with weaker El Niño events released ˜0.2, ˜0.3 and ˜0.3 Pg·C in 2002, 2006 and 2015, respectively. Cumulative peat fire C emissions since 1997 are thought to be ˜2.9 Pg (Miettinen et al., 2017).

As well as C loss from peat fires, the lower water table resulting from channels can promote peat oxidation (via biological degradation; Miettinen et al., 2017); more oxygen from the atmosphere can reach the peat allowing it to be decomposed by aerobic pathways, resulting in the release of e.g. CO_2 to the atmosphere (Freeman et al., 2001).

In intact tropical peatlands, this can be a natural phenomenon that can occur during the short (˜3-month) dry season. Despite the oxidation that can occur in the dry season, an intact tropical peatland over a full year can function as a net sink for CO_2; the wet season typically accumulates more CO_2 than is lost in the dry season (Hirano et al., 2007).

When channels drain tropical peatlands, much more oxidation of the peats can take place, and C loss by oxidation can proceed all year round. Further, as conversion of peat swamp forest often includes removal of the forest, the ability of the ecosystem to continue to sequester C is also considerably reduced (Hirano et al., 2007). As such, the increased rates of oxidation and reduced C sequestration of degraded tropical peatlands can cause them to become overwhelming C sources (Couwenberg et al., 2010; Hirano et al., 2012; Miettinen et al., 2017); oxidation of drained peats in Peninsular Malaysia, Sumatra and Borneo has been estimated to have released ˜0.15 $Pg{\cdot}C{\cdot}yr^{-1}$, or cumulatively, 2.50 Pg·C since 1990 (Miettinen et al., 2017).

Significant amounts of C can also move out of peat swamp forests and degraded peatlands via water flowing out of the peat dome. Moore et al. (2013) estimated that fluvial loss of total organic carbon (TOC) from intact peat swamp forest was 63 $g{\cdot}C{\cdot}m^{-2}{\cdot}yr^{-1}$, whereas degraded peat swamp forest lost significantly more ($88-105$ $g{\cdot}C{\cdot}m^{-2}{\cdot}yr^{-1}$) with $7-9$ % of the TOC made up of particulate organic carbon (POC). At intact peat swamp forest this proportion was 2 % (Moore, 2011). Therefore, degraded peat swamp forest was also losing considerably more dissolved organic carbon (DOC) than intact peat swamp forest (where DOC equals TOC minus POC; Moore et al., 2013).

1.2 Riverine systems and their role in the carbon cycle

Rivers and streams used to be thought of as passive pipes that transported material from land to the sea; "gutters down which flow the ruins of continents" (Leopold et al., 1964). It was also believed they were net-autotrophic ecosystems where photosynthesis dominated heterotrophic metabolism, fixing more C than was respired. It wasn't until the 1990s that these assumptions were scrutinised, and completely different systems proposed (Cole et al., 2007).

Riverine systems receive significant quantities of organic matter, inorganic nutrients and microbes from their catchments as water moves through and over soils to their drainage rivers that occupy the

low-lying regions of the catchment (Cuffney, 1988). This input of material acts to prime riverine systems, providing a food source for organisms to break down (McClain et al., 2003). The decomposition of abundant organic matter means that most riverine systems are net-heterotrophic and produce significant amounts of CO_2 (Hope et al., 1994; Cole et al., 2007; Battin et al., 2008; Battin et al., 2009; Raymond et al., 2013). Due to their high capacity for breakdown of organic matter, rivers and streams can be considered as 'terrestrial digestive systems'.

As well as in-stream production of CO_2 via heterotrophic processes, dissolved CO_2 from soil respiration can also reach streams from the catchment via ground- and through-flows (Johnson et al., 2008). Internal production and external delivery of CO_2 to rivers generally means they contain much higher concentrations than the atmosphere, and are said to be 'supersaturated' with respect to the atmosphere. Streams can also be supersaturated with other dissolved gases, such as CH_4, as is commonly the case with peatland streams (Billett and Moore, 2008).

Supersaturation of dissolved gases means the concentration gradient is toward the atmosphere; as such those dissolved gases will be much more easily emitted than absorbed. Further, if there is turbulence at the water surface, this increases the likelihood that gases will be degassed from the water to the air (MacIntyre et al., 1995). Turbulence can be caused by the wind at the water surface, but it is also caused internally as the rivers flow; currents are produced by friction with the bank sides and channel bottom making a physically complex, turbulent environment (MacIntyre et al., 1995). When turbulence exists at the water surface, it promotes gas transfer to the atmosphere.

Globally, it is estimated that streams and rivers emit 1.8 $Pg{\cdot}C{\cdot}yr^{-1}$ whereas inland lakes and reservoirs emit 0.32 Pg $C{\cdot}yr^{-1}$ despite the lakes and reservoirs occupying ~5−times the land surface area (Raymond et al., 2013). In this way, rivers are a significant part of the global C cycle and are a globally significant source of greenhouse gases (Hope et al., 1994; Cole et al., 2007; Battin et al., 2008; Battin et al., 2009).

1.3 Tropical blackwater streams and their high carbon loads

As rivers can be considered as emergent properties of catchment climate and geomorphology (cf. Sioli, 1975), peatland catchments dominated by organic soils produce 'blackwater' streams and rivers. The

waters are tea-coloured owing to comparatively high concentrations of aromatic DOC that derives from plant tissues, which are also known as phenolic acids (Rydin and Jeglum, 2006; Schlesinger and Bernhardt, 2013). Phenolic acids can be sorbed by clay particles in rivers that drain mineral soils and this clarifies the water and lowers the amount of DOC, however, in peatlands the underlying clays are essentially isolated from the water column by a thick layer of organic soil thus the DOC can persist in the water (St. John and Anderson, 1982). Blackwaters, like the organic soils they drain, are generally acidic, nutrient poor (owing to the DOC sorbing inorganic nutrients), have low concentrations of dissolved oxygen and have comparatively high concentrations of DOC (Meyer and Edwards, 1990; Alkhatib et al., 2007; Rixen et al., 2008).

As stated above, channels draining peats are characteristically supersaturated with CO_2 and CH_4 (Dinsmore et al., 2010; Raymond et al., 2013; Billett et al., 2015) and recent investigations have shown that rivers draining peat swamp forests in Indonesia contain very high concentrations of DOC too (Baum et al., 2007; Rixen et al., 2008; Moore et al., 2011; Huang et al., 2012; Moore et al., 2013). For example, the Dumai River in Sumatra reached 5,050 μmol·L^{-1}, the highest reported river DOC concentration in the world (Alkhatib et al., 2007); more than 10−times the world average of 450−479 μmol·DOC·L^{-1} (Huang et al., 2012).

Higher concentrations of DOC allow for a greater rate of breakdown and hence a greater potential to emit CO_2, but this is also dependent on nutrient and oxygen availability and, for example, biodegrading organisms. Further, as peatland catchments are relatively flat, the waters tend to flow comparatively slowly, increasing the residence time of the water in the channel. This increases the potential for the DOC to be broken down in-stream before it discharges to the ocean (Helton et al., 2015).

Very high CO_2 outgassing rates have been reported for Amazonian blackwater rivers and streams (Richey et al., 2002; Mayorga et al., 2005) but data on Southeast Asian blackwater river and stream emissions are scarce. This has been identified as a priority knowledge gap to fill if more accurate global emissions estimates from riverine systems are to be made (Raymond et al., 2013).

The flow of C from one reservoir to another, e.g. from the water to the air, is described as a 'flux' and is presented as a change in amount, over a period of time. The fluxes described here will be the net transfer of gases from the channels to the atmosphere. Current fluxes from tropical riverine systems have been both measured and others estimated: Müller et al. (2015) measured CO_2 fluxes of 5.5±2.6 and

12.7±6.8 g·C·m^{-2}·d^{-1} for the Maludam River in Malaysia, while Aufdenkampe et al. (2011) estimated 2,720 g·C·m^{-2}·yr^{-1}, or 7.4 g·C·m^{-2}·d^{-1}. The fluxes in Aufdenkampe et al. (2011) were obtained using medians from a synthesis of measurements and values reported in the literature, for dissolved gas concentrations and gas transfer velocities (a metric for water turbulence) specific to tropical streams and rivers.

Southeast Asia contains 65 %, or 68.5 Pg, of tropical peatland C (Dargie et al., 2015), and hence many streams and rivers draining the peats are C-dense blackwaters. Indonesian rivers alone are estimated to deliver 8−10% of all TOC discharged to the sea, globally (Alkhatib et al., 2007; Baum et al., 2007). Disturbance of river catchments is believed to have increased global TOC export from land to sea by 1.0 Pg·C·yr^{-1} since pre-industrial times (Regnier et al., 2013). In Indonesia, 45 % of the peat swamp forests have already been lost (Hooijer et al., 2006) and this is likely to affect the nature of the C reaching drainage networks, and also how much of the C is degraded and degassed in-channel (Lapierre et al., 2013). Increased concentrations of DOC resulting from disturbance of catchments can cause streams to emit more CO_2 (Lapierre et al., 2013).

Disturbance of peat swamp forest has been shown to alter the quantity and quality of DOC leaving the land (Moore et al., 2013; Gandois et al., 2014). Moore et al. (2013) reported that the C being lost from disturbed peat swamp forest was millennia-old. Carbon from degraded peat swamp forest has also been shown to be more humified and resistant to biological breakdown (Moore et al., 2013; Evans et al., 2014; Butman et al., 2015; Evans, 2015). It is possible, then, that peat swamp forest disturbance exacerbates greenhouse gas emissions from peatland drainage networks and therefore it is important to ascertain the natural, background greenhouse gas flux in order to compare it to that measured from disturbed peat swamp forest.

The best place to measure quantitative and qualitative differences in TOC flux and greenhouse gas emissions from intact and degraded peat swamp forests, is where streams immediately drain these respective land classes, i.e. at the 'headwaters' (the upstream sections of a riverine system that directly drain higher subcatchments). Headwaters make up the greatest proportion of channel area, have the highest concentrations of dissolved gases and the highest fluxes of gases per unit area (Koprivnjak et al., 2010; Aufdenkampe et al., 2011; Butman and Raymond, 2011). In intact systems, headwaters have been shown to have more recent, labile −and therefore more bioavailable− DOC that is more easily broken

down which could increase CO_2 emissions (Mayorga et al., 2005).

Although headwaters are usually considered natural tributaries, for the purposes of this study man-made channels draining the peat swamp forest will also be referred to as headwaters; they are already known to have high concentrations of DOC, and like other tropical headwaters likely have high concentrations of dissolved gases.

To date no study has investigated greenhouse gas fluxes from intact and degraded peat swamp forest headwaters. This study sets out to address this knowledge gap with a focus on fluxes of CO_2 and CH_4. Although nitrous oxide (N_2O) is also a potent greenhouse gas, it has been found to have a very small ($0-2$ %) contribution to the total CO_2-equivalent flux in a study of channels draining degraded tropical peatlands that investigated the cumulative flux of CO_2, CH_4 and N_2O (Jauhiainen and Silvennoinen, 2012).

1.4 Dissolved CO_2 and CH_4 and their sources in peat channels

1.4.1 Sources of dissolved CO_2 in channels

The dissolved CO_2 present in channels can originate from surrounding catchment soils or in-stream (see Fig. 1.5). CO_2 that derives from soil respiration can be picked up from the surrounding catchment by dissolving in water that is flowing over and through the soil to the river. CO_2 is produced in-stream by a variety of pathways. Firstly, it may arise from dissolved inorganic carbon (DIC); depending on the alkalinity of the water CO_2 may react to form carbonic acid (H_2CO_3), bicarbonate (HCO_3^-) and carbonate (CO_3^{2-}) as in the following reactions:

$$CO_{2(aq)} + H_2O \rightleftharpoons H_2CO_{3(aq)} \tag{1.1}$$

$$H_2CO_{3(aq)} \rightleftharpoons H^+ + HCO_3^- \tag{1.2}$$

$$H^+ + HCO_3^- \rightleftharpoons 2\,H^+ + CO_3^{2-} \tag{1.3}$$

As pH increases, the chemical equilibria move from Eqn. 1.1 to Eqn. 1.3. At pH < 4.3 CO_2 dominates DIC as a dissolved gas (Schlesinger and Bernhardt, 2013). As the pH increases it reacts with H_2O to form H_2CO_3 gradually being converted to HCO_3^- which is the predominant species between pH 6.4 and pH 10.2. CO_3^{2-} then dominates in the higher pH ranges (Manahan, 2010; see Fig. 1.6). DIC is the sum of

inorganic C that was or could become CO_2:

$$\mathrm{DIC} = \sum [CO_{2(aq)}^{*}] + [HCO_3^{-}] + [CO_3^{2-}] \tag{1.4}$$

where $[CO_{2(aq)}^{*}]$ constitutes the sum of dissolved CO_2 and H_2CO_3. As reported pH values of Indonesian peat channels are lower than pH 4.3 (Moore, 2011) it can be assumed that most DIC exists as CO_2, as was demonstrated by Huang et al. (2012).

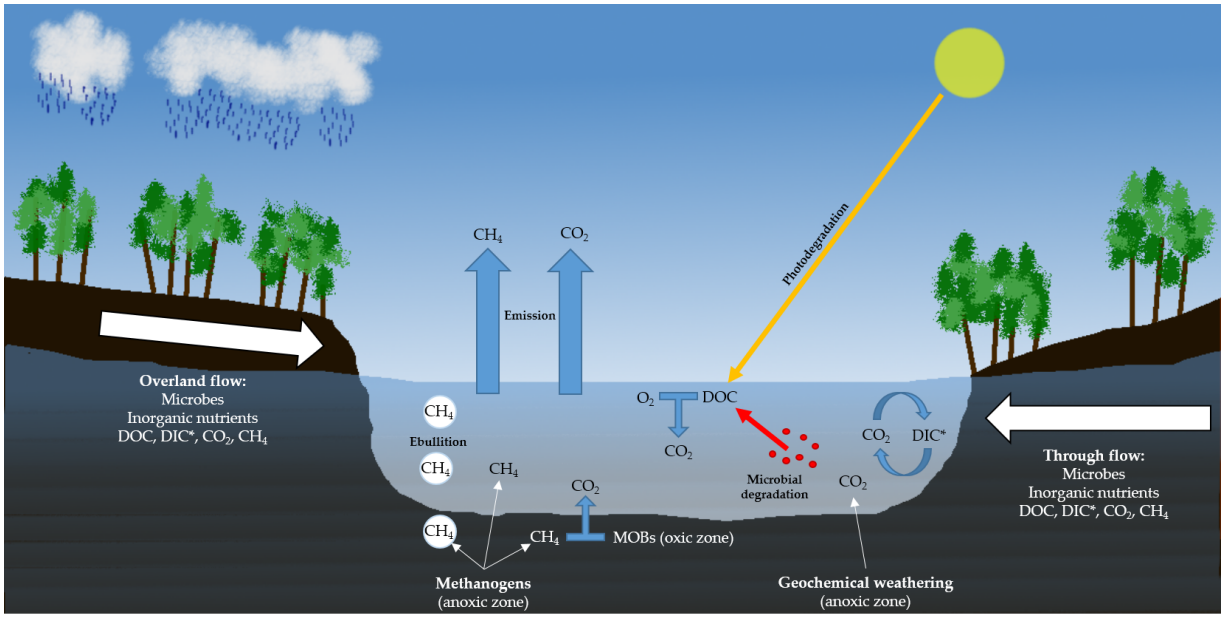

Figure 1.5: Diagram showing the processes by which CO_2 and CH_4 originate in supersaturated streams and channels that drain peats. These processes are described in Sections 1.4.1 and 1.4.2.

Secondly, CO_2 can result from active or passive degradation of DOC whereby the most dominant processes are likely to be biodegradation and photodegradation (Schlesinger and Bernhardt, 2013): microbes use O_2 to break down DOC during respiration, and; photosensitive DOC which has free electrons that can be excited by sunlight can react with dissolved O_2.

The oxic zone of the stream bed may produce CO_2 by normal aerobic reactions, including methane-oxidising bacteria that break down CH_4 to produce CO_2. Historic CO_2 has also been shown to be released via geochemical weathering from deep within the peat profile (Billett et al., 2007, 2012).

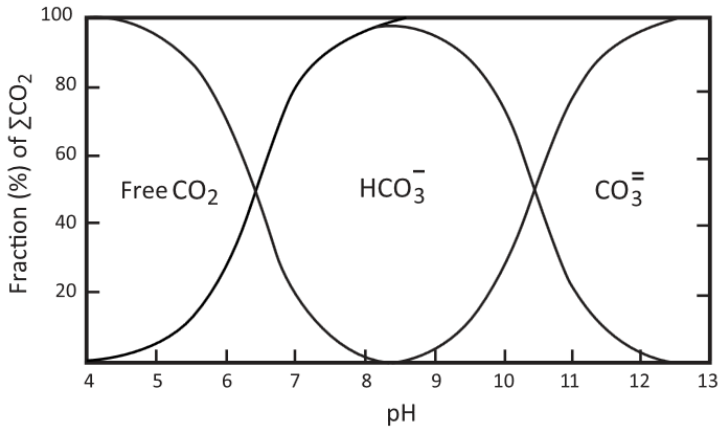

Figure 1.6: Diagram demonstrating DIC species dynamics at a range of pH values. Blackwater stream pH is typically $\leq$4 and so CO_2 dominates DIC (Source: Goldenfum, 2011).

1.4.2 Sources of dissolved CH_4 in channels

Methane is a potent greenhouse gas that is considered to have a 100-year global warming potential of 32 as a single pulse, and a sustained-flux global warming potential of 45, with respect to CO_2; therefore, one mole of CH_4 has the warming potential of 32$-$45 moles of CO_2 (Neubauer and Megonigal, 2015).

In channels, CH_4 is produced by anaerobic respiration in anoxic sediments where methanogenic microbes use C as a terminal electron acceptor. The best known pathways use acetic acid (CH_3COOH) or CO_2 as terminal electron acceptors, and are respectively known as acetoclastic and hydrogenotrophic methanogenesis (Schlesinger and Bernhardt, 2013):

$$CO_2 + 4\,H_2 \longrightarrow CH_4 + 2\,H_2O \tag{1.5}$$

$$CH_3COOH \longrightarrow CH_4 + CO_2 \tag{1.6}$$

Few studies have been conducted on the dominant methanogenic pathway in tropical peatlands, but like their acidic and nutrient-poor equivalents in the temperate zone, findings currently indicate that it is hydrogenotrophic (Inubushi et al., 2005; Holmes et al., 2015).

Methane is less soluble in water than CO_2 and CH_4 bubbles can form in the sediment. Disturbance of the sediment or a low hydrostatic pressure may cause the bubbles to release into the water column (MacIntyre et al., 1995). But because poorly dissolves, those bubbles may reach the surface and release CH_4 directly to the atmosphere, this is known as 'ebullition'. The low solubility of CH_4 can also make it more sensitive to water turbulence, with respect to CO_2; turbulence is more likely to cause CH_4 to come

out of solution and be emitted (MacIntyre et al., 1995).

Methane can also enter the stream by lateral flows (overland and through-flows) from the surrounding catchment. Arrival of CH_4 by lateral flow is made more possible in tropical peats than northern peats, due to the former's higher permeability (or hydraulic conductivity; Baird et al., 2017; Hoyt et al., 2017). Methane arriving in lateral flows could originate from anoxic peats producing the CH_4 by the above-mentioned methanogenic pathways.

Methane can be readily oxidised into CO_2 (and H_2O).

1.4.3 Plant-mediated production and transport of CH_4

Some plants, particularly those in wetland habitats, possess aerenchyma in their roots, stems and leaves. Aerenchyma are air-filled channels that allow plants exchange gases between the soil and the atmosphere. They allow the oxygenation of roots in waterlogged conditions, and also provide a pathway for gases to escape that have built up in the soil, some of which may be toxic to the plant (MacIntyre et al., 1995; Schlesinger and Bernhardt, 2013).

Aerenchymatous plants in wetland ecosystems can play a fundamental role in the CH_4 cycle of a catchment, and therefore the abundance of CH_4 in the channels that might be transported from the catchment. Such plants can a) promote methanogenesis, b) facilitate O_2 transport from the atmosphere to the peat, promoting CH_4 oxidation, and c) facilitate transport of CH_4 from the peat to the atmosphere. These processes will be discussed in later chapters. In all cases the rooting zone, or 'rhizosphere' is of fundamental importance as gases and compounds move between the plant and the soil via the roots (Megonigal and Day, 1992; Kozlowski, 1997).

Jackson et al. (1996) conducted a meta-analysis of root depths in different terrestrial biomes around the world. A primary finding was that root biomass dropped exponentially with depth; 30 % of roots were found in the top 10 cm of soil, a further 20 % in the next 10 cm, and 25 % between 20−40 cm depth. Five of the biomes were forest ecosystems and it was reported that 69 % of roots are found in the top 30 cm of soil in tropical evergreen forests (see Table 1.3). The studies did not include southeast Asian PSF, but this forest would be classed as 'tropical evergreen'. Root biomass per unit area was the highest of the forest biomes in the study of Jackson et al., and this reflects the habit of PSF plants that employ dense root mats near the surface to scavenge metabolites from the otherwise nutrient poor and often waterl

Table 1.3: Root biomass distribution and density in various forest biomes around the world. This table reproduces data reported by Jackson et al. (1996) in a synthesis of global rooting depths across the world's main biomes. The numbers of references used to determine the root biomass of the biomes are also provided.

Forest biome	Root biomass in upper 30 cm (%)	Root biomass ($kg \cdot m^{-2}$)	Number of references
Boreal	83	2.9	4
Temperate coniferous	52	4.4	8
Temperate deciduous	65	4.2	7
Tropical deciduous	70	4.1	3
Tropical evergreen	69	4.9	9

ogged peats (Yule, 2010).

Sulistyanto, 2005 investigated root density in an intact PSF and reported that 551 $g \cdot m^{-3}$ (up to 83 %) of roots were found in the top 25 cm of the peat, nearly 5−times that of the next 25 cm of peat (112 $g \cdot m^{-3}$). This finding indicates that the decline of root biomass with depth may be more rapid than in a typical tropical evergreen forest.

There are no data on rooting depths for degraded PSF, but the catchments are much less vegetated than intact PSF and display a much reduced diversity of flora (Moore, 2011). The vegetative community of degraded PSF typically consists of grasses and ferns, but if the land is degraded to the extent that it regularly floods, little can survive apart from the palm-like *Pandanus*. The reduced quantity and diversity of vegetation in degraded PSF likely impacts the cycling of CH_4 by the processes described above.

1.5 El Niño and its effects on CO_2 and CH_4 in tropical peatlands

The El Niño−Southern Oscillation (ENSO) is a natural phenomenon associated with temperature and precipitation anomalies in the tropics. These anomalies drive the climatic extremes that occur in the tropics over years and decades, and, on land, are associated with droughts and heatwaves, or floods and periods of cold (Cai et al., 2014; Jiménez-Muñoz et al., 2016; L'Heureux et al., 2017; Pandey et al., 2017). ENSO oscillates between two states, El Niño and La Niña, and these states affect different areas of the Pacific Basin differently. For Indonesia (and other countries along the western edge of the Pacific Basin), generally, El Niño is characterised by anomalously warm and dry weather, and La Niña by anomalously cool and wet conditions (Harger, 1995). These anomalous conditions result from above or below average

sea surface temperatures affecting the circulation of trade winds and the temperature and humidity of the air they carry (Wolter and Timlin, 2011; L'Heureux et al., 2017).

Over time scales of a year, or years, a peatland may function as a net-C sink, despite the dry periods during which oxidation can occur. However, events such as El Niño in Indonesia induces rainfall anomalies whereby protracted periods of dryness lead to greater water table drawdown (Harger, 1995; Keil et al., 2008). The longer the periods of water table drawdown, the greater the potential for C loss by e.g. oxidation. Prolonged and more extreme dry seasons caused by El Niño can result in tropical peatlands losing more C than they accumulate and they can become a C source (Wang et al., 2014; Pandey et al., 2017; Zhu et al., 2017).

It has been predicted that the size of the terrestrial C sink in the tropics will shrink as a result of increasing temperatures and frequency of droughts (Wang et al., 2014), i.e. tropical peatlands will have a higher potential to become C sources. This potential will likely become greater as the frequency of El Niño events has been predicted to increase (Cai et al., 2014).

The strength of an El Niño (or La Niña) can be measured using the Multivariate ENSO Index, which is based on the departure from a standardised mean from a group of indices, including sea surface temperature, near-surface air temperature, sea level pressure, etc., measured in standard deviations (Wolter and Timlin, 2011). There have been three strong El Niño events since the satellite technology has existed to measure large-scale environmental parameters such as sea surface temperatures. These three strong ENSOs typically lasted about a year and occurred in 1982-83, 1997-98 and 2015-16 (L'Heureux et al., 2017; see 1.7). Each of these El Niño events was characterised by a suite of environmental indices nearly reaching −or exceeding− 2.5 standard deviations from a standardised mean.

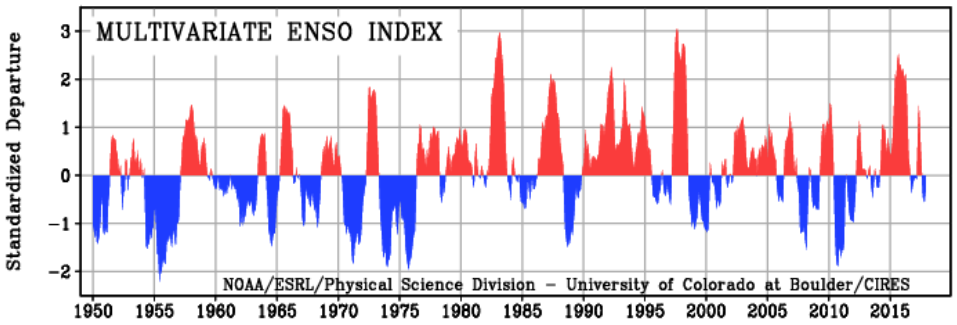

Figure 1.7: Monitoring of the El Niño−Southern Oscillation (ENSO) began in the mid-20th century. El Niño events are shown in red and La Niña events in blue. The three strongest El Niños, since records began, occurred in 1982-83, 1997-98 and 2015-16 when the standardised departure reached or exceeded 2.5 standard deviations from the long-term mean. Source: Earth Systems Research Laboratory, NOAA.

The occurrences of El Niño events have been followed by jumps in the concentration of atmospheric CO_2 (Keeling et al., 1995; Jones et al., 2001); and following the El Niño of 2015, a record rise in atmospheric CO_2 was observed. The rise was linked to droughts in tropical countries during the El Niño (Betts et al., 2016). The droughts reduced the rate of uptake of C by plants (exacerbated by the death of trees) and increase losses of C by fire.

Interannual variation of CH_4 emissions from tropical wetlands has been shown to be more dependent on precipitation, rather than temperature, which is the primary environmental driver in temperate regions (Turetsky et al., 2014). Further, CH_4 emissions have been found to be highest during wet La Niña years (Pandey et al., 2017). Due to this coupling of CH_4 emissions with precipitation and water table depth, El Niño should also produce a response due to drought whereby CH_4 emissions would reduce.

Indonesian peatlands have been shown to be particularly vulnerable to C loss during El Niño events. Fires during the 1997-98 and 2015-16 El Niño events were estimated to have respectively released 0.86 and 0.23$\pm$0.07 Pg of previously stored C to the atmosphere, in fire seasons of 3−4 months duration (Page et al., 2002; Field et al., 2016; Huijnen et al., 2016). Ongoing peat oxidation further increases the total C lost (Miettinen et al., 2017) to the extent that annual C loss from these comparatively small land areas are of the same order of magnitude as global anthropogenic fossil fuel emissions in the same year (Huijnen et al., 2016). There have not yet been any studies of the effects of El Niño on C loss from channels draining peat swamp forest.

Studies of the effects of El Niño on fluvial systems are scarce, but El Niño has been found to impact stream discharge rates and DOC delivery to temperate and sub-tropical streams (Molles and Dahm, 1990; Hudson et al., 2003) and a tropical river in Brazil (Depetris and Kempe, 1990). Changes to discharge rates and DOC delivery should be expected to affect emissions of CO_2 and CH_4 from fluvial systems, as discharge rates suggest a change to water flow velocity and turbulence, and DOC provides one of the sources for CO_2 production For example, the study of the Paraná River in Brazil found that an El Niño caused a considerable increase in precipitation and a once-in-a-century flood. During the flood DOC

concentrations increased 100−200 %, and the DOC was more refractory than during the pre-El Niño period. Changes to dissolved CO_2 in the river coincided with increased DOC delivery and reduced discharge, however, emissions of CO_2 were not studied (Depetris and Kempe, 1990).

In Indonesia, El Niño would be expected to cause drought rather than flooding, therefore the C loss from channels would be expected to be different from the study of Depetris and Kempe (1990); carbon cycling may respond to lower water tables, rather than inundation. Measuring dissolved concentrations and channel emissions of CO_2 and CH_4 during an El Niño have the potential to better understand changes to C cycling in the surrounding peats due to drought (Worral et al., 2005).

1.6 Thesis aims

Tropical peat swamp forest is an ecosystem that is comparatively small in terms of land area, but has a significant role in terms of the global C cycle; it naturally contributes a major portion of total TOC to the oceans, acts as a terrestrial sink for atmospheric CO_2 and is a major source of atmospheric CH_4. Peat swamp forest is under threat from large-scale land-use change, which often involves deforestation and drainage. Deforestation and drainage (i.e. peatland degradation) has been shown to significantly perturb the way in which C is cycled in peat swamp forests, and in a way that has an impact on the global C cycle and global warming (Freeman et al., 2001; Betts et al., 2016; Huijnen et al., 2016).

Peat swamp forest C cycling is coupled to water table depth, which changes with the seasons. Further, anthropogenic degradation is known to interfere with the natural hydrology of peat swamp forest whereby land-use change can cause a significant drop in the peatland water table with respect to intact analogues. Few studies exist that have directly compared, simultaneously in wet and dry seasons, intact and degraded peat swamp forest in bottom-up, process-level investigations of C cycling.

The tropics are thought to produce nearly 80 % of the global riverine CO_2 flux to the atmosphere (Lauwerwald et al., 2015). Many global-scale studies exclude small streams and rivers due to a scarcity of data (Raymond et al., 2013; Wit et al., 2015) even though smaller fluvial systems tend to dominate aquatic surface in a catchment by area. Further, the smallest of the channels, i.e. headwaters, can dominate greenhouse gas emissions in a catchment by unit area (Richey et al., 2002; Mayorga et al., 2005; Billett et al., 2013). The large fluxes are hypothesised to result from the higher dissolved gas and DOC

concentrations that predominate in headwaters, with respect to the rest of the downstream riverine system.

To date, virtually all studies of greenhouse gas and DOC fluxes by lotic systems draining PSF have focussed on rivers and estuaries (e.g. Alkhatib et al., 2007; Baum et al., 2007; Rixen et al., 2008; Wit et al., 2013; Müller et al., 2015). Only two studies have investigated headwater channels: Moore et al. (2013) reported DOC fluxes from channels draining intact and degraded PSF in wet and dry seasons; and Jauhiainen and Silvennonen (2012) reported CO_2, CH_4 and N_2O fluxes from channels draining degraded PSF (also in wet and dry seasons). Moore et al. (2013) found that channels draining these PSF land use types were major loss pathways for POC and DOC, and the quantity and quality of DOC was significantly different between them, indicating there may be a difference in the quantities of greenhouse gases that may be emitted by the channels. But as Moore et al. did not investigate gas fluxes from PSF channels, the study by Jauhiainen and Silvennonen is the only study that reports greenhouse gas fluxes from channels draining PSF. However, the study of Jauhiainen and Silvennonen only investigated channels in catchments that had undergone major disturbance. This thesis therefore reports the first measurements of greenhouse gas fluxes in intact PSF, and is also the first study to explore the differences in channel greenhouse gas fluxes between intact and degraded PSF. This study will therefore contribute significantly to the existing literature on the effect of PSF disturbance on greenhouse gas emissions.

Raymond et al. (2013) estimated that rivers and streams emit 1.8 $Pg{\cdot}C{\cdot}yr^{-1}$, globally. This estimate was one of the highest in the literature, but it included upscaled estimates from the few data available for streams and rivers in southeast Asia, which contributed a significant proportion to the global total. However, Raymond et al. acknowledged that more studies in southeast Asia were needed in order to better constrain a global estimate, and further that studies of southeast Asian streams and rivers were a research priority.

More recent studies of greenhouse gas emissions from southeast Asian streams and rivers suggest that fluxes are much more moderate than those estimated by Raymond et al. (Wit et al., 2015), and therefore their global estimate is a significant overestimation. This thesis, therefore, also presents scarce data that can allow the freshwater greenhouse gas flux community make better estimates of gas fluxes in streams both in southeast Asia, providing data on headwaters that may dominate catchment fluxes. Given the supposed importance of southeast Asian riverine systems for total riverine greenhouse gas

emissions by Raymond et al., these data are critical for making more accurate estimates of global CO_2 and CH_4 emissions from freshwater ecosystems.

The primary aims of this thesis are to: a) report fluxes of CO_2 and CH_4 from channels draining intact PSF, which are not yet reported in the literature; b) compare fluxes of CO_2 and ceCH4 with degraded PSF, filling a gap in the knowledge pertaining to the change in C-cycling and greenhouse gas emissions that results from degradation of PSF; c) to present data that promote understanding of the drivers of those greenhouse gas fluxes, between wet and dry seasons and between land classes; and d) report on the effects of the 2015 El Niño event on channel greenhouse gas emissions. The latter aim was not originally planned as an investigation, but as the event occurred in the first year of sampling it was decided to create a study of it and compare it to a non-El Niño year (2016). These data are particularly novel as severe El Niño events are not frequent and are difficult to predict. No 'bottom-up' studies report the effects of an El Niño on greenhouse gas fluxes from channels draining PSF.

Specific hypotheses will be presented in each data chapter, except for Chapter 5 which investigates the El Niño event: as a severe El Niño is a rare event whereby so little data concerning its effects exists regarding bottom-up C-cycling and greenhouse gas fluxes, hypotheses were not formulated. Chapter 5 therefore represents a rare, on-the-ground observation of the El Niño event and its impacts on greenhouse gas emissions from the channels.

Chapter 2 (Materials and Methods) will present the main study sites, their locations, and characteristics. A rationale will be provided pertaining to the use of floating chambers as a measurement technique, this technique forming the basis of the study. Further, it will present the general methods employed for obtaining the diffusive fluxes of CO_2 and CH_4 from the channels, including all field, laboratory and data analyses that were common to each investigation in this thesis.

The first two data chapters (Chapters 3 and 4) directly compare, respectively, CO_2 and CH_4 emissions, from channels draining intact and degraded peat swamp forest. These gases are the most important anthropogenic greenhouse gases with CO_2 currently the most important in terms of global climate change, and CH_4, which is expected to overtake CO_2 in its importance later this century. Terrestrial emissions of CO_2 and CH_4 from peat swamp forest behave differently with respect to the water table; i.e. a low water table typically results in higher CO_2 emissions and lower CH_4 emissions, and vice versa. For this reason, the gases are dealt with in separate chapters which respectively establish the baseline differ-

ences in CO_2 and CH_4 emissions from the channels, in intact and degraded peat swamp forest. These chapters constitute the first studies of the emissions of the two most important greenhouse gases, from channels draining intact and degraded PSF.

The third data chapter (Chapter 5) will look at the effect that the 2015 El Niño had on emissions of CO_2 and CH_4 from channels draining intact and degraded peat swamp forest. This chapter therefore presents the effects of an extremely dry episode with respect to more climatically-normal years, and how peat swamp forest responds to such events in terms of the CO_2 and CH_4 emitted from channels.

Finally, Chapter 6 (Thesis Synthesis), synthesises and summarises the findings of the land-use change comparison (intact/degraded) and the investigation of the 2015 El Niño event; both are shown to have an impact on peat swamp forest hydrology and channel emissions of CO_2 and CH_4, and therefore offer further insights into how C cycling changes as a result of peatland degradation and drought. These findings will be put into the context of −and will be synthesised with− existing knowledge about the behaviour of the peatland C cycle, and the implications for the global C cycle. Chapter 6 also makes suggestions for further relevant investigations.

Chapter 2

Materials and Methods

2.1 Introduction

This chapter introduces the geography and climate of the region in which the investigations were carried out. It will cover the study sites and their locations, general character, recent disturbance histories, and the sampling locations. Spatial and temporal sampling strategies will also be presented.

This thesis involves determining water-atmosphere fluxes of CO_2 and CH_4, and the physical properties of the environment that might affect these fluxes. The general methods commonly used for each of the investigations in this thesis will be described, including equipment construction, measurement of fluxes, sample collection and analyses, and the calculations and statistical analyses used.

Materials and methods specific to certain chapters will be found in the Materials and Methods sections of their respective chapters.

2.2 Study region, field sites and sampling strategy

2.2.1 Study region

Site selection

The study required areas of intact and degraded tropical peat swamp forest to be in close proximity. The province of Central Kalimantan, located in Indonesian Borneo (see Fig. 2.1), has large expanses of both intact and degraded peat swamp forest adjacent to each other, separated by the Sabangau River (see Fig.

2.2). In Southeast Asia, tropical peatlands typically form as domes that have greater peat thickness in the middle and which slope gently down towards their edges (Page et al., 1999). Whilst peat swamp forest previously covered large areas of the coastal and sub-coastal lowlands of Central Kalimantan, many hundreds of thousands of hectares have been deforested and drained (degraded) in the province since the 1990s (Rais and Ichsan, 2008; Koh et al., 2011).

The most significant project that involved the degradation of peat swamp forest in the province was the designation of 1.1 Mha of peat swamp forest east of the Sabangau River to be turned over to rice agriculture. This ambitious project, the Mega Rice Project, led to deforestation and peatland drainage in the latter half of the 1990s. However, the project ultimately failed, as a result of poor planning and excessive drainage, and was halted at the end of the 1990s and the land abandoned (Boehm and Siegert, 2001). In this thesis, this deforested and drained area will be referred to as the 'degraded land class' where all the study sites representative of degraded peat swamp forest were located.

To the west of the Sabangau River is the Sabangau National Park, a 0.57 Mha expanse of peat swamp forest that is now classified as a protected area, having been subjected to a period of selective logging followed by illegal logging during the 1990s and early 2000s (Gaveau et al., 2013). As a result of designation of the Sabangau National Park and the work of the Borneo Nature Foundation in collaboration with CIMTROP (University of Palangkaraya), the Sabangau peat swamp forest has had strengthened protection since 2004, such that illegal incursions are now minimal. The Sabangau forest covers a large peat dome between the rivers Sabangau, to the east, and the Katigan, to the west. The peat is domed, with a maximum recorded depth approaching 13 m (Page et al., 1999). There is a series of forest sub-types from the edge to the centre of the peat dome and the peat surface consists of a continuum of hummocks and hollows. Water drains off the dome as run-off overland or through the upper part of the peat column (Page et al., 1999; Baird et al., 2017). For the purposes of this thesis, this area is regarded as the 'intact land class', in which the sites representing intact peat swamp forest were located.

Having degraded peat swamp forest in such close proximity to a near-natural analogue has led to numerous studies being conducted to investigate the effects of disturbance and degradation of peat swamp forest in this area, which include investigations into changes in carbon cycling and balance (e.g. Jauhiainen et al., 2008; Hirano et al., 2012; Moore et al., 2013).

Importantly, both the intact and degraded land classes have drainage channels. These channels

are not a natural feature of the peat swamp forest and were created for different reasons: the small, narrow channels at the intact site were dug by illegal loggers for extraction of timber to the river and did not significantly impact the water table of the forest. In contrast, to the east of the Sabangau river, in the former Mega Rice Project area, the channels were constructed to drain the land and control the water table (Moore, 2011). The project was abandoned prior to the implementation of effective water table management thus this area of peatland has uncontrolled drainage. Channels in both locations allowed for gas flux and water chemistry measurements to be compared between two contrasting land use types.

Figure 2.1: The island of Borneo is made up of the kingdom of Brunei and the Malaysian provinces of Sarawak and Sabah in the north (highlighted in pink), and the four Indonesian provinces of Kalimantan in the southern part of the island. The study sites were in Central Kalimantan (Kalimantan Tengah), two degrees south of the equator, indicated by the red star. The equator passes through Kalimantan and is indicated by the red line (Source: LandsatLook Viewer, 2013).

Catchment character

At the current time, there is 4.0 Mha of peat swamp forest in Borneo, mostly located in the low-lying coastal areas, and with a large proportion of this in the province of Central Kalimantan (Wulffraat et al., 2017). These coastal areas are very flat and have been conducive to the development of peat swamp forest since sea level dropped ~26k years ago (Page et al., 2004). Several rivers flow approximately north

to south in the region, discharging into the Java Sea. Investigations reported in this thesis took place at sites located between the Sabangau and Kahayan rivers.

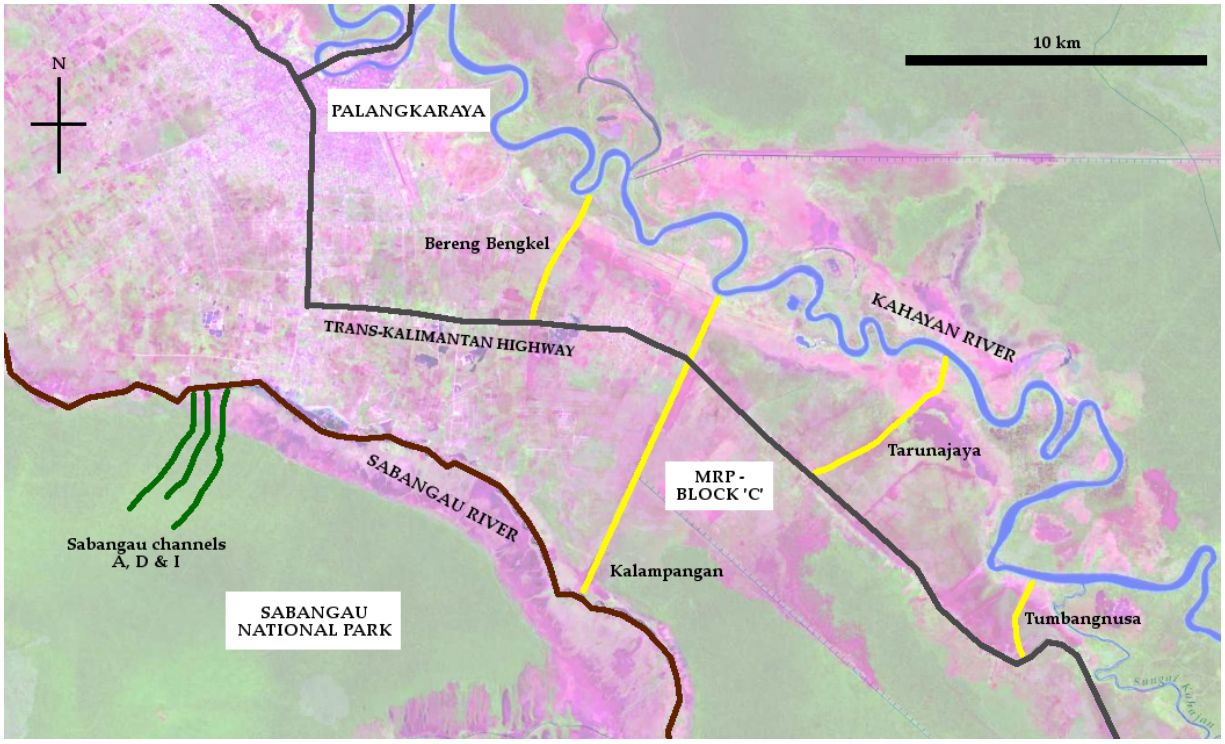

Figure 2.2: Map of the study region near the provincial city of Palangkaraya. The map is a Landsat false colour image where green shows intact, forested areas and violet indicates degraded regions. The intact area is mostly to the west of the Sabangau River, and the degraded area to the east. Intact and degraded channels used in the study are respectively coloured green and yellow. The intact sites flow from the Sabangau National Park and discharge into the blackwater Sabangau River. One degraded study site, Kalampangan, discharges into the Sabangau River. The other degraded sites disharge into the whitewater Kahayan River. The Trans-Kalimantan Highway approximately marks the Sabangau-Kahayan catchment boundary.

The Sabangau catchment is dominated by peat soils and is drained by the Sabangau River, a blackwater river with high concentrations of DOC (Moore et al., 2011). The Kahayan is the longest river in Central Kalimantan (˜600 km) and the catchment is comprised of both peat and mineral soils, in the lowland and upland areas, respectively. Clays transported in the river from the upland catchment area are sufficient to sorb most DOC exported from the lowland peatlands and, therefore, the Kahayan River has the character and chemistry of a typical muddy, tropical whitewater (Haraguchi et al., 2007). The blackwater Sabangau and whitewater Kahayan are therefore geochemically distinct; apart from the Sabangau River having a much higher concentration of DOC, it has a lower pH and less dissolved oxygen than the Kahayan (Haraguchi et al., 2007).

There is a very gradual rise in catchment elevation from the sea to the headwaters of the Sabangau; Kya, the source of the 176 km Sabangau River is just 12 m above sea level (Haraguchi et al., 2007; Page et al., 2009b). The 200 km downstream portion of the Kahayan runs through similarly low-lying land (Haraguchi et al., 2007). As the rise in elevation from the sea is very gradual (the Sabangau River rises on average only 1 m in 12.5 km), ocean tides can have a significant effect on the rivers: at low tides the rivers can drain freely into the sea, but at high tides can cause the water level to rise significantly along the river length with sea water infiltrating significant distances upstream, a phenomenon known as 'tidal reach'. The blackwater Sabangau, for instance, has very little naturally occurring chloride, but this ion has been detected 100 km upriver during tidal reach (Haraguchi et al., 2007).

As the study channels drain directly into the Sabangau and Kahayan Rivers, the channel waters can also be affected by tidal reach. Sea water does not reach as far as the study sites, but the rise in water depth causes river water to invade up the channels as was frequently encountered during sampling.

For the Sabangau River this makes no relevant difference as its blackwater geochemistry is no different to that of the channels. When the Kayahan's white waters are pushed up peat draining blackwater channels, the DOC can be sorbed by clay particles, and measurements revealed and increase in both pH and dissolved oxygen concentrations during this time. As the degraded channels all drained into the Kahayan River they could be affected by water chemistry changes due to tidal reach pushing non peat-derived waters up their lengths. The fluxes could have been impacted by a change in water chemistry, so to avoid potential complications in interpreting flux data from peat-draining channels, sampling and flux measurements were only conducted when the water was flowing from the peat channels to the river, and not the other way around.

Regional climate

Central Kalimantan is situated in the intertropical convergence zone, two degrees south of the equator. At this latitude there is comparatively little variation in day length or average daily temperatures throughout the year. It has a tropical monsoon climate which is hot and humid with daily temperatures averaging 26.7 ^{o}C throughout the year and relative humidity rarely dropping below 60% (Page et al., 2004; Evans et al., 2014).

The year consists of two seasons; a longer wet season that is typically 9 months-long between

October and May, and a shorter dry season of 3 months, typically between July and September. Mean average rainfall for the area is 2,700 mm·yr^{-1} (Page et al., 2004). Rainfall is highest at the peak of the wet season between November and January (˜350 mm per month) and lowest between July and September (75−100 mm per month; Hooijer et al., 2008; see Fig. 2.3).

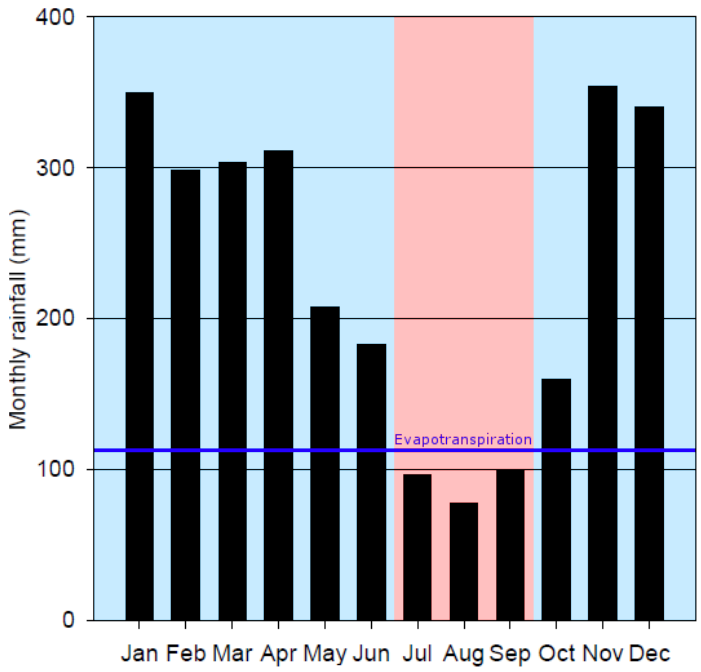

Figure 2.3: Monthly rainfall in Central Kalimantan averaged from data for 1984−2006 (figure adapted from Moore et al., 2011). The wet season months have a blue background. The dry season months, when evapotranspiration exceeds rainfall, have a red background. For half the year, precipitation is near or over 300 mm per month.

Water is constantly flowing down the gradient of the peat domes and out to the rivers that drain them (Baird et al., 2017). During the wet season, regular rainfall maintains high water levels in the peat, channels and rivers. In the peak months of the wet season, the water table is at or near the peat surface and the intact land class takes on an inundated, swamp-like character.

At the degraded land class during the wet season, the water table can be decimetres below the peat surface nearer the middle of the peat dome, but at the dome periphery, the peat adjacent to drainage rivers can become inundated as water rises above the peat surface to form an extensive floodplain. The investigations in this thesis were located in areas adjacent to rivers.

As the wet season transitions to the dry season, rainfall becomes less frequent. As tropical peat domes are reliant on rainfall for water input, and water is always moving out of the peat dome, dry season months are typified by water export exceeding water input and water levels drop; Hooijer et al.

(2008) defined the dry season as evapotranspiration exceeding precipitation. The amount the water table can drop in tropical peatlands depends largely on the depth of the channels draining them (Baird et al., 2017), therefore the water table drops less in intact peat swamp forest than degraded peat swamp forest, and the water table amplitude is also less in intact than degraded peat swamp forest (Takahashi et al., 2003; Hooijer et al., 2008).

The region is also subject to the effects of El Niño and La Niña which can both affect precipitation and water table depths, as described for Indonesia as a whole in Chapter 1.

2.2.2 Site descriptions

The intact land class channels

The Sabangau National Park (henceforth, Sabangau Forest) is enclosed by the Katingan and Sabangau Rivers to the west and east, respectively. It does have a history of moderate human disturbance and selective logging, but that has not compromised the natural hydrological functioning of the peat dome, and therefore it maintains a peat swamp forest vegetation and soil carbon store (Gaveau et al., 2013; Moore et al., 2013). As these functions are maintained the peat swamp forest is considered to be intact, rather than pristine or degraded.

Figure 2.4: The channels in the Sabangau Forest were originally dug to remove harvested timber from the forest. Their dimensions are uniform; rarely more than 2 m wide and 1 m deep, being sufficient to extract logs. The channels have not been used since logging ceased in 2003/04.

The loggers dug channels in the peat to float timber out of the forest when water levels were high enough, and are not a natural feature of peat swamp forest (see Fig. 2.4). The logging channels are fairly uniform in their dimensions; ˜1 m deep and typically not exceeding 2 m wide (see Fig. 2.7; Page et al., 2009b; Moore, 2011). The channels are irregularly sinuous (as they were dug to avoid large tree roots) and are dendritic in nature as they penetrate through the forest towards the centre of the peat dome. Water flows from the centre of the Sabangau Forest peat dome and eventually discharges into either the Katingan River to the west or the Sabangau River to the east.

The three channels used in this study all discharge into the Sabangau River (see Fig. 2.2 and Table 2.1) and were used by Moore et al. (2013) in an investigation into DOC export from peat swamp forest.

The lengths of these channels were reported in Moore (2011) and Moore et al. (2013) as being 10−12 km-long, however, these lengths are incorrect and updated lengths have been provided in Table 2.1.

Seasonal variability in rainfall affects water depth and discharge in the channels. 12 months of

Table 2.1: GPS coordinates of the intact canals at the point at which they exit the forest. LAHG Designation and Local Name correspond to the names of the channels used respectively by the field station and conservation teams and local people. Their lengths are measured from the forest edge, inward towards the centre of the peat dome (data provided by the Borneo Nature Foundation). The river into which they discharge, and the Site Code used for data analyses and discussion of the findings are provided.

LAHG Designation	Local Name	Latitude	Longitude	Length (m)	River	Site Code
A	Erman	2° 18′ 49.4″ S	113° 54′ 10.9″ E	1,640	Sabangau	SAB1
D	Udang	2° 18′ 44.8″ S	113° 54′ 0.6″ E	2,603	Sabangau	SAB2
I	Adun	2° 18′ 21.0″ S	113° 53′ 25.5″ E	2,941	Sabangau	SAB3

discharge data between June 2008-2009 showed that the forest catchment in this study discharged 0.9 $\times$ 10^6 $m^3 \cdot km^{-2} \cdot yr^{-1}$, most of this during the wet season. As this was considerably less than rainfall input into the catchment (2,744 mm during the measurement period) it indicated that water predominantly left the forest by evapotranspiration (Moore, 2011). However, if Moore (2011) significantly overestimated the lengths of the channels, the size of the catchment those channels drain may also be overestimated.

In the wet season the channels at the intact land class can overtop their banks and form a more continuous though hummocky swamp, although water flow is maintained. Flow is faster when the water table is rising or falling during transitions between wet and dry seasons, but is slower or virtually halted at the peaks of the seasons. In the dry season the upstream portions of the channels dry up typically to within ˜1 km of the forest edge (Moore, 2011). As such, sampling was focussed along the kilometre of channels adjacent to the forest edge so that wet and dry season data could be obtained and compared.

In extremely dry periods, such as during El Niño events, the channels can dry up completely (Moore, 2011), firstly forming chains of discontinuous pools due to the irregular nature of the channel bottom, but at the peak of the dry period no open water may be present.

The degraded land class channels

The degraded land class is located in part of the abandoned Mega Rice Project area. The Mega Rice Project area was designated into five blocks, ‘A’ through to ‘E’ where a total of 1.12 Mha of peat swamp

forest was deforested and 4,470 km of drainage channels dug in the peat to drain it. Insufficient hydrological planning for the project meant that the area was drained excessively rendering the soils unsuitable for rice cultivation, and the project was abandoned. The channels in this study were located in Block 'C' which is the largest of the blocks at 0.57 Mha (Rais and Ichsan, 2008).

Although the Mega Rice Project was abandoned, the channels were useful to local people (mostly the Dayak that consider themselves fisherpeople) as they provided access for their boats to reach the rivers that the channels drain into. Many of the channels in Block C have villages adjacent to them so that the inhabitants have easy access to fisheries. The channels are also used for sanitation.

The villages also utilise the abandoned land, for example, for cultivation of crops (such as oil palm), animal husbandry and construction of 'swift houses' to provide swift nests, which are considered a culinary delicacy in Asia. Often, the land needs to be cleared of forest debris or regrowth, and so the land has been regularly burned in the dry season.

The non-cultivated vegetation typically consists of pioneer species that tend to dominate following recent disturbance of peat swamp forest; mainly low-growing ferns, sedges and grasses. Maximum recorded peat depth in this area is 8 m (Page et al., 1999; Page et al., 2002).

In some areas, the drainage channels are comparatively large (see Fig. 2.7) and hence they have a more significant impact on the drainage of their catchments. These areas support limited regeneration of vegetation due to regular dry season fires and wet season floods. These areas do not typically have villages associated with them.

As in Moore (2011) and Moore et al. (2013), the degraded land class is considered to exhibit two different levels of degradation due to the degree of drainage: intermediately degraded peat catchments with smaller channels support some natural regrowth of vegetation and may also have some settlement with limited agricultural cultivation; and severely degraded peat catchments are generally devoid of vegetation and human settlements due to the extreme levels of water table fluctuation. The two studies carried out by Moore found that these two types of degraded peatland land covers behaved differently in terms of DOC loss and the quality and quantity of that DOC.

For the purposes of this study the two degraded land cover classes described above will be considered as one composite group. For discussion purposes, however, some data will be presented using the different degradation classes to illustrate some of the more extreme behaviour exhibited by the severely

degraded land class.

Figure 2.5: Tarunajaya, an intermediately disturbed peatland photographed very shortly after one of the first fires of the 2015 El Niño fire season. The canals here do not dramatically lower the water table and the area is used for grazing cattle in the dry season. The area is increasingly being planted up with oil palm (*Elaeis* sp.).

Three intermediately disturbed sites were visited; Tarunajaya and Tumbangnusa in the first two field seasons, and Tarunajaya and Bereng Bengkel in the last two field seasons. All are north and/or east of the Sabangau River and the Trans-Kalimantan highway. Each of these area comprise separate catchments, and each has one main channel draining into the Kahayan River (see Fig. 2.2 and Table 2.2).

The channels are utilised frequently by local people for boat transport (the access road to Tumbangnusa was entirely destroyed by fire in 2011), fishing, sanitation, and waste −including human sewage− disposal. The channels are significantly larger than at the intact land class being 3−6 m wide and 2−3 m deep (see Fig. 2.7) and therefore the water table is more significantly affected; it is below the surface during the dry season and above the surface for significant periods during the wet season.

Discharge at the intermediately degraded sites is double that of the intact catchment; 1.8×10^6 $m^3 \cdot km^{-2} \cdot yr^{-1}$ despite it receiving less rain input (2,356 mm during the 12-month study period; Moore, 2011).

The degraded site at Kalampangan is much more severely disturbed. Two peat domes are intersected and drained by a 12 km drainage channel and runs from the Sabangau River in the southwest and Kahayan Rivers to the northeast (see Fig. 2.2 and Table 2.2). This channel, the 'Kalampangan Canal', is between 10−25 m wide and 1−7 m deep (see Fig. 2.7). It lowers the water table and drains significant

quantities of water from the surrounding catchments. The water table can reach -1.4 m during the dry season (Hooijer et al., 2008) and discharge is triple that of the forest catchment; 2.7 $\times$ 10^6 $m^3 \cdot km^{-2} \cdot yr^{-1}$ though it receives lower precipitation than the intermediately degraded catchments (2,225 mm in the 12-month study period; Moore, 2011).

Figure 2.6: A view of the Kalampangan Canal looking north-east from the Sabangau River (out of shot). The canal drains two peat domes along its 12 km length, reaching the Kahayan River in the southeast. The canal does not directly discharge into either river but at its ends which terminate ~200 m from the river, there are parallel 'feeder' canals which receive the main canal's waters and channel them into the rivers. It was these feeder canals that were sampled in the investigation.

On the periphery of the catchment next to the Sabangau River (where the sampling took place) the area floods in the wet season (see Fig. 2.8) and in the dry season the water table drops considerably below the peat surface and the peat is prone to fires. These seasonal events make it very difficult for a vegetation cover to re-establish, year on year (Hosciło et al., 2011) and, as a result, a significant portion of catchment is comprised of bare peat. In the dry season the peat dries and oxidises, and, owing to fire impacts, resembles a loose ash which collapses several centimetres underfoot. This loose peat would likely have contributed to the large exports of POC observed by Moore et al. (2013).

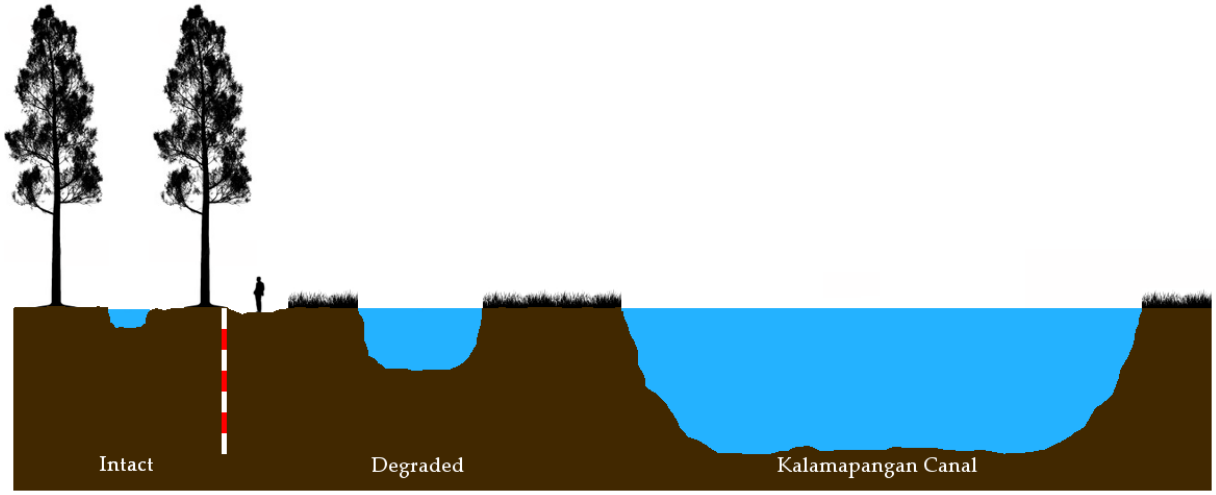

Figure 2.7: Cross-sectional areas of the channels draining the intact and degraded land classes taken from the maximum widths and depths reported in Moore (2011). A white and red scale bar is included where each box indicates 1 m depth. The channels at the intact land class were cut for selective logging in the Sabangau National Park, and measure between 1.5−2.0 m wide and ˜1 m deep. The channels are surrounded by forest. At the degraded land class, the channels used in the study were dug to drain water from the peat domes and were between 3−6 m wide and 2−3 m deep. However, at the severely degraded site, Kalampangan, the drainage is dominated by the large Kalampangan Canal which measures 15−25 m wide and 4−7 m deep.

Sampling at this site was mostly restricted to two feeder channels that run either side of the Kalampangan Canal terminus; the Kalampangan Canal does not discharge directly in to the Sabangau River, but instead stops ˜200 m short of it. The feeder channels are approximately the same size as the channels at the intermediately degraded sites and drain water from the main canal and deliver it to the Sabangau River (see Fig. 2.6).

Figure 2.8: During the wet season the canals in the degraded areas become part of a floodplain due a combination of high water levels and the lack of forest cover which limits transpirational losses.

Table 2.2: GPS coordinates of the degraded canals at the point they discharge into a river. The river into which they discharge and the site code used for data analyses are provided. The Kalampangan Canal also discharges into the Kahayan River, but this northern part of the canal was not sampled. Classification of the degree to which the catchments were disturbed is derived from Moore et al. (2013).

Channel	Latitude	Longitude	River	Site Code	Disturbance
Tarunajaya	2° 17′ 16.8″ S	114° 6′ 25.2″ E	Kahayan	TAR1	Intermediate
Tumbangnusa	2° 21′ 14.4″ S	114° 7′ 55.2″ E	Kahayan	TUN1	Intermediate
Bereng Bengkel	2° 14′ 27.6″ S	114° 0′ 3.6″ E	Kahayan	BER1	Intermediate
Kalampangan	2° 21′ 32.4″ S	113° 59′ 56.4″ E	Sabangau	KALA	Severe

2.2.3 Spatial and temporal sampling strategy

Spatial sampling strategy

Sampling was typically within 1 km of the channels' point of discharge to their respective rivers. This was partly due to the difficulty in negotiating the terrain, but also that during the dry season the upstream portions of the channels were expected to dry up. In order to make comparisons between the wet and dry seasons it was decided to sample those portions of the channels which would most likely contain water in the dry seasons when the water level was lowest. These locations were often near to the channels' points of discharge.

During the wet season, sections of the intact land class channels were located that were free of significant obstacles that might impede the passage of the chambers during high flows. Sometimes the channels would need some light clearance of bankside vegetation that hung over the channel. Further, sticks were driven into the bankside, just a few centimetres above −and parallel to− the water surface. These sticks were used to guide chambers away from isolated hollows at the channel bank where they might get stuck. The channel sections had to be long enough to allow the chambers to drift on the water for 5−10 minutes. Vegetation was not a problem at the degraded channels. But in the dry season the water levels could drop to the point where the channels contained isolated pools which were also sampled.

At the degraded land class, the channels were often accessed by boat in the wet season (when the water level was above the peat surface) and by foot during the dry season. Access to the channels in the

degraded land class became difficult during the dry season, which became a particular issue at TUN1 where the channel was the only means of access to the sampling sites. With insufficient water in the channel, particularly in the El Niño dry season of 2015, access to TUN1 became impracticable and therefore it was decided that a different degraded land class channel had to be found; this was BER1 and was used in the latter two fieldwork seasons. During the wet season, much greater access to the degraded channels was possible compared to the intact sites as the channels were larger and boats could be used, therefore the data gathered in the wet season could span a greater portion of each channel.

Temporal sampling strategy

Both land classes were visited in the wet and dry seasons, in both 2015 and 2016 (see Table 2.3). The first wet and dry seasons (field seasons 1 and 2) during 2015 culminated in a severe El Niño event, during which nearly all the channels had dried up by mid-September. Peat fires were severe and fieldwork was abandoned. The El Niño persisted until November. The wet season that followed saw significantly larger amounts of rainfall than normal and water levels were high, however, due to difficulties in obtaining a visa, it was not possible to return to the field to sample during this season. The dry season of 2016 was late and short, water levels dropped, but not to the levels of a normal dry season. As the area was generally wetter, very few fires occurred in comparison to normal years. Fieldwork recommenced in August 2016 and finished as the wet season was establishing in December. This time period comprises fieldwork seasons 3 and 4. The greatest effort was made to visit sites on a regular rotation, i.e. to visit

Table 2.3: The fieldwork seasons referred to in the thesis. Presented is the dominant season and the start and finish dates of the seasons. Fieldwork ceased early in season three due to the severe El Niño fires.

Fieldwork season	Local season	Fieldwork start	Fieldwork finish
1	Wet	6^{th} April 2015	15^{th} June 2015
2	Dry	23^{rd} July 2015	13^{th} September 2015
3	Dry	12^{th} August 2016	16^{th} October 2016
4	Wet	31^{st} October 2016	10^{th} December 2016

each of the six sampling locations over sets of six sampling days. However, in the first two sampling seasons, TAR1 and TUN1 were much harder to access than SAB1−3 and KALA. TAR1 and TUN1 required transport by motorbike, and a boat and boat driver available for hire at those sites. These sites could also not be visited when the waters of the Kahayan River were entering the channels. The transport, hire,

field support personnel and confirmation that the channels were freely draining all had to be obtained, and sometimes one or more of these requirements could not be met and another site was visited instead (such as those at the intact land class, or at KALA). In the second two sampling seasons this issue was mostly mitigated by hiring dedicated people and transportation to assist with my research. A complete list of site visits are to be found in Tables 2.5 to 2.8.

Visits were limited to the daytime, starting at ˜9 a.m. in the morning and finishing between 4 and 5 p.m. in the afternoon. As the sampling involved visiting different stretches of the channels along its length, the most downstream end was alternately the first or last on successive sampling days in order to avoid sampling bias due to time of day.

2.3 Methods

2.3.1 Measurement of channel CO_2 and CH_4 fluxes

There are three major pathways for gases to exchange between freshwaters and the atmosphere; these are via diffusion and/or turbulent transfer at the air−water interface at the water surface, ebullition, and via aquatic plants that emerge above the water surface (MacIntyre et al., 1995). This thesis is concerned with the diffusive/turbulent flux because it is this flux term that tends to dominate in flowing waters, particularly for CO_2 (Baulch et al., 2011; Crawford et al., 2014). Ebullition of CH_4 can make up a significant proportion of total CH_4 flux in lakes (Huttunen et al., 2003; Bastviken et al., 2011) and some streams (Baulch et al., 2011; Crawford et al., 2014), however it is a challenge to measure as its occurrence can be spatially and temporally stochastic (Crawford et al., 2014). Poor constraining of ebullition has led to frequent estimation errors of total CH_4 fluxes in the literature (Bastviken et al., 2004; Bastviken et al., 2011).

The diffusive flux (F) is given as:

$$F = k \cdot K_H \cdot \Delta P \tag{2.1}$$

with

$$\Delta P = P_{(\text{aq})} - P_{(\text{air})} \tag{2.2}$$

where, k is the gas exchange (or piston) velocity at a given temperature, K_H is Henry's constant that corrects for the solubility of a gas at a given temperature and salinity, and ΔP is the difference in the respective partial pressures of the air near the water surface, $P_{(air)}$, and that of the water, $P_{(aq)}$.

Henry's Law states that as the temperature and salinity of water increases, its solvency potential decreases (Benson and Krause, 1984). A poorly soluble gas such as CH_4 will be more affected by temperature and salinity than a more soluble gas like CO_2.

The gas exchange velocity, k, is a function of the kinetic energy at the water−air interface. It comprises the combination of water turbulence, the kinematic viscosity of the water and the molecular diffusion coefficient of a particular gas (MacIntyre et al., 1995).

The difference in the partial pressures between the water and air give the difference in concentrations and therefore the gradient across which a gas will seek equilibrium. The greater the difference, the faster the more concentrated reservoir will diffuse into the less concentrated reservoir.

F, k and ΔP are all measurable, and obtaining F can be done in indirect and direct ways. Indirect methods work by obtaining the values in Equation 2.1, namely the gas exchange velocity and the difference in partial pressures.

Indirect gas flux measurement methods

Indirect methods are favourable as they are non-invasive and do not interfere with the water surface (which can cause disturbance and might artificially alter the flux). Artificially affecting the flux is a concern with some direct measurement methods (e.g. Matthews et al., 2003). The drawbacks of indirect methods are that they do not directly measure the flux, and errors in the measurement of k or ΔP will give erroneous values for F.

There are several approaches to obtaining k including measuring turbulent flow, measuring wind speed (that might affect turbulence at the water surface), mass-balance models (Cole et al., 2010), and using inert (sometimes radioactive) tracer gases.

Calculating k from wind speed and fetch has been used in several studies of lake fluxes (Cole et al., 2010; Vachon et al., 2010), though they have yielded inconsistent results that do not transfer to other sites and may be more location/system-specific (Vachon and Prairie, 2013). In rivers (>100 m wide) wind fetch has a significant role as a physical driver of fluvial gas fluxes, however for smaller streams

water flow and its associated turbulence was found to be a greater driver of k than wind-shear effects (Alin et al., 2011).

An acoustic Doppler velocimeter (ADV) can be used to measure turbulence near the boundary layer allowing the calculation of k (Vachon et al., 2010). The ADV works by bouncing packets of sound waves off suspended particles in a remote volume of water, thereby not disturbing it. This has been effective in chamber gas flux studies in lakes, but the ADV needs to be attached to the chamber to measure k at the water-headspace interface (Vachon et al., 2010; Gålfalk et al., 2013). In flowing water the ADV would need its own float joined to the chamber which itself can cause turbulence and hence makes it unsuited to measuring k in flowing waters (Gålfalk et al., 2013).

Inert tracer gases such as propane ($CH_3CH_2CH_3$), sulphur hexafluoride (SF_6), radioactive helium (^3He) and radioactive radon (^{222}Rn) have been used to ascertain rates of diffusion from water to the atmosphere (Devol et al., 1987; Kremer et al., 2003; Billett and Harvey, 2013). The gases are pumped into an upstream portion of stream. Concentrations of the gas are then measured in a downstream portion of the stream. Losses of the gas are attributed to gas exchange at the water surface because the inert nature of the gases means that there is no potential for biological or chemical alteration, and hence only physical processes can account for a difference (Matthews et al., 2003). Once dilution of the gas in the stream is accounted for, the rate of diffusion gives k. Gas tracers can pose problems in larger flowing water systems and require days to obtain results (Billett and Harvey, 2013). Gas tracers may be unsuitable for studying channels in tropical peatlands as the channels can overbank during the wet season and may cease to form discrete channels upon which the tracer gas method largely depends; the larger surface area over which the tracer gases could diffuse and be emitted could cause difficulties in accounting for loss of the tracer gas with respect to the channel (Billett and Harvey, 2013).

k, however, can only be approximated as flowing, 'lotic' systems are highly diverse and dynamic environments where the physics of water−atmosphere gas exchange are very complex (MacIntyre et al., 1995). Directly measuring the flux is desirable provided it does not significantly interfere with the water surface.

Direct measurement methods

Direct measurements of the flux can be obtained using a closed environment, or 'headspace', or techniques using eddy covariance or gradient flux (Guérin et al., 2007). Eddy covariance works at a scale that is too large for small streams or channels as it is very difficult to determine the wind footprint (Matthews et al., 2003).

Floating chambers are a commonly used method of directly measuring flux because of their simplicity and affordability (Bastviken et al., 2015). The vast majority of gas flux studies using floating chambers have been in lakes, estuaries and the sea, but they are increasingly being used for flowing river and stream studies. In rivers and streams there are different drivers of water turbulence which include water depth, stream bed roughness and water velocity (MacIntyre et al., 1995). In lakes they are often anchored to the lake bed (e.g. Cole et al., 2010), but this is unsuitable in many streams; anchoring limits their ability to move freely and they can disturb the water surface when they resist the wind. Tethering chambers in flowing waters can significantly increase the flux due to the chamber resisting the flow (Guérin et al., 2007; Lorke et al., 2015).

Floating chambers create an enclosed environment over the water surface. This headspace can then be monitored for changes in gas concentration(s) over a period of time. Fluxes may be measured by a variety of methods which include: a) taking vial samples of the headspace at the start and end of the deployment which are then analysed using a gas chromatograph; b) using a portable gas analyser connected via tubing to chamber inlet and outlet ports to measure fluxes in real-time, and; c) installing compact gas sensor-loggers that can operate remotely (Bastviken et al., 2015; Lorke et al., 2015; see Table 2.4).

Vial samples are useful because they capture a volume of the headspace and can be stored for later analysis. The samples can be analysed in a lab which may have instruments that can measure the concentrations of several gases simultaneously. Vial samples, however, only give snapshots of the gas

Table 2.4: Methods of obtaining gas fluxes using floating chambers.

Sampling method	CO_2	CH_4	Anchored	Drift	Ebullition	Fine-scale
Vial samples	X	X	X	X	X	
Portable gas analyser	X	X	X		X	X
Sensor-logger	X		X	X		X

concentrations in the headspace and so it can be difficult to know if/when the flux rate changed and why; enhanced gas emissions into the headspace by e.g. increased turbulence or ebullition would be more difficult to detect using snapshot samples of the headspace (Bastviken et al., 2011).

A portable greenhouse gas analyser can be connected to the chamber to get real-time, fine-scale changes in headspace concentrations, however there is an inherent drawback in that the limited length of tubing requires that either the chamber is anchored, or that the analyser itself must be able to move with the chamber (especially in a flowing system). Anchoring chambers is not recommended for flowing water gas flux studies (Lorke et al., 2015), and constructing a raft to flow with the chamber without disturbing it, for several minutes, would be very difficult as portable analysers typically weigh several kilograms.

Use of battery-powered sensor-loggers is desirable as they are integral to the chamber and do not need external connections, therefore they can drift unimpeded with the water. Further, they allow a reasonably fine-scale measurement of the flux. Unfortunately, compact CH_4 sensor-loggers are not yet available.

Some studies have criticised the use of chambers because they have been shown to cause considerable overestimation of gas fluxes (Matthews et al., 2003). The chambers impose an artificial environment on the water surface and headspace and create "chamber effects" that affect gas exchange between the water and headspace. These chamber effects include chamber greenhouse heating (Belanger and Korzun, 1991) and non-natural levels of turbulence at the water surface. A chamber can disturb the water because of its mass and resistance to air and water flow. This can artificially increase fluxes inb the chamber if e.g. it is being buffeted by the wind, but it can also shelter the water surface from the wind and reduce fluxes (Matthews et al., 2003).

Chamber design, therefore, is an important factor in reducing the amount of disturbance that a chamber can cause to the water surface. Reflective tape should be used to prevent chamber greenhouse heating (Belanger and Korzun, 1991). To reduce disturbance to the water surface, the chamber 'skirt' should be appropriate (Cole et al., 2010). The chamber skirt is the depth of penetration of the chamber into the water. Using flexible skirt materials has also been shown to improve flux measurement accuracy (Lorke et al., 2015).

As the fluxes and partial pressures of dissolved gases were measured, this allowed for the calcu-

lation of k (as in Equation 2.17). As a data quality check for the fluxes, the k values in this study were compared with those of similar stream types in order to check that the gas exchange velocities were realistic and representative.

This study used floating chambers fitted with CO_2 sensor-loggers to measure the CO_2 flux in real-time. Gas samples of the air and water were used to determine the concentration gradient and thereafter determine k. With k known along with the concentration gradient, the diffusive flux of CH_4 could be calculated (as described in Sections 2.3.9−12).

2.3.2 Floating chamber design and operation

Sensor construction and operation

Standalone battery-powered, small and lightweight sensors with low power consumption and an internal data logger were required for the study. SenseAir ELG CO_2 sensor-loggers were selected for their cheapness and serviceability in a remote field situation, and they have also been used in studies using floating chambers for measurement of CO_2 (Gålfalk et al., 2013; Bastviken et al., 2015; Lorke et al., 2015). Further, their sensitivity (1 ppm resolution) and measurement range (0−10,000 ppm) was suitable for deployments lasting 5−15 minutes. They operate on the principle of non-dispersive infrared (NDIR) spectroscopy, where an infrared beam of a certain wavelength (0.763 μm for CO_2) gets passed through a gas sample, and the degree of attenuation of the beam infers the concentration of the absorbing gas.

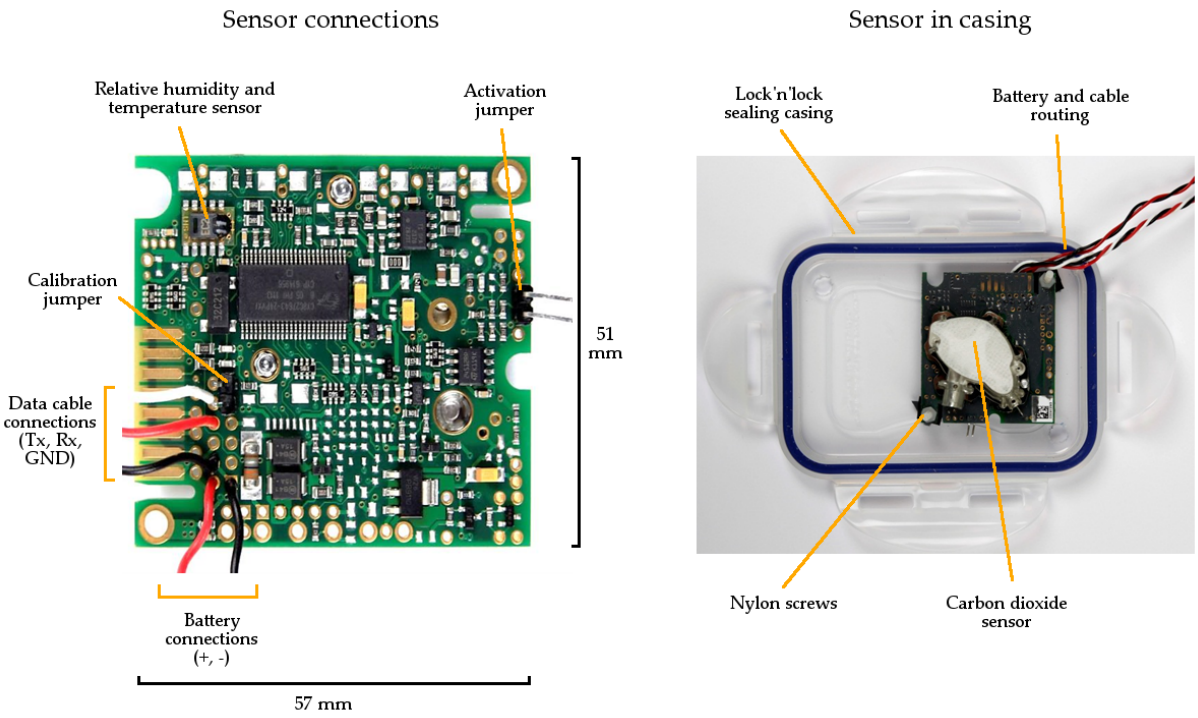

Figure 2.9: Both sides of SenseAir ELG CO_2 sensor-logger. On one side is the relative humidity and temperature sensor, two sets of jumper pins for calibration and sensor activation, and the battery and data cable connections. The battery has positive (+) and negative (-) terminals, and the data cable has transmit (Tx), receive (Rx) and ground (GND) connections. The jumper pins and cables all had to be soldered into place. The sensor was painted three times with an anti-tracking varnish covering all areas except the relative humidity and temperature sensor, the carbon dioxide sensor and the activation jumper pins. The casings for the battery and sensor in this study were circular, not rectangular. Original pictures from Bastviken et al. (2015) Supporting Information.

The sensors also measured relative humidity (0−100 %) and temperature (-40 to 60 ^{o}C). The sensors were prepared as in Bastviken et al. (2015): They arrived as OEM modules to which a battery lead and data cable (with DIN connector) were soldered. The sensors were also varnished with three coats of xylene anti-tracking varnish to protect the sensor electronics from water and chamber humidity (see Fig. 2.9).

A USB-DIN connector cable was also made so that the sensor could be connected to the computer. SenseAir UIP5 software was downloaded from the SenseAir website, after which it was immediately updated to the latest version. The sensors could be programmed (sampling frequency, measurement commencement delay, clock-setting, etc.) and monitored from this software. This software was also used to calibrate the sensors. To make sure the sensors were calibrated properly prior to use in the field, they were placed in a container and sparged with nitrogen gas for 3 hours. This duration was sufficient that all air had left the container and all the sensors could be set to 0 ppm CO_2. They were then left to measure ambient CO_2 overnight and the results checked the next day to ensure they were producing

suitably similar results.

Floating chamber construction and operation

The floating chambers used in this study were functionally identical to those described in Bastviken et al. (2015) but constructed slightly differently to reduce the possibility of chamber disturbance artificially affecting gas exchange.

The chambers in this study were constructed from inverted 7-litre plastic mixing bowls which were curved rather than having flat sides and a flat top. It was believed −but not tested− that the curvature might make them more aerodynamic and less prone to buffeting by wind which has been shown to be an issue for floating chambers in exposed lake flux studies (Matthews et al., 2003).

To accommodate sufficient chamber headspace volume, these curved chambers were taller and had a smaller surface area-to-volume ratio. As the chambers were taller and consequently had a higher centre of gravity, the centre of gravity was lowered again by mounting and stacking the internal components down centrally through the chamber. This central distribution of weight improved chamber stability. The smaller surface area (to volume ratio) was intended to allow the chamber to move more naturally on flowing waters (see Fig. 2.10).

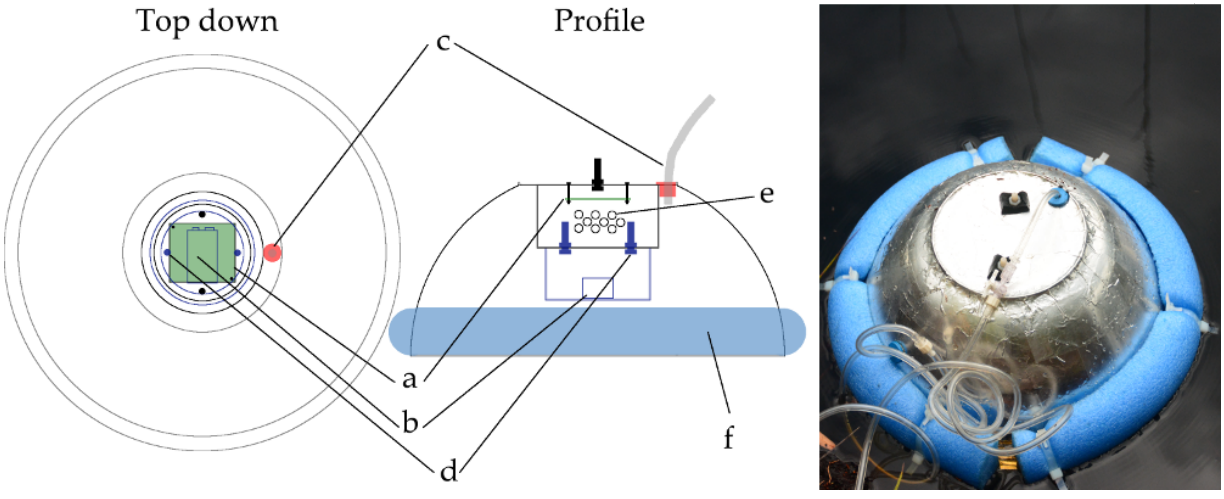

Figure 2.10: Top down and profile schematics, and image of the floating chamber design used in the investigation. The main features are labelled as: a) CO_2 sensor; b) 9-volt battery; c) sampling port composed of bung and pipe; d) nylon screws, e) holes drilled into sensor housing; and f) halved pool noodle (as floatation aid). The chambers were 7 L in volume, 150 mm tall and had internal and total diameters of 305 mm and 345 mm, respectively.

Each chamber was fitted with a battery-powered SenseAir ELG CO_2 sensor-logger mounted in the upper housing. The upper housing was drilled with numerous holes in order to allow gases to flow in and out and be measured by the chamber. A lower, sealed housing contained the battery and sensor data transmission cable to keep them dry at all times. The sampling port consisted of a stopped through which a hole was drilled and Tygon tubing passed. The tubing passed to a depth similar to that of where the sensor was mounted. At the end of the tubing was a stopcock. The stopcock acted as a valve to extract headspace samples. The stopcock was left open upon deployment on the water to prevent air pressure build-up. After deployment it was immediately sealed. Nylon screws were used throughout to minimise weight and because they were unreactive and would not affect the measured gas flux. The chambers were fitted with halved 60 mm-diameter styrofoam rods to act as floatation aids. These floatation aids were of different colours to aid visual identification in the field. All chambers were covered with reflective aluminium foil tape to prevent greenhouse heating of the headspace resulting from sunshine (Belanger and Korzun, 1991).

The total weight of a complete floating chamber was ˜460 g. When in the water the amount of chamber penetrating the surface was 20 mm making the effective volume of the chamber 5.9 L. The effective chamber volume was found by placing the chamber in water and marking the chamber at the water surface. The chamber was inverted, put on weighing scales and filled with water to the mark. The difference in weight (kg) was converted to litres, giving the effective volume of the chamber. The stack was left in place to account for the volume it consumed in the chamber. The clearance of the internal stack with the water surface was 30 mm. The chambers were designed so that the internal stack of components could be removed from the chamber by unscrewing the nuts and bolts attaching it to the chamber top. By removing the internal component stack the chambers then could be stacked which allowed for much easier and more compact carrying in the field. Though $5-10$ chambers would be used in a deployment, 12 chambers were built in total in case of damage or failure.

A couple of chambers had two extra holes drilled, respectively into the side (halfway up the chamber) and the top of the chamber. The holes were the same size as the sampling fort so that septa could be placed in them, allowing them to be used as additional sampling ports. The ports allowed these chambers to be connected to a Los Gatos ultra-portable greenhouse gas analyser (UGGA; Los Gatos Research Inc., USA) which allowed real-time measurement of CO_2 and CH_4. Measuring CO_2 with the UGGA was

useful for checking the data from the sensors (which were sampling simultaneously). The UGGA could be connected simply by connecting two lengths of Tygon tubing; one length from the top port of the chamber to the inlet on the UGGA, and one length from the side port to the exhaust port on the UGGA.

As the chamber deployments were expected to be fairly short, lasting up to 10 minutes, the sensor logging period was set to the finest time-scale which was 2 readings per minute (i.e. every 30 s). The logging was started by connecting a 'jumper' (a small connector that closes a circuit) to some pins on the sensor circuit board.

Data were transferred at the end of each day to a computer after which the sensor-logger memory was wiped. At this time, the battery was checked to ensure it had enough charge to last the next set of deployments (>7 volts), and the sensor-logger's on-board clock was synchronised with that of the computer.

Floating chamber deployment

Upon arriving at a site a test deployment was made to check whether the channel current was strong enough to carry the chambers downstream. Further, the channel section also needed to be long enough so that the chamber would take at least 5 minutes to travel its length. If this was the case an end point would be identified downstream where chambers would be collected from, to end the deployment. The end point was typically 50−100 m from the start point. During the test deployment, the chambers were watched and obstacles identified and removed that might obstruct the passage of the chambers. GPS coordinates of the start and end points of the drift section were recorded using a Garmin eTrex 20x.

Before starting each chamber deployment, environmental measurements were taken: air temperature and pressure were measured with a Comet C3121 thermometer-hygrometer; water temperature, pH and electrical conductivity were measured with a HANNA HI-98129 pH/EC/TDS hand-held probe; and dissolved oxygen was measured using a Cole-Parmer Traceable Dissolved Oxygen Pocket Tester. (In the third and fourth sampling seasons, a hand-held anemometer was available to measure wind speed.)

Immediately prior to chamber deployment, samples of gas were taken. All samples were taken with syringes and transferred to pre-evacuated 12 mL Exetainer vials, i.e. all gas samples were over-pressurised. Care was taken to make sure breath did not contaminate the gas samples. The gas samples collected were a 20 mL sample of atmospheric air, and a 20 mL gas sample taken from a 2 minute syringe

equilibration of 75 mL of channel water and 25 mL of atmospheric air. A further 20 mL gas sample of a chamber headspace was taken immediately before the chambers were deployed, which will be explained below.

Chambers were deployed in channels typically in a group of five, but 30 seconds apart giving time for the channel current (or the wind) to carry the chambers away from the deployment point. The chambers were colour-coded to allow easy identification which was important for knowing how long the chambers had been in the channel, and if the chambers had passed each other and changed order. Knowing the drift duration and the length of the section of the channel allowed the chamber velocity to be calculated.

Before placing the chamber in the channel, they were wafted gently for ˜25 seconds to purge the chamber and sensor housing of any contamination by breath. To prevent over-pressurisation of the headspace resulting from sudden placement of the chambers in the water, the chambers were gently lowered into the water with a slight tilt on one side before lowering the other side. In addition to this, the sampling port was left open to allow air to escape, before being closed immediately. Once the first chamber was in the channel a stopwatch was started. The remaining chambers were deployed in this manner at 30-second intervals with the last having a sample of the headspace taken.

As the last chamber was placed on the water surface, a syringe was connected to the sampling port of the chamber to take a sample of the headspace. The syringe was 'pumped' once to encourage air circulation in the chamber without disturbing it. 20 mL of headspace was extracted and transferred to an evacuated 12 mL Exetainer vial. The sampling port was closed, the syringe removed and the chamber set to drift.

Upon reaching the end point of the drift section the chambers were immediately removed from the channel and the drift duration recorded. The chamber that had a headspace sample taken at the start also had a headspace sample taken in the same manner at the end, before being lifted from the water.

Once all the deployments were completed, the channel depth and width were measured at five equidistant points along the drift section and the water velocity was measured. As channel depth and velocity were very variable over the seasons, several methods were employed for establishing water velocity. If the current was strong enough to carry the chambers, the water velocity was taken from the fastest chamber in each deployment. If the channel was deep enough (>25 cm) a Valeport 002 electro-

magnetic current meter (impeller) was used at the points where the depth and width were measured. If the water was too shallow, particles below the channel water meniscus were timed for how long it took them to move 2 m. This was repeated several times.

2.3.3 Sample storage

At the field site there was no refrigeration facility. All samples were stored in the dark in sealed boxes. The boxes were kept in the coolest place available; in the most shaded building in the camp, on the floor, where the temperature was ~20 ^{o}C. They were stored like this for a maximum of 2.5 months. They were then taken back to the UK after the field season had ended. The gas samples were immediately transferred into boxes and stored at ~18 ^{o}C prior to analysis. The water samples were transferred into boxes and stored in a fridge at 4 ^{o}C.

2.3.4 Water table measurement

Water table data for the intact land class was provided by the Borneo Nature Foundation. It comprises data from six dip wells, three of which are adjacent to SAB2, and another three adjacent to SAB3. At both SAB2 and SAB3 the dip wells are respectively located approximately 100, 300 and 500 m from the forest edge, and 20 m out from the channels themselves. The dip wells were constructed from a perforated plastic pipe that was driven into the peat down to the underlying rock. The wetted sections of dip sticks inserted into the dip wells were measured to ascertain the water level in the peat. They were sampled on a monthly basis from 2015−18 as part of continuing long-term water table monitoring of the forest. No dip well data were available for SAB1. No such means of measuring the water table were available at the degraded land class.

2.3.5 Quantitative DOC analysis

Further to the gas samples, water samples were collected to determine DOC quantity and quality at the points at which deployments were made. These were collected by taking 20 mL of channel water into a syringe and passing through a Whatman 0.45 μm GF/F glass fibre filter directly into a 12 mL vial.

The samples were immediately stored in the dark and, as a fridge was not available at the research station, they were placed in the coolest part of a building (at ambient temperature). As it was intended to

analyse the samples for DOC quality (such as aromaticity), but the necessary equipment to do the analysis was in the UK, the samples were not acidified as this can alter the properties of the DOC (Worrall et al., 2006; Cook et al., 2016; Peacock et al., 2016). The longest period the samples were stored at ambient temperature was 10 weeks. Immediately after a field season was over the samples were brought back to the Open University where they were analysed for DOC concentrations.

For analysis the samples were transferred to 40 mL vials for use with a Shimadzu ASI-V autosampler. The autosampler carousel was raised using inserts in order to raise the vials closer to the sampling needle to allow for the small volume of sample (12 mL). The samples were subsequently analysed by a Shimadzu TOC-V_{CPN} Total Organic Carboniser (fitted with a platinum catalyst) which used high-temperature catalytic oxidation at $> 680\,^{o}$C to determine DOC concentrations. The instrument was calibrated with hydrogen sodium napthalate standards as described in Moore et al. (2011).

Two 20 μL replicate injections were used by the analyser for each sample. Each injection was sparged for 90 seconds and washed twice. If the two concentrations differed by more than a standard deviation of 0.1 σ or 2% of the coefficient of variation a third replicate injection was used. 12 mL blank and 75 mg L^{-1} hydrogen sodium napthalate standards were inserted every ten samples through the run, as well at the start and end, in order to detect and correct for any drift in the instrument during analysis.

As the samples were not preserved by acidification some DOC losses were expected; Cook et al. (2016) found that the DOC concentration of untreated tropical water samples cold-stored at 4 ^{o}C reduced by $8-11$ % from their original concentrations after 12 weeks of storage. Further, the study found that DOC concentrations of samples stored at ambient room temperature (33 ^{o}C) reduced a further 6.1 % than those samples stored at 4 ^{o}C. Although DOC losses in these tropical samples were significant in these storage experiments, over 82 % of the DOC remained. The samples in this experiment were stored at lower ambient temperatures and analysed within a shorter time frame, and therefore it was expected that the samples would lose a similar but smaller amount of DOC yet still be suitable for qualitative analysis.

Aromaticity of DOC is commonly considered a proxy for recalcitrance and it has been found that the DOC in more aromatic water samples degrades more slowly, with the more labile DOC in the samples being degraded preferentially (Peacock et al., 2015). DOC from the degraded land class has been found to be more aromatic than the intact land class (Moore, 2011), therefore less degradation of the DOC

should have occurred in the samples from the degraded land class than the intact land class, whilst in storage over the same timeframe.

2.3.6 Qualitative DOC analysis

A Cole-Parmer UV/visible spectrophotometer (230 VAC, 50 Hz) and 3 mL quartz cuvette was used to analyse the aromatic content of the samples. The instrument was calibrated using potassium hydrogen phthalate (KHP). The calibration standards were made by putting 2.125 g of KHP in a 1 L volumetric flask which was dried at 120 °C for 1 hour. 1 L of deionised water was then added to make a 1000 mg L^{-1} stock solution. This solution was tested against manufacturer's KHP standards to ensure accuracy of the concentration. This solution was then diluted to 100, 75, 50, 25, 20, 15, 10 and 5 mg L^{-1} standards and was used to calibrate the instrument.

Specific ultraviolet absorption at 254 nm ($SUVA_{254}$) can be used as a proxy for determining aromaticity within in a DOC sample by using the equation described by Weishaar et al. (2003):

$$(6.52 \times SUVA_{254}) + 3.63 \tag{2.3}$$

with:

$$SUVA_{254} = A_{254}/C_{\mathrm{DOC}} \times 100 \tag{2.4}$$

where A_{254} is the absorbance at 254 nm and C_{DOC} is the DOC concentration.

As the DOC concentrations in the filtered channel water samples were high (typically over 50 mg·L^{-1} and could therefore could fully attenuate the spectrophotometer beam, the samples were diluted 1:1 with Milli-Q ultrapure water. The samples were gently shaken so that the diluted sample was homogenised. The instrument was set to measure absorbance at 254 nm, and before analysing each sample a blank of ultrapure water was used to ensure the instrument was reading zero absorbance so that it was clear the instrument had not drifted. C_{DOC} was multiplied by two to account for the dilution of the sample and then the aromaticity of the sample was calculated as described in the above equations. The cuvettes were thoroughly rinsed and dried between analysis of each sample.

2.3.7 Radiocarbon measurements and molecular sieve cartridge construction and deployment

Radiocarbon (^{14}C) dating is a widely used method for determining the age of organic materials (Evans et al., 2007; Moore et al., 2013) and carbon gases in channels (Billett et al., 2007, 2015; Garnett et al., 2012, 2013). ^{14}C is a naturally occurring isotope of cosmogenic origin that gradually increases in concentration in the atmosphere (see Fig. 2.11 left pane) with respect to ^{12}C. This dating method can be used for material that pre-dates atomic bomb testing (pre-1955), after which large amounts of ^{14}C were release to the atmosphere (see Fig. 2.11 right pane). As a plant photosynthesises, it captures CO_2, consisting of both $^{14}CO_2$ and $^{12}CO_2$. The ratio of ^{14}C to ^{12}C in the plant tissues reflects the atmospheric concentration at the time of CO_2 fixation.

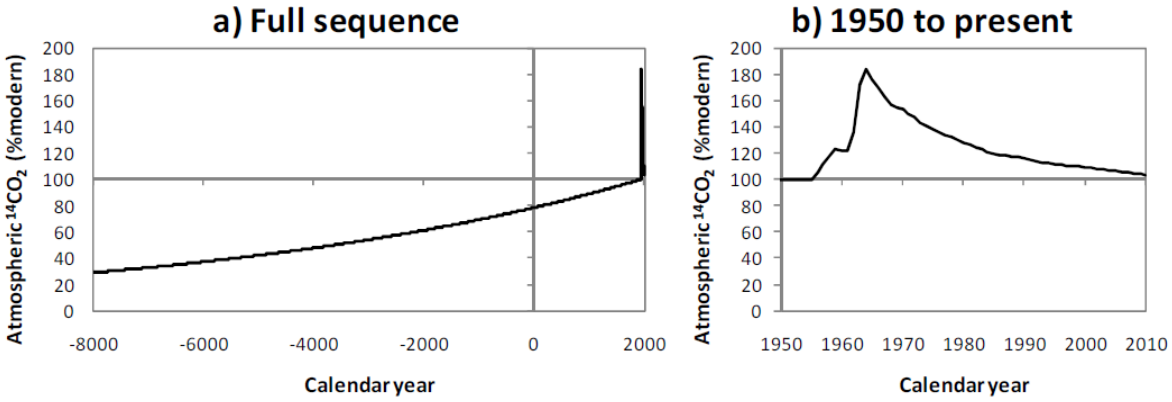

Figure 2.11: Historic (left) and modern (right) atmospheric ^{14}C concentrations. Figure sourced from Moore et al. (2013) supplementary materials.

Molecular sieve cartridges containing CO_2-adsorbing zeolite clays (see Fig. 2.12) were used to collect dissolved CO_2 from the channels for ^{14}C analysis, as this CO_2 would come from the breakdown of organic carbon from the surrounding catchment. The molecular sieves were therefore used to test whether there was a significant difference in the age of the organic carbon that was being degraded between the land use types. The molecular sieves were constructed as described in Garnett et al. (2012).

It was critical to deploy the cartridges for sufficient time that they adsorb adequate sample for radiocarbon analysis (more than 3 mL and ideally between 5 to 7 mL; Mark Garnett, personal communication). A period of one month was deemed sufficient following measurements of flow rates and dissolved CO_2 concentrations obtained during the pilot fieldwork season.

21 cartridges were deployed for one calendar month between the beginning of May and the be-

ginning of June 2015. 3 cartridges were located in each channel at points allowing the largest possible coverage of channel, i.e. at the upstream, midstream and downstream points of the stretches of channel where gas flux and other measurements were made.

Figure 2.12: A deconstructed molecular sieve cartridge with (from bottom to top) the outer black casing, blue packing foam, and glass pipe containing zeolite clays and a hydrophobic filter at the upstream end. The sieve is arranged in the photo as if water was flowing from the right.

It was important to ensure that the cartridges were not exposed to the air as the clays would rapidly adsorb atmospheric CO_2 which would have a highly modern signature and therefore contaminate the samples. It was therefore important to ensure that they were always deployed in locations that would contain sufficient water to keep them covered for the duration of the deployment. They had to be deployed in areas that met several criteria:

- They were deployed in locations in the channel where there would be sufficient water present during the dry season that they could be deployed in the same place.
- The water would exceed 20 cm depth at the time they would be recovered in the dry season.
- At the intermediately degraded sites, they were sufficiently upstream that water invasion from the Kahayan would not reach the cartridges.
- They were located in places in which local people would not easily discover and unwittingly interfere with them.

To deploy the molecular sieve cartridges, ~1 kg rocks were attached to the cartridge casings at the sleeves to act both as an anchor and, once on the channel bottom, would elevate the sampling end and effect

a pitch of ~10°, facing upstream. This was intended to reduce the possibility of the sampling end being clogged by sediment that might have otherwise collected around the cartridge. Once a sieve was submerged under the water a clip was released from the tube connecting the hydrophobic filter to the pipe containing the zeolite clays. This was done underwater so that the clays were not contaminated with CO_2 from the atmosphere. As some of the channels were deep, the cartridges were lowered using twine threaded through the head and tail ends of the probe so as to guide the orientation of the sampling end upstream. Sticks were also used to act as extra anchors to prevent the sieve cartridges being lost during potential high flows in the channels. The time, date, sieve cartridge ID, location description, location photo and GPS coordinates were recorded at this time.

The wet season deployments were successful. Due to very low channel water levels and fires during the 2015 dry season, molecular sieves could not be deployed as was intended and therefore no comparison was possible for the measurements made during the wet season.

When retrieving the molecular sieves, they were carefully raised to just below the water surface so that the clip could be replaced onto the tube, preventing contamination by air. They were then stored in the dark in the coolest part of the field station until the fieldwork season had finished. They were then shipped back to the UK and then sent to the NERC Radiocarbon Facility in East Kilbride for analysis.

CO_2 trapped by the zeolite clays was liberated by heating whilst purging with nitrogen gas, and then converted to graphite by Fe/Zn reduction. The graphite pellets were then analysed by Accelerator Mass Spectrometry (AMS) to establish the ^{14}C content relative to ^{12}C. The ages of the samples were provided as conventional radiocarbon years before present (BP) where present refers to AD 1950.

2.3.8 Flux calculation: Sample and data analysis

Several stages were required to obtain fluxes for CO_2 and CH_4 which have been summarised in the workflow diagram in Fig. 2.13, and have been described in the following sections.

Once all the CO_2 flux data had been obtained using the floating chambers, the data needed to be compiled and the linear fluxes identified. The start and end points of the fluxes were entered into a spreadsheet and then those concentrations adjusted due to drift in the SenseAir CO_2 sensor-loggers in the field. The adjusted linear fluxes were then subject to a test of linearity.

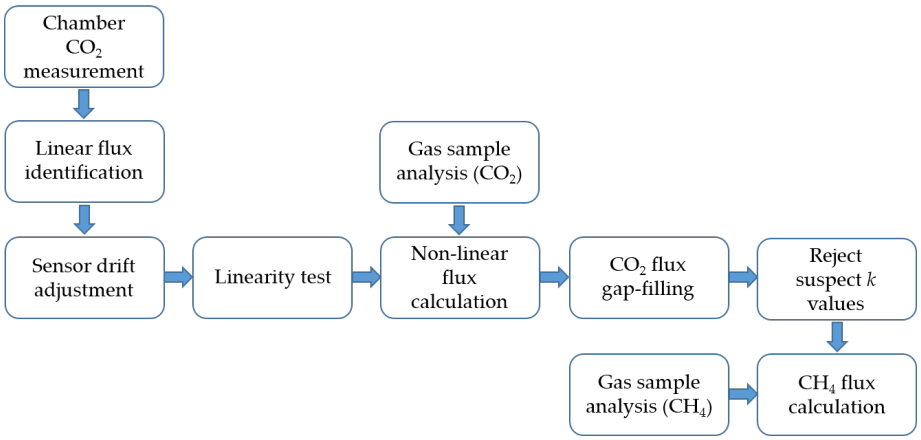

Figure 2.13: A diagram of the workflow demonstrating the steps required to obtain fluxes for CO_2 and CH_4.

Gas samples were analysed for CO_2 concentrations to calculate more accurate non-linear fluxes, although due to time restrictions not all of the gas samples could be analysed. A strong relationship was found between the data that had both linear and non-linear fluxes and, therefore, that relationship was used to estimate non-linear fluxes from those data with only linear fluxes.

Some fluxes in the dataset had gas exchange velocity (or k) values that were suspected of being erroneous due to a few gas measurement problems (which k was derived from). As the non-linear fluxes were dependent on k, these fluxes were likely flawed and were omitted from the dataset. For the remaining CO_2 fluxes, corresponding CH_4 fluxes could be calculated once the gas samples had been analysed for CH_4 content.

2.3.9 Linear flux identification

I wrote a computer script to extract the data from the CO_2 sensor logs into the `R` statistical programming environment. For every sensor, the days' CO_2 measurements were plotted and the start and end points of the linear flux identified. The linear flux typically occurred following a 'settling period' after the chamber was deployed in the channel (see Fig. 2.14).

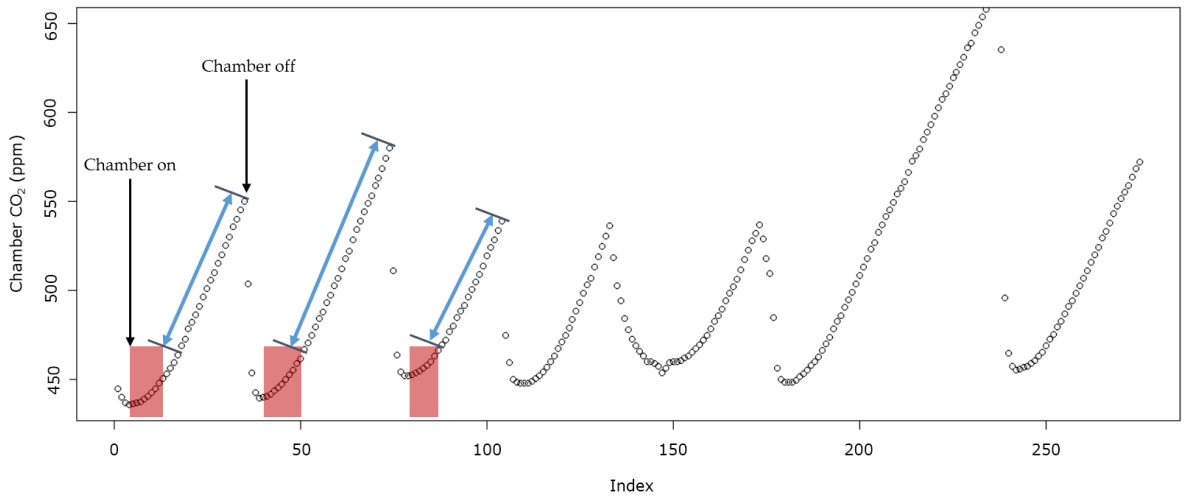

Figure 2.14: Example of sensor data demonstrating the chamber settling period (red boxes) and the data that would be used for a linear flux (blue lines). Linear fluxes were tested for linearity (R^2 >0.95). Data points are at 30-second intervals (an Index of 1 = 30 s).

The start and end points of the linear flux were entered into a spreadsheet.

2.3.10 Sensor drift adjustment: correcting for sensor auto-calibration

The problem posed by sensor auto-calibration

The SenseAir CO_2 sensor-loggers were built for indoor use and have an in-built auto-calibration feature (SenseAir, 2018). The auto-calibration works by using SenseAir's 'automatic baseline correction' (ABC) algorithm that records the lowest CO_2 concentration within a pre-configured time interval. The algorithm gradually corrects for measurement 'drift' by assuming that the value is 400 ppm CO_2 (which might be expected in an indoor environment) and adjusting the zero point.

The ABC feature was not explicitly mentioned in the product documentation, nor in Bastviken et al. (2015) which outlined the use of the SenseAir sensors for measuring CO_2 in the field, and as such, this feature was unexpected. It was only much later in the sampling campaign that sensor drift was recognised to be a problem (i.e. calculated fluxes were becoming higher), and that the problem stemmed from the ABC feature; the sensors were being used intensively in a high CO_2 environment (i.e. the chamber headspace), whereby it was less likely that the sensors would encounter 400 ppm within its pre-configured time interval. Hence, the sensor's zero point was, periodically, being adjusted to headspace

CO_2 concentrations significantly higher than 400 ppm. This had the effect of causing the sensor's measurement of e.g. 400 ppm to be e.g. 500 ppm, i.e., near-ambient would be measured as being higher, and with continued use of the sensors ABC would cause the measured value to increase with respect to the actual concentration (see Fig. 2.15). Further, the range of the sensor measurements generally increased over time, presumably as a result of their increasing and differential drift due to ABC. This indicates that imprecision was increasing and 'agreement' between sensors was decreasing. The drop in between-sensor precision is evidenced by the larger ranges in measured CO_2 minima across the sampling period which should be very similar (as in the first sampling season; see right pane of Fig. 2.16).

If CO_2 concentrations were measured as higher than they actually were, this would likely cause the fluxes (that are the basis of this thesis) also to be higher than they were. Further, as the drift of the sensor-loggers became more significant over time, the data collected in later seasons would be more affected and accurate comparisons could not be drawn.

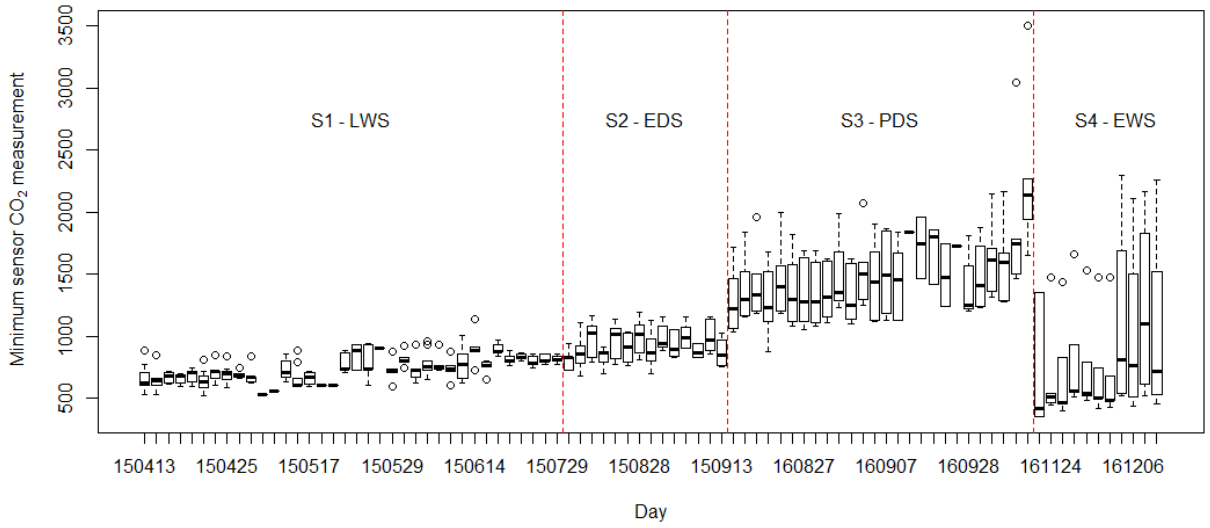

Figure 2.15: Box plot showing the minimum CO_2 concentrations measured by the sensors on each day of sampling. Typically, five sensors were used per day. The data demonstrate that the minimum concentration increased through the sampling seasons as a result of the sensors' in-built 'automatic baseline correction' (ABC) algorithm, with the exception of EWS (season 4) when the sensors were re-calibrated. The precision of the minimum readings also reduced as sampling progressed.

As chambers were wafted in the air before use to ensure the headspace and sensor were as close to ambient CO_2 concentration as possible before each deployment (i.e. ~400 ppm), the minimum value measured by a sensor on each day was assumed to be approximately ambient, and therefore the drift due to ABC was estimated, and the measured values adjusted as described in the following section.

Adjusting the data to correct for sensor auto-calibration

Five sensors were calibrated to ambient CO_2 (405 ppm); sensor 1 was calibrated correctly whereas the four others (sensors 4, 9, 8 and 6, respectively) were calibrated to measure ambient CO_2 as 700, 1,000, 2,400 and 2,700 ppm, respectively, to mimic the drift that occurred in the field due to auto-calibration (see Fig. 2.15).

To determine how different sensor calibrations might affect measurement, the sensors were put in the same busy office in mid-afternoon and left out through the night. This was so that they simultaneously measured a large concentration range of CO_2 that would be high when the office was occupied, and would gradually drop to ambient levels (˜400 ppm) once the office was empty (see left pane of Fig. 2.16).

Box plots of the office CO_2 data revealed that as calibration increased the range of values increased (see centre pane of Fig. 2.16). Further, the parts per million differences between the five number summary statistics of the box plots (maximum, third quartile, median, first quartile and minimum) were larger at higher calibrations (third quartile−maximum of sensor 1 $<$ third quartile−maximum of e.g. sensor 4). Furthermore, whilst the box and whiskers demarking the five number summary statistics for each sensor were proportionally in the same positions, there was a non-regular 'stretching effect'; each successive 'part per million' in the scale was larger than the one preceding it, and this effect became larger as the respective calibration of the sensors increased.

The five number summary statistics for each sensor were plotted against their sensor's respective calibration (see right pane of Fig. 2.16). To adjust for the incorrect calibration and its effect of non-regularly expanding the measurement scale, linear models were plotted for each of the summary statistics (all $R^2 \geq$0.998) and the common point of convergence of the models identified by taking the median of the intersection coordinates of every possible model combination ($n = 10$).

For the correctly calibrated sensor (calibrated to 405 ppm when CO_2 concentration was 405 ppm) the scale would consist of regular one part per million units. As a common point of convergence was found between the models of the summary statistics, the rate of the expansion of the CO_2 measurement scale of incorrectly calibrated sensors in relation to the correctly calibrated sensor, incorrect measurements could be adjusted so they were closer to being correct.

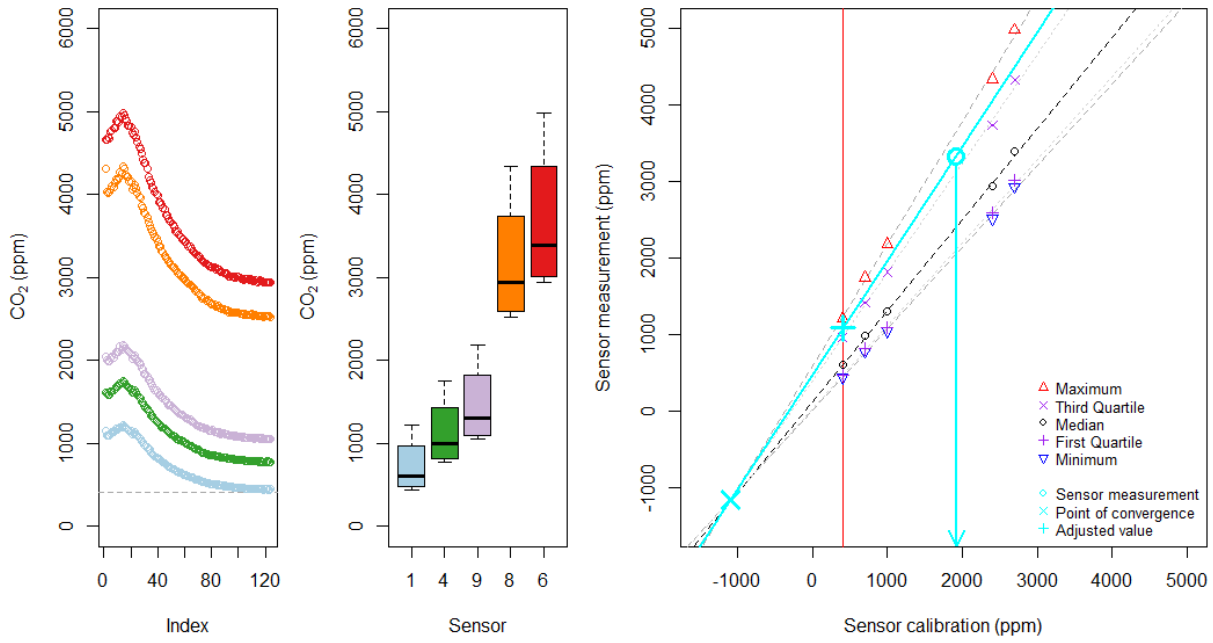

Figure 2.16: Assessment and adjustment of data from incorrectly calibrated SenseAir CO_2 sensor-loggers. In the left and centre panes, blue represents the correctly calibrated sensor and green, purple, orange and red represent the sensors calibrated to 700, 1000, 2400 and 2700 ppm. Left pane: CO_2 concentration measured by sensors that were calibrated differently (against ambient concentration) in a busy office that emptied in the evening. Centre pane: Box plots of the data in the left pane demonstrate that as calibration increased, the range of measured values increased, and within that range, the measurement scale expanded non-regularly. Right pane: each vertical group of data points respectively represents the box plot summary statistics for each sensor. Linear models for the summary statistics (dashed lines; all $R^2 \geq 0.998$) converged together at the same point. The cyan points and lines are used to demonstrate how adjustments were made to the measured values and improve the flux dataset (see Section text for explanation). The vertical red line represents the point on the x-axis of a properly calibrated sensor where the measurement scale on the y-axis is completely uniform (1 ppm increments).

To adjust incorrect values measured by sensors that had had their calibration drift due to ABC, two pieces of information were needed; a) the CO_2 measurement, and b) the 'calibration' at which that measurement was made. The 'calibration' of a sensor was set as the minimum CO_2 measured by that sensor on each particular day, which inherently assumes that the lowest value was actually near-ambient (˜405 ppm). Although this may not have been absolutely accurate, natural variation in atmospheric CO_2 was not expected to fluctuate greatly.

For each sensor, the starting CO_2 concentration for each flux was plotted against the 'calibration' and a linear model constructed from this point, to the point of convergence of the summary statistic models. The adjusted CO_2 concentration was taken to be the CO_2 value when the 'calibration', or x

value, of the model was 405 ppm (see the intersection point of the red and cyan lines in the right pane of Fig. 2.16). This process was repeated for each end point of each flux. Each flux was then recalculated by using the adjusted start and end CO_2 concentration values.

It was possible to test whether the adjusted sensor-logger CO_2 measurements were accurate: Fortunately, a correctly calibrated Los Gatos UGGA was used in the field on a few separate occasions to measure real-time fluxes of CO_2 and CH_4 simultaneously with sensor-loggers that had drifted (by differing amounts) due to ABC.

As the UGGA could confirm that the adjustments made to the data made the concentrations and subsequent fluxes more accurate, the adjustment was applied to the entire dataset.

Testing the correction for sensor auto-calibration

The Los Gatos UGGA was used in conjunction with the chamber sensors during the post-El Niño dry season (PDS) in September 2016 (see Fig. 2.17). These data were valuable for demonstrating that the autocalibration problem associated with the CO_2 sensors could be solved by the process described earlier in the chapter (see 'Adjusting the data to correct for sensor auto-calibration').

Over seven sampling days, 37 UGGA-chamber deployments were made. The average minimum ambient CO_2 measured by the UGGA over those seven sampling days was 405.1 ppm. The sensors, if correctly calibrated, would have also measured ˜405 ppm CO_2 in ambient air. However, CO_2 minima from the sensors over these days were between 1,724 and 1,961 ppm indicating clearly that the calibration of the sensors had drifted considerably.

For each of the 37 fluxes measured simultaneously in the UGGA-chamber configuration, the maximum values of each respective UGGA and sensor flux were obtained. The sensor measurements were corrected by creating a linear model that passed through the point of convergence of the calibration test (see right pane of Fig. 2.16), to coordinates where x was the minimum value of the sensor that day (the assumed calibration), and where y was the value measured by the sensor for that flux. The corrected value was taken as the y value along the linear model where x was 405 ppm CO_2 (i.e. what would have been a correctly calibrated sensor). The corrected data are presented in Fig. 2.17, left pane) where it is clear that the maximum drifted values (red) were much higher than the corrected data (black) which cluster around the 1:1 line (where UGGA ppm CO_2 = sensor ppm CO_2). The correction was not perfect

(R^2 = 0.56) but it effectively scaled the measured CO_2 values to being similar to those recorded by the UGGA. One of the reasons for this imprecision would have been that the minimum recorded values from the sensors may not have been the actual amount of drift in the sensor, but it was the only available data upon which a correction factor could be produced.

Three sets of CO_2 fluxes were then calculated for each of the 37 UGGA-chamber deployments; one set based on measurements by the UGGA, one set from the corrected data, and another for the original data (see Fig. 2.17, right pane). As the 37 UGGA-chamber deployments all took place over differing deployment times, a hypothetical (approximately average) deployment time of six minutes was used to calculate their values. The absolute values of the fluxes are not important in this instance; the data present the effectiveness of the improved accuracy and scaling that the correction method achieves.

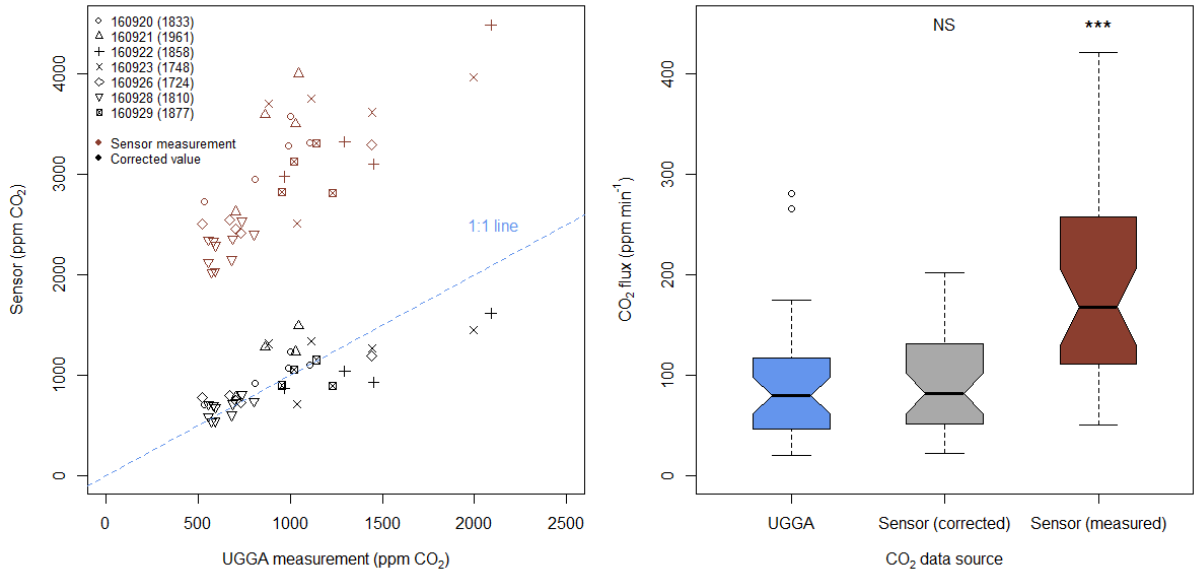

Figure 2.17: A scatter plot of CO_2 measurements by the sensors, as compared to the UGGA (left pane). In the key (top left), the sampling days (given in the date form YYMMDD) show the minimum value of CO_2 measured by the sensor that day (in brackets). This value was used to estimate sensor drift. The original sensor data (red) are much higher than CO_2 measurements by the UGGA. When the correction was applied to the sensor measurements, they became much more similar to those measured by the UGGA (equivalence in highlighted by the blue 1:1 line). CO_2 fluxes (n = 37) were then calculated for the UGGA, corrected sensor and measured sensor data (right pane) over a hypothetical 6-minute deployment period. The corrected fluxes were not significantly different to the fluxes of the UGGA (p = 0.998), indicating that the correction method was effective. However, the orignal measured fluxes were significantly higher ($p = 2.84 \times 10^{-6}$), being nearly double those of the UGGA.

A Welch two sample t-test found that the corrected sensor data were not significantly different to the fluxes measured by the UGGA, and were in fact very similar (t = -0.002, df = 67.3, $p = 0.998$, means = 90.91 and 90.94 ppm·min^{-1} for the UGGA and corrected data, respectively). Conversely it was found

that the original sensor data produced fluxes significantly higher than the UGGA (Welch two sample t-test; t = 5.15, df = 62.1, $p = 2.84 \times 10^{-6}$), where the mean CO_2 flux calculated from the original data was nearly twice that of the UGGA (188.1 ppm·min^{-1}).

Being that the sensor drift was so great in these data, with the drift amounts being amongst the greatest in the entire dataset (see Fig. 2.15), the correction method appears to have been highly effective in resolving the sensor calibration issue.

2.3.11 Testing for linearity

An `R` script accessed the spreadsheet data with the start and end points of the fluxes, and reconstructed the fluxes from the sensor data. Each individual flux was tested for linearity, and all with R^2 <0.95 were rejected from the dataset. Rejections due to R^2 <0.95 were made as a diffusive flux would be expected to be very close to linear on a timescale of minutes. Non-linear fluxes might suggest deployment or chamber issues, such as the sampling ports being open (the headspace was not a closed environment) or the chamber becoming stuck causing significant disturbance to the water surface.

2.3.12 Gas sample analysis

Using an Ultra-portable Greenhouse Gas Analyser in a closed loop configuration

Prior to calculating CO_2 and CH_4 fluxes, it was necessary to analyse the atmospheric and dissolved gas samples. This was done using the UGGA in a closed loop configuration (see Fig. 2.18) based on that described by Baird et al. (2010).

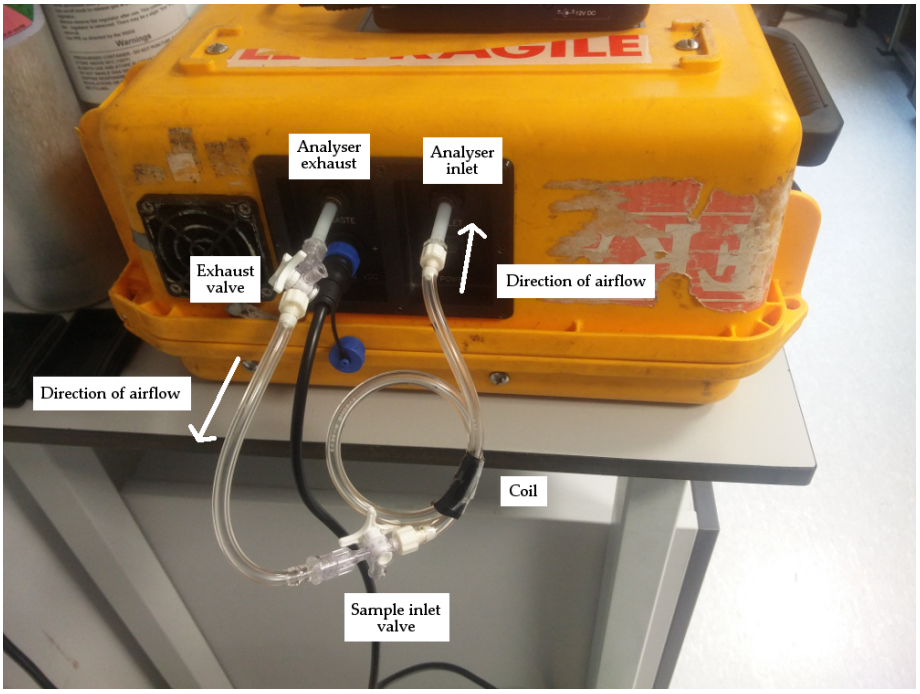

Figure 2.18: Annotated image of closed loop used in conjunction with a Los Gatos Ultraportable Greenhouse Gas Analyser. Tygon tubing loops from the exhaust to the inlet ports of the analyser create a closed circuit and static mix of gas concentrations. A sample is injected into the loop via the sample inlet port. After a settling period the change in concentration of the gases is recorded. The exhaust valve is then opened to return the loop to ambient concentrations of gases.

The UGGA is capable of measuring concentrations of CO_2, CH_4 and water vapour (H_2O) simultaneously in real time, with the shortest sampling frequency being 1 s^{-1}. The UGGA uses Off-axis Integrated Cavity Output Spectroscopy for detecting the gases using two diode lasers of different wavelengths. One laser (1.5 μm) is used to detect CO_2 and another laser (1.65 μm), CH_4 and H_2O. The lasers are oriented marginally off-axis with respect to a mirror-lined cavity that the beams and gas enter. The cavity uses curved, reflective mirrors that reflect the off-axis laser beams thousands of times internally, effectively making the laser path several kilometres in length (Baer et al., 2002; see Fig. 2.19).

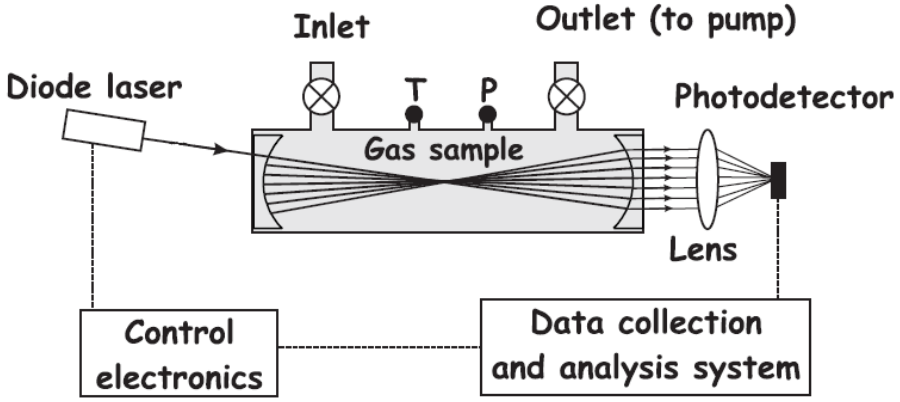

Figure 2.19: A schematic of the Off-axis Integrated Cavity Output Spectroscopy system used by the UGGA. Samples are injected into a mirror-lined cavity. The mirrors are curved at the ends to bounce the beams of off-axis lasers for numerous kilometres within the cavity, allowing for enhanced detection of target gases. The closed loop connects the inlet and outlet ports, creating a closed system. Edited from schematic found in Baer et al. (2002).

The closed loop was composed of Tygon tubing with two valves inserted, one for exhaust gases, the other as a sample inlet. In theory, when the valves are closed it creates a closed system where no gases enter or leave and hence the concentrations of gases being measured by the analyser are essentially unchanging. These concentrations provide a background level by which to measure change in concentrations when a sample is injected into the system.

The measurement procedure started with closing the loop and recording the gas concentrations, along with ambient temperature and pressure. A syringe containing 4 mL of sample was connected to the loop, the valve opened, sample injected, and the inlet valve closed again. A few seconds were allowed for the injected gases to mix with the background gases so that a reasonably uniform (± 3 ppm) concentration filled the loop. Once the gases were well-mixed readings were taken of the new CO_2 and CH_4 concentrations in the loop. The exhaust valve was then opened to allow the loop to return to ambient concentrations. The measurements were taken as parts per million in dry air and hence are equivalent to microatmospheres (μatm). The process was repeated for each sample, of which there were two main types; atmospheric and equilibrated samples, respectively. For every 30 samples run on the UGGA, standards of 0.2, 1.0 and 2.0 % CO_2 (e.g. 2,000, 10,000 and 20,000 ppm) were respectively measured in triplicates to ensure there was no significant drift in measurement.

As the loop itself contained air and hence some CO_2 and CH_4, the samples were diluted when they were injected into the loop. As the loop and sample volumes were known, as well as the start and end concentrations of the gases in the loop, the concentrations could be calculated by using the equations in the next section.

Calculating CO_2 and CH_4 concentration in the atmospheric and headspace samples

The volume of the sample in the syringe at standard temperature and pressure, V_{samp} (mL), is given by

$$V_{samp} = V_{syr} \cdot \frac{P_{samp}}{T_{samp}} \cdot \frac{1\ (\mathrm{K})}{101.325\ (\mathrm{kPa})} \tag{2.5}$$

where V_{syr} is the volume of the syringe (mL), and P and T are respectively the pressure (kPa) and temperature (K) at the time of sample analysis.

The number of moles in the sample as a proportion of the total within the loop (G_{mol}) is found using

$$G_{mol} = \frac{V_{samp}}{10^3} \Big/ V_{UGGA} \tag{2.6}$$

where V_{UGGA} (mL) is the volume of the closed loop that is contained within the UGGA.

The concentration of the gas sample C_{samp} (ppm) is found with

$$C_{samp} = \left(C_{end} \cdot 10^6 \cdot (V_{loop} + G_{mol}) - \frac{C_{ini} \cdot 10^6 \cdot V_{loop}}{G_{mol}} \Big/ G_{mol} \right) \cdot 10^6 \tag{2.7}$$

where C_{start} and C_{end} are respectively the concentrations of the gas (ppm) before and after the sample injection as measured by the UGGA, and V_{loop} is the volume (L) of the closed loop that is separate to the UGGA (i.e. the Tygon tubing and valves).

The above calculations were performed for both CO_2 and CH_4. The concentrations of both gases were then converted to partial pressures. The partial pressure of an individual gas in a sample, P_{samp} (μatm), is the pressure that the gas itself exerts as a proportion of the total mix of gases in a given volume. This was calculated with

$$P_{samp} = P_{atm} \cdot \frac{C_{samp}}{10^6} \tag{2.8}$$

where P_{atm} is the mean recorded atmospheric pressure (Pa) on the day of sampling.

Calculating CO_2 and CH_4 concentration in the equilibrated water samples

Unlike the atmospheric and headspace gas samples which simply had to be run through the closed loop UGGA to find their CO_2 and CH_4 concentrations, the equilibrated samples were a mix of 3:1 water-air; the samples were diluted by air and this component had to be removed to find the dissolved gas concentrations in the water.

The number of moles of the target gas (CO_2 or CH_4) in the equilibrated air (n_{EA}) was found using the Ideal Gas Law which states that

$$P \cdot V = n \cdot R \cdot T \tag{2.9}$$

where P is the pressure (atm), V is the volume (L), n is the number of moles (mol), R is the Universal Gas Constant (0.082056 atm·L·K^{-1}·mol^{-1}) and T is the temperature (K). Therefore

$$n_{EA} = \frac{(P_{EA} - P_{AA}) \cdot V_{SH}}{R \cdot T_W} \tag{2.10}$$

where P_{EA} is the partial pressure of the target gas in the equilibrated sample, P_{AA} is the partial pressure of the target gas in the equilibrated air, V_{SH} is the volume of the syringe headspace and T_W was the temperature of the water when the sample was taken. P_{EA} and P_{AA} were calculated using Equations 2.5−2.8.

The number of moles of the target gas (CO_2 or CH_4) in the equilibrated water (n_{EW}) was found using

$$n_{EW} = P_{EA} \cdot V_{SW} \cdot K_H \tag{2.11}$$

where V_{SW} is the volume of the water in the syringe (L), and K_H is Henry's constant (mol·L^{-1}·atm^{-1}) which determines the solubility of a gas depending on the temperature and salinity of the water in which the gas is dissolved. This is a gas-specific coefficient that needed to be calculated respectively for CO_2 and CH_4, using

$$\ln K_H = A_1 + A_2 \cdot \left(\frac{100}{T}\right) + A_3 \cdot \ln\left(\frac{T}{100}\right) + S \cdot \left(B_1 - B_2 \cdot \left(\frac{T}{100}\right) + B_3 \cdot \left(\frac{T}{100}\right)^2\right) \tag{2.12}$$

where T is the temperature of the water (K), S is the salinity (‰) and A_1, A_2, A_3, B_1, B_2 and B_3 are constants for calculating the solubility of the target gas; the constants in Weiss (1974) were used for CO_2 and the constants in Weisenburg and Guinasso (1979) were used for CH_4 (see Appendix Table 7.1). Measured salinities in the channels were very low (observed range 0.02−0.10 mS·cm^{-1} or 2−10 ‰) and therefore the second half of Equation 2.12 which accounts for salinity had a negligible effect on the value of K_H.

With the number of moles known in the gas and water fractions of the syringe, the concentration of dissolved CO_2 (C_{EW}; μM) in the original channel water was found using

$$C_{EW} = \frac{n_{EA} + n_{EW}}{V_{SW}} \tag{2.13}$$

where n_{EA} is the number of moles of CO_2 in the equilibrated syringe headspace, n_{EW} is the number of moles of CO_2 in the equilibrated syringe water and V_{SW} is the volume of water in the syringe (L).

The partial pressure of the target gas in the headspace when at equilibrium with that of the water (P_{aq}; μatm) was found with

$$P_{aq} = \frac{C_{EW}}{K_H} \tag{2.14}$$

which used the same value for K_H as calculated in Equation 2.12.

As the partial pressures of the dissolved gases were known, the fluxes of the gases could be calculated.

2.3.13 Use of the Los Gatos UGGA to measure gas fluxes

A Los Gatos UGGA was available for use in the field in the last two field seasons, which took place in 2016; the post-El Niño dry season (PDS) and early wet season (EWS). Due to time and sampling constraints it was only used in PDS.

A chamber was specially modified to for use by the UGGA by drilling an extra hole halfway down a chamber side into which a septum was fitted. The septum was also drilled with a hole wide enough to accept Tygon tubing, and therefore this port was exactly the same as used for the sampling port at the top of the chamber (see 'Floating chamber design and operation' earlier in this chapter). The Tygon tubing was removed from the top sampling port, this allowing the chamber to be directly connected to the UGGA via longer lengths of Tygon tubing (approximately 1.5 m). One piece of Tygon tubing was fitted from the top sampling port to the analyser inlet (see Gas sample section in this chapter), and the side sampling port on the chamber was connected to the analyser exhaust on the UGGA. This configuration created an airflow from the top of the chamber (where the CO_2 sensor was located) to the analyser, and the exhaust gases were pumped back by the UGGA into the chamber via the side port. Like the analysis of gas samples in a closed loop, the system was similarly closed when in operation. The location of the side port halfway up the side of the chamber was to ensure that water from the channel could not enter the gas analysis system.

UGGA-chamber deployments could only be made when water flow in the channels was negligible as the UGGA needed to be connected to the floating chamber by the Tygon tubing. Flowing water would have required the UGGA to be able to float with the chamber in tandem, in another raft, without disturbing the chamber or itself getting stuck. This was deemed impracticable as the UGGA was heavy (~15 kg), the tubing connecting the UGGA to the chamber could potentially snag on overhanging vegeta-

tion, and the UGGA itself was an expensive piece of equipment that would be ruined if the UGGA was submerged. The UGGA therefore was only useful for measuring real time CO_2 and CH_4 fluxes when channel flow was negligible, so that those measurements could be made from the bank side where the UGGA could be placed on a solid surface.

Gas flux measurements were made using the UGGA-chamber combination much in the same way as deploying the chambers normally: the sensor (and UGGA) were set to start measuring and the chamber was gently wafted in the ambient air for $\tilde{3}0$ seconds; the chamber was then gently lowered on to the water surface and was left for $6-10$ minutes. The data from both the sensor and the UGGA were retrieved at the end of the day. As the measurements were simultaneous, the CO_2 data could be compared directly, and the much more accurate UGGA measurements could be used as a quality check for the measurements of the CO_2 sensor.

2.3.14 Use of the Los Gatos UGGA to determine CH_4 fluxes and ebullition

Although the UGGA measured CH_4 in real time, it was not suitable for making measurements during normal drifting chamber deployments when the channel water was flowing.

In order to ascertain CH_4 fluxes in the channels, samples of the chamber headspace from one of the chambers were taken at the start and finish of each group of chamber deployments. These start and finish headspace gas samples were then intended to be analysed by the closed injection loop method, where the difference in concentrations would give the flux over the deployment period.

The diffusive CH_4 flux could be calculated from the gas exchange velocity determined from the CO_2 flux measured by the sensors, and the CH_4 concentrations in the water, the ambient air and the chamber headspace at the start of the deployment (which should also approximate ambient air). With this information the concentration of CH_4 in the chamber headspace at the end of the deployment could be calculated. If the end concentration of CH_4 from the headspace was higher than that calculated from the diffusive flux, this non-diffusive CH_4 would have been considered as CH_4 arising from ebullition. The gas samples were stored until a field season finished and then shipped back to the UK for analysis.

A serious setback occurred when the UGGA analyser was seriously damaged in transit as a result of poor handling by the couriers. It was not possible to analyse gas samples for several months after finishing fieldwork whilst the analyser was sent back to the USA for repairs. As a result, only a small

fraction of the gas samples collected during the project could be analysed.

A further major problem arose when it came to analysing the chamber headspace gas samples: it was found that the UGGA in the closed loop set up was not sensitive to near-ambient concentrations for CH_4 (and CO_2, see Gas sample analysis section earlier in this chapter) and so ebullition could not be estimated and, therefore, a likely significant part of total CH_4 flux could not be determined in this study.

Fortunately, I have taken a post at the University of Nottingham where Dr. Sofie Sjögersten, who undertakes gas flux research in southeast Asian peatlands, has a laboratory. This laboratory has a gas chromatograph (GC) that can measure CO_2, CH_4 and N_2O simultaneously, and with the sensitivity needed to measure near-ambient concentrations of these gases. The GC at Nottingham is also fitted with an autosampler, so that the large amount of samples I have can be analysed. Dr. Sofie Sjögersten has authorised these gas analyses to take place, and as a result we will also have channel N_2O flux data, in addition to estimates of the ebullitive CH_4 being emitted from the channels.

2.3.15 Non-linear flux calculation

Linear vs. non-linear fluxes

The simple equations for calculating the diffusive flux of a gas, F, imply that F is partly determined by the difference in the concentrations of the gas between the air and equilibration point at the water surface, i.e. the concentration gradient, ΔP in Equations 2.1 and 2.2.

However, as the chamber headspace is a closed system and the volume minuscule with respect to the volume of the supersaturated channel, the concentration in the headspace can change comparatively quickly with respect to the channel water as there is, in effect, an inexhaustible supply of supersaturated gas in the water. In other words, the effective gas concentration in the water over time periods of minutes does not change whilst the headspace concentration significantly increases.

As the headspace concentration increases with time and approaches the concentration in the water, the concentration gradient decreases and causes the instantaneous flux to decrease with time. In natural water-air gas fluxes, the atmospheric reservoir is so large that it is not significantly altered at a timescale of minutes, therefore the instantaneous flux would remain essentially the same. Using headspace measurements and the simple equation in Equation 2.1 will underestimate the gas flux and has led to significant biases in the reporting of diffusive gas fluxes (Kutzbach et al., 2007). However, a solution was pro-

vided to account for the constant decrease of the instantaneous flux due to a decreasing ΔP in Bastviken et al. (2004) and Cole et al. (2010). Their solution is broken down (as it was performed by my `R` script) in the following section.

Calculating the non-linear flux of CO_2

For the remaining data the start and end concentrations (ppm) were converted to partial pressures (μatm) using Equation 2.8.

Although the equations in this section can be used for CH_4, CO_2 was the only gas measured for its concentration change in the chamber headspace, and hence was the only gas that could provide a calculated value for k. Once k was established for CO_2 it could be found for CH_4, and subsequently, the diffusive flux of CH_4 from the channels. Calculation of the CH_4 flux, which used some of the equations below will be covered in the following section.

C is the difference in partial pressure of the target gas between the water and the air (μatm)

$$C = P_{aq} - P_{ini} \tag{2.15}$$

where P_{ini} is the partial pressure of the target gas at the start of the linear flux, and P_{aq} is the value derived from Equation 2.14.

Kappa ($\varkappa$) is how much the partial pressure of the target gas would change in the chamber headspace, given a certain concentration gradient, over a defined period of time; as the concentration of the headspace increases, the concentration gradient decreases, and therefore if k remains constant the flux will reduce, as stated by Equation 2.1. $\varkappa$ is calculated by

$$\varkappa = -\ln\left(\frac{P_{aq} - P_{end}}{C}\right) \Big/ t_{end} - t_{ini} \tag{2.16}$$

where P_{end} is the partial pressure at the end of the linear flux (μatm), and t_{end} and t_{ini} are respectively the end and start times of the linear flux with that duration given in units of days.

The gas exchange velocity (k; $m{\cdot}d^{-1}$) is a metric of turbulence at the air-water interface, where higher values of k will lead to relatively higher rates of gas emissions from the water. This is calculated with

$$k = \frac{\varkappa \cdot V_{CH}}{A_{CH} \cdot K_H \cdot R \cdot T_{CH}} \tag{2.17}$$

where V_{CH} is the volume of the chamber headspace (L), A_{CH} is the area of the chamber headspace in contact with the water surface (m^2), K_H is Henry's constant calculated for the temperature of the water as in Equation 2.12 and T_{CH} is the temperature of the chamber headspace (K).

Finally, the flux (F; g·CO_2·m^{-2}·d^{-1}) of the target gas can be calculated using

$$F = \left(\frac{k \cdot K_H \cdot C}{10^3}\right) \cdot V_{CH} \Big/ R \cdot T_W \tag{2.18}$$

which was multiplied by 0.273 (the proportion of the mass of C in a molecule of CO_2).

2.3.16 Gap-filling CO_2 fluxes that didn't have corresponding dissolved CO_2 concentrations

A total of 2,095 chamber deployments were made in the study. 278 of those deployments could not have a non-linear flux calculated as equilibrated water samples were not available.

A linear model was constructed from observations where original and non-linear-corrected fluxes were available (2,095 - 278 = 1,817 observations; see Fig. 2.20).

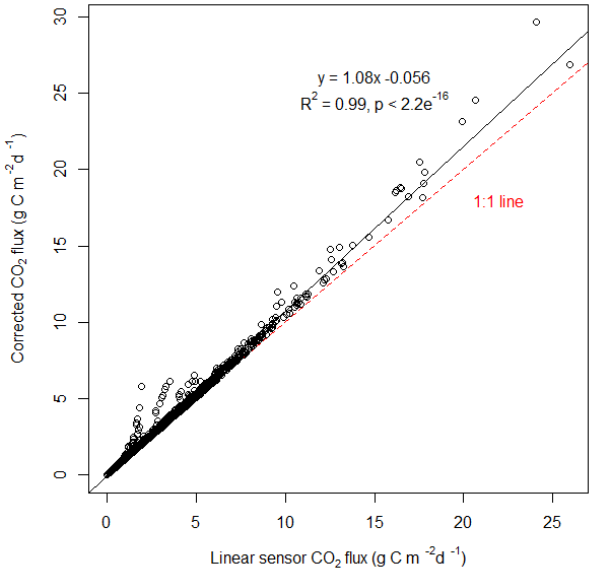

Figure 2.20: 1,817 chamber deployments had both non-linear-calculated CO_2 fluxes and original linear CO_2 fluxes. These were used to construct a linear model. The model equation was used to correct 278 linear fluxes so that the whole CO_2 flux dataset could be used for analysis.

It demonstrated that on average the non-linear fluxes were ~8 % higher than the original linear fluxes. The equation derived from the linear model

$$y = 1.083 \cdot x - 0.059 \tag{2.19}$$

was applied to those fluxes where the non-linear correction could not be calculated, and where y is the estimated non-linear flux and x is the linear flux of the observation without a corresponding dissolved gas sample. This gap-filling process allowed all 2,241 observations to be included in the analysis of CO_2 fluxes.

2.3.17 Rejection of the suspect gas exchange velocity (k) values

Converting k to k_{600}

Gas exchange velocities for CO_2 ($k_{[CO_2]}$) were calculated using Equation 2.17. $k_{[CO_2]}$ values were then converted to k_{600} which allows exchange velocities to be compared between any gas and at any temperature (Cole et al., 2010). Schmidt numbers (Sc) are dependent on temperature and specific to respective gases and the subscript of 600 in k_{600} refers to a Schmidt number of 600 which corresponds to CO_2 at 20 °C, the gas and temperature that k is typically normalised to for comparing k for other gases and temperatures. As in Cole et al. (2010), this was calculated by

$$k_{600} = k \Big/ \left(\frac{600}{Sc}\right)^{n} \tag{2.20}$$

where the exponent n is a diffusion coefficient dependent on turbulence at the boundary layer (Jähne and Haussecker, 1998) and Sc is the Schmidt number. n = 0.5 ($\frac{1}{2}$) has been used for lakes with low wind speeds and in riverine CO_2 flux studies (Cole et al., 2010; Lorke et al., 2015). Sc was calculated using

$$Sc = A + B \cdot T + (C \cdot T)^2 + (D \cdot T)^3 + (E \cdot T)^4 \tag{2.21}$$

where T is the water temperature (°C) and A, B, C, D and E are coefficients of Schmidt number versus temperature for freshwater and which vary depending on the gas in question (Wanninkhof, 2014; see Appendix Table 7.2 for the list of constants).

Exclusion of data with suspect k values

Examination of the dataset revealed 103 gas exchange velocities that were excessively high (10−46 m·d^{-1}), likely indicating a source of error; values of 10−26 m·d^{-1} would be expected in the ocean at high wind speeds (10−15 m·s^{-1}; Wanninkhof et al., 2009). Similar values were observed for k_{600} when chambers were anchored (which could significantly increase k) in a fast flowing stream (0.4−0.9 m·s^{-1}; Lorke et

al., 2015).

The 103 outlying gas exchange velocities in this dataset seem very unlikely for slack peatland streams. These high values consistently occurred at the lowest recorded partial pressures of dissolved CO_2 from 3 days of data, all at KALA, and where all values were <1000 μatm CO_2 but the CO_2 fluxes measured by the sensors were within the range usually encountered at KALA. This suggested a problem with the dissolved CO_2 partial pressure measurements and that these were a source of error. This error could have arisen as a result of the Los Gatos UGGA losing sensitivity at nearer-ambient concentrations. This also appeared to be the case in a study conducted by Baird et al. (2010) which specifically looked at the precision of the Los Gatos UGGA used in an injection loop set up: all CH_4 standards over 2.5−times ambient air concentration (˜1.9 ppm) were within ±5 %, however at ˜1.4−times ambient, precision dropped to 24 % (CO_2 was not investigated, but it is reasonable to assume a similar effect). It was concluded that the dissolved CO_2 concentrations were underestimated which gave rise to extreme gas exchange velocities being calculated. Accordingly, these gas exchange velocities were excluded from the dataset and analyses.

Ambient atmospheric concentrations were assumed due to UGGA sensitivity issues

The k data provided evidence that the UGGA was losing sensitivity and accuracy at near-ambient concentrations when analysing samples in a closed-loop configuration, which was an issue described in Baird et al. (2010). Measurement of gas standards (described in Section 2.3.8), which were all ≥2,000 ppm CO_2, did not seem to be affected, i.e. the measured concentrations were within ± 5 % of the actual standard concentrations.

The atmospheric gas samples were expected to be near-ambient atmospheric concentration, but those that were measured were often approximately 1.5 to 2−times the expected concentration (600−800 ppm). As the atmospheric concentrations were key for calculating the partial pressures of the atmospheric and equilibrated CO_2 and CH_4, it was decided that assuming atmospheric concentrations would be better than using those determined by the closed-loop UGGA.

Atmospheric CO_2 and CH_4 were assumed to be 405 and 1.97 ppm, respectively, and the fluxes were recalculated as in Section 2.3.9. It was expected that this would make little difference to the cal-

culated fluxes because of the magnitude of the differences in concentrations between the atmosphere and the supersaturated water. To test this, fluxes were also calculated with ±7 % the assumed ambient concentrations, i.e. 405±30 ppm CO_2 and 1.97±0.15 ppm CH_4. As expected, these upper and lower estimates made little difference to the CO_2 and CH_4 fluxes which were typically within 95−99 % of the actual assumed ambient concentrations. Therefore, natural variation of CO_2 and CH_4 within these upper and lower amounts would have little difference on the derived fluxes.

2.3.18 Calculation of the methane flux

According to Cole et al. (2010), piston velocities and Schmidt numbers (Sc) are related:

$$\frac{k_{gas1}}{k_{gas2}} = \left(\frac{Sc_{gas1}}{Sc_{gas2}}\right)^{n} \tag{2.22}$$

therefore the gas exchange velocity for CH_4 can be found with

$$k_{[CH_4]} = k_{[CO_2]} \Big/ \left(\frac{Sc_{[CO_2]}}{Sc_{[CH_4]}}\right)^{\frac{1}{2}} \tag{2.23}$$

where n = 0.5 as in Equation 2.20.

The diffusive flux of CH_4 was calculated using Equations 2.15 to 2.18 by substituting values relevant to CH_4: $k_{[CH_4]}$, the partial pressure of CH_4 in the water, and Henry's constant (K_H) for CH_4, the latter being calculated using Equation 2.12 by using the Bunsen coefficients provided in Weisenburg and Guinasso (1979). The fluxes ($g{\cdot}CO_2{\cdot}m^{-2}{\cdot}d^{-1}$) were multiplied by 0.75 (the proportion that C has of the mass of a molecule of CH_4) and 10^3 for presentation as $mg{\cdot}C{\cdot}m^{-2}{\cdot}d^{-1}$.

2.3.19 Statistical analysis

The open source and freely available `R` language (version 3.0.2 "Frisbee Sailing"; R Development Core Team, 2013; see http://www.R-project.org) and `R Studio` (version 1.0.136) environment was used for all statistical analyses. All data subject to analyses were checked for normality using quantile-quantile plots prior to choosing a suitable test. As standard, an F test of equal variances was conducted prior to selecting a t-test.

Much of the data were non-normal, thus non-parametric tests (such as Wilcoxon's rank sum test) were used to compare between land classes. Further, the dataset contained many outliers and therefore median values are reported. Effect sizes are reported as standard, using Pearson's r, which was

calculated with:

$$r = \sqrt{\frac{z}{N}} \tag{2.24}$$

where z is the z-score and N is the number of observations, respectively, from the Wilcoxon's rank sum test (Rosenthal, 1991).

Where independent t-tests were used, Pearson's r was calculated using:

$$r = \sqrt{\frac{|t^2|}{|t^2| + df}} \tag{2.25}$$

where t is the test statistic and df denotes the degrees of freedom given in the t-test (Rosnow and Rosenthal, 2005).

2.3.20 Graphical representation of data

The behaviour of individual sites often differed, especially between the intermediately degraded and severely degraded sites. To highlight this, red box plots were used for the severely degraded site, KALA, and yellow for the intermediately degraded TAR1 and TUN1. All intact sites (SAB1 to SAB3) were coloured green.

Analyses were conducted only at a land class level, where green represents the intact land class, and yellow, the degraded. Statistical significance is indicated with '***', '**' or '*', for probability (p) values of $<$0.001, $<$0.01, and $\leq$0.05, respectively. Non-significant results ($p >$0.05) are indicated by 'NS'.

All box plots have the number of observations recorded for each site/land class above the box at the top of the plot. When land classes are compared, the notches about the medians represent an approximate 95 % confidence interval (CI_{95}), calculated using:

$$CI_{95} = \pm 1.58 \cdot \frac{IQR}{\sqrt{n}} \tag{2.26}$$

where IQR is the interquartile range and n is the number of observations. This method for calculating confidence intervals for medians was described in McGill et al. (1978).

2.3.21 Clarification of terminology

This thesis compares the differences between intact and degraded land classes, both of which consist of three replicate sites or channels. Sites may be used when discussing the catchment, whereas the channels

refer to the channels draining those sites. In addition, when talking more broadly about the land classes, in terms of the wider implications (such as what may occur at a landscape scale), peat swamp forest (or PSF) may be used for convenience, as in, for example, Moore et al. (2013). For clarity, degraded PSF does not consist of a forest, but rather it indicates its former state prior to degradation.

2.3.22 Sample and data summaries

The following tables present the numbers of samples and measurements taken during the late wet season (LWS; Table 2.5), El Niño dry season (EDS; Table 2.6), post-El Niño dry season (PDS; Table 2.7) and early wet season (EWS; Table 2.8). In reference to the table headers: 'Deps' refer to the total numbers of chamber deployments, but does not represent the data used for analysis; 'CO_2' refers to the number of CO_2 measurements analysed in this thesis; 'CH_4' refers to the number of CH_4 calculations analysed in this thesis; 'Air hi' refers to the number of atmospheric gas samples, the number of samples used in analyses is in brackets; 'Air lo' refers to the number of gas samples taken near the water surface, the number of samples used in analyses is in brackets; 'Diss gass' refers to the number of dissolved gas samples taken, the number of samples used in analyses is in brackets; 'Head' refers to the number of chamber headspace gas samples taken, the number of samples used in analyses is in brackets; 'TOC' refers to the number of water samples taken that were analysed for DOC concentration using the TOC analyser, the number of samples used in analyses is in brackets; 'T (air)' refers to the number of air temperature measurements analysed in this thesis, 'P (air)' refers to the number of air pressure measurements analysed in this thesis; 'T (H_2O)' refers to the number of water temperature measurements analysed in this thesis; 'DO' refers to the number of dissolved oxygen measurements analysed in this thesis; 'EC' refers to the number of electrical conductivity measurements analysed in this thesis; and 'Other' notes when other data were collected whereby 'MS' represents molecular sieve deployment/retrieval, 'UGGA' represents the use of the Los Gatos UGGA and 'DOC' represents DOC quality (aromaticity) measurements with the spectrophotometer. In some instances a record of the actual number of samples taken was not available, such cases are marked with '?'.

Totals are provided in Table 2.9.

Table 2.5: Daily totals of measurements and samples taken during LWS, but if there was a difference between the number collected and the number used in analyses the latter are in parentheses. The date is given as YYMMDD.

Date	Site	Deps	CO_2	CH_4	Air hi	Air lo	Diss gas	Head	TOC	T (air)	P (air)	T (H_2O)	DO	EC	Other
150406	SAB2-3	0	0	0	13 (0)	0	13 (12)	0	0	0	0	0	0	0	
150409	KALA	0	0	0	25 (0)	25 (0)	20 (20)	0	0	0	0	0	0	0	
150410	SAB1	0	0	0	7 (0)	0	7 (7)	0	0	6	6	6	0	0	
150413	KALA	10	10	10	12 (0)	0	12 (6)	11 (0)	6 (6)	12	12	14	0	0	
150414	TAR1	10	0	0	7 (0)	0	7 (7)	6 (0)	5 (5)	6	6	7	0	0	
150415	SAB1	25	25	25	5 (0)	0	5 (5)	5 (0)	5 (5)	10	10	10	0	0	
150417	SAB2	25	25	25	10 (0)	0	10 (5)	10 (0)	6 (6)	9	9	8	8	0	
150418	SAB3	15	15	15	6 (0)	0	6 (3)	6 (0)	5 (5)	5	5	5	5	0	
150423	KALA	30	30	30	12 (0)	12 (0)	12 (6)	12 (0)	8 (8)	12	12	12	12	0	
150424	SAB1	20	20	20	4 (0)	0	4 (4)	0	5 (5)	3	3	3	3	0	
150425	KALA	26	26	26	7 (0)	7 (0)	7 (4)	7 (0)	0	4	4	4	3	0	
150427	SAB2	19	19	19	8 (0)	8 (0)	8 (4)	8 (0)	5 (5)	8	8	8	8	0	
150428	SAB3	30	30	30	12 (0)	12 (0)	12 (6)	12 (0)	10 (10)	7	7	11	11	0	
150503	TUN1	5	5	5	5 (0)	0	20 (20)	0	5 (5)	5	5	11	11	0	
150504	TAR1	7	0	0	7 (0)	0	28 (28)	0	7 (7)	7	7	7	7	0	
150505	SAB1	15	15	15	6 (0)	6 (0)	6 (3)	6 (0)	3 (3)	3	6	5	5	0	
150508	SAB2	23	23	23	12 (0)	12 (0)	12 (6)	10 (0)	10 (10)	12	12	12	12	0	
150509	KALA/SAB1-3	0	0	0	0	0	0	0	0	0	0	0	0	0	MS
150510	TUN1	0	0	0	0	0	0	0	0	0	0	0	0	0	MS
150511	TAR1	0	0	0	5 (0)	0	15 (15)	0	? (5)	0	0	0	0	0	MS
150512	SAB3	0	0	0	13 (0)	0	39 (39)	0	13 (13)	13	13	13	13	0	
150517	KALA	12	12	12	10 (0)	10 (0)	10 (5)	10 (0)	5 (5)	10	10	10	10	0	
150518	TAR1	15	0	0	6 (0)	0	18 (18)	0	7 (7)	5	5	6	6	0	
150519	TUN1	18	18	18	6 (0)	0	18 (18)	0	6 (6)	6	6	6	6	0	
150522	SAB1	0	0	0	0	0	40 (40)	0	0	0	0	0	0	0	
150525	SAB2	24	24	24	8 (0)	8 (0)	8 (4)	8 (0)	5 (5)	3	3	4	4	0	
150526	SAB2	34	34	34	12 (0)	8 (0)	12 (8)	8 (0)	9 (9)	4	4	5	5	0	
150527	KALA	22	22	22	10 (0)	8 (0)	10 (6)	8 (0)	8 (8)	9	9	7	9	0	
150528	TUN1	18	18	0	18 (0)	0	18 (0)	0	6 (6)	6	6	6	6	0	
150529	KALA	45	45	0	9 (0)	0	9 (0)	0	5 (5)	9	9	4	4	0	
150603	SAB1	25	25	0	10 (0)	10 (0)	10 (0)	10 (0)	5 (5)	2	3	4	4	0	
150604	TAR1	36	36	36	0	0	0	0	3 (3)	7	7	4	3	0	
150605	TUN1/TAR1	0	0	0	0	0	0	0	0	0	0	0	0	0	MS
150606	KALA/SAB1-3	0	0	0	0	0	0	0	0	0	0	0	0	0	MS
150607	KALA	45	45	0	9 (0)	0	9 (0)	0	0	7	7	0	0	0	
150608	KALA	30	30	0	7 (0)	0	7 (0)	0	0	8	8	0	2	0	
150612	KALA	27	27	0	10 (0)	0	10 (0)	0	7 (7)	0	0	0	0	0	
150613	SAB3	34	34	0	12 (0)	12 (0)	12 (0)	12 (0)	6 (6)	8	8	9	9	0	
150614	SAB1	20	20	0	12 (0)	6 (0)	24 (0)	6 (0)	9 (9)	12	12	12	12	0	
150615	TAR1	35	35	35	0	0	0	0	10 (10)	7	7	9	7	0	

Table 2.6: Daily totals of measurements and samples taken during EDS, but if there was a difference between the number collected and the number used in analyses the latter are in parentheses. The date is given as YYMMDD.

Date	Site	Deps	CO_2	CH_4	Air hi	Air lo	Diss gas	Head	TOC	T (air)	P (air)	T (H_2O)	DO	EC	Other
150723	SAB1	33	33	33	?	?	? (3)	?	? (5)	6	6	13	13	0	
150725	KALA	15	15	15	?	?	? (3)	?	? (5)	6	6	5	5	0	
150726	SAB2	23	23	23	?	?	? (3)	?	? (5)	5	5	9	9	0	
150727	SAB3	30	30	30	?	?	? (6)	?	? (6)	12	12	12	11	0	
150728	TAR1	30	30	30	?	?	? (6)	?	? (6)	4	4	4	4	0	
150729	TAR1	30	30	30	?	?	? (6)	?	? (10)	4	4	10	10	0	
150808	TUN1	0	0	0	?	?	? (0)	?	? (1)	0	0	0	0	0	
150816	SAB1	22	22	22	?	?	? (3)	?	? (6)	4	4	4	4	0	
150820	KALA	34	34	30	?	?	? (3)	?	? (10)	2	2	1	1	0	
150821	SAB2	20	20	20	?	?	? (3)	?	? (10)	5	5	6	6	0	
150823	BAH1	30	0	0	?	?	? (0)	?	? (10)	6	6	10	10	0	
150824	TAR1	30	30	30	?	?	? (6)	?	? (10)	6	6	6	6	0	
150825	SAB3	28	28	28	?	?	? (5)	?	? (9)	5	5	7	7	0	
150828	SAB2	30	30	30	?	?	? (4)	?	? (6)	6	6	6	6	0	
150829	KALA	61	61	61	?	?	? (6)	?	? (10)	5	5	3	6	0	
150831	SAB1	19	19	19	?	?	? (3)	?	? (5)	3	3	3	3	0	
150907	SAB3	28	28	28	?	?	? (3)	?	? (5)	4	4	8	8	0	
150908	TUN1	8	8	8	?	?	? (6)	?	? (5)	3	3	3	3	0	
150909	BAH1	6	0	0	?	?	? (0)	?	? (5)	3	3	3	3	0	
150910	TAR1	0	0	0	?	?	? (5)	?	? (6)	4	4	5	5	0	
150912	TAR1	29	29	29	?	?	? (6)	?	? (6)	6	6	3	3	0	
150913	KALA	12	12	12	?	?	? (6)	?	? (0)	3	3	3	3	0	
150928	TAR1	0	0	0	?	?	? (0)	?	? (1)	3	3	3	3	0	

Table 2.7: Daily totals of measurements and samples taken during PDS, but if there was a difference between the number collected and the number used in analyses the latter are in parentheses. The date is given as YYMMDD.

Date	Site	Deps	CO_2	CH_4	Air hi	Air lo	Diss gas	Head	TOC	T (air)	P (air)	T (H_2O)	DO	EC	Other
160815	KALA	15	15	15	6 (0)	6 (0)	6 (3)	6 (0)	0	3	3	2	2	0	
160819	SAB1	34	34	34	6 (0)	6 (0)	6 (3)	6 (0)	6 (6)	6	6	6	6	6	
160820	SAB3	35	35	35	9 (0)	9 (0)	9 (4)	6 (0)	6 (6)	4	4	3	6	6	
160821	KALA	15	15	15	6 (0)	5 (0)	6 (3)	6 (0)	3 (3)	4	4	3	3	3	
160822	SAB2	0	0	0	6 (0)	6 (0)	6 (0)	6 (0)	3 (3)	0	0	0	0	0	
160825	SAB2	34	34	34	0	0	3 (3)	0	0	3	3	3	3	3	
160826	BER1	23	23	23	6 (0)	4 (0)	10 (8)	4 (0)	6 (6)	5	5	5	5	5	
160827	TAR1	30	30	30	6 (0)	4 (0)	10 (8)	4 (0)	6 (6)	6	6	4	4	4	
160830	SUN1	40	0	0	8 (0)	4 (0)	8 (8)	4 (0)	8 (8)	8	8	8	8	8	
160831	BER1	30	30	30	6 (0)	6 (0)	6 (3)	6 (0)	3 (3)	6	6	6	6	6	
160901	SEB1	34	34	34	9 (0)	6 (0)	9 (6)	7 (0)	7 (6)	5	5	5	5	5	
160902	KALA	20	20	20	2 (0)	2 (0)	2 (1)	2 (0)	3 (3)	2	3	3	3	3	
160905	SEB3	30	30	30	0	0	? (6)	0	6 (6)	3	3	3	3	3	
160906	TAR1	30	30	30	8 (0)	8 (0)	8 (4)	8 (0)	6 (6)	5	5	5	5	5	
160907	BER1	30	30	30	0	0	? (3)	0	3 (3)	6	6	6	6	6	
160908	SUN1	37	0	0	0	0	14 (0)	0	? (8)	8	8	8	8	7	
160920	SAB1	4	4	4	2 (0)	0	2 (2)	0	2 (2)	4	4	2	2	2	UGGA
160921	SAB1	33	33	33	3 (0)	0	3 (3)	0	3 (3)	10	10	4	4	4	UGGA
160922	SAB2	26	26	26	3 (0)	3 (0)	3 (3)	0	3 (3)	10	10	4	4	4	UGGA
160923	SAB3	30	30	30	3 (0)	3 (0)	3 (3)	0	3 (3)	9	9	3	3	3	UGGA
160926	SUN1	9	0	0	3 (0)	3 (0)	3 (3)	6 (0)	3 (3)	7	7	5	5	3	UGGA
160928	KALA	19	19	19	?	?	? (3)	?	? (3)	5	5	4	3	2	UGGA
160929	KALA	20	20	20	?	?	? (6)	?	? (3)	5	5	3	4	2	UGGA
161009	BER1	15	15	15	?	?	? (3)	?	? (0)	3	3	3	0	3	
161011	TAR1	30	30	30	?	?	? (3)	?	? (0)	6	6	6	0	6	
161012	SAB2	30	30	0	?	?	? (3)	?	? (0)	6	0	6	0	6	

Table 2.8: Daily totals of measurements and samples taken during EWS, but if there was a difference between the number collected and the number used in analyses the latter are in parentheses. The date is given as YYMMDD.

Date	Site	Deps	CO_2	CH_4	Air hi	Air lo	Diss gas	Head	TOC	T (air)	P (air)	T (H_2O)	DO	EC	Other
161101	SAB1/KALA	0	0	0	0	0	0	0	6 (4)	0	0	0	0	0	DOC
161104	SAB1/KALA	0	0	0	0	0	0	0	6 (4)	0	0	0	0	0	DOC
161110	SAB1/KALA	0	0	0	0	0	0	0	6 (4)	0	0	0	0	0	DOC
161121	SAB1/KALA	0	0	0	0	0	0	0	6 (4)	0	0	0	0	0	DOC
161122	SAB1	39	39	39	?	?	? (3)	?	? (0)	5	5	4	0	4	
161123	KALA	20	20	20	?	?	? (6)	?	6 (0)	12	12	6	0	6	
161124	SAB3	39	39	39	?	?	? (4)	?	? (0)	5	5	4	0	4	
161126	SUN1	30	0	0	?	?	? (6)	?	6 (0)	6	6	6	0	6	
161127	SAB2	29	29	29	?	?	? (4)	?	? (0)	4	4	4	0	4	
161128	BER1	45	45	45	?	?	? (6)	?	? (0)	9	9	5	0	6	
161129	TAR1	45	45	45	?	?	? (6)	?	? (0)	9	9	9	0	9	
161130	SAB1/KALA	0	0	0	0	0	0	0	6 (4)	0	0	0	0	0	DOC
161203	BER1	45	45	45	?	?	? (6)	?	? (0)	9	9	9	0	9	
161204	SAB2	60	60	60	?	?	? (8)	?	? (0)	12	12	13	0	13	
161206	TAR1	45	45	45	?	?	? (6)	?	? (0)	9	9	9	0	9	
161208	SUN1	24	0	0	?	?	? (6)	?	? (0)	6	6	6	0	6	
161210	KALA	30	30	30	?	?	? (6)	?	? (0)	6	6	6	0	6	

Table 2.9: Summary of total numbers of measurements, and the number of those measurements that were used for analyses in this thesis. At the time of compiling a complete list of the samples was not available, except those that had been analysed. As many samples would have been collected, a much greater than sign '$\gg$' is used to indicate that the the total number of samples may have been approximately 50−100 % higher than the value given.

Measurements/samples	Table header	Total	Used in analyses
Chamber deployments	Deps	2,303	2,095
CO_2 fluxes	CO_2	2,095	2,095
CH_4 fluxes	CH_4	1,817	1,817
Atmospheric air samples	Air hi	$\gg$ 395	0
Near-surface air samples	Air lo	$\gg$ 219	0
Dissolved gas samples	Diss gas	$\gg$ 534	561
Headspace gas samples	Head	$\gg$ 228	0
Dissolved organic carbon (quantity)	TOC	$\gg$ 386	434
Dissolved organic carbon (quality)	Other - DOC	20	20
Air temperature measurements	T (air)	558	558
Air pressure measurements	P (air)	557	557
Water temperature measurements	T (H_2O)	537	537
Dissolved oxygen measurements	DO	409	409
Electrical conductivity measurements	EC	187	187
UGGA measurements	Other - UGGA	37	37
Molecular sieves	Other - MS	21	12

Chapter 3

Effects of degradation of peat swamp forest on channel emissions of carbon dioxide

Authors: Kent, M.S.[1,2], Page, S.E.[3], Evans, C.D.[4], Idrus[5,6], Hanafi[6], Sandy[5], Bina[5,6], Bastviken, D.[7], Garnett, M.H.[8], Ripoll, B.[6] Pangala, S.[2,9] and Gauci, V.[2]

Institutions: [1]*School of Agricultural and Environmental Sciences, University of Nottingham, Sutton Bonington Campus, College Road, Loughborough, LE12 5RD.* [2]*School of Environment, Earth and Ecosystem Sciences, Faculty of Science, Technology, Engineering and Mathematics, The Open University, Walton Hall, Milton Keynes, MK7 6AA.* [3]*Department of Geography, University of Leicester, University Road, Leicester, LE1 7RH.* [4]*Centre for Ecology and Hydrology, Environment Centre Wales, Deiniol Road, Bangor, LL57 2UW.* [5]*Center for International Cooperation in Sustainable Management of Tropical Peatland (CIMTROP), University of Palangkaraya, Jalan Yos Sudarso, Kampus UNPAR Tunjung Nyahu, Palangkaraya 73111, Central Kalimantan, Indonesia.* [6]*Borneo Nature Foundation, Jalan Bukit Raya No. 82, Bukit Raya, Palangkaraya 73112, Central Kalimantan, Indonesia.* [7]*Department of Thematic Studies, Linköping University, Campus Valla, Linköping, Sweden.* [8]*Natural Environment Research Council Radiocarbon Facility, Rankine Avenue, Scottish Enterprise Technology Park, East Kilbride, G75 0QF.* [9]*Lancaster Environment Centre, Lancaster University, Lancaster, LA1 4YQ.*

Abstract

Tropical peatlands contain a disproportionately large amount of carbon (C) in their soils, per unit area, compared with temperate peatlands. Significant amounts of tropical peatland have been deforested and drained in recent decades. This degradation can fundamentally disrupt the hydrology and C storage capacity of these ecosystems. Peat swamp forest, which often acts as a C sink, is particularly vulnerable to degradation whereby degraded areas have become a globally significant C source; petagrams of C have been lost from degraded Indonesian peatlands alone since the 1990s. Several terrestrial peat swamp forest CO_2 emission studies exist, yet fluvial emissions studies are scarce despite peat-draining channels being a significant loss pathway for terrestrial C. Losses can occur due to translocation of dissolved and/or particulate C to rivers and oceans, or by in-stream degradation of C substrates, whereby the resultant CO_2 can be released directly to the atmosphere. This is the first study of seasonal CO_2 emissions from channels draining intact and degraded peat swamp forest. Both intact and degraded channels were supersaturated with CO_2. The intact channels contained >13,000 μatm in the wet season, ~2−times as much as the degraded channels. The intact channels had low dissolved oxygen concentrations (possibly indicating high rates of heterotrophy), but much CO_2 could have arrived via lateral flows, owing to the higher water table. Dissolved CO_2 dropped ~50 % at both channel types in the dry season. CO_2 emission was driven by supersaturation rather than by gas exchange velocities. Despite intact channels emitting twice as much CO_2 per unit area than degraded channels (medians = 4.68 and 1.81 $g{\cdot}C{\cdot}m^{-2}{\cdot}d^{-1}$ in wet and dry seasons, respectively), the degraded channels had a greater areal extent and therefore potentially emit more in total. Further, the intact channels were cycling recently photosynthesised C, whereas CO_2 emitted by degraded channels was several centuries old.

3.1 Introduction

Peatlands, including tropical peat swamp forests, are recognised as globally important stores of C, most of which is millennia old (Limpens et al., 2008). Peatlands typically form in wet climates where rainfall is sufficient to maintain the water table near or above the surface for significant periods of the year. The high water table acts as a barrier to oxygen and this considerably restrains aerobic breakdown of C-rich soil organic matter. Anaerobic breakdown, which is not oxygen dependent, is the dominant pathway

of soil organic matter degradation in most naturally functioning peatlands. As anaerobic breakdown is a much slower degrading process than aerobic breakdown, accumulation of soil organic matter may exceed degradation causing soil C stocks to increase with time (Rydin and Jeglum, 2006).

Globally, peat soils hold 485−745 Pg·C (see Chapter 1). Tropical peatlands represent 14−17 % of C held in peat soils, globally. Approximately 54 % of tropical peat C is found in Indonesia, mostly in the peatlands of Borneo and Sumatra. Considering that Indonesian peatlands make up just 5.2 % of global peatland area (207,000 km^2 of 3,970,000 km^2; Page et al., 2011), they contain a disproportionately high amount of C compared to other peatlands.

Tropical wetlands (including peat swamp forest) are globally significant not just for the C they contain but also the greenhouse gases they accumulate and emit. They naturally act as a globally important sink for carbon dioxide (CO_2), storing it as soil organic matter, and in so doing contribute to cooling the climate. (Limpens et al., 2008; Yu et al., 2011; Page and Baird, 2016).

Degradation of peat swamp forest, for example as a result of deforestation, drainage and fire, results in the release of globally significant quantities of greenhouse gases to the atmosphere as a result of both peat oxidation and combustion. Fires resulting from the 1997 and 2015 El Niño events released 2.97−9.43 and 0.89 Pg·CO_2-equivalents, respectively (Lohberger et al., 2017). In Southeast Asia, peat swamp forest degradation is a consequence of land use change which is occurring on a large and rapid scale (Hergoualc'h and Verchot, 2014; Miettinen et al., 2017).

Land use change of peat swamp forest generally requires removal of the forest vegetation, and drainage by cutting channels through the peat. These channels drain the large amounts of water that would otherwise be stored in and/or reside above the peat for significant periods in the year (Wulffraat et al., 2017). Without water acting as a barrier to prevent oxygen from entering the peat, aerobic breakdown can take place. Once the peat begins to oxidise and degrade, previously stored C can be released to the atmosphere (Couwenberg et al., 2010). As a result of this drop in water table, previous sinks and stores of C are becoming significant sources (Miettinen et al., 2017).

In some instances, such as the ex-Mega Rice Project in Central Kalimantan, Borneo, degradation was so extreme the land had to be abandoned; the channels adversely affected the water table so that the land became prone to seasonal flooding and fires during the wet and dry seasons, respectively. These seasonal extremes appear to prevent natural forest regeneration and what secondary forest has managed

to establish is of a different ecological composition due to the severely altered hydrological conditions (Page et al., 2009b). As the hydrology and ecological communities are altered in degraded peat swamp forest, this leads to significant changes in ecosystem biogeochemistry indicating that there has been a significant change to the way C is cycled with respect to intact peat swamp forest. Similarly, land converted for e.g. oil palm also alters peat swamp forest C chemistry (Materić et al., 2017; this study used DOC samples I took from my sampling sites).

Degradation of peat swamp forest is known to significantly impact C export to channels, affecting the quality and quantity of dissolved and particulate organic carbon (DOC and POC, respectively; Moore et al., 2013; Evans et al., 2014; Evans, 2015). Studying channel geochemistry can therefore be an effective way of assessing changes to ecosystem functioning following disturbance (e.g. Moore et al., 2013; Materić et al., 2017).

As the channels drain comparatively large areas of peatland compared to the actual channel area itself, they receive a lot of organic and inorganic material from the surrounding catchments; as water passes over and through the peat volume it entrains DOC and POC, inorganic nutrients, enzymes and microbes (Cuffney, 1988). Analysing the quality and quantity of these ecosystem products, and the differences between waters that drain intact peat swamp forest and degraded peat swamp forest could, therefore, provide information on the ecological and biogeochemical changes that take place in a peat swamp forest catchment when it is disturbed (Materić et al., 2017), particularly in terms of ecosystem C balance (Moore et al., 2013). Overland and through-flows of water on and in the peat will also entrain dissolved gases such as CO_2 and deliver them to the channels.

Moore et al. (2013) found that degraded peat swamp forest was losing ~50 % more total organic carbon (DOC and POC) via its drainage channels than intact peat swamp forest. Further, radiocarbon-dating of the DOC demonstrated that the average radiocarbon age of degraded peat swamp forest DOC was ancient and had originated from deep peat layers $\leq$5,000 years-old), whereas the intact peat swamp forest DOC was modern and had been recently photosynthesised. DOC from deep peat layers remains mostly in long-term storage in an intact peat swamp forest system, but degradation, in particular drainage, was shown to mobilise old C from deep within the peat column.

With increased delivery of DOC and POC to channels following peat swamp forest disturbance and degradation, it is possible that emissions of CO_2 could increase if the material being delivered is

readily degradable (Lapierre et al., 2013; Butman et al., 2015). River and stream systems have frequently been shown to be significant sources of greenhouse gases such as CO_2 and CH_4; this is particularly the case for peat-draining streams which can be supersaturated with CO_2 and CH_4 (Billett and Moore, 2008). Similar studies have not yet been conducted in intact and degraded peat swamp forest, but as the streams and rivers draining these landscapes are a significant part of local to global-scale C cycling, we therefore have an incomplete picture of peat swamp forest catchment scale C cycling.

Fluxes of C are known to vary according to season. The climate in Indonesia is, like many countries within the Intertropical Convergence Zone, categorised into distinct wet and dry seasons. The frequency and intensity of rains varies greatly throughout the year, with the majority of total annual rainfall, 92−95 %, falling during the wet season (Moore, 2011). In most wet season months, rainfall in the study location in southern Borneo exceeds 300 mm, whereas in the dry season it can fall below 100 mm per month (Hooijer et al., 2008).

Net water input (rainfall minus evapotranspiration) has a direct effect on how much water is present in a peat swamp forest catchment and its associated waterways, including channels. In turn, the position of the water table relative to the peat surface will affect the biogeochemistry of the peat with several investigations having detected seasonal effects on C emission and export in response to the rise and fall of the water table (Hirano et al., 2007; Jauhiainen et al., 2008; Jauhiainen and Silvennoinen, 2012; Moore et al., 2011, 2013). It is therefore important to capture this seasonal variation if accurate estimates are to be made of annual fluxes of CO_2. Water flow over and through the peat is key to delivering dissolved CO_2 and DOC that can subsequently be broken down in-stream to produce further CO_2. As such, a seasonal variation in channel fluxes is expected, with the highest emissions occurring in the wet season when delivery of terrigenous DOC and CO_2 is at its highest rates. In the dry season, less delivery can take place and may be restricted to mostly groundwater flows through the peat. Further, water drawdown in the peat soil of degraded peat swamp forest is likely to be much greater than in intact peat swamp forest which could have two affects on CO_2 emissions from the channels: a) the volume of wetted peat adjacent to the channel could be smaller in degraded peat swamp forest, meaning there is a smaller total reservoir of DOC and CO_2 that could act as a source to the channel; and b) DOC being leached from deeper layers of degraded peats owing to the lower water table is more likely to be resistant to breakdown, both in the peat and in-stream.

This study aims to quantify how much CO_2 is contained in waters within channels draining intact and degraded tropical peatland, and how much is being emitted to the atmosphere. It will compare land uses (land classes) using intact peat swamp forest as a baseline in order to for establish how land use change in the form of deforestation and drainage affects the emission of these important greenhouse gases. The changes in CO_2 fluxes will be attributed to some of the physicochemical changes that result from seasonal differences, as well as deforestation and drainage. Finally, using radiocarbon dating, it will determine the source of the CO_2 it is emitting; whether that C is recently photosynthesised and suggests a peat swamp forest C sink, or whether is old and comes from previously stored C in the peat. The latter would provide further evidence that degradation of peat swamp forest causes it to become a source of ancient CO_2 to the atmosphere, just as Moore et al. (2013) found that degraded peat swamp forest was releasing large quantities of ancient DOC to the channels draining them.

3.1.1 Hypotheses

Peat swamp forest environment and biogeochemistry

- H_0: Intact and degraded peat swamp forest are fundamentally the same in terms of their environmental conditions and biogeochemical functioning that drive CO_2fluxes.
- H_1: Deforestation and drainage of peat swamp forest fundamentally alters the environmental conditions and biogeochemical functioning in such a way that, in comparison to intact peat swamp forest, C cycling and emission of CO_2 is altered (see below).

Carbon dioxide emissions

- H_0: CO_2 emissions are the same from channels draining both intact and degraded peat swamp forest, in both wet and dry seasons.
- $H_{1.1}$: CO_2 emissions are higher from channels draining intact peat swamp forest as an intact forest is more metabolically active than deforested peat swamp forest.

Radiocarbon age of dissolved CO_2

- H_0: ^{14}C-enrichment of dissolved CO_2 is the same for channels draining both intact and degraded peat swamp forest. A modern radiocarbon signature would suggest an age less than ˜70 years.
- H_1: The dissolved CO_2 of the intact channels will have a modern radiocarbon age. Dissolved CO_2 in the degraded channels will have a ^{14}C-enrichment lower than 100 %, and hence will be 'pre-modern', and likely hundreds to thousands of years old.

3.2 Materials and Methods

3.2.1 Study sites and sampling periods

The study sites were located in the province of Central Kalimantan, Indonesia. Of all the Indonesian and Malaysian provinces in Borneo, Central Kalimantan has the largest area of extant peat swamp forest; ˜4 Mha, of which >1 Mha has been degraded (Wulffraat et al., 2016). South and southwest of the provincial capital, Palangkaraya, are two large expanses of respectively intact and degraded peat swamp forest. The intact and degraded peat swamp forest is separated by the Sabangau River which runs south to the Java Sea. Both areas historically formed a continuous peat swamp forest ecosystem (de Vries, 2003).

Three ex-logging channels were sampled in intact peat swamp forest, in the Sabangau National Park, west of the Sabangau River. Light, selective logging activities occurred in the forest in recent decades, but the channels that were dug are comparatively small and do not greatly affect the water table of the forest peat dome throughout a year (Moore, 2011). The three channels are designated as 'SAB1', 'SAB2' and 'SAB3', respectively. They are 100s−1000s m long and reach part-way towards the centre of the peat dome, extending eastwards through the forest before discharging into the Sabangau River (Moore, 2011; see Fig. 3.1).

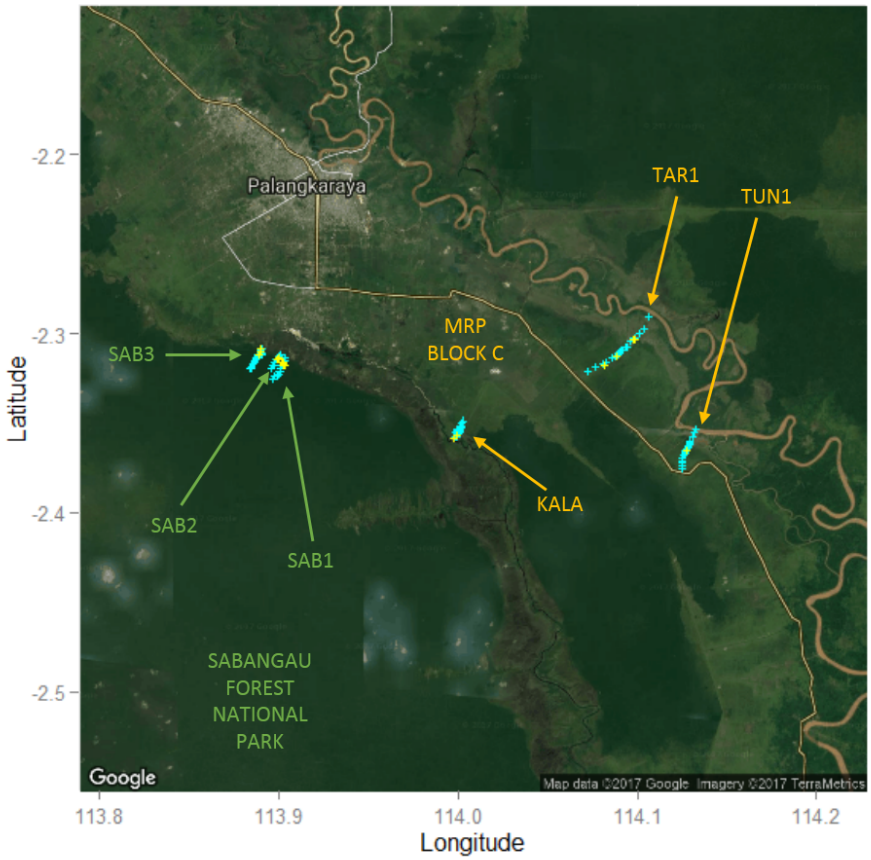

Figure 3.1: Map of the sampling region in Central Kalimantan, Indonesian Borneo. The provincial capital, Palangkaraya, is labelled. Wet season sampling locations are shown in light blue and dry season sampling locations in yellow. These do not indicate the extent of the channels, only the sampling locations. Much greater stretches of the channels were accessible during the late wet season, whereas the channels dried up to their downstream portions or even to puddles in the dry season. The intact Sabangau Forest National Park and degraded Mega Rice Project Block 'C' lie on opposite sides of the Sabangau River. (Source map © 2017 Google.)

North and east of the Sabangau River is a large expanse of degraded peat swamp forest. The peat swamp forest was deforested and drained for the now-defunct Mega Rice Project and is known as 'Block C', the largest of the five designated blocks of the ex-Mega Rice Project (Rais and Ichsan, 2008). Block C varies in terms of the length and depth of the channels that were constructed to drain this peatland, but in all cases they are much larger than those in the intact forest (Rais and Ichsan, 2008). The largest of the channels in the degraded peat swamp forest in the study, located in the Kalampangan (KALA) area, have the greatest impact on hydrological regulation of the catchment. The other degraded channels at Tarunajaya (TAR1) and Tumbangnusa (TUN1) are smaller and have less of an impact on catchment hydrology. As such, as the size, particularly the depth, of the channels increases, so does the hydrological impact and

degree of degradation to the surrounding catchment increase (Moore et al., 2013).

As described by Moore (2011) and Moore et al. (2013), TAR1 and TUN1 were considered to have undergone intermediate levels of degradation and were drained by intermediate-sized channels. The channels at TAR1 and TUN1 both discharge into the Kahayan River. The third degraded site, KALA, is more severely degraded as it has a very large 12 km-long channel running through the centre of −and significantly draining− two peat domes (see Chapter 2). The Kalampangan Canal reaches from the Kahayan River at its north east end to the Sabangau River at its south west end but does not directly discharge into these rivers. Running parallel to the ends of the canal and on both sides there are 'feeder channels' that receive water from the canal and discharge it into the rivers (Moore, 2011; see Fig. 3.2 and see Fig. 2.6 in Chapter 2). Sampling was only conducted at the Sabangau end of the Kalampangan Canal catchment; both feeder channels were used for sampling and because they drain the same catchment (Moore et al., 2013), and are referred to singularly as one site, KALA.

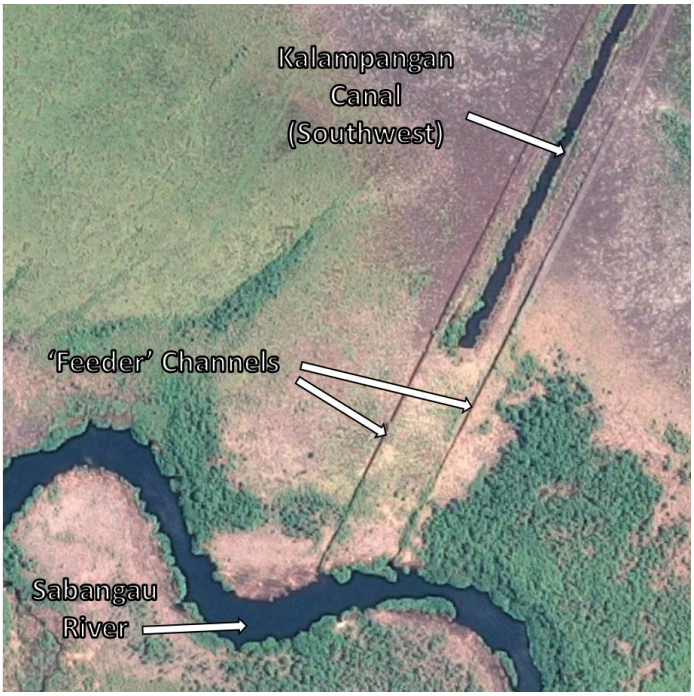

Figure 3.2: The Kalampangan Canal at KALA does not discharge its waters directly into the rivers at either of its ends. This is an aerial of the southwest end of the Kalampangan Canal showing the feeder channels that run parallel to, and drain, the canal. Here the feeder channels connect to the Sabangau River, and in the northeast end they connect to the Kahayan River. Both rivers flow southeast to the Java Sea. (Source map © 2018 Google.)

The six sampling sites (SAB1−SAB3 at the intact land class and TAR1, TUN1 and KALA at the degraded land class) were visited in a randomised rotation throughout the sampling period, i.e. a rotation would

include all sites, but the order of the sites would change between rotations. One site would be visited per day. The sampling periods occurred in the late part of wet season and the dry season of 2015. The dry season sampling occurred from July to September 2015, during the severe El Niño, which exacerbated a very low rainfall anomaly and conditions were unusually dry (Jiménez-Muñoz et al., 2016; L'Heureux et al., 2017). Fieldwork eventually had to be abandoned due to a national emergency being called by the Indonesian government as a result of the forest and peatland fires and accompanying extreme levels of air pollution (Koplitz et al., 2016).

The intact sites were accessed by foot in both seasons, as were the degraded sites in the dry season. During the wet season, the degraded sites could be accessed by boat and therefore a much greater coverage of the channel was possible (see Fig. 3.1).

3.2.2 Sampling methodology

Field measurements

Floating chambers were used to measure CO_2 fluxes from the channel surface (see Materials and Methods chapter for detailed descriptions of construction and deployment). Floating chambers have mostly been used to measure freshwater gas fluxes in lentic systems where it is common practice to anchor them in position (e.g. Cole et al., 2010). As the channels in this study were flowing, anchoring the chambers would likely have caused significant disturbance to the water, resulting in artificially enlarged gas emissions (Lorke et al., 2015). This study employed a novel design of floating chamber whereby battery-powered CO_2 sensors were installed into the chamber roof, allowing the floating chamber to move freely with the channel current, i.e. they could drift. As the chamber could drift in the channel, artificially enlarged fluxes due to water disturbance by the chamber were minimised (Lorke et al., 2015). The CO_2 sensors were SenseAir ELG sensor-loggers were set up as described in Bastviken et al. (2015), with the smallest measurement interval set at 2 min^{-1}. Chamber deployments consisted of five chambers being drifted for 5−10 minutes, depending on water flow velocity. Six deployments were typically made in a day, meaning that ˜30 individual fluxes were obtained per day. The data were plotted and each flux had a linear portion ($R^2 > 0.95$) identified at the start of the measurement period.

Dissolved gas samples were gathered by 2-minute syringe equilibration of a mix of 1:3 atmospheric air and channel water sampled from the top 10 cm of the channel, and samples of the channel

water were taken from the top 10 cm of the channel for analysis of total organic carbon (as described in Chapter 2). Environmental measurements of air temperature, air pressure, water temperature, pH, electrical conductivity and dissolved oxygen were taken by handheld probes as described in Chapter 2 (section 3.2). In this study a handheld anemometer was used to measure wind speed. The wind direction was ascertained by using smoke, and measurements were conducted for 1 minute after which an average over that period was calculated. Water velocity measurements were taken using a Valeport 002 electromagnetic current meter, if the channel was sufficiently deep enough to accommodate the impeller ($>$ 25 cm; in the dry season the water level was often too low). The impeller was inserted facing the flow of the water and averages were taken from 1-minute deployments. The sensitivity of the probe was restricted to $0.046-5.0$ m$\cdot$s^{-1}.

Laboratory measurements

Dissolved gas samples were analysed at the Open University, Milton Keynes, UK, using a Los Gatos Ultra-portable Greenhouse Gas Analyser (UGGA) and the injection loop method described by Baird et al. (2010). Partial pressures of the original dissolved gases were calculated by accounting for the dilution of ambient air during equilibration (see Chapter 2).

Total organic carbon was analysed by a Shimadzu TOC-V_{CPN} at the Open University, and DOC aromaticity was measured at the field station using a Cole-Parmer UV/visible spectrophotometer (230 VAC, 50 Hz), as described in Chapter 2.

Radiocarbon deployment and analysis

To establish the radiocarbon ages of the dissolved CO_2 in each of the channels, three molecular sieve cartridges were deployed in each the channels for one month during the latter part of the wet season. The functioning and use of the molecular sieve cartridges is described in Garnett et al. (2012) and Chapter 2. Once the molecular sieve cartridges had been retrieved, they were sent to the NERC Radiocarbon Facility in East Kilbride for analysis of ^{14}C-content. The unique lab codes of the samples, and the results of the analyses are provided in the Appendix Table 7.3. As analysis of the molecular sieves was expensive (approximately GBP300 per sieve), only three of nine intact samples were used in order to keep costs down. This also maximised the potential for all nine of the degraded samples to be radiocarbon-dated.

Dry season radiocarbon samples were not obtained as the trap rates of the molecular sieve cartridges could have been too slow to capture sufficient CO_2 before the water in the channels became too shallow. If the water was too shallow the molecular sieve cartridge samples could a) have been tarnished with atmospheric CO_2, or b) have become visible to local fisherpeople who might have tampered with them. Dry season radiocarbon ages would have been expected to be older as the CO_2 present in the channels would have come from the breakdown of deeper parts of the peat profile (Garnett et al., 2012).

Annual emission estimates

Annual flux estimates (F_{ann}) were calculated simply by multiplying the daily median fluxes by the number of days of their respective seasons, and adding the totals together using Equation 3.1:

$$F_{ann} = 273 \times \widetilde{F_{wet}} + 93 \times \widetilde{F_{dry}} \tag{3.1}$$

where 273 and 93 are the numbers of days in the wet and dry seasons (see Chapter 1), respectively, and $\widetilde{F_{wet}}$ and $\widetilde{F_{dry}}$ and the median fluxes of CO_2 ($g{\cdot}C{\cdot}m^{-2}{\cdot}d^{-1}$) in the wet and dry seasons, respectively.

3.2.3 Statistical analysis

Statistical analyses were performed as described in Chapter 2.

3.3 Results and Discussion

3.3.1 Water table and channel depth

Three years of water table depth data provided by the Borneo Nature Foundation recorded from January 2015 indicated that, in normal years, the normal water table amplitude at the intact land class typically ranged from near (or just above) the peat surface in wet seasons, and -25 cm in dry seasons (see Fig. 3.3). The exception was during the dry season of 2015, an El Niño year, during which it fell below -100 cm. This chapter, which discusses the differences between the wet and dry seasons of 2015 (LWS and EDS), therefore deals with the greatest seasonal differences in terms of water table encountered in the study period.

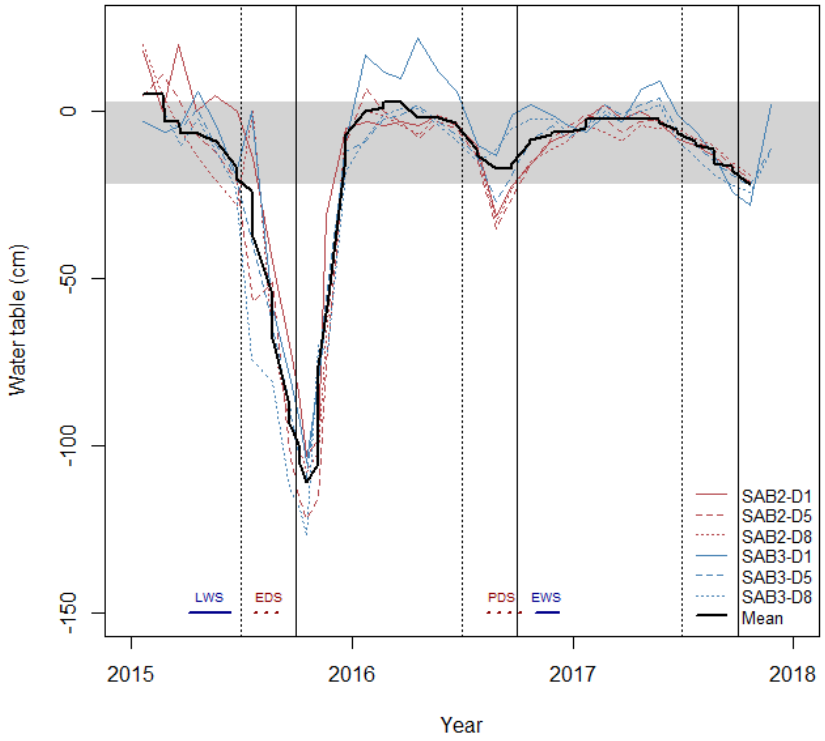

Figure 3.3: Water table data at the intact land class using measurements from three dipwells adjacent to both of the SAB2 and SAB3 channels. The water table data spans nearly three complete years with the mean water table in bold black. Typical starts of the dry and wet seasons (see Chapter 2) are represented by dashed and solid vertical lines, respectively. The four sampling seasons (see Chapter 2) are shown as solid blue and dashed red lines towards the base of the plot, respectively representing wet and dry seasons. Of the three years of water table data available, the extended dry season of 2015 (an El Niño) showed an uncharactersitic drop in water deble depth as compared to the mean range observed in the two following years (highlighted by the horizontal grey band; data provided courtesy of Borneo Nature Foundation.)

No water table data were available for the degraded land class during the study period. A study by Sundari et al. (2012) collected water table data at a degraded forest site (DF in Fig. 3.4), which is ˜400 m from the severely degraded site in this study (KALA). Over a two-year sampling period, the water table at DF was consistently lower than an intact forest site (UF) in the Sabangau National Park, near the intact land class investigated in this study (see Fig. 3.4).

What was not observed at DF in Sundari et al. (2012), despite being close to KALA, was that the water table at KALA could exceed 100 cm above ground during the wet season peaks. During these periods the channels would become subsumed by a larger floodplain surrounding the channels. This was also observed to occur at the other degraded sites in this study (TAR1, TUN1 and BER1) though the water table was not so high above the soil surface. DF may therefore be part of another catchment

which may not be so severely degraded as KALA as it is dominated by −and appears to support− secondary forest (regrowth following disturbance; Sundari et al., 2012) where KALA currently does not show significant signs of recovery. It is clear though that nearby channels in this area of Block C are having large impacts on the hydrology of the catchment, with respect to UF.

Water table amplitude at the degraded site in the Sundari et al. (2012) study was much greater than in the intact site, being 1.6 and 1.1 m, respectively. The amplitude of the water tables in this study were also larger at the degraded land class than at the intact land class which provides further evidence that degraded peat swamp forest is less able to hydrologically regulate itself.

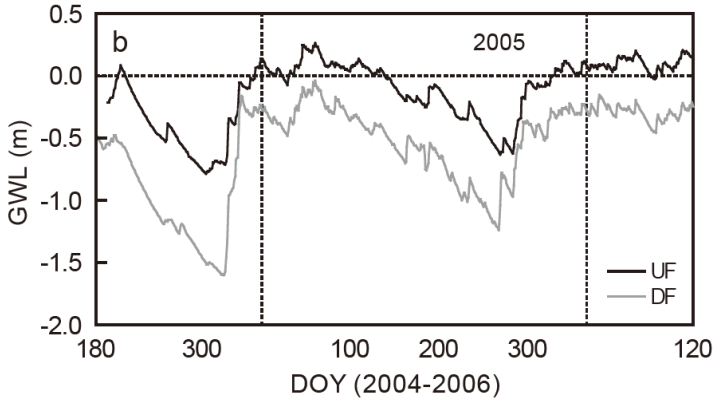

Figure 3.4: Water table (GWL = groundwater level) data for intact and degraded peat swamp forest sites located near (within 2 km) to the intact and degraded study sites in this investigation. Data were gathered over two years shown here as the day in the year (DOY) between 2004−06. The dashed vertical lines indicate the first day of a year. The water table in the intact area (UF) was consistently higher than the degraded area (DF). Typically the DF water table was ~50 cm lower than the UF water table, but during dry periods the difference could be more ($\leq$100 cm), and during wet periods could be less ($\geq$5 cm). This indicates that degraded peat swamp forest is less hydrologically stable than intact peat swamp forest. Plot reproduced from Sundari et al. (2012).

Sundari et al. (2012) found that soil respiration responded strongly to changes in the water table at both the UF and DF sites; CO_2 efflux decreased in UF which resulted from anoxia when the water table was high. In DF, soil respiration increased when the water table dropped below -0.8 m. These changes in rates of soil respiration suggest that changes to dissolved CO_2 in the channels could be expected. As the amount of water reaching the channels could reduce, so too could the amount of dissolved CO_2 and degradable organic material.

In the late wet season channel depths were significantly higher at the degraded land class (median = 150 cm) than at the intact land class (median = 45 cm; Wilcoxon's rank sum test; W = 65, p = 0.0002, r = -0.87; see Fig. 3.5, left pane). These median channel depth values represent the approximate channel

depths at their respective land classes, demonstrating that the channels are significantly deeper at the degraded land class. In the right pane of Fig. 3.5, the channel depths are represented as water level relative to the soil surface. At the degraded land class in the late wet season, the water level was nearly 150 cm above the peat surface; the channels had been subsumed into a floodplain that filled the lower part of its catchment. This significant flooding was distinctly different to the intact land class where the channels were at times overbanked, but only by ˜10 to 20 cm, however the water level relative to the peat surface was not significantly different in the late wet season; median water levels relative to the peat were -12 cm and 2 cm for the intact and degraded land classes, respectively. The slightly lower level at the intact land class may have resulted from the vegetation actively transpiring the water, whereas at the degraded land class negligible vegetation existed to carry out this process on a large scale.

Wet season flooding of degraded catchments could occur a) because the lack of forest cover would limit the amount of surface and groundwater that can be transpired back to the atmosphere, and/or b) because oxidised peat layers could be subsiding causing elevation to decrease so that it is more similar to the adjacent rivers. Degradation clearly affects the hydrological functioning of peat swamp forest with respect to its natural, forested state. As a result, degraded catchments can be inundated by metres of water, for several months, during the peak of the wet season. The greater variance in channel and water table depths at the degraded land class, in both the wet and dry seasons, is due to the deeper channels impairing the catchments ability to maintain its water table.

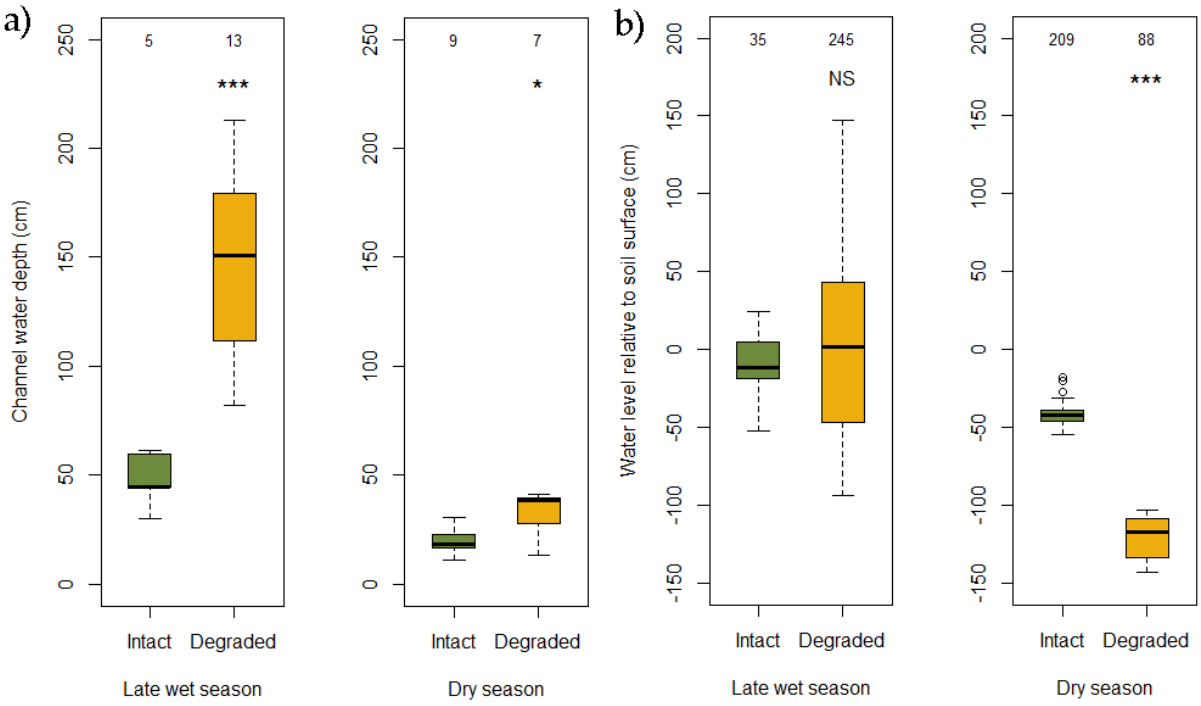

Figure 3.5: Panel a) Average channel water depth measurements at the intact and degraded land classes in the late wet and dry seasons of 2015. Water depth was significantly different in the wet season (p = 0.0002). In the dry season water depth lowered at both land classes, but the statistical significance was marginal (p = 0.054). The values for the wet season represent the median depths of the channels at their respective land classes. Panel b) Channel water level measurements the channel relative to the soil surface in the late wet and dry seasons of 2015. In the wet season, the channels at both land classes were mostly at bankfull and statistically non-signifcant, however the degraded land class was much more variable and it also flooded up to 1.5 m above the soil surface. In the dry season, water levels dropped at both land classes, however the drop at the degraded land class (median = 117 cm) was statistically much greater than at the intact land class (median = 42 cm; Wilcoxon's rank sum test, $p < 2.2 \times 10^{-16}$).

In the dry season the channels' water depths dropped. Median depths were 18.5 and 38.3 cm for intact and degraded land classes, respectively. Depths were marginally significantly different, and the effect size was also smaller than during the late wet season (Wilcoxon's rank sum test; W = 13, p = 0.054, r = -0.48). When the water depth measurements were converted to water level relative to the peat surface (see Fig. 3.6), it showed the water table had dropped to -42 cm at the intact land class. This was significantly less than the degraded land class which reached a median of -117 cm (Wilcoxon's rank sum test; W = 15,136, $p < 2.2 \times 10^{-16}$).

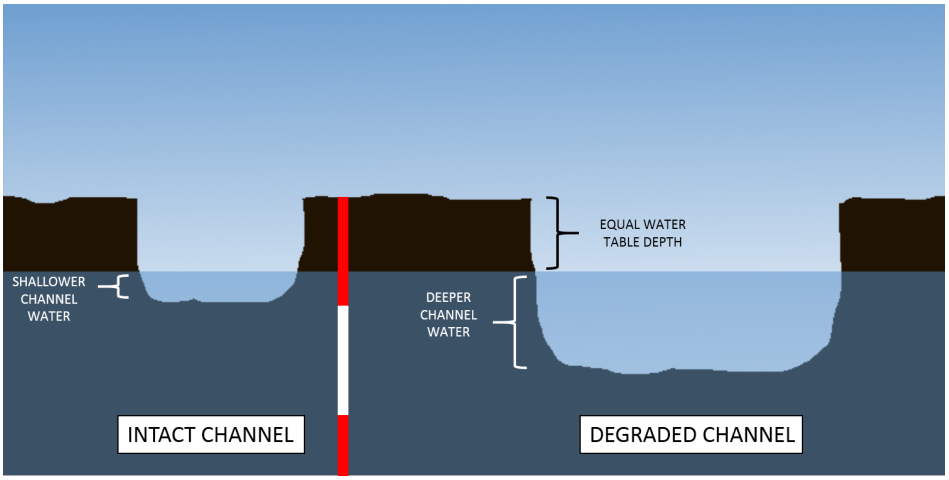

Figure 3.6: Schematic of the channels at the intact and degraded land classes. The channels at the degraded land class were approximately a metre deeper than the channels at the intact land class. The channel depth in the degraded channels would have to be much higher to have an equal water table with the intact land class. If the channel depth is near equal then the water table would have to be much lower.

The water table data provided by the Borneo Nature Foundation showed that water table amplitude at the intact land class is normally from the peat surface to -25 cm depth. The low rainfall during the dry season (during 2015 El Niño) caused an uncharacteristic drop to over -100 cm, reaching levels comparable to the degraded land class. Although no water table data were available for the degraded land class, the channel depth measurements broadly agree with the findings of Sundari et al. (2012) in that the degraded land class is significantly lower throughout the year, with respect to the intact land class. The exception to the findings of Sundari et al. was that during the wet season the water level at the degraded land class can be much higher than the peat surface when it floods. This happens at the periphery of the peat dome where the data were collected. This finding provides further evidence that the degraded land class is far less able to hydrologically regulate itself and experiences much greater seasonal extremes, potentially making it difficult for vegetation to recover in such areas.

3.3.2 Air and water temperatures

Air temperature and sunlight have effects on water temperature. In freshwater ecosystems, where salinity is negligible, water temperature largely dictates the solubility of gases; as water warms the solubility of gases reduces and promotes a higher rate of gas emission to the atmosphere (e.g. Benson and Krause, 1984). Air and water temperatures were measured at several points each day (see Fig. 3.7).

Air temperatures were highly and significantly different between land classes, with large effect

sizes ($r > 0.5$) in both late wet and dry seasons (Wilcoxon's rank sum tests; respectively, W = 11,732, $p <$ 2.2 $\times 10^{-16}$, r = -0.74 and W = 2,141.5, $p = 3.34 \times 10^{-9}$, r = -0.59).

Water temperatures were similarly significantly different between land classes, again with large effect sizes in both late wet and dry seasons (Wilcoxon's rank sum tests; respectively, W = 12,075, $p < 2.2 \times 10^{-16}$, r = -0.86 and W = 3,072.5, $p = 2.78 \times 10^{-12}$, r = -0.63).

Water and air temperatures were most significantly different, and had the strongest effects sizes, in the late wet season.

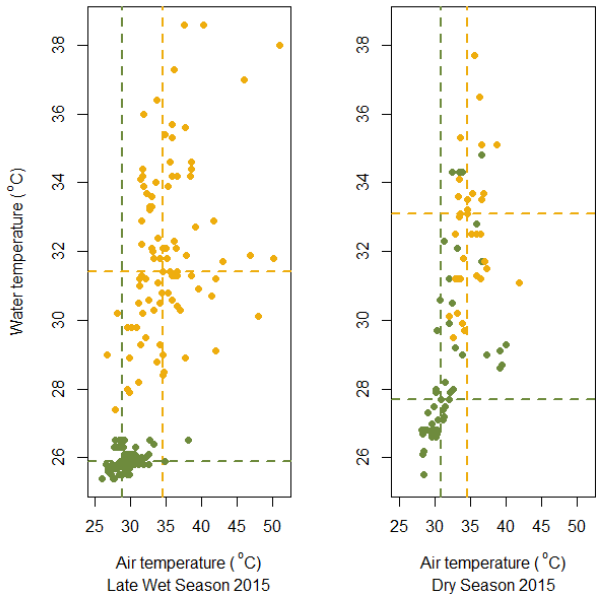

Figure 3.7: Daytime air and water temperatures at the intact (green) and degraded (yellow) land classes, in the late wet and dry seasons of 2015. Median values are indicated by the dashed lines. Air and water temperatures were significantly different between land classes in both seasons. Median water and air temperatures at the intact land class were 3−5 °C cooler than the degraded land class. In the wet season, water and air temperatures were more constrained than the degraded land class, due to the forest canopy producing a microclimate effect. The microclimate effect in the intact land class was still evident in the dry season, except for measurements taken at the more exposed forest fringe. Temperature fluctuated more at the forest fringe in a similar way to the degraded land class.

In the late wet season, intact land class daytime air and water temperatures were lower, and very constrained compared to the degraded land class which demonstrated a high variability. In the late wet season, median recorded air and water temperatures were 28.8 and 25.9 °C for the intact sites and 34.6 and 31.4 °C for the degraded sites; the air and water at the degraded land class was on average 5−6 °C warmer than for the intact land class. In the dry season median air temperatures increased to 30.8 and 34.6 °C for the intact and degraded land classes, respectively, and the difference between the land

classes was not as great as the late wet season. Water temperatures were still 5−6 °C apart but increased to medians of 27.7 and 33.1 °C for intact and degraded land classes, respectively.

The higher temperatures at the degraded sites result from the lack of forest cover and, as a result, no canopy interception of sunlight. Further, exposed dark, bare peat surfaces were much more abundant at the degraded sites (particularly at KALA) resulting in a low albedo, greater absorption of solar energy and release back into the air as heat (Price et al., 1998). As such, air and water temperatures were higher.

Also evident in the temperature data is the effect of abundant surface water (pools and runnels) and higher humidity in the wet season which modulate the temperature within the intact forest, creating a moister, cooler microclimate (Gotsch et al., 2014). Air and water temperatures within the intact forest during the wet season were much more constrained than in the dry season when comparatively little standing surface water was present.

3.3.3 Electrical conductivity

The electrical conductivity (EC) meter ceased functioning after the pilot field season after being placed in storage and therefore it was not possible to collect EC data during the late wet and El Niño dry seasons (LWS and EDS), or TUN1. Another EC meter was procured for the final two field seasons (the post-El Niño and early wet seasons, or PDS and EWS, respectively), and therefore EC data from these field seasons are presented. These EC data are from the sites and also the rivers into which they drain, as the water from these rivers could sometimes invade into the channels as a result of tidal reach or high rainfall in the catchment (see Fig. 3.8). These data were gathered to examine whether saline waters had entered the channel which may have resulted in the flocculation of DOC.

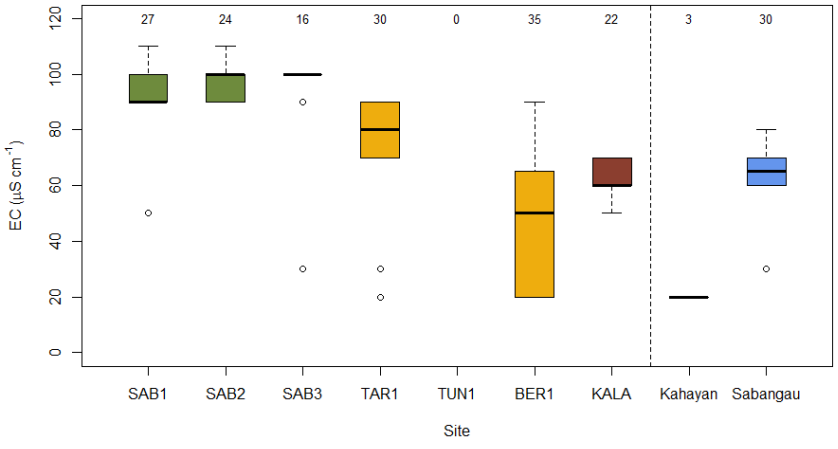

Figure 3.8: Electrical conductivity at the intact and degraded land classes in the post-El Niño dry season (PDS) and early wet season (EWS) of 2016. Also included in the right hand portion of the plot are some EC measurements from the Kahayan River (into which the channels of the intermediately degraded sites discharge), and the Sabangau Rivers (into which the channels of the intact and severely degraded sites discharge). Readings did not exceed 110 μS·cm^{-1} which indicated that there had not been any influence from saline waters invading the channels.

The intact sites had the highest EC values with 97 % of observations falling between 90−110 μS·cm^{-1}, but these higher values were still characteristic for those of freshwaters (Weiss, 1974). 90 μS·cm^{-1} was the highest value recorded at any of the degraded sites, and they fell as low as 20 μS·cm^{-1}. Median EC values at the degraded sites were 80, 50 and 60 μS·cm^{-1} for TAR1, BER1 and KALA, respectively.

The Kahayan River, into which the channels at TAR1 and BER1 drain, typically had a very low EC (20 μS·cm^{-1}). The lower EC values for TAR1 and BER1 suggest a possible influence on water chemistry from the Kahayan River, but as EC was never higher than the intact sites, and that in all cases the EC was low, it did not suggest any influence of tidal reach and saline waters. The Sabangau River had a higher EC than the Kahayan River (median = 65 μS·cm^{-1}), but still this was very low, also suggesting that KALA was not influenced by invading saline waters. The results demonstrate that increased salinity from tidal reach did not affect DOC or gas flux measurements.

3.3.4 Dissolved oxygen

Higher water temperatures would be expected to reduce the solubility of dissolved gases in the channel waters, however dissolved oxygen concentrations increased at both land classes during the warmer dry season. Further, between land classes, the degraded sites had significantly higher dissolved oxygen concentrations in both sampling seasons (Wilcoxon's rank sum tests; W = 1,530.5 and 805.5, $p = 5.85 \times 10^{-14}$ and $p = 1.58 \times 10^{-7}$, r = -0.55 and -0.47 for late wet and dry seasons, respectively; see Fig. 3.9).

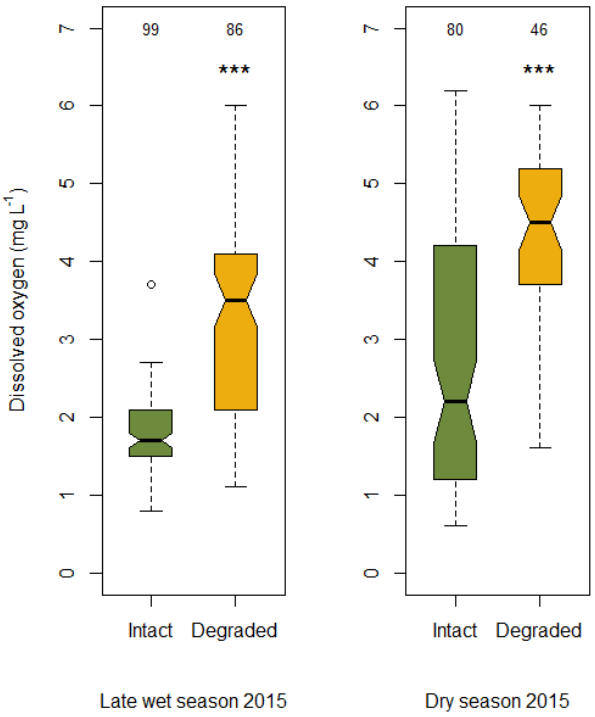

Figure 3.9: Median dissolved oxygen concentrations at the degraded land class were approximately double those of the intact land class. In both seasons concentrations were significantly different, but less so in the dry season (late wet season $p = 5.85 \times 10^{-14}$; dry season $p = 1.58 \times 10^{-7}$. In the wet season, the intact and degraded land classes contained 1.7 and 3.5 mg·L^{-1}, respectively, and in the dry season the concentrations were 2.2 and 4.5 mg·L^{-1}, respectively.

At the degraded sites median oxygen concentrations were ˜2−times those of the intact sites in both seasons; in late wet and dry seasons, respectively, 3.5 and 4.5 mg·L^{-1} compared to 1.7 and 2.2 mg·L^{-1} for the intact sites. In freshwater environments, at the temperatures encountered, surface water would contain a dissolved oxygen concentration of approximately 8.3−6.4 mg·L^{-1} were it to be in equilibrium with the atmosphere (Benson and Krause, 1984). This suggests that oxygen was being consumed, most likely by heterotrophic processes, in the channels of both land classes. As the channels at the intact land class contained significantly less oxygen it indicates that more oxygen was being consumed in the intact channels, indicating higher amounts of aerobic, heterotrophic metabolism (e.g. Hondzo and Steinberger, 2008; Rixen et al., 2008).

If the dissolved oxygen concentrations were to be presented as percentage saturation, the differences between land classes would be further amplified; water temperatures at the degraded land class were warmer, and hence less oxygen can dissolve in them than at the cooler, intact land class. There are two main reasons for why dissolved O_2 may be lower at the intact land class: a) O_2 could have been consumed by higher rates of in-stream degradation processes such as heterotrophic breakdown or

photolysis, or b) if the catchment is the main source of dissolved O_2 to the channels and that this O_2 is arriving faster than the channel can achieve equilibrium with the atmosphere, then the pore water at the intact land class may be more depleted in O_2 than the degraded land class.

Identifying the sources and sinks of O_2 in the channels was beyond the scope of the study; biological oxygen demand/oxygen utilisation experiments were not conducted, nor measurements of pore water concentrations in the surrounding peats, therefore the reasons can only be speculated about. However, pore water O_2 measurements carried out at the intact land class by Pangala et al. (2013), and at the degraded land class by Adji et al. (2014) suggest that pore water O_2 was lower at the degraded land class than at the intact land class (2−8 and 5−13 μmol L^{-1}, respectively). From these measurements it appears that the degraded land class might have lower concentrations of dissolved O_2 in the channels if lateral transport from the catchment was the primary driver of O_2 levels. However, it is highly likely lateral transport of O_2 does take place. Degradation of DOC is therefore favoured as an explanation of the lower O_2 concentrations in the channels for reasons explained below.

These channels, classed as 'blackwaters' (see Materials and Methods), are characteristically high in dissolved organic carbon (DOC) which would provide the substrate for microbial metabolism in the channel. Low oxygen concentrations could be caused by breakdown of a) leaf litter (O'Brien et al., 2017), which would be considerably higher at the forested intact land class, or b) abundant DOC that is more labile and bioavailable, which is more the case for the intact land class rather than the degraded land class (Moore et al., 2013). High concentrations of DOC (Rixen et al., 2008; Wit et al., 2015) and dissolved CO_2 (Müller-Dum et al., 2019; that might derive from DOC degradation) in blackwaters have been shown to be inversely correlated to dissolved oxygen concentrations. The water is noticeably darker in the intact channels compared to the degraded channels, indicating higher concentrations of DOC.

A previous study that used the same intact and degraded peat swamp forest channels found that the channels in degraded the degraded sites had lower concentrations of DOC, and a higher aromaticity of that DOC compared to the peat channels at the intact sites. The more aromatic DOC was comparatively more recalcitrant and less bioavailable and more resistant to breakdown by biological means (Moore, 2011; Moore et al., 2013). The much higher oxygen concentrations encountered at the degraded land class in this study indicate that dissolved oxygen concentrations were not a limiting factor for heterotrophic metabolism, and less heterotrophy is occurring, than at the intact land class. Lower rates of

heterotrophy would produce proportionally less dissolved CO_2 in the channels. As the intact channels had much lower dissolved oxygen concentrations, it is likely that higher rates of heterotrophic respiration are occurring there, consequently producing larger quantities of dissolved CO_2.

In terms of water table, air and water temperatures and dissolved oxygen, it is clear that degradation has myriad effects on the peat swamp forest microclimate and channel geochemistry, in ways that are relevant to CO_2 emissions from the channels, which will be discussed in the next section.

3.3.5 Quantity and quality of DOC

Across the three sampling seasons (LWS, EDS and PDS) where DOC measurements were made at all sites, median DOC concentrations were consistently highest at the intact sites, ranging from 54.4 to 58.1 mg·L^{-1} (see Fig. 3.10). At the degraded sites, median concentrations were 46.6, 45.4, 22.5 and 29.3 mg·DOC·L^{-1} for TAR1, TUN1, BER1 and KALA, respectively.

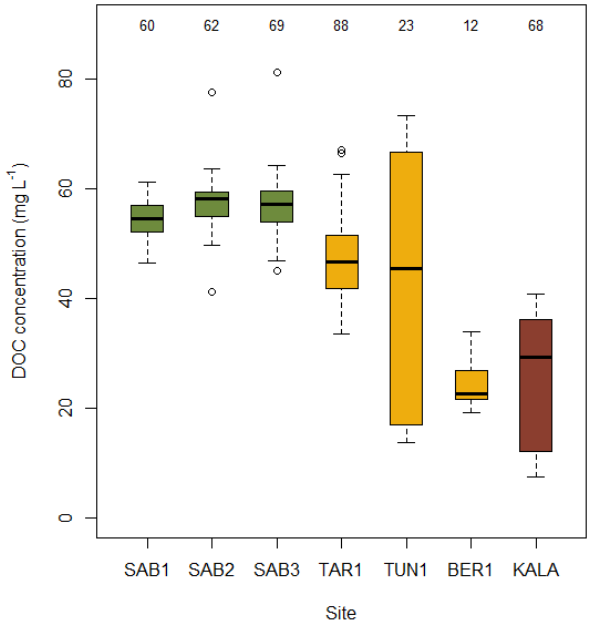

Figure 3.10: DOC concentrations at each of the sites, spanning the LWS, EDS and PDS field seasons. Median intact DOC concentration was consistently highest at the intact sites (54.4 to 58.1 mg·L^{-1}), with DOC concentration generally declining as severity of degradation of the PSF catchments increased; DOC concentrations were 46.6, 45.4, 22.5 mg·L^{-1} respectively for TAR1, TUN1 and BER1 (the intermediately degraded sites), and 29.3 mg·L^{-1} for KALA, the severely degraded site.

The results show a general trend whereby DOC concentration in the channels reduces with increasing disturbance, the exception being BER1 which had the lowest median DOC concentration, but this may have been due to significantly fewer sampling days occurring at this site, with respect to the others.

DOC concentrations in the channels were significantly different between intact and degraded land classes in both seasons (Welch's two sample t-tests; respectively, t = 9.03, $p = 2.54 \times 10^{-14}$, r = -0.61 and t = 10.66, $p < 2.2 \times 10^{-16}$, r = -0.67; see Fig. 3.11). Concentrations remained similar at both land classes in both wet and dry seasons, however the interquartile range was much larger for the degraded land class in the dry season indicating that lower concentrations of DOC were more common.

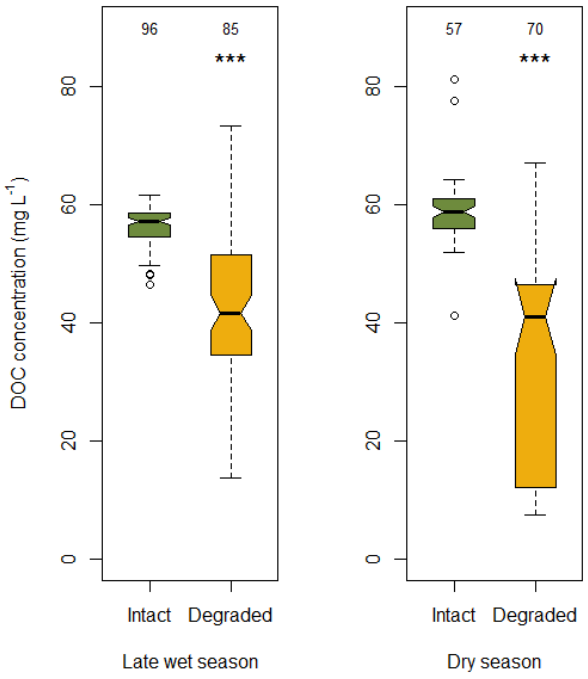

Figure 3.11: DOC concentrations at the intact and degraded land classes in the late wet and dry seasons. In the late wet season, the intact land class (median = 57.1 mg·DOC·L^{-1}) had significantly higher DOC concentrations than the degraded land class (median = 41.7 mg·DOC·L^{-1}; $p = 2.54 \times 10^{-14}$). Similarly, in the El Niño dry season, the intact land class had significantly higher DOC concentrations than the degraded land class (respective medians = 58.8 and 41.0 mg·DOC·L^{-1}; $p < 2.2 \times 10^{-16}$).

These results agree broadly with DOC concentrations presented in Moore et al. (2013) where there was no particular seasonal trend in DOC concentrations in these channels (particularly, see Supplementary Materials), whereas a seasonal signal was evident in the Sabangau River (Moore et al., 2011). These results show that lateral input of DOC is important for these peat-draining channels, as during the dry season there was negligible rain to deliver leachates and organic material to the channels where they would provide DOC.

In the final sampling season (early wet season; EWS) both DOC concentration and aromaticity were investigated as part of a DOC degradation experiment, but for logistical reasons it was only possible to gather samples from two sites; SAB1 from the intact land class, and KALA from the degraded land

class. The values represent paired starting values at the beginning of an incubation whereby the water samples were collected fresh and analysed within a few hours of collection (see Fig. 3.12).

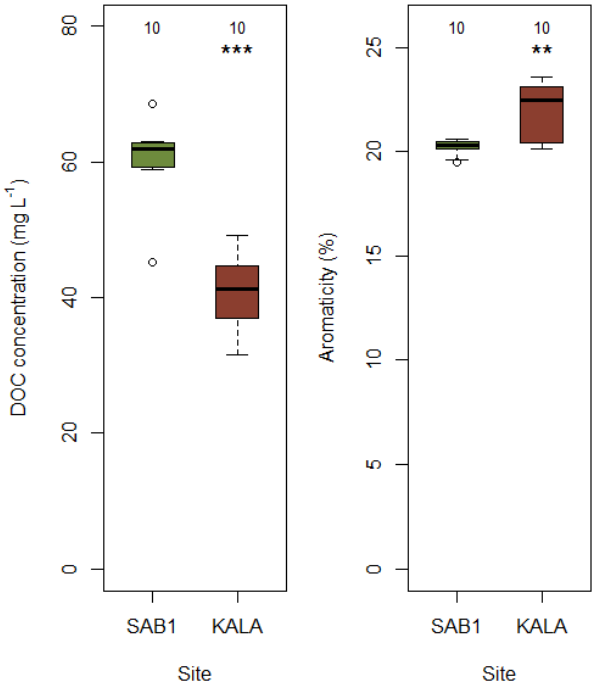

Figure 3.12: DOC concentrations and aromaticity of SAB1 and KALA in the final sampling season, EWS. SAB1 had a significantly higher DOC concentration than KALA (respective medians = 61.9 and 41.4 mg·DOC·L^{-1}; $p = 9.00 \times 10^{-7}$), and the DOC from KALA was significantly more aromatic than SAB1 (respective medians = 22.5 % and 20.3 %; $p = 0.00135$).

Median channel DOC concentrations at SAB1 (61.9 mg·L^{-1}) were significantly higher than at KALA (41.4 mg·L^{-1}; two sample t-test, t = 7.28, $p = 9.00 \times 10^{-7}$, r = -0.80). This trend very much resembled the findings from the earlier seasons in this study that DOC concentrations at sites and the intact land class are significantly higher the sites at the degraded land class sites. These samples from EWS, which were analysed within hours of collection, also suggest that DOC losses in the samples that were stored untreated for up to 12 weeks (LWS, EDS and PDS) were in the region of 8 % for the intact sites, but were perhaps negligible for the degraded sites. The difference between the two land classes is therefore likely to be an underestimate. If DOC losses were smaller for the degraded sites this suggests more aromatic, recalcitrant DOC is present in the channels of the degraded land class.

Aromaticity was also measured in the EWS water samples and was found to be significantly higher at KALA than at SAB1, where median aromaticities were 22.5 and 20.3 %, respectively (two sample t-test, t = -3.79, $p = 0.00135$, r = -0.54). This is in agreement with the findings of Moore et al. (2013) who demonstrated that channel DOC at the degraded land class was typically hundreds to thousands

of years-old and originated in deep peat layers. In that study the DOC from the intact channels had a modern radiocarbon signature, indicating more labile, less aromatic substrate addition from the surrounding catchment into the channels. These data also suggest that the lower dissolved oxygen levels in the channels at the intact land class may be due to greater availability and biodegradation of labile DOC, whereas oxygen was less likely to be consumed by heterotrophic processes at the degraded land class where more aromatic DOC was more present in the channels.

Further analysis of the DOC samples from SAB1 and KALA using Thermal Desorption−Time of Flight−Proton Transfer Reaction−mass spectrometry (TD-ToF-PTR-MS) was conducted by Materić et al. (2017). It was found that the channel DOC molecules from KALA were heavier than at SAB1 (DOC, SAB1 and KALA are referred to as DOM, KI and KD in the paper; see Fig. 3.13). This adds further evidence that the DOC at the degraded sites is less labile and more recalcitrant than the intact sites, and therefore is less likely to be broken down by biological processes in the stream to produce dissolved CO_2 Results of measurements of dissolved CO_2 in the channels will be presented and discussed in the following section.

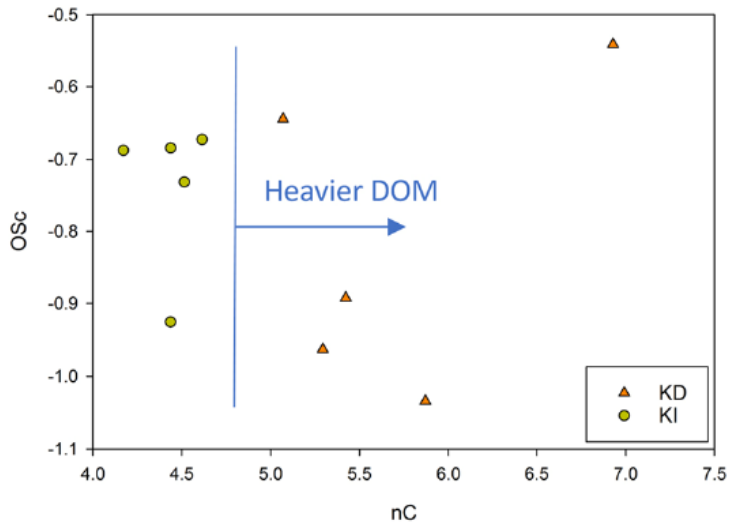

Figure 3.13: Results of TD-ToF-PTR-MS analyis of DOC samples from SAB1 and KALA. There was no clear trend in the mean oxidative state of carbon (OSc) between the two sites, however there was clear separation in the number of carbon atoms per molecule (nC) whereby KALA demostrated the heavier −and therefore larger− molecules. Figure from Materić et al. (2017).

Overall, the DOC in the channels draining degraded peat swamp forest looks to be less abundant and more aromatic than at the intact land class. This is consistent with the water table being generally lower in degraded peats and therefore the organic carbon in the channels is more recalcitrant. DOC abundance did not show significant seasonal variation, and therefore it suggests that overland flows may not be

a dominant method of delivery of DOC to the channels. However, DOC movement over and through the peat was not measured and further studies are required to identify the sources of the DOC in the channels at the two land use types, and how those sources may vary in importance on a seasonal basis.

3.3.6 Partial pressure of dissolved CO_2

During the late wet season, all median partial pressures of dissolved CO_2 at the intact sites were higher than those of the degraded sites and exceeded 13,000 μatm, being 13,523, 13,529 and 13,453 μatm for SAB1−3, respectively. At the degraded sites, the intermediately degraded TAR1 and TUN1 sites had the highest values at 11,668 and 13,485 μatm CO_2, respectively. While TAR1 was markedly lower that the intact sites, TUN1 was in the same range as the intact sites with the median exceeding those of SAB2 and SAB3. The severely degraded site, KALA, had the least dissolved CO_2 at 6,023 μatm, less than half that of either the intact or intermediately degraded sites (see Fig. 3.14). This supports the findings of Moore et al. (2013) that DOC becomes less abundant and more resistant to biological breakdown in response to degradation of the peat swamp forest ecosystem. However, it is also likely that leaf litter inputs to the channels at the intact land class promote heterotrophy and higher dissolved CO_2.

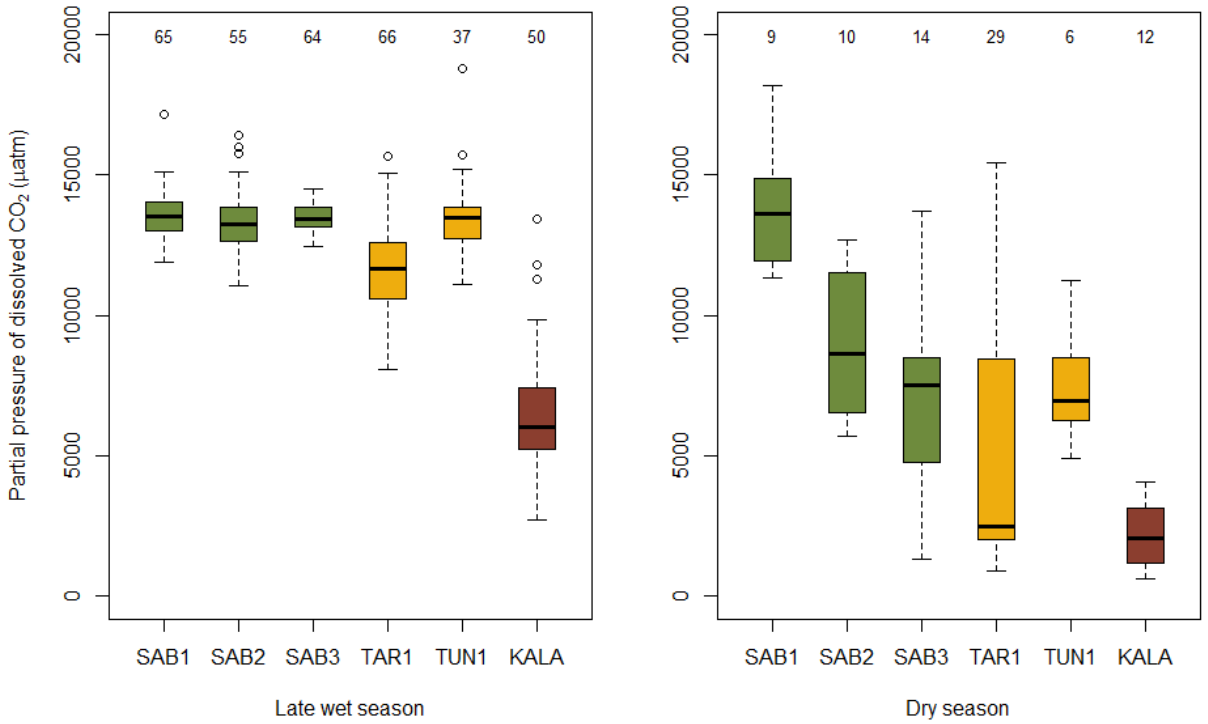

Figure 3.14: Median dissolved CO_2 partial pressures were consistently higher at the intact sites than at the degraded sites, in both late wet and dry seasons of 2015. KALA in the late wet season was much lower than intact and intermediately degraded sites. In this season intact and degraded dissolved CO_2 medians ranged from 13,259 to 13,523, and 6,023 to 13,485 μatm, respectively. In the dry season, intact and degraded dissolved CO_2 respectively ranged from 7,503 to 13,626 and 2,069 to 6,954 μatm. SAB1 was the only site to show an increase, though it was by comparatively little.

In the dry season, partial pressures of dissolved CO_2 decreased markedly at all sites, apart from at SAB1. Intact partial pressures at this time were respectively 13,626, 8,621 and 7,503 μatm at SAB1$-$3, and 2,480, 6,954 and 2,069 μatm at TAR1, TUN1 and KALA. The dry season data mostly displayed greater variance in values than the late wet season data which may be due to the comparatively smaller sampling sizes, and the wider range and extremity of environmental conditions encountered during the dry season. In terms of median dissolved CO_2 values, the degraded sites were consistently ranked TUN1 $>$ TAR1 $>$ KALA.

The partial pressures of dissolved CO_2 at the intermediately degraded TAR1 and TUN1, particularly, were higher than expected. TAR1 and TUN1 were disturbed (deforested and drained) at approximately the same time as KALA, but the degree of the disturbance was less (Moore, 2011). TAR1 and TUN1 have since re-vegetated to an extent, albeit with ferns and grasses, rather than secondary forest. This vegetation likely produces more labile DOC that on reaching the channels can be more readily degraded than the older, more humified and recalcitrant DOC from the KALA catchment peats. Further, both TAR1 and TUN1 had human settlements nearby, as opposed to KALA which was uninhabited. Settlements in the area are nearly always adjacent to channels, which are utilised for sanitation and transport by boat. At TUN1, particularly, there was a strong smell of faeces in the channel. The input of fresh degradable material being flushed from the village could have fertilised the channel and been broken down causing dissolved concentrations of CO_2 to increase above what they would have naturally been without any settlement nearby (e.g. Meybeck and Vörösmarty, 1999).

Water temperatures increased at both sites in the dry season, and leaf litter inputs presumably continued (though reduced lateral flow would reduce the amount of leachate reaching the channels). Continued priming by leaf litter would therefore be expected to cause heterotrophy to increase and oxygen concentrations to decrease, considering that the water volume in the channels is lower in the dry season. However, oxygen concentrations increased and it indicates that leaf litter input may not be the dominant driver of dissolved CO_2. Further, dissolved CO_2 decreased almost 3$-$fold at KALA where

leaf litter input would be negligible, being that there is very little vegetation in the catchment. This may indicate that DOC degradation and lateral flows are the main sources of dissolved CO_2 in the channels.

If the dominant term for dissolved CO_2 in the channels is DOC, then the data suggest that the most degradable (most labile, least humified) DOC of the degraded sites might be found at TUN1, and the least degradable at KALA. However, aromaticity data were only available for KALA and was is not possible to make this comparison. If dissolved CO_2 in the channels is mostly controlled by lateral inputs of CO_2, then the water table could be the dominant term; the water table is a proxy for the volume of wetted peat 'connected' to the channels that could act as a source for dissolved CO_2, such as in the study of Ueda et al. (2000) who noted a hydrological driver of dissolved CO_2 between wet and dry seasons at a coastal swamp in Thailand.

Rainfall declines markedly in the dry season and the water table lowers, sometimes well below the peat surface (Hirano et al., 2009), including in the channels during extremely dry episodes (as was witnessed during the dry season in question). This reduces the volume and connectivity of wetted soil in the catchments, which would consequently limit a) the volume of biologically active soil, and b) the ability of soil organisms and metabolites to be transported to the channels (e.g. Marwanto and Agus, 2014). In the wet season, by comparison, there could be continual transport of organisms and metabolites to the channels by overland and through-flows, which could stimulate higher rates of metabolism in-stream. Further, a biologically active soil could also produce CO_2 that could be entrained by through-flows of water and get deposited in the channels.

The intact land class in the late wet season had a median partial pressure of dissolved CO_2 of 13,359 μatm and a smaller variance in the data than the degraded land class, where median dissolved CO_2 was 11,637 μatm (see Fig. 3.15). A Wilcoxon's rank sum test found degraded dissolved CO_2 to be significantly lower than at the intact land class (W = 9,316, $p = 8.06 \times 10^{-12}$, r = -0.37).

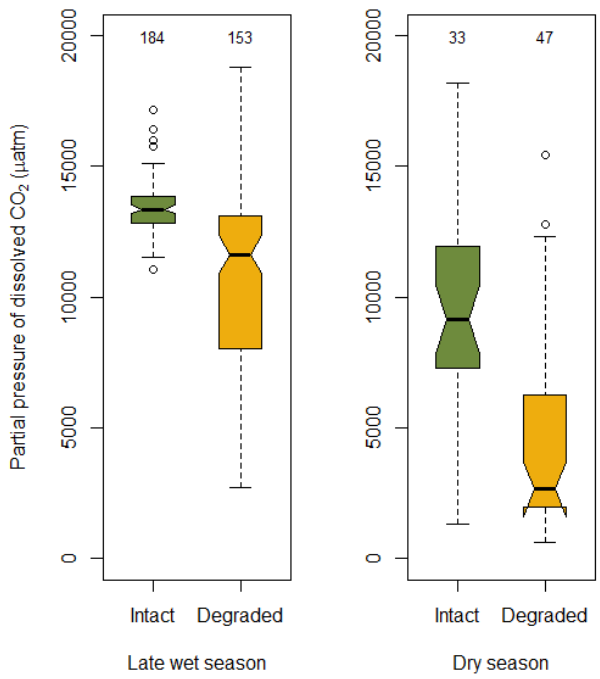

Figure 3.15: Median dissolved CO_2 partial pressures were higher at the intact land class in both sampling seasons, but the values more constrained in the former. In the late wet season, intact and degraded median dissolved partial pressures were respectively 13,359 and 11,637 μatm CO_2, and in the dry season, 9,148 and 2,669 μatm CO_2. In both seasons, degraded dissolved CO_2 was significantly lower than at the intact land class (late wet season: $p = 8.06 \times 10^{-16}$; dry season: $p = 7.74 \times 10^{-6}$).

In the dry season, median dissolved CO_2 was lower for both intact and degraded land classes which were 9,148 and 2,669 μatm and constituted 32 % and 77 % reductions in dissolved CO_2, respectively. Degraded dissolved CO_2 remained significantly lower than the intact land class (Wilcoxon's rank sum test, W = 1,112, $p = 7.74 \times 10^{-6}$, r = -0.50).

The partial pressures of dissolved CO_2, particularly for the intact sites in the late wet season (median = 13,358 μatm) were relatively high in terms of those reported for tropical streams and rivers in the literature; Aufdenkampe et al. (2011) estimated a median partial pressure of 4,300 ppm CO_2 in tropical streams. However, most studies are conducted in relatively large rivers rather than upstream reaches or headwaters (Cole et al., 2007; Johnson et al., 2008). The channels investigated in this study are more similar to small headwater streams, and the partial pressure of CO_2 is known to decrease as stream order increases (Dawson et al., 2004; Johnson et al., 2008). This is because the most labile substrates are consumed first, leaving the material that is harder to metabolise to flow downstream (Meyer and Edwards, 1990; Ilina et al., 2014). Richey et al. (2002) observed 14,100 $\pm$ 12,000 μatm in upstream reaches and 6,300 $\pm$ 4,200 μatm in downstream reaches of the central Amazon basin. The upper figure, derived from the

headwater of a tropical peat catchment in Amazonia is certainly in the range encountered in this study, in an equivalent setting. In a very similar ecosystem in Borneo, Müller et al. (2015) measured 6,130−8,943 μatm in a river draining tropical peats in Sarawak, Malaysia. These partial pressures were from a river and whilst high, partial pressures in the headwaters were likely to have been higher.

Dissolved CO_2 was positively correlated with DOC concentration across the LWS, EDS and PDS field seasons (see Fig. 3.16), indicating that breakdown of DOC could be a significant −but seemingly not dominant− driver of dissolved CO_2 in the channels ($R^2 = 0.29$, $p = 1.508 \times 10^{-5}$). Other sources other than DOC breakdown are further suggested by the linear model intercepting the y-axis at 2,097 ppm. It was beyond the scope of this project to identify the sources of dissolved gases within the channels, but it is possible that a significant amount enters the channels via lateral inputs from the catchment, which has been reported in other recent studies of PSF channel geochemistry (e.g. Hoyt et al., 2016, 2017). Further work involving the use of isotopes, e.g. $^{13}CO_2$ and DO^{13}C, could be used to determine the relative importance of water flows and in-stream degradation as sources of CO_2 in the channels at both land classes, and between seasons (Mayorga et al., 2005; Billett et al., 2007; Garnett et al., 2012).

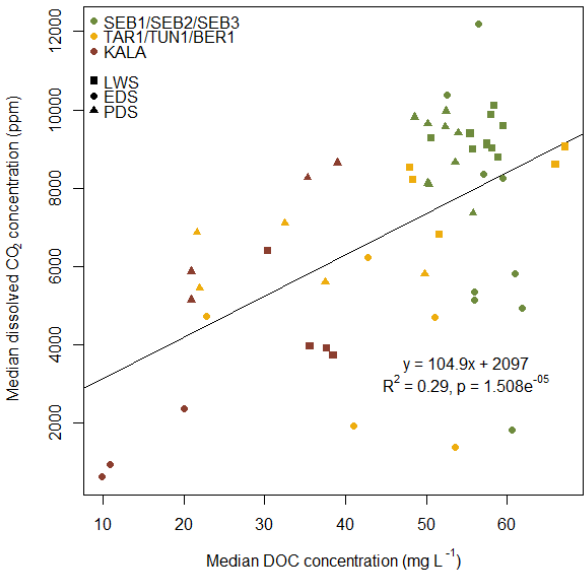

Figure 3.16: Median dissolved CO_2 concentrations were positively correlated to DOC concentrations when data for each available sampling day were plotted ($R^2 = 0.29$, $p = 1.508 \times 10^{-5}$). This suggests that DOC concentrations have a significant influence on the amount of dissolved CO_2 in the channels but the weak R^2 also suggests that other (unmeasured) sources play a role. The intercept on the y-axis of 2,097 ppm CO_2 further suggests that there are other significant sources of CO_2 other than DOC within the channels.

3.3.7 The gas exchange velocity

To correct for the actual non-linearity of the CO_2 fluxes and obtain realistic flux estimates, calculation of the gas exchange velocity was required. Floating chambers have been known to significantly overestimate flux by causing disturbance to the water surface (Matthews et al., 2003; Lorke et al., 2015), which is the interface where gases exchange. Turbulence in this area is expressed as the gas exchange velocity, k, and a chamber causing disturbance would have a higher value of k. To ensure the fluxes obtained from the floating chambers were not the result of excessive turbulence due to chamber disturbance, k values can be examined to check for this effect. As such, acceptable k values act as a quality check for the directly measured CO_2 fluxes.

All gas exchange velocities were converted to k_{600} values (see Chapter 2) for comparison with other gas exchange velocities in the literature.

k_{600} was generally higher at the intact sites during the late wet season. Median values were 0.92, 0.85 and 1.15 m·d^{-1} for SAB1−3, respectively (see Fig. 3.17). At the degraded land class, TAR1, TUN1 and KALA respectively had k_{600} values of 0.81, 0.53 and 0.88 m·d^{-1}.

The channels in the forest were much shallower than those at the degraded sites. The forest typically receives more rainfall than the degraded areas (Moore, 2011) and therefore a larger volume of water will be moving through and out of the peat dome. Water flows were typically faster and flowed for more study days than at the degraded sites which, when water had overtopped the channel banks, swiftly became part of a wider floodplain. The floodplain had negligible flows which were not measurable with the impeller (sensitivity 0.046−5.0 m·s^{-1}).

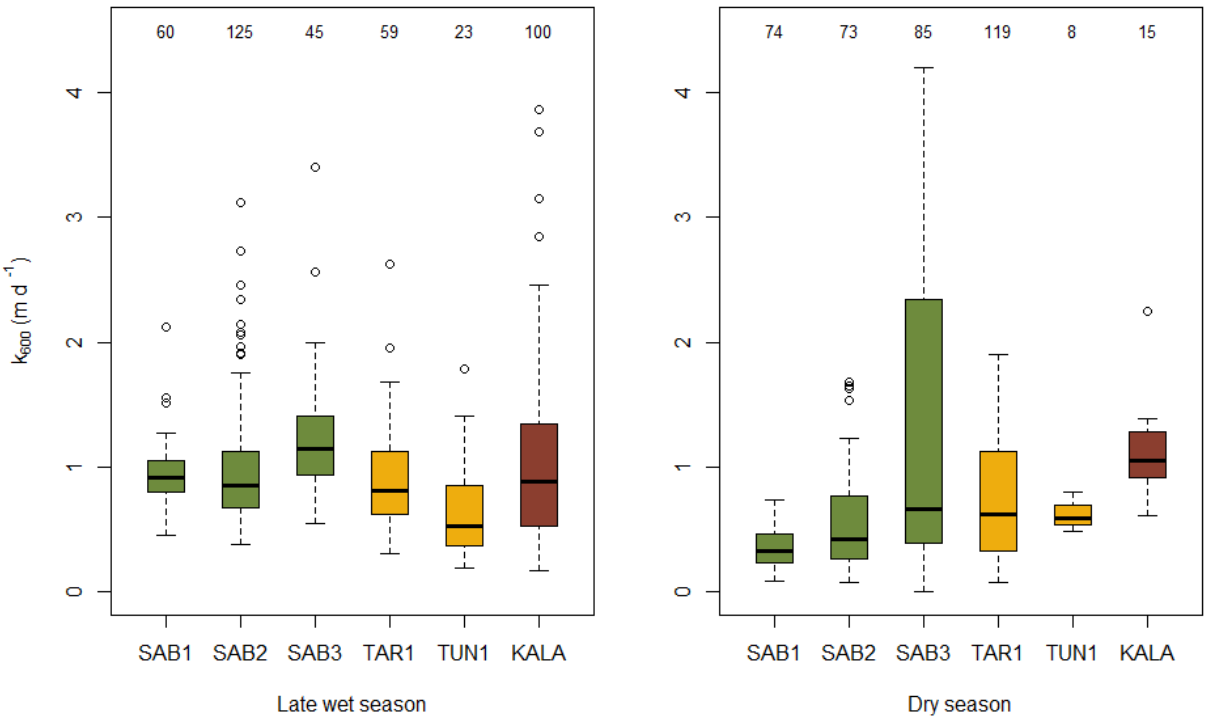

Figure 3.17: k_{600} in the late wet season and dry season of 2015. During the late wet season, intact k_{600} ranged from 0.85 to 1.15 m·d^{-1} and degraded ranged from 0.53 to 0.88 m·d^{-1}. In the dry season, k_{600} decreased at the intact sites and mostly increased at the degraded sites; ranging from 0.33 to 0.67, and 0.59 to 1.06 m·d^{-1}, respectively.

In the dry season gas exchange velocities were lower at all intact sites than during the dry season, likely owing to greatly reduced flow rates as the channels had dried and became puddles. It was not possible to measure flows as they were so weak and closely resembled soil through-flows. Median k_{600} was 0.33, 0.42 and 0.67 m·d^{-1} for SAB1−3, respectively. At the degraded sites, k_{600} increased at TUN1 (to 0.59 m·d^{-1}) and greatly increased at KALA (to 1.06 m·d^{-1}). k_{600} at TAR1 reduced to 0.62 m·d^{-1}.

On a land class basis, late wet season k_{600} medians were 0.92 and 0.83 m·d^{-1} for intact and degraded sites, respectively (see Fig. 3.18). A Wilcoxon's rank sum test found that k_{600} was significantly higher at the intact sites, but that the effect was small (W = 12,442, p = 7.13 $\times 10^{-5}$, r = -0.21).

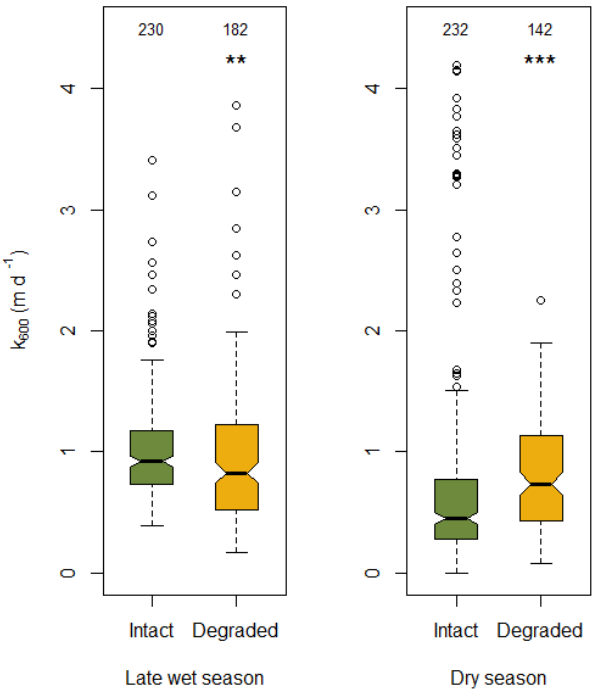

Figure 3.18: k_{600} by land class in the late wet and dry seasons of 2015. k_{600} was significantly different between land classes in both seasons. There was a general reduction of k_{600} in the dry season with respect to the wet season. In the late wet season, median k_{600} values were 0.92 and 0.83 m·d^{-1} for the intact and degraded land classes, respectively. In the dry season, median values were 0.45 and 0.73 m·d^{-1} for intact and degraded sites, respectively.

Dry season k_{600} medians were 0.45 and 0.73 m·d^{-1} for intact and degraded land classes, respectively, decreasing at both intact and degraded land classes with respect to the late wet season. A Wilcoxon's rank sum test found that the gas exchange velocity between land classes was more significantly different in the dry season, though again the effect size was small (W = 24,533, p = 0.0026, r = -0.15).

To compare with k_{600} values reported in the literature, annual estimates were calculated using the seasonal medians and weighting them according to the proportion that the season takes up in the year, giving 0.76 and 0.80 m·d^{-1} for the intact and degraded land classes, respectively.

Overall, k_{600} values were low compared to those commonly found in the literature, but these include few studies of tropical streams (Raymond et al., 2012) and these values are the first for small, tropical peatland headwater channels. The peatland headwaters in this study have low channel slopes and water velocities which, as the two primary drivers of the scale of the gas exchange velocity (Raymond et al., 2012), mean that k_{600} will be similar to the lower range of values found in the literature. At the height of both the wet and dry seasons, water flow through the peat swamp forest channels can reduce to a negligible rate, respectively because of inundation or water levels dropping so low that the

channels becomes discontinuous and stop flowing.

Aufdenkampe et al. (2011) estimated median k_{600} in tropical streams ($<$ 60−100 m wide) to be 4.128·m d^{-1}, and in seasonally inundated tropical wetlands, 0.576 m·d^{-1}. These global, landscape-type estimates were calculated using atmospheric circulation, and existing values of CO_2 partial pressures, k_{600}, and flux measurements from those landscapes.

The median values in this study were much lower than those for streams estimated in Aufdenkampe et al. (2011), but in that study the stream definition included anything up to 60 m wide. The channels in this study are considerably smaller, being <1 to ~3 m wide, their waters comparatively slack and slow-flowing and, at the intact sites where a closed canopy exists, they experience negligible winds (virtually all wind measurements with an anemometer measured 0.0 m·s^{-1}, see Appendix Fig. 7.2). Therefore, the lower values seem reasonable in comparison to the tropical streams described in Aufdenkampe et al. (2011).

The median k_{600} values in this study are higher than the seasonally inundated wetlands k_{600} median of 0.576 m·d^{-1} in the study by Aufdenkampe et al. (2011). The sites in this study do not truly represent natural wetlands, which would not contain man-made drainage channels built to facilitate water export out of the wetland; in a natural wetland the water would stand for longer periods and drain more slowly. However, there were some periods of the year in this study when the water did stand and flows were slow to unmeasurable, and so it is reasonable that k_{600} was higher, although not substantially higher than 0.576 m·d^{-1}.

Streams more comparable in size located in the Upper Rhine Valley in southwest Germany yielded a mean value of 2.1±2.5 m·d^{-1}, using very similar equipment and methodology (Lorke et al., 2015). This value is still higher than I recorded, but the channels would have had a different bed roughness and substrate, and general channel geomorphology, which all contribute to turbulent eddy generation in the channel (MacIntyre et al., 1995). In the Rhine Valley study, the mean flow rate (which would in part contribute to k) was 0.30±0.07 m·s^{-1} which was ~50 % faster than the mean flow rate of 0.21±0.07 m·s^{-1} at the sites in this study (means ± standard deviation).

There were a number of outlying observations that were very different to −and nearly always much higher than− the vast majority of data points. These resulted from heavy rain, high flows or strong winds, or unstable chambers that may have collided with each other or the channel bank, or

got stuck. In most cases, these effects were artefacts of using floating chambers and are known in the literature as 'chamber effects' (Belanger and Korzun, 1991). As elevated k_{600} values may result from numerous chamber effects that themselves arise from a variety of physical sources, it was deemed impractical to attempt to measure and record them all individually for each chamber. All elevated values were included in the analyses. The analyses identified outliers in the dataset (such as the circles on the box plots) and therefore those values should be treated with some caution as they may have arisen from chamber effects.

3.3.8 Flow velocity as a driver of gas exchange velocity

Channel flow velocity data were available for 10 sampling days at the intact sites. The flow velocity was calculated from the fastest time one of five chambers took to get from the upstream drift start point to the downstream drift end point. Gas exchange velocity is a function of turbulence at the water surface, and faster flows could induce greater turbulence (e.g. Lorke et al., 2015). Flow velocities were plotted against k_{600} to see what influence it had on the gas exchange velocity (see Fig. 3.19).

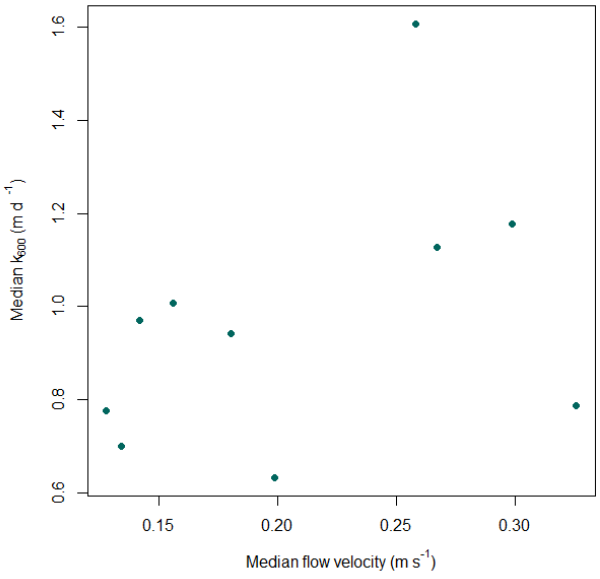

Figure 3.19: A subset of gas exchange and water velocities (from the intact site in the wet season) did not show a significant relationship. This indicates that there are other, more significant drivers.

Flow and gas exchange velocities did not produce a significant correlation (Linear model; R^2 = 0.059, $p = 0.25$) indicating that there were other −potentially more significant− drivers of k_{600}. These could include bed roughness and substrate, and general channel geomorphology which were not measured or

categorised (MacIntyre et al., 1995).

3.3.9 CO_2 fluxes

In the late wet season a total of 656 chamber deployments were made; 309 and 347 at the intact and degraded sites, respectively. In the dry season 481 chamber deployments were made; respectively, 232 and 249 at the intact and degraded sites. The reduced number in the dry season was due to an intense El Niño which caused the channels to dry up to the point where fieldwork had to be stopped.

In the late wet season, all median CO_2 fluxes at the intact sites (SAB1−3) were higher than at the degraded sites. Fluxes at both intermediately degraded sites (TAR1 and TUN1) were higher than those at the severely degraded site (KALA; see Fig. 3.20). Median CO_2 fluxes in the late wet season at the intact sites were 4.55, 4.41 and 6.29 g·C·m^{-2}·d^{-1} for SAB1−3, respectively. Median fluxes at the degraded sites were 3.60, 2.98 and 2.17 g·C·m^{-2}·d^{-1} for TAR1, TUN1 and KALA, respectively.

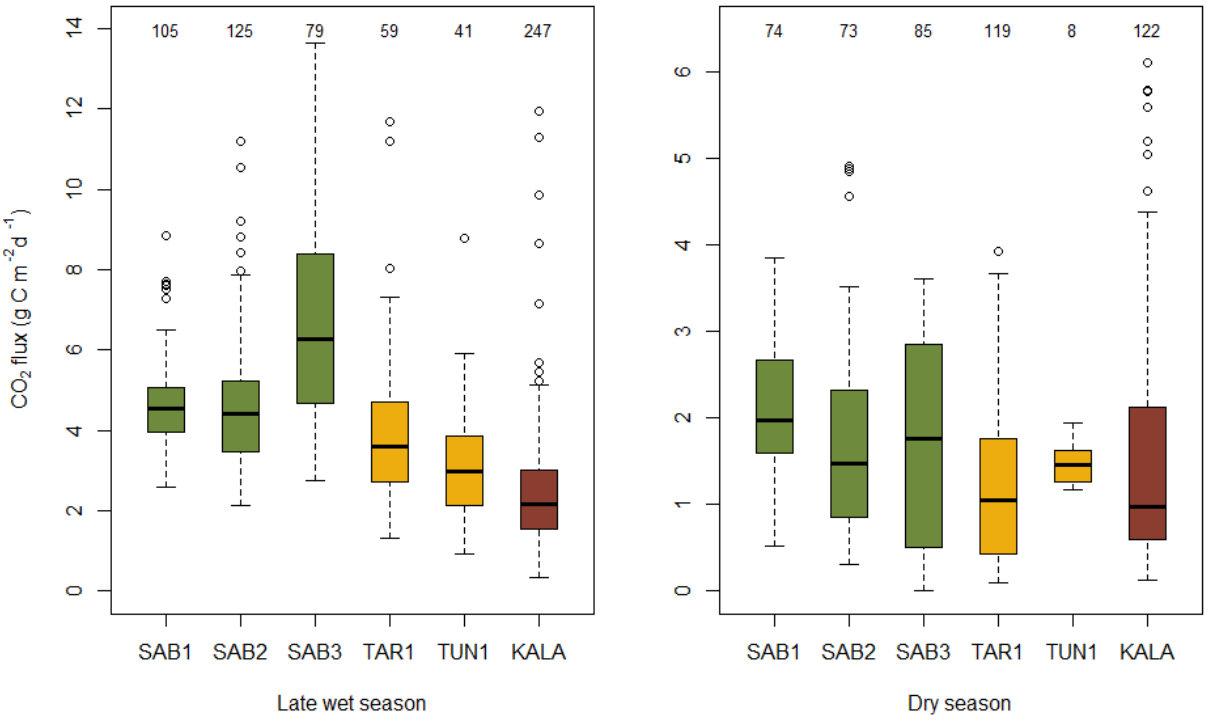

Figure 3.20: CO_2 fluxes by site, in the late wet and dry seasons of 2015. Note the different y-axis scales. In the late wet season, the median intact fluxes ranged from 4.41 to 6.29 g·C·m^{-2}·d^{-1}. The degraded CO_2 fluxes ranged from 2.17 g·C·m^{-2}·d^{-1} at KALA to 3.60 g·C·m^{-2}·d^{-1} at TAR1. In the dry season, all sites yielded lower median fluxes; they ranged from 1.48 to 1.97, and 0.98 to 1.46 g·C·m^{-2}·d^{-1} at the intact and degraded sites, respectively.

All sites had significantly lower fluxes in the dry season, and the differences between the intact and degraded CO_2 fluxes were smaller. CO_2 fluxes dropped to 1.97, 1.48 and 1.76 g·C·m^{-2}·d^{-1} for SAB1−3, respectively, and 1.05, 1.46 and 0.98 g·C·m^{-2}·d^{-1} for TAR1, TUN1 and KALA, respectively.

In both sampling seasons, CO_2 fluxes were significantly higher at the intact land class than at the degraded land class (see Fig. 3.21). In the late wet season, the median fluxes for the intact land class were nearly double those of the degraded sites at 4.68 and 2.49 g·C·m^{-2}·d^{-1}, respectively. A Wilcoxon's rank sum test found that CO_2 fluxes were very significantly higher at the intact land class and demonstrated a large effect size between land classes (W = 85,288, $p < 2.2 \times 10^{-16}$, r = -0.61). In the dry season, intact and degraded CO_2 median fluxes were 1.81 and 1.07 g·C·m^{-2}·d^{-1}, respectively. Again, fluxes at the intact land class were significantly higher, again being nearly double those of the degraded land class, but the effect size was small (Wilcoxon's rank sum test; W = 37,378, $p = 2.50 \times 10^{-8}$, r = -0.25).

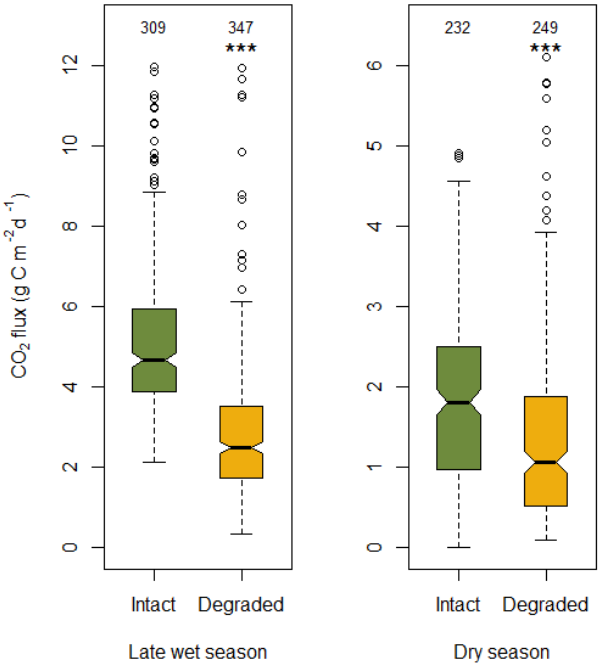

Figure 3.21: CO_2 fluxes by land class in the late wet and dry seasons of 2015. Note the different y-axis scales. The intact site had significantly higher fluxes in both the late wet season and the dry season ($p < 2.2 \times 10^{-16}$ and $p = 2.50 \times 10^{-8}$, respectively), though the difference was greater in the late wet season. Median CO_2 fluxes in the late wet season were 4.68 and 2.49 g·C·m^{-2}·d^{-1} for the intact and degraded sites, respectively. Both land classes' median CO_2 fluxes for the dry season were lower than the late wet season; 1.81 and 1.07 g·C·m^{-2}·d^{-1} for the intact and degraded sites, respectively.

In the late wet season and dry season, intact CO_2 flux medians were respectively 1.9− and 1.7−times higher than the degraded land class.

CO_2 fluxes from a degraded channel in Kalimantan were reported in Jauhiainen and Silvennoinen (2012) where the site was described as 'settled' peat swamp forest and was located within the KALA catchment area. They reported mean CO_2 effluxes of 2.68 and 2.29 g·C·m^{-2}·d^{-1} in the wet and dry seasons, respectively. These values are somewhat higher than those in this study where the equivalent means were 2.46 and 1.53 g·C·m^{-2}·d^{-1}. It was not deemed appropriate to report mean values in this study; the influence of numerous outliers originating from possible chamber effects likely do not represent real world fluxes and would artificially inflate the average. In this study, the median fluxes for KALA in the wet and dry seasons were 2.17 and 0.98 g·C·m^{-2}·d^{-1}, respectively. These values are much lower than the values given by Jauhiainen and Silvennoinen (2012), being respectively 81 and 43 % of wet and dry season fluxes given in their study.

The most striking difference between the results of this study and that of Jauhiainen and Silvennoinen (2012) were the CO_2 fluxes during the dry season; the median flux in this study was 0.98 g·CO_2-C·m^{-2}·d^{-1} whereas in Jauhiainen and Silvennoinen (2012) the mean CO_2 flux was 134 % higher, being 2.29 g·CO_2-C·m^{-2}d^{-1}. The other difference of note is that 2.29 g·CO_2-C·m^{-2}·d^{-1} does not constitute a large reduction in flux with respect to the wet season, which was only 15 % higher, being 2.68 g·CO_2-C·m^{-2}·d^{-1}. In this study, the wet season value was 121 % higher than the dry season.

The much lower dry season CO_2 flux in this study was likely influenced greatly by the severe El Niño that was taking place during the sampling period; dissolved CO_2 concentrations markedly declined, seemingly as a response to lower water levels. Lower dissolved CO_2 in the channels would cause CO_2 fluxes to decline if the gas exchange velocity was to stay the same. Lower dissolved CO_2 would be expected in a normal dry season, but not to the same extent as seen here in the El Niño as water table drawdown would not be as severe.

The fluxes in this study are of the same order of magnitude as in Jauhiainen and Silvennoinen (2012) and therefore may represent natural variation at KALA in El Niño and non-El Niño years, respectively; the data presented in Jauhiainen and Silvennoinen (2012) were collected in 2007, a moderate La Niña year (Kashino et al., 2009) when associated increases in precipitation can result in a higher water table (Hodson et al., 2011). As 2007 was a La Niña year, the higher CO_2 fluxes reported by Jauhiainen and Silvennoinen (2012) and the lower El Niño CO_2 fluxes reported in this study appear reasonable.

As Jauhiainen and Silvennoinen (2012) did not report concentrations or partial pressures of dis-

solved CO_2, nor any gas transfer velocities, it is not possible to scrutinise the possible causes for the higher fluxes they reported. However, the higher values they reported may also have been in part caused by a) their choice of reporting mean values of their fluxes, or b) their chamber design.

The data reported in this study were highly non-normal and a significant number of elevated fluxes appeared to be caused by chamber effects. As such, medians were reported and non-parametric analyses were performed in order to reduce the influence of chamber effects on the reported fluxes. If outliers existed in the Jauhiainen and Silvennoinen (2012) dataset (which would be expected as chamber effects are difficult to avoid in environments that cannot be controlled), and as the mean is more sensitive to outliers, it could be that their reported values are higher than if they had reported median values.

Chamber design can also influence measured fluxes as they can be more or less prone to chamber effects (Cole et al., 2010; Lorke et al., 2015). For example, some chambers might be less stable in windy conditions and increase disturbance at the water surface. On the other hand, some chambers may shelter the water surface from the wind which might reduce disturbance at the water surface. As such, a poorer chamber design might promote a background signal in the flux data. The chamber used by Jauhiainen and Silvennoinen (2012) was constructed using a tall cylinder and had a wide square float around it that sat on the water surface. Their chamber may have been subjected to greater buffeting by the wind and could have disturbed a comparatively large water surface area compared to its headspace area. Without any gas exchange velocity data, it is not possible to examine more closely whether the chamber design could have been elevating the fluxes through increased disturbance to the water surface. As such, the mean and median values of CO_2 fluxes, respectively reported in Jauhiainen and Silvennoinen (2012) and in this study, must be compared to existing measurements and estimates for similar streams and ecosystems.

Aufdenkampe et al. (2011) estimated tropical streams on average emit 7.5 $g{\cdot}C{\cdot}m^{-2}{\cdot}d^{-1}$. The higher fluxes of ~5 $g{\cdot}C{\cdot}m^{-2}{\cdot}d^{-1}$, measured at the intact sites in this study are about 33 % less. This is most likely because these headwaters a) are slack and slow-flowing, b) there is very little change in elevation with distance, and c) there are no topographical features, per se, to increase the gas exchange velocity, or provide hotspots of evasion. It is possible, therefore, that a more significant amount of CO_2 is emitted downstream by the rivers that the channels flow into (Dawson et al., 2004).

3.3.10 Radiocarbon age of CO_2

Analysis of the CO_2-C trapped by the zeolite sieves found the degraded land class to be significantly less enriched with ^{14}C (Welch two sample t-test, t = 8.38, df = 8.18, p = 2.74 $\times 10^{-5}$, r = 0.90; see Fig. 3.22). All of the samples from the intact channels had a 'modern' radiocarbon age (relative to AD 1950), whereas the samples from the degraded channels all had 'pre-modern' ages. The radiocarbon ages at the degraded land class ranged from 341±37 to 1655±36 years old, and the median age was 684. The youngest radiocarbon ages of the degraded land class were generally from the intermediately degraded sites TAR1 and TUN1, and the oldest radiocarbon ages were from severely degraded KALA (see Appendix Table 7.3 for list of samples analysed for their radiocarbon ages).

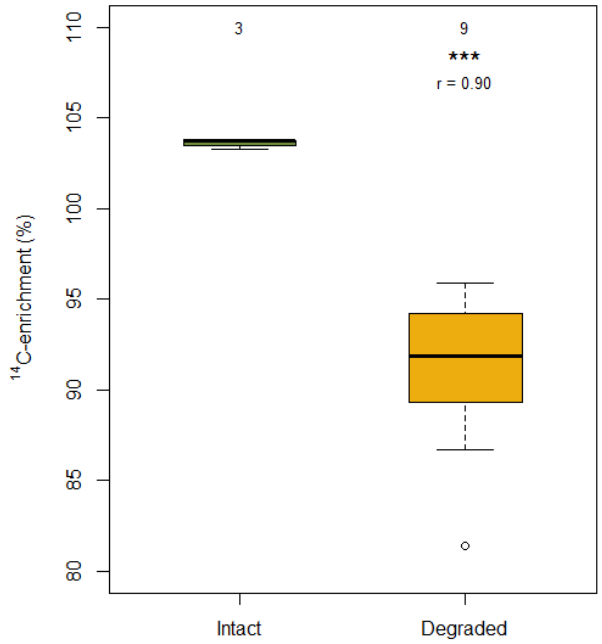

Figure 3.22: ^{14}C-enrichment of the dissolved CO_2 trapped by the zeolite sieves. The sieves were deployed in the intact and degraded channels for a month in the late wet season. All intact samples had a 'modern' radiocarbon age (>100 % ^{14}C-enrichment). The CO_2-C of the degraded channels was found to be pre-modern where radiocarbon ages ranged from 341±37 to 1655±36 years old.

The radiocarbon ages suggest that the CO_2 in the intact channels was overwhelmingly modern and likely was generated from labile, recently photosynthesised C substrates. At the degraded land class however, the radiocarbon ages suggest that there was negligible input of recently photosynthesised C. Most of the CO_2 present in the degraded channels appears to be coming from the breakdown of older, deeper peats

that are many hundreds of years old. This older dissolved CO_2 is probably just as likely to be emitted to the atmosphere as more modern CO_2 (Mark Garnett, personal communication).

From a catchment perspective, the intact channels appear to be year-round emitters of CO_2 whereas the surrounding ecosystem, and the intact peat swamp forest ecosystem as a whole, is a net-sink for CO_2 (Moore et al., 2013). Although emissions are lower at the degraded land class, the CO_2 being evaded from the channels stems from degradation of old/ancient peats. The lack of modern CO_2 gives another indication that degraded peats can undergo a regime shift and become an overwhelming source of C to the atmosphere; the peat swamp forest C sink function can be lost, and may continue to destabilise.

3.4 Conclusions

This study demonstrated that degradation of peat swamp forest can have numerous effects on the environmental conditions and biogeochemical cycling, which have the potential to affect CO_2 fluxes from drainage channels. The most significant factor driving CO_2 fluxes at both intact and degraded peat swamp forest appeared to be the depth of the water table. CO_2 emissions were higher when the water table was high during the wet season and CO_2 emissions reduced significantly when the water table dropped during the dry season. The degraded land class had much deeper channels than the intact land class ($2-7$ m and $\tilde{1}$ m, respectively) and the deeper channels therefore affected the ability of the degraded peatland to regulate its water table. The water table was consistently lower at the degraded land class, except in the case of the severely degraded site, KALA, where the water table rose high above the peat surface and became a floodplain in the wet season. Water table amplitudes at the degraded sites were also much greater than at the intact sites.

Air and water temperatures were found to be higher in both seasons in degraded peat swamp forest as there is no forest to facilitate a microclimate. There was also greater abundance of dissolved oxygen in both seasons in the degraded channels. The gas exchange velocities appeared to be reasonable for the type of channels, and therefore the chamber flux measurements considered to be reliable. Dissolved CO_2 was higher at the intact land class during both seasons, and because the gas exchange velocities between the land classes were not considerably different, the main driver of CO_2 flux was considered to be dissolved CO_2. The CO_2 fluxes were consequently much higher for the channels at the intact land class.

However, the CO_2 evaded from the channels at the intact class is considered to be modern, whereas for the channels draining intermediately degraded peat swamp forest the CO_2 was many hundreds of years old, and over 1,000 years-old at KALA, the severely degraded site.

Less dissolved CO_2 was present in the channels at the degraded land class. This could have resulted from a) lower rates of respiration of organic matter in degraded peat swamp forest and/or less throughflow of porewater that could transport CO_2 resulting from edaphic respiration to the channels, or b) DOC quantity and quality was poorer in/reaching the channels of the degraded land class, limiting in-stream respiration. It is likely that these possibilities are not mutually exclusive and the abundance of CO_2 in the channels is controlled by moth mechanisms. Further work is required to identify the relative importance of these mechanisms as drivers of CO_2 concentrations in channels draining peat swamp forest.

The intermediately degraded sites had higher than expected concentrations of DOC and CO_2 which may have resulted from re-vegetation of the catchments by herbaceous plants (Moore, 2011), or from nearby human settlements using the channels for sanitation. The severely degraded site at KALA consistently had the lowest dissolved CO_2 suggesting a low quality of substrate and/or a smaller community of organisms involved in degradation of organic matter, in the surrounding peats, or within the channel waters. Further study is required to more fully understand the sources of DOC and CO_2 within the channels, and the make-up of the degrading microbial communities and their metabolic rates and/or potentials.

The dry season water table was significantly lower than in the wet season and, as mentioned above when discussing the difference between the water tables at the intact and degraded land classes, dissolved CO_2 concentrations dropped in the channels at both land classes may have dropped for the same reasons: a) less overland and through-flow could reduce delivery of dissolved CO_2 and/or more labile C substrates to the channels; and b) lower water tables could result in a smaller wetted volume of peat being in contact with the channel hence restricting the amount of CO_2 and DOC that can be transported to it (see Fig. 3.23). Further, the DOC would come from deeper layers in the peat and hence would be expected to be more recalcitrant. The seasonal differences suggest that biogeochemical conditions at the intact land class become more similar to degraded peat swamp forest when the water table is lower, and hence the water table may be an effective proxy for assessing and categorising the condition −or

level of degradation– of peat swamp forest, from a C-cycling perspective.

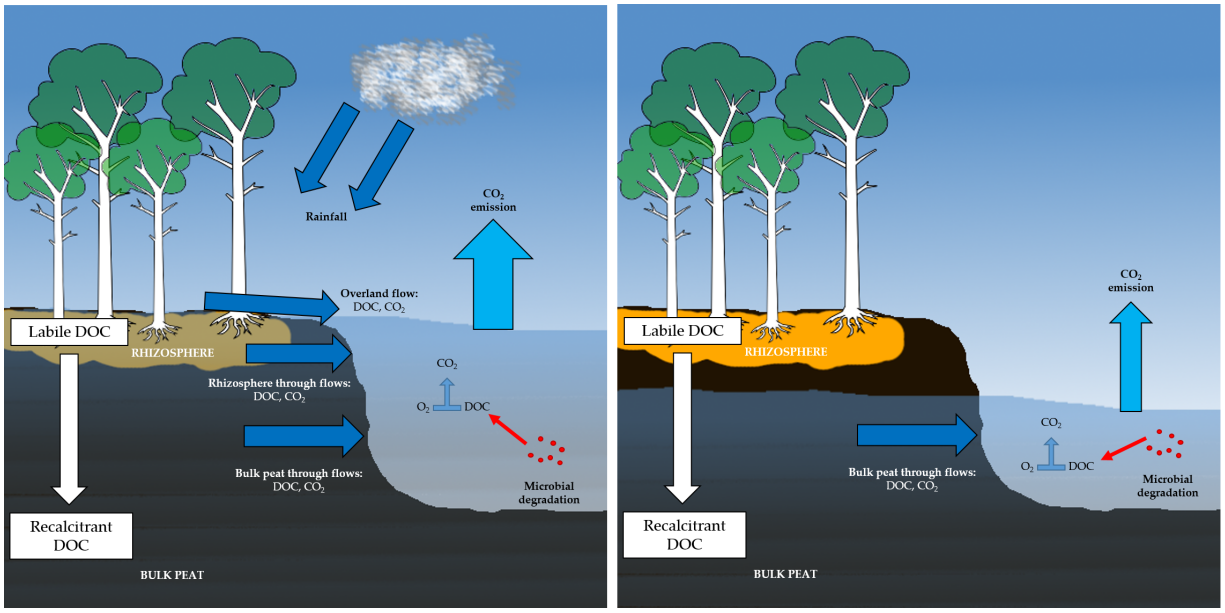

Figure 3.23: Schematic of the main sources of DOC and CO_2 to a channel draining intact peat swamp forest in a wet and dry season (left and right panes, respectively). In the wet season when rains are frequent and intense, the water table is kept higher and overland flows can constitute a significant source of CO_2 and DOC to the channels. The peat near the surface contains the most labile carbon and nutrients, and hence this material would promote degradation and emission of CO_2 in and by the channels. Though dissolved CO_2 may enter the channel by overland- and through-flows, however, anoxic layers that are submerged may not produce a substantial quantity of CO_2. Conversely, in the dry season when the water table is lower, the deeper peat layers may yield significantly more recalcitrant DOC and there are negligible overland flows to provide more labile material. Further, a reduced wetted volume of peat connected to the channel could reduce the potential size of reservoir that may yield carbon to the channels. CO_2 emissions in the dry season therefore are consequently lower.

k_{600} values were quite low compared to those found in the literature but appear suitable for the peat swamp forest environment, with this study providing the first reported values for headwater channels in this ecosystem. k_{600} was higher at the intact land class than at the degraded land class in the wet season. This was not directly attributable to water flow, but it was likely a factor as correlations have been found in other studies (e.g. Lorke et al., 2015). Intact channel flows may have persisted for a while longer during the wet season, when the channels at the degraded land class could have already merged into extensive floodplains, which may explain the higher k_{600} at the intact land class. In the dry season, intact channels were forming still, discontinuous puddles and k_{600} dropped, but k_{600} at the degraded land class was more or less the same. The gas exchange velocity may have stayed the same as it can be driven by both channel flow and exposure to the wind.

As both intact and degraded peat swamp forest have highly dynamic hydrological regimes (still

or flowing) within a year, care should be taken to obtain accurate annual k_{600} averages.

As k_{600} was not greatly different between intact and degraded peat swamp forest, the evaded CO_2 followed the trend of dissolved CO_2; the degraded sites consistently emitted less than intact sites. There was less dissolved CO_2 and the concentration gradient between the supersaturated water and the atmosphere was less steep. Intact peat swamp forest emitted approximately twice the amount of CO_2 than the degraded peat swamp forest, in both wet and dry seasons, with emission during the latter season being about half the amount of the dry season.

At the intact land class the channels may emit more CO_2 than the catchment soils; Jauhiainen et al. (2005) estimated peat soil emissions of 953 $g{\cdot}CO_2\text{-}C{\cdot}m^{-2}{\cdot}yr^{-1}$ in the same intact forest, whereas the channels measured in this study produced ~50 % more at 1,447 $g{\cdot}CO_2\text{-}C{\cdot}m^{-2}{\cdot}yr^{-1}$. At the degraded land class, peat soils have been measured to produce between 823 and 1,014 $g{\cdot}CO_2\text{-}C{\cdot}m^{-2}{\cdot}yr^{-1}$ (Hirano et al., 2009). The channels in this study emitted less CO_2 than the peat surfaces in Hirano et al. (2009), the annual estimate in this study being 779 $g{\cdot}CO_2\text{-}C{\cdot}m^{-2}$.

Given the above soil and channel emissions estimates, it is likely that, per square metre, the degraded soils emit more CO_2 than the channels as the water table can be below the peat surface for extended periods; the lower the water table, the greater the volume of oxidisable peat, and the greater the potential for CO_2 emissions (Couwenberg et al., 2010). However, terrestrially-derived CO_2, as well as that from degradation of terrigenous DOC may still be emitted by rivers as it makes its way to the sea and so the channels may be facilitating a greater loss of C, which is yet to be quantified for these peat catchments.

This bottom-up study allows for a better understanding of catchment-based C cycling in peat swamp forest and the roles that channels have in terms of landscape scale CO_2 fluxes (Billett et al., 2015); these can be interpreted in conjunction with existing landscape scale data obtained from flux towers (e.g. Hirano et al., 2007, 2009), which themselves are not able to constrain fluxes from the various point sources that contribute to the total measured flux (Matthews et al., 2003). The study areas used in this investigation have been the subject of several C balance and greenhouse gas flux studies, both terrestrial and aquatic, and which have used a variety of methods. The data reported are a useful addition for providing a more complete description of catchment and landscape-scale C cycling in peat swamp forest.

This study has provided further evidence that deforestation and drainage of peat swamp forest

induces a systematic change to the ecosystem, whereby catchment C cycling and emissions of CO_2 have been significantly altered. This study has quantified another pathway by which C can be lost which, in terms of degraded peat swamp forest, cannot be replaced or accumulated as it can be in intact peat swamp forest; the degraded catchments in this study have already released many centuries-worth of previously stored C within the two decades since they underwent deforestation and drainage. Without any significant signs of regeneration of peat swamp forest vegetation, or when that regeneration is actively prevented, the rapid C loss from degraded peat swamp forest is likely to continue.

3.5 Author contributions

V.G., S.E.P., C.D.E. and S.P. conceived of the study. M.S.K., D.B., M.H.G., V.G., C.D.E., S.P. and S.E.P. devised the methods. M.S.K., I., H. and S. carried out the fieldwork. I., B. and B.R. collected and collated the hydrological data in the Sabangau Forest. M.H.G. processed the molecular sieve (radiocarbon) samples. M.S.K. carried out the data analysis and wrote the manuscript. V.G., S.E.P. and C.D.E. provided comments on an early version of the manuscript.

Chapter 4

Effects of peat swamp forest degradation on channel emissions of methane

Authors: Kent, M.S.[1,2], Page, S.E.[3], Evans, C.D.[4], Idrus[5,6], Sandy[6], Bastviken, D.[7], Pangala, S.[2,8] and Gauci, V.[2]

Institutions: [1]*School of Agricultural and Environmental Sciences, University of Nottingham, Sutton Bonington Campus, College Road, Loughborough, LE12 5RD.* [2]*School of Environment, Earth and Ecosystem Sciences, Faculty of Science, Technology, Engineering and Mathematics, The Open University, Walton Hall, Milton Keynes, MK7 6AA.* [3]*Department of Geography, University of Leicester, University Road, Leicester, LE1 7RH.* [4]*Centre for Ecology and Hydrology, Environment Centre Wales, Deiniol Road, Bangor, LL57 2UW.* [5]*Center for International Cooperation in Sustainable Management of Tropical Peatland (CIMTROP), University of Palangkaraya, Jalan Yos Sudarso, Kampus UNPAR Tunjung Nyahu, Palangkaraya 73111, Central Kalimantan, Indonesia.* [6]*Borneo Nature Foundation, Jalan Bukit Raya No. 82, Bukit Raya, Palangkaraya 73112, Central Kalimantan, Indonesia.* [7]*Department of Thematic Studies, Linköping University, Campus Valla, Linköping, Sweden.* [8]*Lancaster Environment Centre, Lancaster University, Lancaster, LA1 4YQ.*

Abstract

Methane (CH_4) is a powerful greenhouse gas that may become the dominant greenhouse gas warming our atmosphere, later this century. Tropical wetlands emit 10−23 % of the total amount of CH_4 to reach our atmosphere. Wetland CH_4 production is primarily hydrology-dependent. Developing countries have been rapidly draining large areas of wetlands, often fundamentally altering their hydrology and CH_4 cycling. Coverage of degraded (deforested and drained) tropical peat swamp forest (PSF), a normally carbon-dense wetland found mostly in southeast Asia, has overwhelmingly risen in recent decades. Comparatively little work has been done on ground-level PSF CH_4 emissions and the processes governing those emissions. Fluvial systems draining peat can be a significant source of CH_4 within a catchment. This is the first investigation of emissions from channels draining intact and degraded PSF. Intact PSF channels were used as a baseline to assess the impacts of land-use change on CH_4. Degraded PSF channels were relatively strong and persistent emitters of CH_4, releasing 13.3 and 29.6 mg·CH_4-C·m^{-2}·d^{-1}, respectively, in wet and dry seasons. During the wet season, intact PSF channels emitted considerably less CH_4 (2.1 mg·CH_4-C·m^{-2}·d^{-1}). However, CH_4 emission in the dry season rose ˜4−times to 7.8 mg·CH_4-C·m^{-2}·d^{-1}, whereas at the degraded PSF that rise was only ˜2−times. Dissolved CH_4 rose despite lower water tables and more abundant dissolved oxygen was present that might otherwise inhibit methanogenesis and promote methanotrophy. Seasonal temperature changes could not account for changes in rates of methanogenesis. It appeared that most CH_4 derives from lateral flow from deeper peats, and in intact systems this CH_4 is normally oxidised, or translocated by trees. Further, the study found that intact PSF can cycle CH_4 similarly to degraded PSF, when water tables are low. Degradation was concluded to fundamentally alter CH_4 cycling in PSF.

4.1 Introduction

Wetlands, globally, are the largest single source of methane (CH_4) to the atmosphere. They contribute 20−39 % of total CH_4 emissions which amounts to 100−231 Tg·yr^{-1} (Laanbroek, 2010). Wetlands are typically inundated with water for significant periods of the year and this provides the anoxic conditions necessary for methanogenesis (Schlesinger and Bernhardt, 2013).

Of the total wetland emission of CH_4 to the atmosphere, 50−60 % comes from tropical wetlands

(Bloom et al., 2012). This is a disproportionately large amount as the greatest extents of wetlands are found in temperate zones (Köchy et al., 2015).

Methanogenesis in tropical wetlands is driven primarily by precipitation, rather than temperature, the latter being the primary driver in temperate regions (Turetsky et al., 2014). However, it is not precipitation alone that dictates the rate of methanogenesis, it is whether the hydrology of a wetland permits an aboveground water table so that the soils become anoxic (Couwenberg et al., 2010).

Countries in the tropics are generally in a state of development. Tropical nations primarily kick-start their economies by exploiting their natural resources. This has led to considerable amounts of wetland being drained (Barbier, 1993; Junk et al., 2013). In Southeast Asia, up to 50 % of peat swamp forest (a particularly carbon-dense wetland) has been deforested or converted for agricultural use (Junk et al., 2013).

Large tracts of peat swamp forest in Indonesia have been deforested and drained, using channels cut through the peat surface. The channels have greatly altered the hydrology of such peatlands and have led to the water table residing beneath the peat surface for protracted periods of time (Sundari et al., 2012). As a result of altered water tables, the production and/or emission of CH_4 is likely to change (Couwenberg et al., 2010). Further, degraded areas of peat swamp forest receive significantly less rain than intact areas (McAlpine et al., 2018; see Chapter 2). Reduced rain input to the catchment could lead to exacerbated water table drawdown. As yet, no comparative study has been conducted to investigate how degradation affects channel emission of CH_4 with respect to an intact peat swamp forest ecosystem.

Intact peat swamp forest soils have been shown to be a source of CH_4 during wet seasons and a weak sink of CH_4 during dry seasons (Jauhiainen et al., 2005). Annual terrestrial emissions from intact peat swamp forest in Central Kalimantan, Indonesia have been estimated to be quite low compared to peatlands in the temperate zone (1.36 ± 0.57 g·C·m^{-2}·yr^{-1}; Jauhiainen et al., 2005; Couwenberg et al., 2010). Degraded peat swamp forest in South Kalimantan was estimated to have lower CH_4 emissions than the intact peat swamp forest in Jauhiainen et al. (2005), but the difference was not substantial (1.2 ± 0.4 g·C·m^{-2}·yr^{-1}; Inubushi et al., 2003). Neither the study by Jauhiainen et al. (2005) nor Inubushi et al. (2003) included CH_4 emissions from trees, which can act as a major source of CH_4 in wetlands (Pangala et al., 2013).

A study by Pangala et al. (2013) found that wet season emissions of CH_4 from peat hollows in

intact PSF were lower (0.11±0.03 g·C·m^{-2}·yr^{-1}) but that significantly more was being lost via tree stems (0.18±0.02 g·C·m^{-2}·yr^{-1}). This finding indicates that trees dominate terrestrial ecosystem emission of CH_4 from PSF. In degraded PSF, the contribution to ecosystem CH_4 emission by tree-mediated pathways would be expected to be negligible, as they are comparatively rare (see Chapter 2).

Methane can also be transported via lateral flow as the swamp forest peat is known to be much more permeable than peats of the temperate zone (Baird et al., 2017; Hoyt et al., 2017). If channels exist in the peat a significant portion of CH_4 could be transported and emitted from the channel surface.

There are currently no data on channel emissions of CH_4 except for some measurements carried out by Jauhiainen and Silvennoinen (2012), however this included only degraded peat swamp forest. Peat-draining channels are characteristically supersaturated with CH_4, therefore they may make a significant contribution to total catchment CH_4 flux. This contribution could be higher than in temperate peat catchments, owing to the higher permeability and greater translocation potential of CH_4.

Degraded peats have been known undergo compaction and that would reduce the permeability of the surface peat (Tonks et al., 2017), but Baird et al. (2017) considered that rates of peat oxidation in degraded peat swamp forest are currently what would be expected from permeable, non-compacted peat. This is supported by the findings of Arai et al. (2014) that degraded peats in Kalampangan, Central Kalimantan, had a high porosity (~90 %). There is a possibility that large quantities of CH_4 are reaching the channels in both intact and degraded peat swamp forest.

There are several sources and sinks of CH_4 that could affect CH_4 emissions from the channels, examples of those sources and sinks in an intact peat swamp forest are presented in Fig. 4.1. In terms of the dominant sources of CH_4 in or to the channels, CH_4 can be produced a) in-stream by methanogenesis in anoxic sediments (MacIntyre et al., 1995); b) in the anoxic bulk peat (Sundh et al., 1994; Bubier et al., 1995), and c) in the rhizosphere as a result of deposition of root exudates (Girkin et al., 2018). The first source is dependent on sediment temperature, water flow velocity and oxygen content, and hydrostatic pressure on the channel bed (Jones et al., 1995; Chanton and Whiting, 1995; Truax et al., 1995), but these are not expected to be very different between the channels of the two land use types; for instance, water depths and flow rates were of the same order of magnitude according to Moore (2011) (also see Appendix Fig. 7.1). The latter two sources, bulk peat and rhizosphere methanogenesis, are dependent on water flowing through the peat to carry dissolved CH_4 to the channels without it being oxidised. How-

ever, upon reaching the channel the CH_4 can be oxidised in-stream in the presence of dissolved oxygen.

A major limiting factor on the amount of CH_4 reaching the channels via through flows in the peat could be due to plant-mediated transport: aerenchymatous plants, which are typical of wetland ecosystems such as peat swamp forest, can passively transport CH_4 from the rhizosphere to the atmosphere (Pangala et al., 2013) before it reaches the channels. This requires the rhizosphere to be sufficiently moist to allow gas exchange across the root cortex (Brix et al., 1992; Whiting and Chanton, 1996). Further, plants also translocate O_2 from the atmosphere to the rhizosphere and this could lead to the oxidation of CH_4 near the roots. This passive oxidation can also reduce the size of the potential CH_4 reservoir that might otherwise reach the channels. However, degraded peatland typically has far less vegetation, and so these processes are less likely to apply to such land use types.

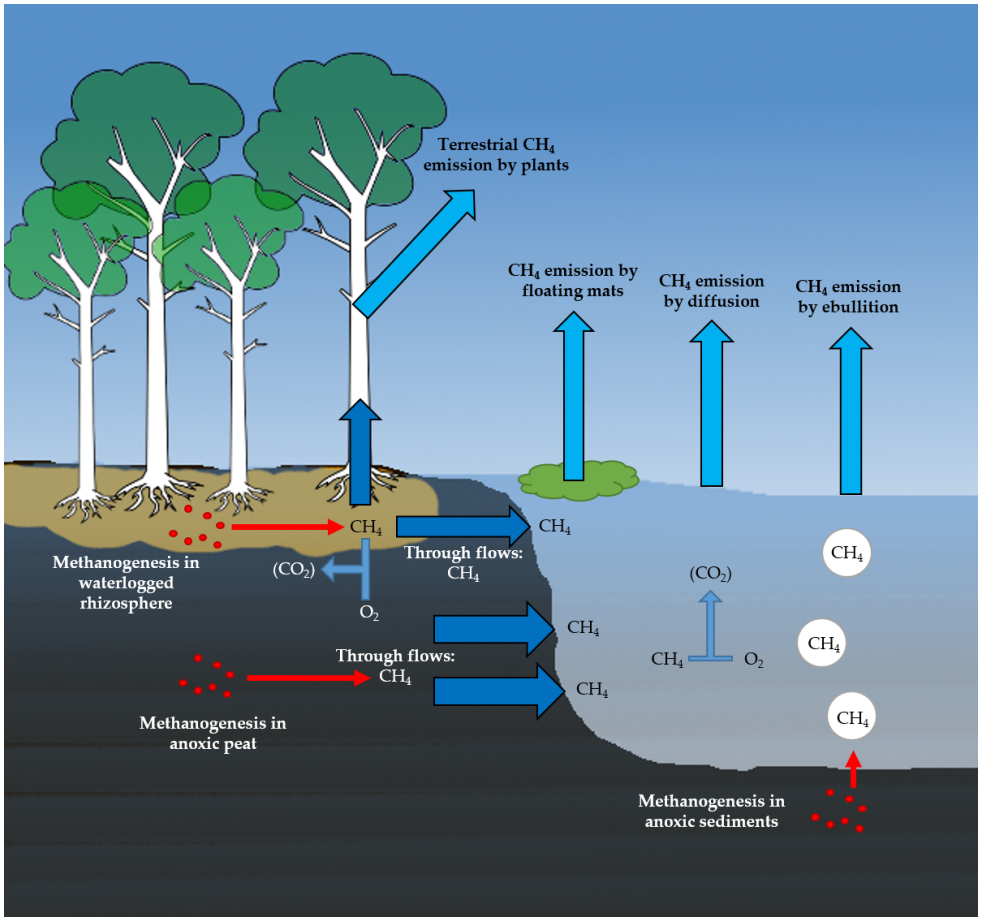

Figure 4.1: Sources and sinks of CH_4 for a channel in an intact peat swamp forest. The main terrrestrial sources of methanogenesis in the peat are in the rhizosphere and in the deeper bulk peat. CH_4 can also be produced in the bottom sediments of the channel. CH_4 may be transported from the peat to the atmosphere by plant-mediated transport, or oxidised in the rhizosphere, before it reaches the channel. Emissions from the channels may be by floating mats of vegetation, by diffusion of free CH_4 in the water column, or by bubble ebullition from the bottom sediment.

The position of the water table at the study sites may therefore play an important role in the amount of CH_4 reaching the channels, and the amount of CH_4 they can emit. This study took place simultaneously with the CO_2 emission study in Chapter 3; in the late wet and dry seasons of 2015. There was a major change in the water table during this time, to the extent that the water table dropped beneath the beds of the channels. Such a significant drop in the water table could considerably reduce the volume of wetted peat and/or rhizosphere and therefore could have a large impact on CH_4 emissions between seasons.

This study aims to quantify the amount of dissolved CH_4 present in channels draining both intact and degraded peat swamp forest, and establish how much CH_4 may be being emitted from the channel surface, with the exception of floating mats of vegetation (MacIntyre et al., 1995) as these did not occur at the study sites. In a wet and a dry season, intact peat swamp forest will be treated as a 'baseline peat swamp forest' from which to assess the changes to CH_4 cycling that result from deforestation and drainage. The sources and sinks of CH_4 were not measured, but the abundance of dissolved CH_4 and CH_4 fluxes could be used to infer some changes to CH_4 production and degradation in the peat, provided that CH_4 production is not overwhelmingly dominated by the bottom sediments of the channels.

4.1.1 Hypotheses

- H_0: CH_4 emissions are the same from channels draining both intact and degraded peat swamp forest.
- H_1: CH_4 emissions will be higher in degraded peat swamp forest as there are comparatively very few plants to mediate transport to the atmosphere, or a substantial rhizosphere to facilitate CH_4 oxidation, with respect to intact peat swamp forest.

4.2 Materials and Methods

This investigation was carried out in the same locations, simultaneously with the CO_2 investigation in Chapter 3. The CO_2 fluxes were used to estimate the diffusive flux of CH_4 (see Materials and Methods for detailed explanation). The same air and water temperatures, and other environmental measurements, used to calculate CO_2 fluxes in Chapter 3 were also used to calculate CH_4 fluxes in this investigation. Annual flux estimates reported in this chapter were calculated as in Chapter 3.

Critically, this chapter does not include CH_4 ebullition data. Ebullition is often the dominant emission pathway with respect to total CH_4 fluxes from freshwater systems. The investigation was set out to obtain ebullitive fluxes by: a) using CO_2 flux data to infer the gas exchange velocity in the channels and henceforth the diffusive component of the CH_4 flux, and b) taking gas measurements of the chamber headspace to determine the total flux of CH_4 and then subtracting the diffusive component of the total flux, to give the ebullitive flux.

Two critical problems were encountered that meant that the headspace gas samples couldn't be analysed. Firstly, the Los Gatos UGGA analyser was seriously damaged in transit when being shipped back to the UK from Indonesia. The UGGA had to be sent to the USA to be repaired and consequently this consumed months on analytical time. Secondly, it was discovered that the UGGA lost its precision when measuring near-ambient concentrations of CH_4 (and CO_2, when used in it closed-loop configuration (method and measurement problems are described in the Chapter 2). The headspace samples by nature only captured the comparatively short period of deployment time (between $5-10$ minutes) and this was not sufficient to raise the headspace concentration far enough above ambient concentration. As a result, the UGGA could not be used for this kind of analysis.

The data presented in this thesis pertain only to diffusive fluxes. However, having taken up a position at the University of Nottingham I now have access to a GC fitted with an autosampler. It is now possible to analyse those headspace samples accurately and also obtain data for CH_4, CO_2 and N_2O, simultaneously. I have arranged to work with a colleague, Dr. Sofie Sjögersten, who investigates gas fluxes in tropical peatlands, and we will analyse the headspace and other samples I have remaining. From these analyses of three gases it will be possible to produce a more complete picture of greenhouse gas fluxes from the study channels than was originally possible during my studentship.

4.3 Results and Discussion

4.3.1 Water table and channel depth

This section presents data from the late wet season of 2015 (LWS) and the dry season during the 2015 El Niño event (EDS). As was discussed more extensively in Chapter 3, there was a very large drop in the water table during the dry season with respect to the average range of the water table measured over

three years; the usual range in from just above the peat surface to -25 cm, but during EDS it dropped below -100 cm (see Fig. 4.2), left pane). The water table was therefore beyond the reach of most plants' roots (see Chapter 1) and therefore, as will be discussed in this chapter, could have significant consequences for the production and vegetative transportation of CH_4 in and from the peat soils.

There was no significant difference in the late wet season in terms of water level relative to the peat surface, where the channels at both land classes were mostly at or near bankfull; i.e. the water level in the channels at both land classes was at or near the same level as the peat surface (median water levels were -12 cm and 2 cm at the intact and degraded land classes, respectively; see Fig. 4.2, right pane). At the degraded land class, however, the water level was much more variable and dropped below the peat surface as well as forming a floodplain above it, whereby the total amplitude was almost 250 cm compared to ~75 cm at the intact land class. The greater water level amplitude was captured when waters were high during the peak of the wet season, and then it dropping lower than the peat surface as the wet season transitioned into the dry season.

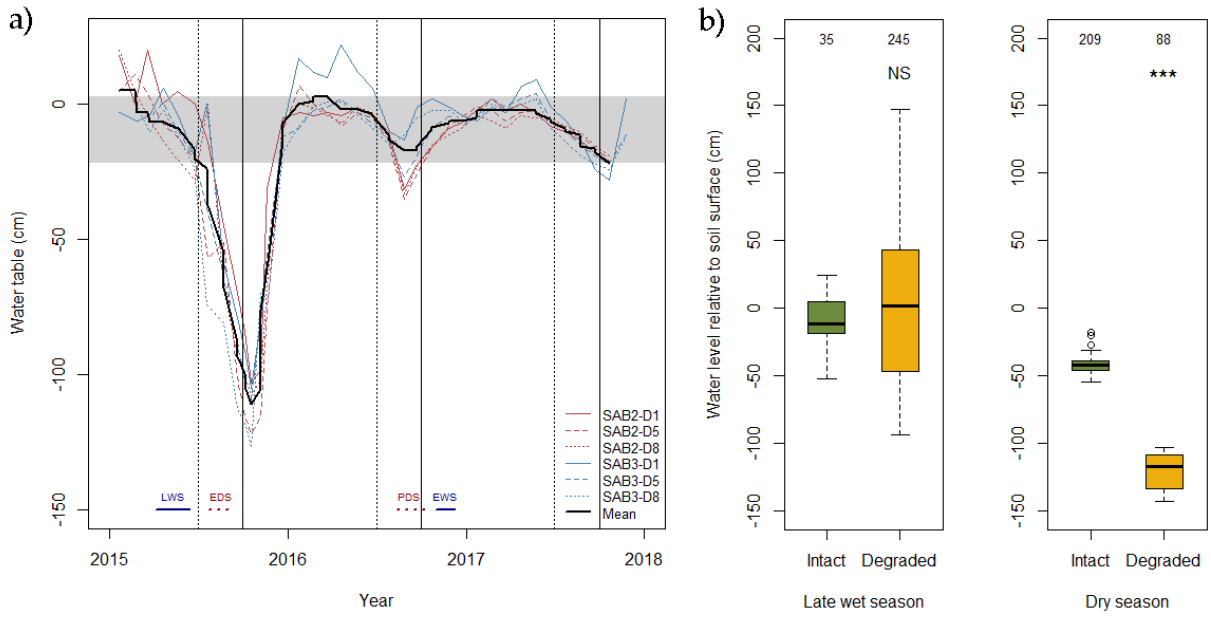

Figure 4.2: Pane a) A 3-year water table dataset provided by the Borneo Nature Foundation for the intact land class. It shows measurements from six dip wells; three adjacent to SAB2, and three adjacent to SAB3. The mean water level is shown as a bold black line. The data presented in this section pertain to the LWS and EDS sampling seasons (indicated toward the bottome of the plot), the latter conducting during the 2015 El Niño event. During EDS, the water table depth dropped well below normal range (highlighted by the horizontal grey band). Sundari et al. (2012) observed that the water table at the degraded land class did not exceed that of the intact land class during the dry season. No water table data were collected for the degraded land class, but Pane b) shows that the water level in the channels was always lower at the degraded land class than at the intact land class during EDS.)

In the dry season, the water table as determined from the channels was significantly lower at the degraded land class (median = -117 cm) with respect to the intact land class (median = -42 cm). This supports the findings of Sundari et al. (2012) that demonstrated that the water level in intact PSF was always higher than degraded PSF, and that degraded PSF underwent greater seasonal extremes. Though water table data were not available for the degraded land class, it is reasonable to assume from the water level data collected in this study, and water table data collected by Sundari et al., that the water table at the degraded land class was lower than at the intact land class during the dry season.

Air and water temperatures were significantly higher (by 3−6 ^{o}C) at the degraded land class in both the late wet season and the dry season. The greatest differences between land classes occurred in the wet season, owing to a cooling microclimate effect at the intact land class (see Chapter 3). Water temperature would have a significant effect on the solubility of CH_4, owing to its poorer solubility in water than CO_2. A lower solubility would promote emission of CH_4 to the atmosphere (Benson and Krause, 1984).

The degraded land class had about twice as much dissolved oxygen in the channel waters than the intact land class, during both seasons. The warmer water temperatures at the degraded land class would have caused a reduction in the solubility of oxygen, with respect to the cooler waters of the intact land class (Benson and Krause, 1984). However, the intact land class had less oxygen due to its consumption by heterotrophic processes (see Chapter 3).

The degraded land class had reasonably well-oxygenated waters (see Chapter 3) which could have inhibited methanogenesis in the channel sediments. Aeration of the sediments could be enhanced particularly if the channel was flowing (Jones et al., 1995; Truax et al., 1995). The same could be true of the intact land class, except that with less oxygen present, the capacity for aerating the sediments and

inhibiting methanogenesis would be less than the degraded land class. In terms of the oxygen content of the water, the degraded land class has a greater potential for oxidising sediments and reducing CH_4 production.

4.3.2 Dissolved CH_4

In the late wet season median dissolved CH_4 was much higher at the degraded sites than at the intact; medians for TAR1, TUN1 and KALA were 579, 2,361 and 1,115 μatm, respectively, while only 133, 186 and 94 μatm at SAB1−3 (see Fig. 4.3).

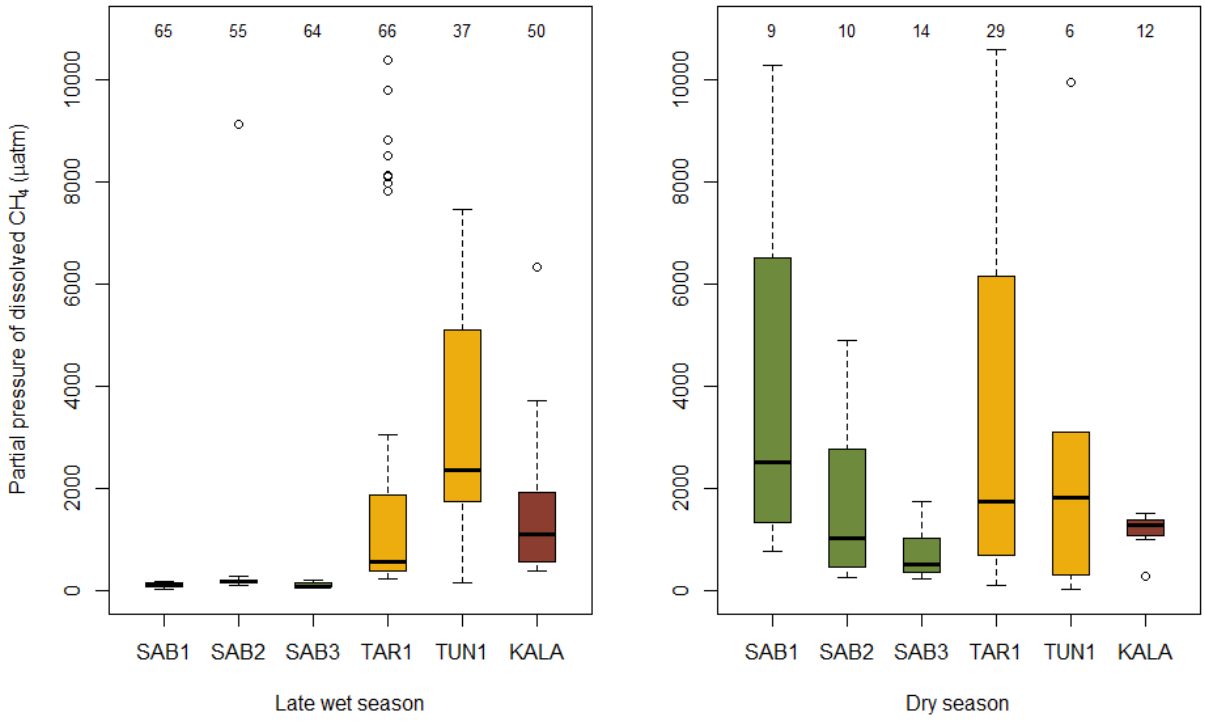

Figure 4.3: Dissolved CH_4 by site. In the late wet season intact dissolved CH_4 was very constrained and comparatively low where medians ranged from 94 to 186 μatm. Dissolved CH_4 at the degraded sites had much greater variances and were much higher, medians ranging from 579 to 2,361 μatm. In the dry season the degraded sites remained in the same range with 1,285 to 1,837 μatm, whereas the intact sites increased markedly to a range similar to the degraded sites (medians = 515−2,518 μatm).

Median dissolved CH_4 at the intact sites increased markedly in the dry season; 2,518, 1,023, 515 μatm for SAB1−3, respectively. At the degraded sites there was some change, but the values remained similar to those of the late wet season; 1,749, 1,837 and 1,285 μatm for TAR1, TUN1 and KALA, respectively.

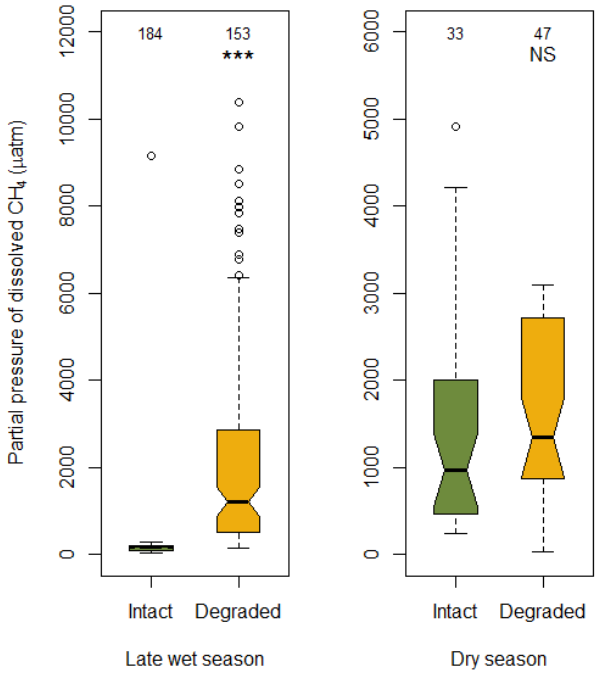

Figure 4.4: Partial pressures of dissolved CH_4 by land class in the late wet and dry seasons. In the late wet season, the intact land class median was 166 μatm CH_4 and partial pressures were significantly lower than the degraded land class (median = 1,215 μatm CH_4; $p < 2.2 \times 10^{-16}$). In the dry season, the degraded land class median increased slightly to 1,341 μatm CH_4, but the intact land class median rose 5.8−times to 968 μatm and the partial pressures were not significantly different to the degraded land class. Low water levels could have retarded the intact forest's ability to oxidise CH_4 in the rhizosphere, or translocate CH_4 via trees' aerenchyma.

During the late wet season, median dissolved CH_4 was over 7-times higher at the degraded land class; 1,215 μatm, compared to 166 μatm at the intact sites, which demonstrated comparatively little variance in the partial pressures (see Fig. 4.4). Dissolved CH_4 was highly constrained and demonstrated little variation, whilst greater ranges of values were found at the degraded land class; the intact land class (n = 184), apart from a single, seemingly anomalous value of 9,138 μatm, occupied a range between 44 and 280 μatm CH_4. Only 5 % of values at the degraded land class (n = 8 of 153 observations) were low enough that they occupied that range. A Wilcoxon's rank sum test found the land classes to be very significantly different with a large effect size; W = 314, $p < 2.2 \times 10^{-16}$, r = -0.66. This clearly demonstrates that deforestation and drainage significantly changes the way in which CH_4 is cycled in peat swamp forest ecosystems.

CH_4 is produced in abundance in wetland soils, largely due to their comparatively deep and anoxic soils. As a result of these conditions, wetlands are the largest single source of CH_4 emitted to

the atmosphere (Ito and Inatomi, 2012). Most of the CH_4 is oxidised to CO_2 in oxygenated soils or the water column, before it reaches the atmosphere (Schlesinger and Bernhardt, 2013). The comparatively low amounts of dissolved CH_4 in the intact channels during the wet season may result from a few phenomena, that are not mutually exclusive: a) that the intact land class channel sediments were producing negligible CH_4 that was dissolving as free CH_4, compared to the channels at the degraded land class; b) that rhizosphere oxidation was occurring in the intact land class peats, whereas at the degraded land class oxidation rates were much lower; and/or c) more CH_4 may have been transported out of the peat by plant-mediated transport at the intact land class, whereas little of this was occurring at the degraded land class. None of these processes were measured and so further study is required to understand the mechanisms driving CH_4 abundance in the channels, but the aforementioned possibilities will be discussed below.

One of the clearest differences between the intact and degraded land classes was the vegetation cover; a metabolically active forest ecosystem at the intact land class, whereas at the degraded land class it was much more sparsely vegetated, with ferns, reeds and grasses. Therefore, root density at the degraded land class could reasonably be expected to be significantly lower. As the rhizosphere in the forest could be more voluminous and complex than at the degraded land class, this could promote greater larger amounts of plant-mediated transport of CH_4 out of the peat, whilst also providing a much better environment for methanotrophs and methane oxidation due to the ingress of O_2 into the peat from the aerenchymatous plants. Both processes would reduce the amount of CH_4 that could be transported to the channels, and therefore it could be expected that the greatest effect of these processes would be evident at the intact land class.

Very low partial pressures of CH_4 were detected in the water at the intact land class and so it is possible that the larger amounts of plants present were promoting oxidation and/or tree-mediated translocation of CH_4 to the atmosphere. It is also less likely that the degraded sites will be dominated by aerenchymatous plants which specialise in waterlogged soils, as the degraded catchments likely have drier upper peat profiles owing to the greater degree of drainage and lower average annual water table (Sundari et al., 2012). This indicates that even if vegetation cover were equal, the degraded land class may be less able to mediate oxidation of CH_4, or CH_4 transport, by plants. Further study could inform as to the potential for CH_4 oxidation/transport by plants, by surveying the vegetation at the sites. Soil

moisture is an important component of the rhizosphere where water provides a solute in which microbes can live, nutrients and gases can dissolve and reactions occur. Drier upper peats at the degraded land class could also make the soil less hospitable to methanotrophs as well as reduce the potential for plant-mediated transport of CH_4.

The low rainfall anomaly of the 2015 dry season during the El Niño meant that channels became much shallower and/or became a discontinuous set of puddles. In some cases the channels dried out completely and water levels dropped below the channel bed. As the channels are cut into the peat surface and there was little or no water being retained above the channel bottom this meant that the water table was considerably below the actual peat surface. The water table was therefore out of reach to much of the rhizosphere (see Chapter 1); this was confirmed by a study by Jauhiainen et al. (2005) in the same study region which found that 83 % of the rhizosphere was located in the top 25 cm of the peat.

Given that plants dominate CH_4 emission when in freshwater environments (Chanton and Whiting, 1995), and the above vegetation-related processes and the effect they could have on the abundance of CH_4 in channels draining tropical peatlands, it appears that in-stream differences in CH_4 production are less likely to account for the seasonal differences in dissolved CH_4 between the two land classes. Hyporheic production of CH_4 in the sediments is usually lost as gas bubbles that rise quickly through the water column and burst on the surface without much dissolution of CH_4 along the way; a gas bubble may lose ˜15 % of its volume in 3 m of travel from sediment to surface (Chanton and Whiting, 1995). Therefore the degraded land class would have to be producing CH_4 bubbles in the bottom sediments at nearly 50−times the rate of the intact land class to account for the 7.3−fold difference between the two land classes during the wet season. Methane production would then have to rise significantly at the intact land class during the dry season. Methanogenesis is a Q_{10} temperature-dependent process, but the ˜5 °C difference between the water temperatures at the two land classes would be insufficient to account for such a large difference in the rate of methanogenesis (Dunfield et al., 1993). Further, there is only a 1.5 °C rise in water temperature at the intact land class between the two seasons and that would not account for a nearly 6−fold rise in methanogenesis in the dry season with respect to the wet season. Additionally, as the channels at the degraded land class contained approximately double the amount of O_2 than the intact land class (see Chapter 3), there was a much greater potential for the CH_4 to be oxidised both in the channel and in the sediments, and that would mean the differences in rates in methanogenesis may

have to be even higher. Though methanogenesis is likely to occur in the anoxic bottom sediments, it does not look to be a significant source of CH_4 to the channels.

At the degraded land class, median dissolved CH_4 was slightly (non-significantly) higher, being 1,341 μatm. At the intact site, however, dissolved CH_4 increased substantially to a median of 968 μatm, 5.8−times that of the late wet season. A Wilcoxon's rank sum test reported that there was no significant difference in dissolved CH_4 partial pressures between the land classes; W = 569, $p = 0.19$, r = -0.15. Due to the extreme conditions exacerbating a soil drought, the intact land class appeared to behave similarly to the degraded land class in both seasons.

Whereas variation at the sites was comparatively low at the intact sites during the wet season, it increased markedly during the dry season at SAB1 and SAB2. This is likely due to the channels drying to the point where they became a discontinuous set of puddles. Without the water forming a continuous flowing body which mixes its contents, localised spatial differences in CH_4 became apparent.

The partial pressures of dissolved CH_4 are high compared to those reported for peatland streams, though the literature is dominated by investigations in temperate areas and few data are available for the tropics (Raymond et al., 2013). For instance, a study of surface waters in the Mer Bleue peatland, Canada, had dissolved CH_4 partial pressures that ranged from 18−160 μatm (Billett and Moore, 2008). The partial pressures in this study are an order of magnitude higher. This likely is a result of a) higher soil temperatures b) water table depth and, potentially, c) deeper peats (Bubier et al., 1995; Turetsky et al., 2014).

Methanogenesis is a temperature dependent process whereby CH_4 production increases as temperature increases (Dunfield et al., 1993; Segers, 1998). As the tropics are considerably warmer than the northern hemisphere for much of the year, the elevated soil temperatures may create better conditions for methanogenesis. Hirano et al. (2007) measured soil temperatures in the region to be 25−30°C. This temperature range is near-optimal for the hydrogenotrophic methanogenesis pathway that dominates in peatlands (Svensson, 1984). Dunfield et al. (1993) found that CH_4 production could be between 16 to 20−times faster at 25−30°C than at 0−15°C, which is closer to the temperature range for most temperate peatlands.

Peatlands in the tropics are, on average, deeper than those in the northern hemisphere; average peat depth in Indonesia is 5.5 m (Page et al, 2011) whilst in the northern hemisphere it is 2.3 m (Gorham,

1991). Although CH_4 production gradually declines with peat depth (Roulet et al., 1992; Sundh et al., 1994), the overall amount of peat producing CH_4 could be greater in the tropics, leading to larger quantities reaching the channels.

Hope et al. (2001) reported upstream mean dissolved CH_4 partial pressures of 908 μatm. In certain areas of the catchment values did exceed 1,000 μatm and in one year exceeded 1,800 μatm. These values are approaching the partial pressures encountered in this study. The high CH_4 partial pressures reported by Hope et al. (2001) were measured in Scottish peatland headwaters. It is therefore possible that in a tropical peatland headwater setting, where ambient and soil temperatures will be higher and will favour methanogenesis that these partial pressures are feasible. Ueda et al. (2000) reported dissolved CH_4 surface water concentrations in a tropical peat swamp as high as 108 μM. This is considerably higher than 1.8 μM (or 879 μatm) reported in Hope et al. (2001).

4.3.3 Estimated diffusive flux of CH_4

Calculated diffusive fluxes of CH_4 in the wet season were 1.52, 2.61, 2.14 mg·C·m^{-2}·d^{-1} for SAB1−3, respectively, and 10.84, 17.07, 14.07 mg·C·m^{-2}·d^{-1} for TAR1, TUN1 and KALA, respectively.

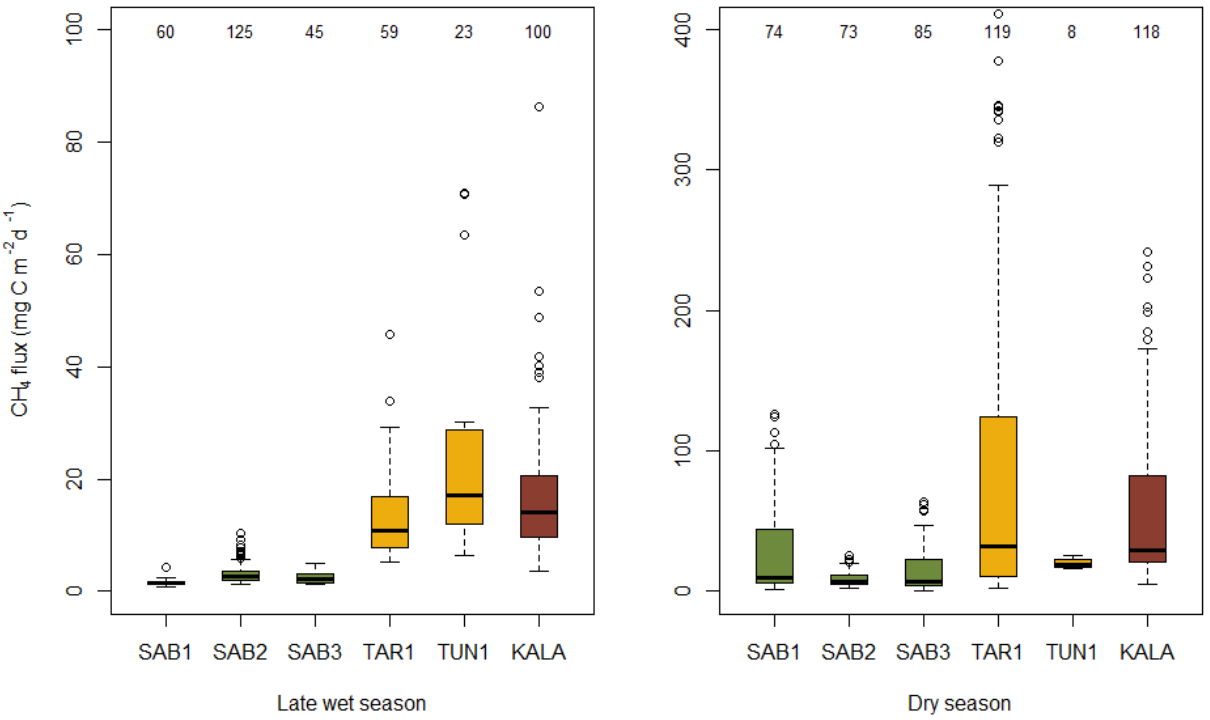

Figure 4.5: Estimated diffusive CH_4 fluxes by site, in the late wet and dry seasons of 2015. Note the different y-axis scales. In the late wet season, the median intact fluxes ranged from 1.52 to 2.61 mg·C·m^{-2}·d^{-1}. The degraded sites were much higher ranging from 10.84 to 17.07 mg·C·m^{-2}·d^{-1}. In the dry season, diffusive CH_4 emissions increased at all sites; ranging from 6.79 to 9.43 mg·C·m^{-2}·d^{-1} at the intact sites to 19.35 to 32.52 mg·C·m^{-2}·d^{-1} at the degraded sites.

Diffusive fluxes increased at all sites in the dry season, however water volume and surface area were both greatly reduced due to the lack of rain and so, in terms of aquatic CH_4 emission from total catchment fluxes, emissions would be low with respect to the wet season. Calculated CH_4 fluxes were 9.43, 7.16, 6.79 mg·C·m^{-2}·d^{-1} for SAB1−3, respectively, and 32.52, 19.35, 29.71 mg·C·m^{-2}·d^{-1} for TAR1, TUN1 and KALA, respectively.

Sampling at TUN1 was very restricted due to difficulty with accessing the site when it was dry and the data reflect only one day in that season. However, the value occupies a similar range to TAR1 and KALA and the median is higher than all the intact sites, as were TAR1 and KALA. In the wet season, TUN1 had the highest diffusive flux of CH_4 and perhaps for the dry season it is an underestimation.

At a land class level during the wet season: the degraded channels were calculated to emit significantly more CH_4 by diffusion than the intact channels, with a strong effect between land classes (Wilcoxon's rank sum test; W = 376, $p < 2.2 \times 10^{-16}$, r = -0.67). The degraded land class median was 6.29−times higher than the intact land class median, being 13.30 mg·CH_4-C·m^{-2}·d^{-1} and 2.11 mg·CH_4-C·m^{-2}·d^{-1}, respectively.

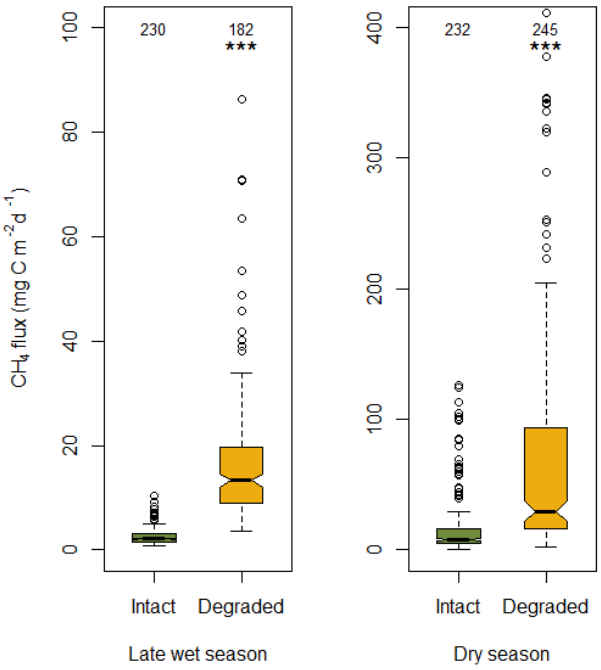

Figure 4.6: Estimated diffusive CH_4 fluxes by land class, in the late wet and dry seasons of 2015. Note the different y-axis scales. The degraded land class had significantly higher fluxes than the intact land class in the late wet season ($p < 2.2 \times 10^{-16}$) and there was much greater variability in the data (medians were 2.11 and 13.30 mg·CH_4-C·m^{-2}·d^{-1} for intact and degraded land classes, respectively). In the dry season median diffusive fluxes rose at both land classes. The degraded site maintained significantly higher fluxes ($p < 2.2 \times 10^{-16}$), though the proportional difference between land classes was less (medians were 7.76 and 29.64 mg·CH_4-C·m^{-2}·d^{-1} for intact and degraded land classes, respectively).

During the dry season, CH_4 flux increased at both land classes and the same pattern emerged: the calculated diffusive flux at the degraded land class was significantly higher (3.8−times) than at the intact land class (Wilcoxon's rank sum test; W = 11,113, $p < 2.2 \times 10^{-16}$, r = -0.52). The effect size, though still strong, was reduced. The degraded median was 29.64 mg·CH_4-C·m^{-2}·d^{-1} and the intact median was 7.76 mg·CH_4-C·m^{-2}·d^{-1}. These dry season medians were 3.7 and 2.2−times higher than the wet season medians for the intact and degraded land classes, respectively. The forest channels, therefore, produced the greatest seasonal response, switching from emitting just a little CH_4 to emitting substantially more, per unit area.

As mentioned previously, the actual area the channel water covered was small in the dry season compared to the wet season, and so this likely constitutes a net-reduction of CH_4 emissions from the channels with respect to total CH_4 emissions.

In the case of CH_4, the diffusive flux is not total flux as CH_4 can bubble up from sediments to the atmosphere without dissolving in the channel water (Chanton and Whiting, 1995). CH_4 bubble ebullition can dominate total CH_4 flux, particularly in lakes (Bastviken et al., 2011), and therefore the fluxes reported should be considered an underestimate of total CH_4 flux.

In the study of Jauhiainen and Silvennoinen (2012), mean 'diffusive' CH_4 emissions were given as 4.5−224.3 mg·CH_4-C·m^{-2}·d^{-1} for a channel that was both similar and close to KALA. Their reporting of this 'diffusive flux', however, is likely an oversight, and is extremely likely to be erroneous; their method of taking headspace samples from floating chambers could not have excluded nor constrained CH_4 ebullition from channel sediments. They also state that "visible gas bubbles surfacing on canal waters (ebullition) was [sic] noticed at several locations during the data collections [sic]." If those bubbles were not caused by fish or other things disturbing the channel's sediments, and was due to CH_4 ebullition, their flux is far more likely to be the sum of diffusive and ebullitive CH_4 fluxes.

As what are likely to be cumulative diffusive and ebullitive fluxes in Jauhiainen and Silvennoinen

(2012) were significantly higher than the diffusive fluxes reported in this study, it indicates that ebullition may overwhelmingly dominate total flux by almost an order of magnitude. The contribution of ebullition to total CH_4 flux has been shown to be generally lower in streams and rivers than lakes (12.8−60 %; Crawford et al., 2014). As flow in the channels can drop to unmeasurable levels (using the hand-held impeller in this study) during the peaks of the wet and dry seasons, the channels can, for significant periods of the year, largely behave similarly to lakes in terms of their gas exchange velocity. A dominant ebullitive contribution to total CH_4 flux is therefore possible at times of low flow.

CH_4 fluxes are known to vary significantly within the day, which is partly controlled by temperature; Bastviken et al. (2004) reported 9−158 % higher emissions in the daytime, in boreal lakes. All measurements were made during the day and therefore the diffusive flux may be an overestimate depending on whether temperature affects diffusion more than ebullition.

Although there is a lot of variation in the literature, the fluxes reported here are quite low, even compared with studies of temperate rivers. At the lower end Jones and Mulholland (1998) reported 0.3−10 mg·CH_4-C·m^{-2}·d^{-1} and de Angelis and Scranton (1993) reported 6.1 mg·CH_4-C·m^{-2}·d^{-1}, for the Walker Branch and Hudson rivers, respectively. Higher ranges were reported by Lilley et al. (1996) and Hope et al. (2001), being 0−238 and 0−345 mg·CH_4-C·m^{-2}·d^{-1}, respectively in Pacific Northwest and Scottish rivers. The latter are both higher than the fluxes of Jauhiainen and Silvennoinen (2012), but within the same order of magnitude.

In the context of the catchments, the streams act as year-round CH_4 sources. In comparison, intact peat swamp forest soils in the area were estimated to be a weak sink of CH_4 on an annual basis (-0.156 to -0.276 g·CH_4-C·m^{-2}·yr^{-1}) while degraded peat swamp forest soils were a source of CH_4 (0.147−0.206 g·CH_4-C·m^{-2}·yr^{-1}; Jauhiainen et al., 2008). Again, with little forest to introduce recently photosynthesised carbon into the channels at the degraded sites, it is likely that the vast majority of the CH_4 must be coming from the peat and, at the degraded land class particularly, may be ancient in origin (cf. Moore et al., 2013).

4.4 Conclusions

Degradation in the form of deforestation and drainage affects the ability of peat swamp forest to regulate its near-surface water table, and as methanogenesis is a process that requires in waterlogged, anoxic soils, CH_4 cycling in can be greatly perturbed. Although water table drawdown was significant during the dry season (which was during an El Niño), it would likely have been in the range of $1-2$ m (Sundari et al., 2012). As the peats are deeper than this at both land classes (see Chapter 2), there would still be some metres of peat that would remain wetted and anoxic, and these conditions would promote methanogenesis.

Dissolved CH_4 was much higher in degraded peat swamp forest with respect to intact peat swamp forest, during the wet season. Partial pressures were low at the intact sites, likely due either to methane being removed by bacterial oxidation near the soil surface, or trees translocating the CH_4 to the atmosphere via their aerenchyma. The degraded peat swamp forest, lacking trees that would provide oxygen and habitat for methane oxidising bacteria, or significant amounts of aerenchyma, consequently had considerably more dissolved CH_4 in the water; it likely was not being oxidised or translocated, as it were at the intact sites. It is much less likely that the differences in dissolved CH_4 concentrations were due to differences in the rates of methanogenesis between land classes or seasons. In the dry season, there was no significant difference between the land classes despite the degraded sites having similar partial pressures to those they had in the wet season; intact dissolved CH_4 had risen considerably, likely due to extreme water table drawdown and soil drought resulting from the low rainfall anomaly of the 2015 El Niño. Further study is required to understand the relative contributions of rhizosphere oxidation, tree-mediated transport and sediment and bulk peat methanogenesis and methanotrophy as sinks and sources of channel CH_4.

Calculated CH_4 emission was consistently higher at the degraded sites. This occurred as a result of the high partial pressures of dissolved CH_4, and during the dry season, in combination with the higher k_{600} (see Chapter 3). The higher gas exchange velocity was probably affected by the open, unforested nature of the sites, and winds could disturb the water surface. As a combination of reduced CH_4 destruction and/or tree root translocation, and greater gas exchange velocities due to exposure, degraded peat swamp forest channels become a significant source of CH_4.

The channels largely appear to be hotspots of CH_4 emission with respect to the peat and trees (of

the intact land class) within their respective catchments: This study found that intact channels in the wet season emitted 2.11 mg·C·m^{-2}·d^{-1} which is much higher than the emissions reported in Pangala et al. (2013); the peat surface and trees emitted 0.29 and 0.50 mg·CH_4-C·m^{-2}·d^{-1}, respectively.

In terms of annual estimates, the intact land class channels emitted 1.26 g·C·m^{-2}·yr^{-1}, which is less than the 1.36 g·C·m^{-2}·yr^{-1} which was estimated to come from the peat surface (Jauhiainen et al., 2005). Channels at the degraded land class emitted much more CH_4 (6.35 g·C·m^{-2}·yr^{-1}) than degraded peat swamp forest soils in South Kalimantan (1.20 g·C·m^{-2}·yr^{-1}; Inubushi et al., 2003).

On a catchment basis, Block C probably emits considerably more CH_4 from its channels (and floodplains) than the Sabangau Forest. However, the size of the catchments and seasonal surface water extent need to be properly quantified before accurate estimates can be made about the channels' contribution to catchment CH_4 flux (see Chapter 3). If conversion and/or degradation of intact peat swamp forest continues, this will cause CH_4 emissions to increase in the future.

This study did not include the ebullitive term for CH_4 which so far has not been investigated and constrained for intact or degraded peat swamp forest. Jauhiainen and Silvennoinen (2012) measured a larger total flux of CH_4 from a degraded channel near KALA, where mean flux ranged from 4.5−224 mg·CH_4-C·m^{-2}·d^{-1} in wet and dry seasons, respectively. Given that the diffusive fluxes measured in this study are considerably smaller, it may be that ebullition of CH_4 is a far more significant contributor to total CH_4 flux. Ebullition of CH_4 from peat swamp forest channels is therefore an important term to constrain to fully understand CH_4 cycling and emission in these ecosystems.

Jauhiainen et al. (2005) stated that "CO_2 is clearly a more important greenhouse gas than CH_4" in reference to carbon fluxes from the same intact tropical peat swamp forest. The findings of this investigation necessitate a reconsideration of that statement given the much higher CH_4 fluxes from the channels of the intact forest during periods of extreme dryness, and from the channels and floodplains of degraded peat swamp forest throughout the year. The floodplains, in particular, constitute a significant evasive surface area in the wet season which is the dominant season for 75 % of the year. As the frequency of flooding over the last 30 years has increased, and is expected to continue increasing (Wells et al., 2016), it is likely that continued land use change will amplify the switch in ecosystem functioning and landscape-scale evasion of greenhouses gases, particularly of CH_4.

Tropical wetlands are already the most significant source of CH_4 globally, in terms of land type

(Kirschke et al., 2013). Continued degradation of tropical wetlands such as peat swamp forest could therefore be making them an even more significant source of the second most significant anthropogenic greenhouse gas (Myhre et al., 2013). Better understanding of tropical wetland CH_4 cycling and emission from intact and degraded areas is needed, as CH_4 looks to become the dominant anthropogenic greenhouse gas later this century (Zhang et al., 2017).

4.5 Author contributions

V.G., S.E.P., C.D.E. ans S.P. conceived of the study. M.S.K., D.B., V.G., C.D.E., S.P. and S.E.P. devised the methods. M.S.K., I. and S. carried out the fieldwork. M.S.K. carried out the data analysis and wrote the manuscript. V.G., S.E.P. and C.D.E. provided comments on an early version of the manuscript.

Chapter 5

The effects of a strong El Niño event on greenhouse gas emissions from channels draining intact and degraded peat swamp forest

Authors: Kent, M.S.[1,2], Page, S.E.[3], Evans, C.D.[4], Hanafi[5], Idrus[5,6], Bastviken, D.[7] and Gauci, V.[2]

Institutions: [1]*School of Agricultural and Environmental Sciences, University of Nottingham, Sutton Bonington Campus, College Road, Loughborough, LE12 5RD.* [2]*School of Environment, Earth and Ecosystem Sciences, Faculty of Science, Technology, Engineering and Mathematics, The Open University, Walton Hall, Milton Keynes, MK7 6AA.* [3]*Department of Geography, University of Leicester, University Road, Leicester, LE1 7RH.* [4]*Centre for Ecology and Hydrology, Environment Centre Wales, Deiniol Road, Bangor, LL57 2UW.* [5]*Borneo Nature Foundation, Jalan Bukit Raya No. 82, Bukit Raya, Palangkaraya 73112, Central Kalimantan, Indonesia.* [6]*Center for International Cooperation in Sustainable Management of Tropical Peatland (CIMTROP), University of Palangkaraya, Jalan Yos Sudarso, Kampus UNPAR Tunjung Nyahu, Palangkaraya 73111, Central Kalimantan, Indonesia.* [7]*Department of Thematic Studies, Linköping University, Campus Valla, Linköping, Sweden.*

Abstract

Peat swamp forests (PSF) are entirely dependent on rain to maintain their characteristically waterlogged soils. By having waterlogged soils for most of the year, decomposition of the peat is retarded and organic matter accumulates such that PSF acts as a carbon (C) sink and a substantial terrestrial C store, containing 3,350±110 Mg·C·ha^{-1}. During an El Niño event, the anomalously low rainfall can result in drought for PSF, which can cause the water table to drop considerably lower beneath the peat surface, and for longer periods, than normal years. Enhanced water table drawdown promotes greater peat oxidation and a reduction in soil moisture, both of which may influence PSF C cycling and emission of carbon dioxide (CO_2) and methane (CH_4). Work presented in Chapters 3 and 4 demonstrates that channels are loss pathways of CO_2 and CH_4 from PSF and degraded peat. Here I present data on emissions of CO_2 and CH_4 from channels draining intact and degraded PSF during and after the 2015 El Niño event. CO_2 evasion from the channels dropped significantly from wet to dry seasons and by up to ~50 % during the El Niño. Methane emissions were up to 11−times higher from channels draining degraded PSF (10−30 mg·CH_4-C·m^{-2}·d^{-1}). However, the El Niño greatly perturbed intact PSF CH_4 cycling with dissolved CH_4 concentrations comparable to those found in degraded PSF and with CH_4 fluxes twice as large as any other sampling season at intact PSF (7.5 mg·CH_4-C·m^{-2}·d^{-1}). The drying caused by the El Niño was sufficiently strong to have caused intact PSF to behave similarly to degraded PSF in terms of having comparatively high dissolved concentrations and emissions of CH_4, thus shedding light on potential mechanisms that may be responsible for observed changes in C-cycling processes that result from degradation. The data presented here show that intact PSF may still be vulnerable to switches in ecosystem CH_4 cycling during strong El Niños such as that of 2015.

5.1 Introduction

The El Niño−Southern Oscillation (ENSO) drives climatic extremes in the tropics. In this chapter, data are presented to examine the effects of the 2015 El Niño event on greenhouse gas evasion from channels draining intact and degraded peat swamp forest.

An El Niño typically causes anomalously warm and dry weather in Indonesia (Harger, 1995), the country with the largest amount of tropical peatlands, globally. The peatlands in Indonesia are peat

swamp forests.

Tropical peat swamp forest receives all its water from rainfall. The significantly reduced amount of rain during El Niño can cause the water table to drop considerably lower than is normal (i.e. a long-term average). The water table dictates how much of a peat swamp forest's soils are anoxic (waterlogged) or oxic (exposed to the air) which can alter the cycling of C and affect emissions of CO_2 and CH_4. On an ecosystem scale, waterlogging of peats generally promotes the production and emission of CH_4 and exposure of the peats to oxygen generally promotes the production of CO_2.

From satellite data collected at a broad scale, tropical wetlands (which include tropical peatlands) have been shown to respond to protracted drought and inundation caused by strong El Niño and La Niña events in that they release globally-significant quantities of CO_2 and CH_4; the atmospheric growth rates of CO_2 and CH_4 jumped following the 2015−16 El Niño and 2011−12 La Niña, respectively (Betts et al., 2016; Pandey et al., 2017).

As the occurrence of strong El Niños and La Niñas are challenging to predict, and are not particularly frequent (there have been three strong El Niños since 1950; L'Heureux et al., 2017), it is difficult to plan to study their effects on ecosystem C-cycling and CO_2 and CH_4 emissions in bottom-up studies, and hence it presents a challenge with respect to obtaining a clear understanding of the mechanisms that promote the large-scale responses that have been observed using satellites.

Peat swamp forest soils are particularly C-dense and have been estimated to contain 3,350±110 $Mg{\cdot}C{\cdot}ha^{-1}$ (Tonks et al., 2017). Carbon loss and emission of CO_2 by Indonesian peat swamp forest has been shown to accelerate during El Niño events, mostly due to fire and peat oxidation. Intact peat swamp forest is significantly less susceptible to fire (Siegert et al., 2001) and peat oxidation (Miettinen et al., 2017), but the burning and oxidation of degraded peat swamp forest has resulted in the loss of petagrams of C since being deforested and drained. Drainage channels have also been shown to be a major loss pathway for peat C, particularly for degraded peat swamp forest.

Drought, which is exacerbated by El Niño, had been shown to affect the composition of microbial communities in tropical peat (Kwon et al., 2013), which has been shown to alter the way C is cycled in the peat (Fenner and Freeman, 2011). Such changes due to drought have been shown to affect the production and emission of CO_2 and CH_4 in a moist tropical forest (Davidson et al., 2008). As a considerable proportion of CO_2 and CH_4 can enter channels laterally (Hoyt et al., 2017), changes in the rates of

the production and transfer of those gases from the adjacent peat to the water could affect the rates of emission of the gases from the channel.

Chapters 3 and 4 demonstrated that channels draining peat swamp forest were a source of CO_2 and CH_4. Further, those chapters demonstrated that CO_2 emissions were higher in intact peat swamp forest than degraded peat swamp forest, whereas the converse was true for CH_4. It is not yet known whether −or how− emissions may vary from channels draining peat swamp forest during an El Niño, however, due to its exacerbation of drought and water table drawdown, it seems likely.

This study addresses the question: Can El Niño events affect diffusive fluxes of CO_2 and CH_4 from channels draining intact and degraded peat swamp forest?

5.2 Materials and Methods

5.2.1 Study sites

The study sites were as mentioned in Chapter 2 except that, due to logistical issues, BER1 was substituted for TUN1 (see Fig. 5.1) in the later two sampling seasons (in 2016). BER1 was similar to TUN1 in that it occupied intermediately degraded peat swamp forest, where the channel discharged into the Kahayan River and there was a human settlement adjacent to the channel.

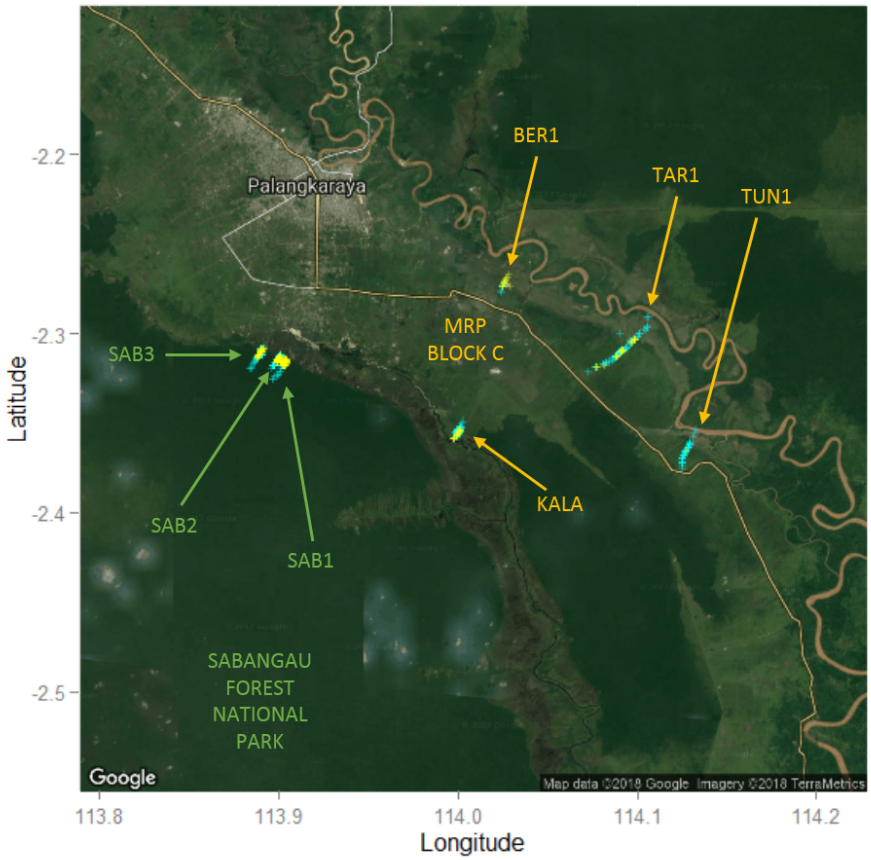

Figure 5.1: Map of the sampling region in Central Kalimantan, Indonesian Borneo. The provincial capital, Palangkaraya, is labelled. Wet season sampling locations are shown in light blue and dry season sampling locations in yellow. These do not indicate the extent of the channels, only the sampling locations. Much greater stretches of the channels were accessible during the late wet seasons than the dry seasons (see Chapter 3). The intact Sabangau Forest National Park and degraded Mega Rice Project Block 'C' lie on opposite sides of the Sabangau River. In the first two seasons, running up to and including the 2015 El Niño, TUN1 was used as the third degraded site, but due to logistical issues this site was replaced with another degraded site BER1 for the later two sampling seasons in 2016. (Source map © 2018 Google.)

The floating chamber gas flux and environmental measurement methods employed in this study were identical to Chapters 3 and 4, and are described fully in Chapter 2. Water table data were provided courtesy of Borneo Nature Foundation (see also Chapters 3 and 4), a conservation operation monitoring in the Sabangau Forest.

Sampling took place in four excursions; two in a wet and dry season in 2015 (LWS and EDS, respectively) during that year's strong El Niño event, and two in a dry and wet season in 2016 (PDS and EWS, respectively), the year that followed the El Niño. The early wet season of 2015 and the late wet season of 2016 could not be sampled, i.e. no data could be collected for the entire wet season immediately

following the El Niño.

The abbreviations refer to: the late wet season in 2015 (LWS) when waters were lowering and the channels becoming drier as the season transitioned into the dry season; the El Niño dry season in 2015 (EDS) when the El Niño was at its peak in terms of a terrestrial rainfall and temperature anomaly; the post-El Niño dry season in 2016 (PDS), and; the early wet season of 2016 (EWS) when the dry season was transitioning into the wet season, i.e. when the water table was rising and channel water depth increasing as a result of increased precipitation (see Table 5.1).

Fewer observations were made in EWS as compared to the other sampling seasons as another separate experiment was being conducted. The EWS dataset comprises a day's-worth of observations for each of the sampling sites.

Analyses addressed the differences (in e.g. gas fluxes) between the wet seasons (LWS and EWS) and the dry seasons (EDS and PDS), considering LWS and EDS to be directly affected by the El Niño, and PDS and EWS to represent more normal, non-El Niño years. The precipitation anomaly exacerbated by the 2015 El Niño, with respect to non-El Niño years was evidenced by the Sabangau Forest water table data.

The sampling seasons conducted in the wet seasons (LWS and EWS) only constituted a few months of the total season, respectively before and after the peaks of their respective seasons. To reflect this, they were named according to whether they were before or after the wet season peak, i.e. early or late wet season. This is because the phase of the wet season can have an effect on gas fluxes, for both CO_2 and CH_4 (Bartlett and Harriss, 1993). Rewetting of dried peat, for instance when rains return following a dry season, can stimulate high rates of degradation and CO_2 emission (Fenner and Freeman, 2011). Hydrostatic pressure exerted by the channel water on the stream sediments, when high, can reduce ebullition of CH_4 (Maeck et al., 2014). When hydrostatic pressure is low, for instance when channel waters are subsiding, CH_4 ebullition can increase. As these intra-seasonal effects have been shown to affect gas fluxes (Bartlett et al., 1988, 1990) they have been reported as early or late wet seasons. The early wet season is when rains are returning and the water is rising toward the peak, and the late wet season is when rainfall is gradually reducing and water levels are lowering.

Table 5.1: Fieldwork took place in two campaigns that each comprised a wet and dry season, in 2015 and 2016, respectively. In between those two campaigns was a wet season (both early and late phases) during which no data were collected. Wet seasons are separated into two phases; when the rains return after the wet season the water levels are 'rising', and as rainfall reduces after the peak of the wet season the water levels are 'lowering'. Fieldwork was prematurely ended for EDS due to severe fires at the degraded land class (which were exacerbated by the El Niño).

Year	Season	Water Table	Sampled	Season No.	Season Code	Season Months	Months Sampled
2015	Wet	Lowering	X	1	LWS	April−June	April−June
2015	Dry	Low	X	2	EDS	July−October	July−September
2015−16	Wet	Rising		N/A	N/A	November−March	N/A
2016	Wet	Lowering		N/A	N/A	April−June	N/A
2016	Dry	Low	X	3	PDS	July−October	August−October
2016−17	Wet	Rising	X	4	EWS	October−March	November−December

5.2.2 Statistical analysis

All statistical analyses were performed as described in Chapter 2.

5.3 Results and Discussion

This section presents data relating to i) the water table, ii) the dissolved CO_2 and CH_4 in the channels, and iii) the emissions of CO_2 and CH_4 from the channels, during the wet season (LWS) and dry season (EDS) of the 2015 El Niño, and in the dry season (PDS) and following wet season (EWS) of 2016, after the El Niño.

The water table is considered a causal factor for the amounts of dissolved CO_2 and CH_4 in the channels, and the dissolved gases are considered a driver for the emissions of CO_2 and CH_4 from the channels.

The section begins by presenting water table data gathered by the Borneo Nature Foundation at the intact land class, and a discussion of water table data gathered by Sundari et al. (2012) between 2004−06 during which a weak El Niño event occurred (in 2004; see Fig. 3.4 in Chapter 1) at a site nearby the degraded land class.

The water table, dissolved gas and gas emission data are initially presented as an overview of how they varied chronologically, which emphasises the distinct differences between EDS and the other seasons and, therefore, when a strong El Niño can be considered to have its greatest effect in relation to the

types of data collected. Following the chronological data presentation is an analytical presentation that considers the differences between the wet and dry seasons, respectively, during and after the El Niño; the effects of a strong El Niño in terms of the collected data are more clearly highlighted at a seasonal scale than by comparing 2015 (the El Niño year) with 2016 (the non-El Niño year).

5.3.1 Water table data

In the wet seasons during and after the El Niño there was no significant difference in water table depths (Two sample t-test, t = -1.21, df = 28, p = 0.24; see Fig. 5.2). Mean water depths at LWS and EWS were -9.89 cm and -6.17 cm, respectively.

The water table during the El Niño dry season (EDS) in 2015 was significantly lower than the post-El Niño dry season (PDS) in 2016, and the effect size was large (Two sample t-test, t = -5.48, df = 34, p = 4.08 $\times 10^{-6}$, r = 0.68). The mean water table during PDS was lower than both wet seasons (-16.78 cm), as would be expected as there is less rainfall, but the mean during EDS was substantially lower (-60.83 cm). Although water table data were not available for the degraded land class, channel water level data at these sites indicated that the water table was significantly lower at the degraded land class than at the intact land class (see Chapters 2 and 3).

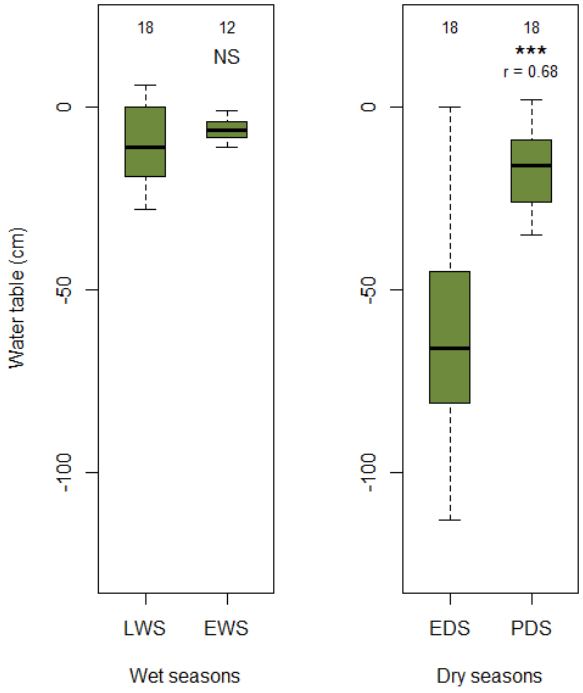

Figure 5.2: Comparisons of seasonal water table data at the intact land class. In the left pane are data from the two wet seasons, LWS in 2015 and EWS in 2016. There was no significant difference in water table depth in the wet seasons. The El Niño dry deason (EDS) had a significantly lower water table (p = 4.08 $\times 10^{-6}$) than the dry season following the El Niño (PDS), likely as there was no rainfall anomaly (shown in the right pane). If PDS consititutes a more normal dry season (mean water table = -16.78 cm), the El Niño affects a considerable departure from the norm (mean water table = -60.83 cm). (Data provided courtesy of Borneo Nature Foundation.)

5.3.2 Overview of partial pressures of CO_2 and CH_4 across the four sampling seasons

The intact sites generally responded similarly across the seasons, i.e. the values increased or decreased in unison (see Fig. 5.3). This was true for both dissolved CO_2 and CH_4. At the degraded sites values did not change together; some sites showed an increase where others decreased. This indicates that the degraded sites are more different to each other −or more unstable− than the intact sites and, as a result of this, patterns of dissolved CO_2 and CH_4 in degraded peat swamp forest may be harder to predict without constraining the factors that may cause the variability.

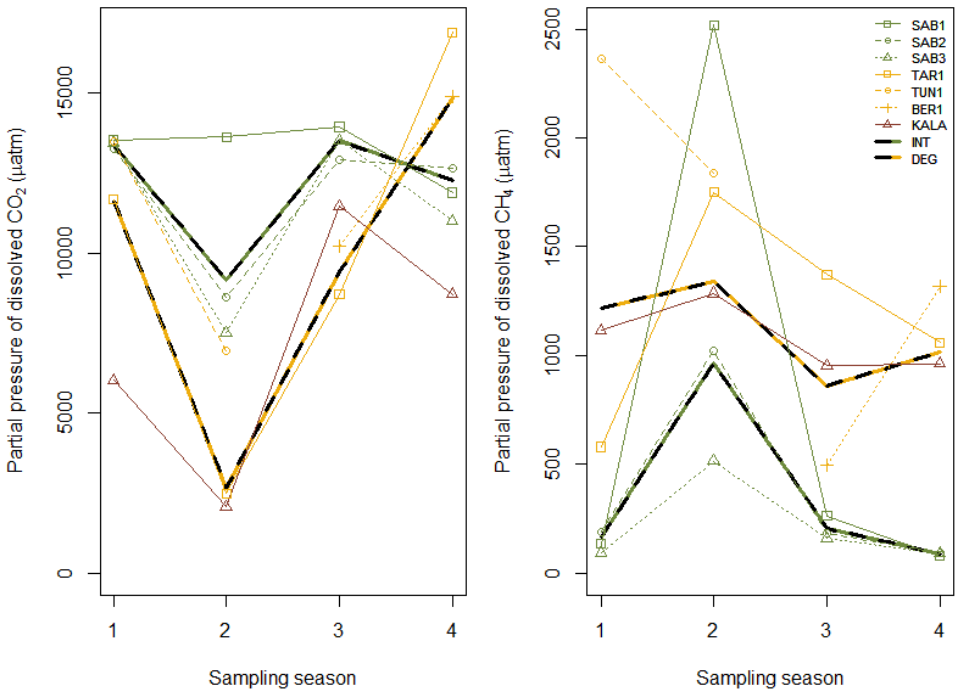

Figure 5.3: Seasonal changes in the partial pressures of CO_2 (left) and CH_4 (right) where seasons 1, 2, 3 and 4 are LWS, EDS, PDS and EWS, respectively. Lines are drawn to demonstrate the relative behaviours of the individual sites in the study. Two bolder, dashed lines mark the intact and degraded land classes and their median values. Dissolved CO_2 at the intact land class was higher in seasons $1-3$, but high values from TAR1 and BER1 in season 4 meant that median dissolved CO_2 at the degraded land class season exceeded those observed at the intact land class. Dissolved CH_4 at the degraded land class was consistently higher than at the intact land class across all sampling seasons.

Median partial pressures of CO_2 were consistently lower at the degraded sites than at the intact sites, except in season 4 (EWS). In the early wet season of 2016, after the 2015 El Niño, partial pressures of dissolved CO_2 at the intermediately degraded sites, TAR1 and BER1, both exceeded those of the intact sites and were the highest values encountered in the study. These high CO_2 partial pressures at TAR1 and BER1 meant the median partial pressure of CO_2 at the degraded land class was, also for the first time in the study, higher than the intact median.

TAR1 and BER1 are both used by nearby human settlements for sanitation and waste, which could add more labile C to the channels, where that would not be the case at KALA. The degradation of labile C at TAR1 and BER1 may have resulted in the high levels of CO_2 that were not observed at KALA, which is uninhabited. The increase in dissolved CO_2 maybe caused by something else to do with the catchment character at the intermediately degraded sites that KALA does not have, such as the much greater vegetation cover, that might provide labile C to the channels. This study, however, cannot determine the reason why dissolved CO_2 exceeded all intact sites, which are covered by a metabolically active peat swamp forest.

Dissolved CO_2 in the intact channels dropped considerably as the water table lowered during EDS (see Fig. 5.4), and may have dropped to even lower levels during the peak of the El Niño dry season in October 2015, however, the vast proportion of the channels were dry at this point and samples could not be collected. It is likely that the same effect of lowering water tables affected the dissolved partial pressures at the degraded land class, though water table drawdown could have been even greater than at the intact land class (see Fig. 3.4).

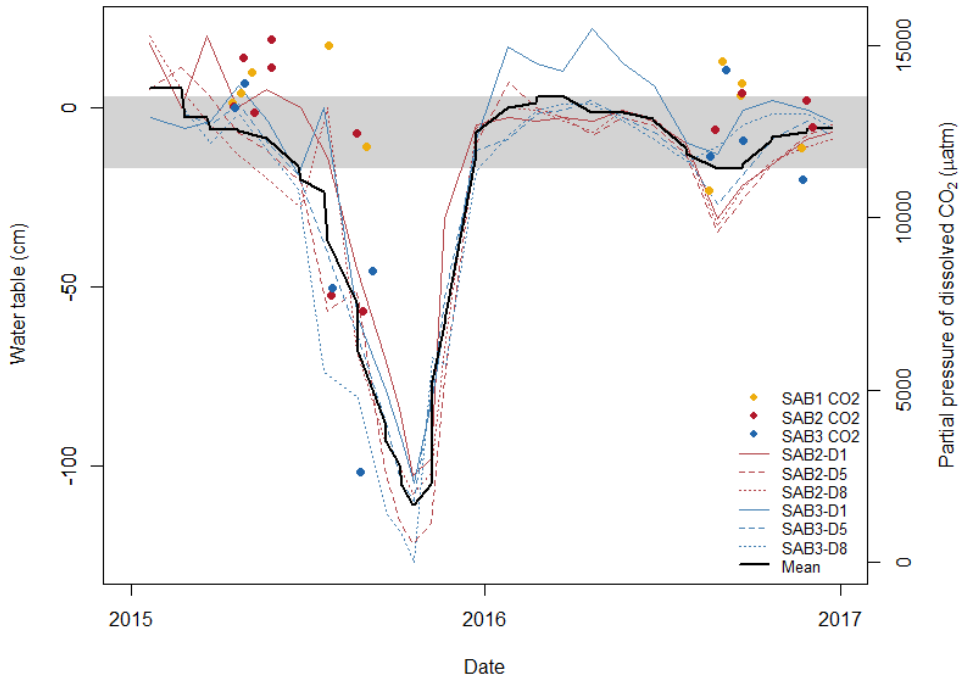

Figure 5.4: Monthly water table data from six dip wells located in the intact land class (shown with lines). The bold black line is the smoothed mean water table. Dissolved CO_2 (indicated by points) in the channels dropped sharply during the El Niño dry season when the water table dropped markedly. The grey horizontal band shows the range in water table amplitude for the following 2016−17 year which did not have anomalous rainfall or water table depths. Yellow, red and blue data represent SAB1, SAB2 and SAB3, respectively. There is more stochasticity in partial pressures with respect to the water table as partial pressure data were collected at a finer temporal scale; some events that affected water table over periods of days may not show at a monthly scale.

Partial pressures of CH_4 all followed a similar pattern at the intact sites, where they were consistently and significantly lower than at the degraded sites (see Fig. 5.3). However, there was a sharp rise in dissolved CH_4 during the El Niño dry season when, at SAB1, an intact site had a higher median of dissolved CH_4 than any of the degraded sites. This was the highest median partial pressure of CH_4 that was encountered in the study, of any of the sites.

The intact and degraded land classes both behaved broadly similarly, in terms if increases and decreases in dissolved CH_4, for the first three seasons. In the early wet season, however, the trend diverged where the intact land class showed a decrease, and the degraded land class showed an increase, in dissolved CH_4, with respect to the post-El Niño dry season (PDS).

At the intact land class, there was a strong response to the anomalous water table drawdown during EDS in the later half of 2015; dissolved CH_4 partial pressures increased and were 4 to 11−times higher than those recorded in the other sampling seasons (see Fig. 5.5).

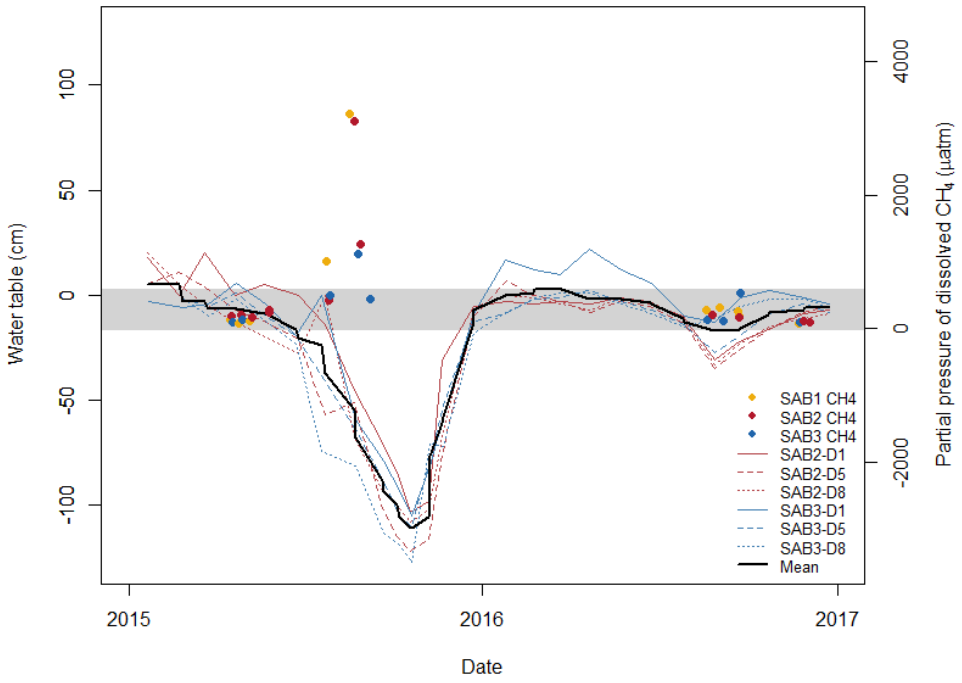

Figure 5.5: Monthly water table data from six dip wells located in the intact land class (shown with lines). The bold black line is the smoothed mean water table. Dissolved CH_4 (indicated by points) in the channels rose significantly during the El Niño dry season when the water table dropped markedly. The grey horizontal band shows the range in water table amplitude for the following 2016−17 year which did not have anomalous rainfall or water table depths. The grey band also approximately represents the upper 25 cm of the peat, where 83 % of the rhizosphere. The water table was deeper than -25 cm for the majority of the El Niño dry season. Yellow, red and blue data represent SAB1, SAB2 and SAB3, respectively. There is more stochasticity in partial pressures with respect to the water table as partial pressure data were collected at a finer temporal scale; some events that affected water table over periods of days may not show at a monthly scale.

The water table depth data and dissolved gas data were recorded independently, at different temporal scales; the water table data recorded by the Borneo Nature Foundation were monthly observations, whereas measurements of the dissolved gases were made daily to weekly. To explore the relationship between water table depth and the partial pressures of dissolved CO_2 and CH_4 in the channels of the intact land class (see Fig. 5.6), the water table data were transformed so that each observation connected via a gradual, linear change in depth to its neighbour (i.e. gap filling). Though this may not necessarily reflect the actual, naturally fluctuating water table (due to rainfall, etc.) it was the only way of exploring the relationship statistically.

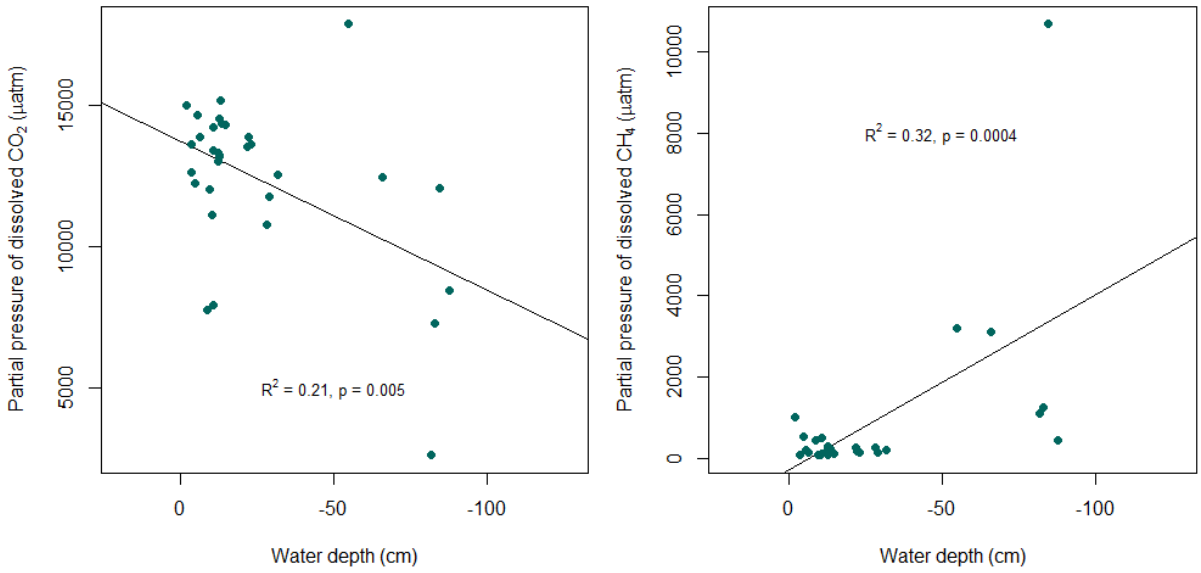

Figure 5.6: CO_2 (left pane) and CH_4 (right pane) resolved as a response to water depth at the intact land class. Dissolved CO_2 concentrations dropped significantly as the water table lowered (p = 0.005), and dissolved CH_4 concentrations rose significantly when the water table lowered (p = 0.0004).

Statistically significant relationships were found for the partial pressures of both CO_2 and CH_4 with respect to the water table depth; dissolved CO_2 reduced with water table depth (R^2 = 0.21, p = 0.005) whereas CH_4 increased (R^2 = 0.32, p = 0.0004), however the R^2 values were small, and hence the correlations were comparatively weak. This was likely partly due to a) natural variation during normal −i.e. not non-El Niño− months when the water table was within a normally occurring range, and, importantly, b) that the monthly water table depth data could not respond to changes at less than a monthly temporal scale, whereas the dissolved gas concentration data were responding to changes in daily water table depth. To properly explore this relationship a study might measure all variables simultaneously.

5.3.3 Overview of fluxes CO_2 and CH_4 across the four sampling seasons

Fluxes of CO_2 all followed the same general trend as highlighted by the land class medians in Fig. 5.7. Following the initial wet season, CO_2 emissions fell by ˜50 % across all sites and both land classes during the El Niño dry season (EDS). In the dry season of 2016 (PDS), emissions had increased at all sites but the intact land class median CO_2 flux was 19 % lower than, and the degraded land class median was approximately the same as, the initial wet season medians. Median CO_2 fluxes increased again in the early wet season of 2016 (EWS), with respect to the 2016 dry season at both land classes, but the intact

and degraded land classes were respectively less and more than the initial, late wet season (LWS).

There was good cross-land class agreement between both the intact and degraded CH_4 flux medians: CH_4 emissions increased markedly in EDS with respect to LWS, increasing over 3−times and over 2−times, at the intact and degraded land classes, respectively. CH_4 fluxes then fell to approximately the values of LWS in PDS, and then reduced again during EWS.

Estimated diffusive fluxes of CH_4 at the intact sites strongly followed the overall land class trend, but this was not the case for the degraded sites; CH_4 flux at TUN1 increased only a little in EDS with respect to LWS; KALA had very high CH_4 emissions during PDS compared to the other sites; and CH_4 emissions increased at BER1 during EWS with respect to the PDS, whereas for all the other intact and degraded sites CH_4 fluxes decreased.

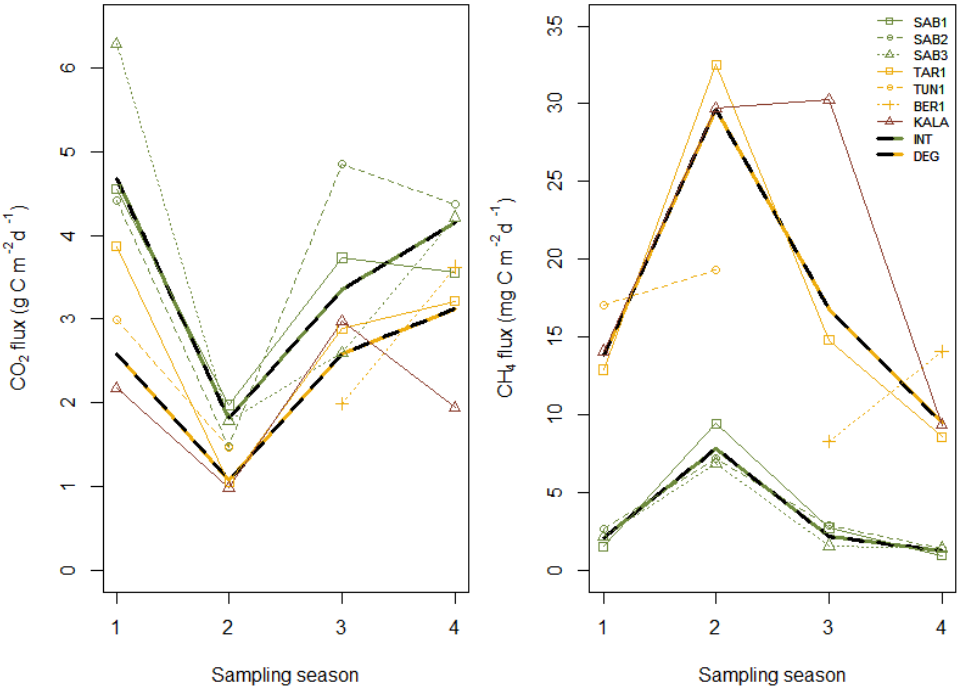

Figure 5.7: Seasonal changes in the fluxes of CO_2 (left) and CH_4 (right) where seasons 1, 2, 3 and 4 are LWS, EDS, PDS and EWS, respectively. Lines are drawn to demonstrate the relative behaviours of the individual sites in the study. Two bolder, dashed lines mark the intact and degraded land classes and their median values. The intact land class emitted consistently more CO_2 across the sampling seasons, whereas the degraded land class was estimated to have emitted (by diffusion) considerably more CH_4.

5.3.4 Wet season comparison

Carbon dioxide

Fluxes of CO_2 at both sites followed the same pattern as dissolved CO_2 in the channel water; at the intact land class partial pressures and fluxes of CO_2 were lower, and at the degraded land class CO_2 partial pressures and fluxes were higher, respectively in EWS at the end of the study (2016), with respect to LWS at the beginning of the study (2015; see Fig. 5.8).

The median partial pressure of dissolved CO_2 was significantly lower during EWS compared to the LWS, that led into the El Niño (Wilcoxon's rank sum test, W = 1,427, p = 4.21 $\times$ 10^{-5}, r = -0.29); during LWS the median martial pressure was 13,359 μatm CO_2 was measured, whereas during EWS the median partial pressure was 8 % lower, measuring 12,276 μatm CO_2.

At the degraded land class, the median partial pressure of dissolved CO_2 was significantly higher (Wilcoxon's rank-sum test, W = 1,316, p = 5.83 $\times$ 10^{-7}, r = -0.36), being 28 % higher in EWS (14,856 μatm CO_2) compared to LWS (11,637 μatm CO_2).

Although statistically significant, the lower partial pressure of dissolved CO_2 at the intact land class could be within a naturally fluctuating range of variation, which may or may not have been directly influenced by the 2015 El Niño. The degraded land class, however, had a 28 % increase in dissolved CO_2.

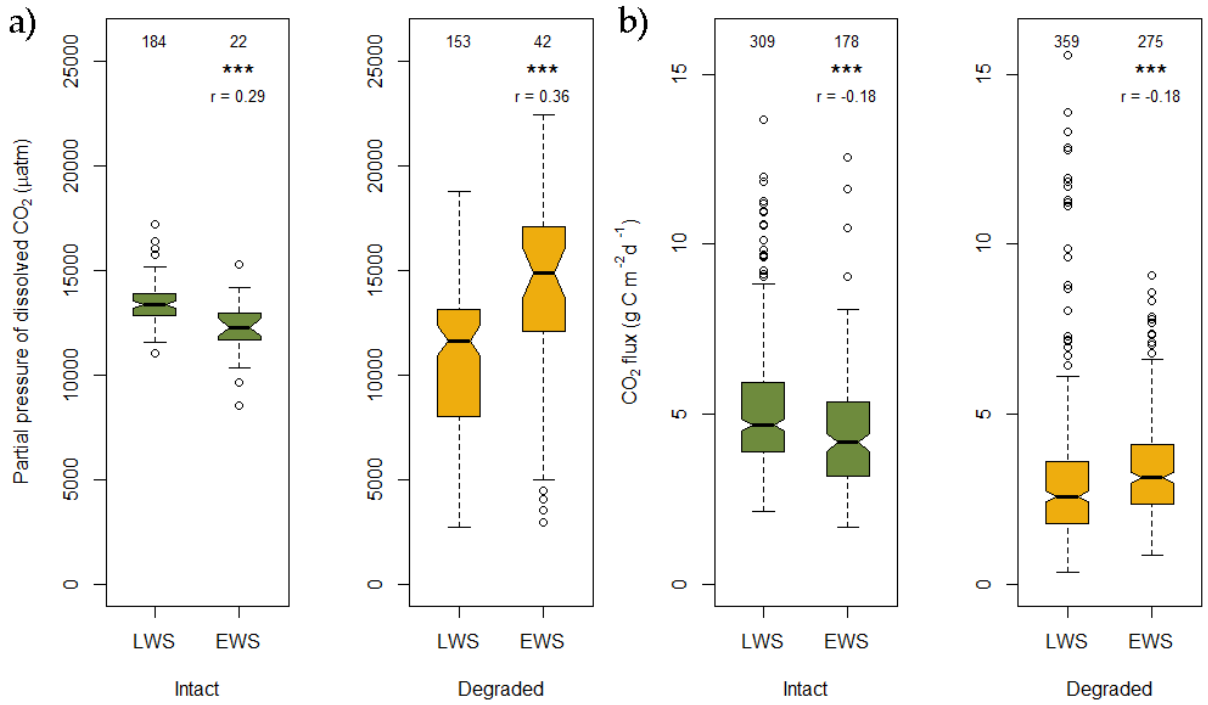

Figure 5.8: Partial pressures (a) and fluxes (b) of CO_2 measured from channels draining intact and degraded peat swamp forest, in the pre-El Niño wet season (LWS) in 2015 and the early wet season of 2016 (EWS), respectively. Dissolved CO_2 was significantly lower in EWS than LWS at the intact land class (p = 4.21 $\times$ 10^{-5}), but was significantly higher at the degraded land class (p = 5.83 $\times$ 10^{-7}). Fluxes of CO_2 followed the same pattern as dissolved CO_2 in that the intact land class emitted significantly less (p = 1.07 $\times$ 10^{-4}), and the degraded land class emitted significantly more (p = 7.19 $\times$ 10^{-6}) CO_2 in EWS with respect to LWS.

Fluxes of CO_2 followed the pattern of dissolved CO_2 at both land classes. The flux of CO_2 at the intact land class was significantly lower in the early wet season of 2016 than in the late wet season of 2015 (Wilcoxon's rank sum test, W = 27,986, p = 1.07 $\times$ 10^{-4}, r = -0.18); the median in 2015 was 4.68 g·C·m^{-2}·d^{-1} and in 2016, was 11 % lower, being 4.15 g·C·m^{-2}·d^{-1}.

At the degraded land class, median CO_2 flux was significantly higher in the early wet season of 2016, with respect to the late wet season of 2015 (Wilcoxon's rank sum test, W = 35,997, p = 7.19 $\times$ 10^{-6}, r = -0.18); there was an increase of 26 % from 2.49 to 3.13 g·C·m^{-2}·d^{-1}.

Methane

At the intact land class, median dissolved CH_4 partial pressure in the channels was significantly lower, dropping by 47 % from 166.5 to 87.9 μatm (Wilcoxon's rank sum test, W = 1,452, p = 1.81 $\times$ 10^{-5}, r = -0.30; see Fig. 5.9).

At the degraded land class, median dissolved CH_4 dropped from 1,215.2 to 1,017.4 μatm, but this difference was not statistically significant (Wilcoxon's rank sum test, W = 2,728, p = 0.95, r = -0.005).

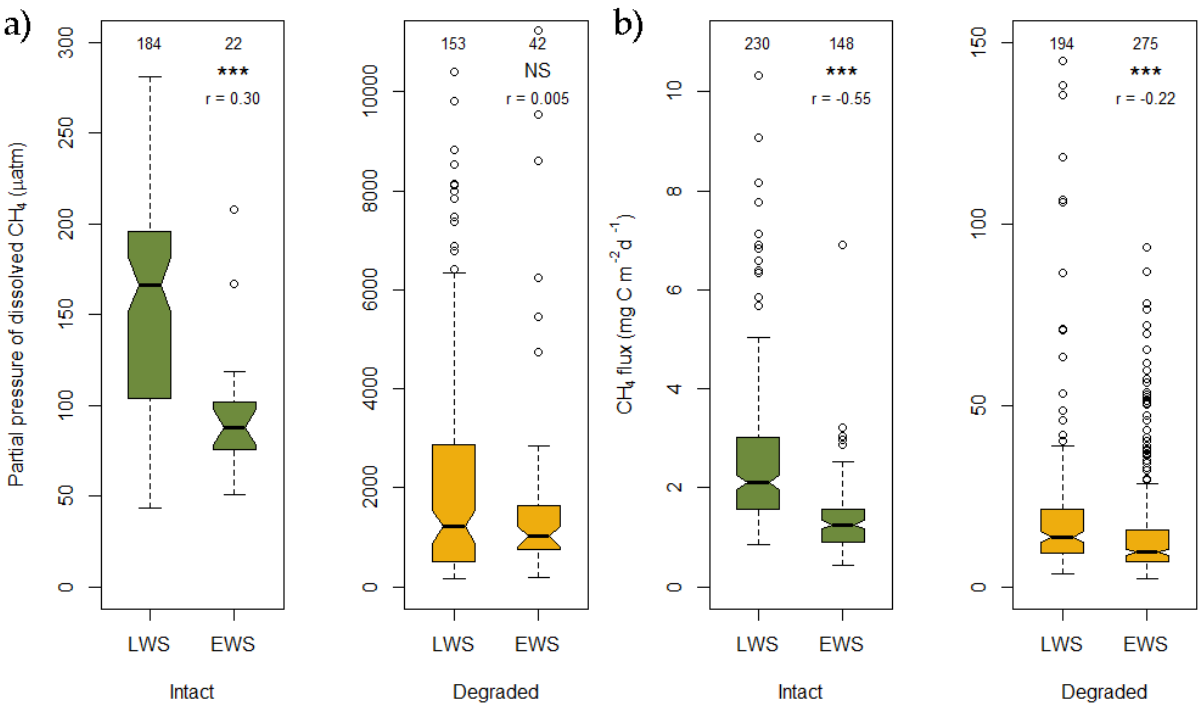

Figure 5.9: Partial pressures (a) and diffusive fluxes (b) of CH_4 measured from channels draining intact and degraded peat swamp forest, in the pre-El Niño wet season (LWS) in 2015 and the early wet season of 2016 (EWS), respectively. Note the different y-axis scales in both plots. Dissolved CH_4 was significantly lower in EWS than LWS at the intact land class ($p = 1.81 \times 10^{-5}$), but was not significantly different at the degraded land class. Estimated fluxes of CH_4 were significantly lower in EWS with respect to LWS at both the intact ($p < 2.2 \times 10^{-16}$) and degraded ($p = 1.23 \times 10^{-6}$) land classes.

Diffusive fluxes of CH_4 were significantly different at both land classes, between the 2015 and 2016 wet seasons, even though dissolved CH_4 at the degraded land class was not significantly different. This suggests that the gas exchange velocity was significantly higher during LWS with respect to EWS (see Chapter 3). The difference in the gas transfer velocity would likely have been due to differences in wind strength as the flux measurements were taken during periods of inundation (and low flows) at the degraded land class.

Median calculated diffusive flux of CH_4 at the intact land class was significantly lower between the 2015 and 2016 wet seasons, and the effect size was large (Wilcoxon's rank sum test, W = 28,096, $p < 2.2 \times 10^{-16}$, r = -0.55). It reduced by 41 % from 2.11 to 1.25 mg·CH_4-C·m^{-2}·d^{-1}, although figures in these ranges may be within a naturally varying range (see Fig. 5.7b).

The estimated diffusive flux of CH_4 at the degraded land class was also significantly lower during EWS with respect to LWS (Wilcoxon's rank sum test, W = 33,687, $p = 1.23 \times 10^{-6}$, r = -0.22). However, it reduced by a smaller amount (31 %) than the intact land class, going from a median of 13.81 to 9.48

$mg{\cdot}CH_4{\text{-}}C{\cdot}m^{-2}{\cdot}d^{-1}$.

5.3.5 Dry season comparison

Carbon dioxide

The dry seasons yielded the lowest partial pressures of dissolved CO_2 in the study, with the lowest occurred during the El Niño of 2015. This was true of both the intact and degraded land classes.

During the El Niño (EDS), median dissolved CO_2 at the intact land class measured 9,148 μatm, rising to 13,541 μatm during EDS (see Fig. 5.10); EDS was 32 % lower than PDS, this being a significant reduction which neared a large effect size (Wilcoxon's rank sum test, W = 231, $p = 5.97 \times 10^{-5}$, r = -0.49).

At the degraded land class, the lower median dissolved CO_2 during EDS was more pronounced, it being 71 % lower with respect to PDS. During the El Niño the partial pressure of CO_2 in the channel measured 2,669 μatm, rising to 9,419 μatm in the next dry season, which constituted a significant difference with a large effect size (Wilcoxon's rank sum test, W = 258, $p = 3.50 \times 10^{-7}$, r = -0.56).

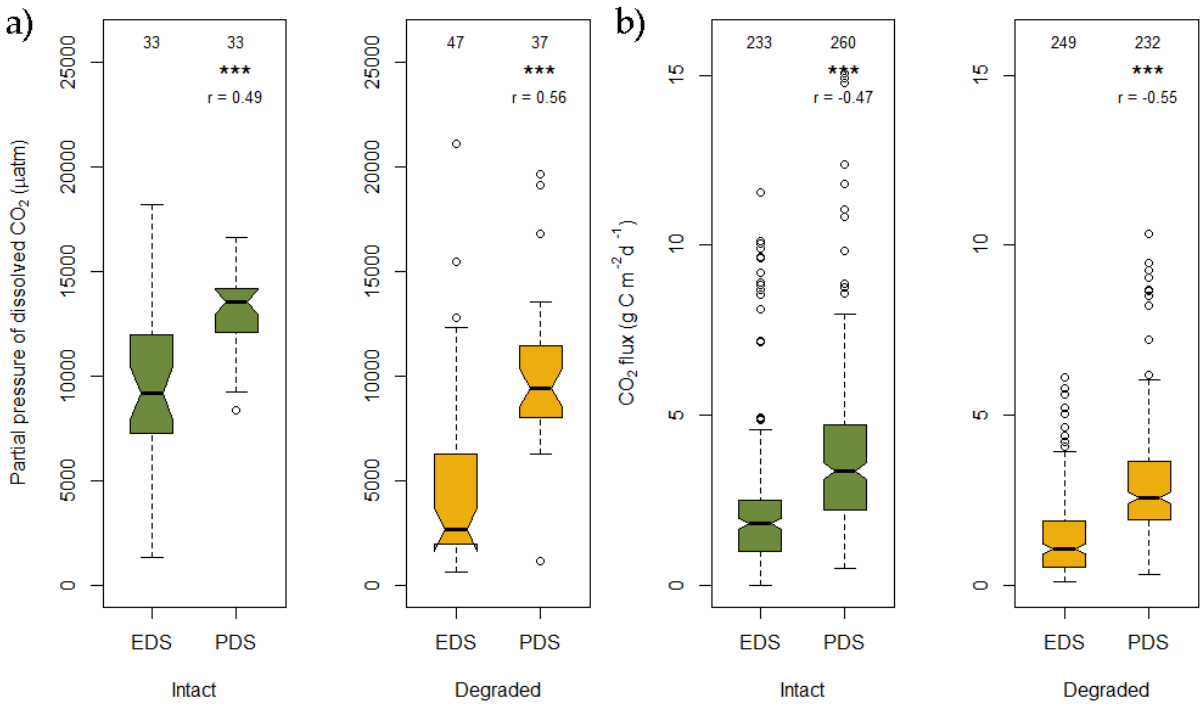

Figure 5.10: Partial pressures (a) and fluxes (b) of CO_2 measured from channels draining intact and degraded peat swamp forest, during the El Niño dry season (EDS) in 2015 and the post-El Niño dry season in 2016 (PDS), respectively. Partial pressures of CO_2 were significantly lower in EDS with respect to PDS, at both the intact ($p = 5.97 \times 10^{-5}$) and degraded ($p = 3.50 \times 10^{-7}$) land classes. Fluxes of CO_2 were also significantly lower in EDS with respect to PDS, at both the intact and degraded land classes, which both had p-values less than 2.2×10^{-16}.

Median CO_2 fluxes during the EDS were also the lowest recorded in the study, reflecting the reduced partial pressures of CO_2 in the channels.

Median CO_2 flux at the intact land class during EDS was 46 % lower than the dry season following the El Niño, and measured 1.81 and 3.36 g·C·m^{-2}·d^{-1}, respectively. This was a statistically significant difference with a medium−large effect size (Wilcoxon's rank sum test, W = 13,897, $p < 2.2 \times 10^{-16}$, r = -0.47).

The degraded land class, proportionally, had a lower flux of CO_2 during EDS than during PDS, with respect to the intact land class. Median CO_2 flux during PDS was 2.58 g·C·m^{-2}·d^{-1}, whereas it was 58 % lower and 1.07 g·C·m^{-2}·d^{-1} during the El Niño. A Wilcoxon's rank sum test found this to be statistically significant and there was a large effect size; W = 10,558, $p < 2.2 \times 10^{-16}$, r = -0.55.

Methane

The El Niño dry season (EDS) had consistently higher median partial pressures and median diffusive fluxes of CH_4, at both land classes, with respect to the post-El Niño dry season of 2016 (PDS).

Median dissolved CH_4 at the intact land class was 365 % higher in the El Niño dry season than in the 2016 dry season, respectively being measured at 968 to 208 μatm CH_4 (see Fig. 5.11). This was statistically significant with a very strong effect size (Wilcoxon's rank sum test, W = 1,032, $p = 4.22 \times 10^{-10}$, r = -0.77).

At the degraded land class the difference between the 2015 and 2016 dry season dissolved CH_4 was not as pronounced and with a much smaller effect size than at the intact land class, but the difference was still significantly different (Wilcoxon's rank sum test, W = 923, $p = 0.03$, r = -0.24). During EDS, median partial pressure of CH_4 in the channels was 1,341 μatm, which was 56 % higher than PDS when it measured 860 μatm.

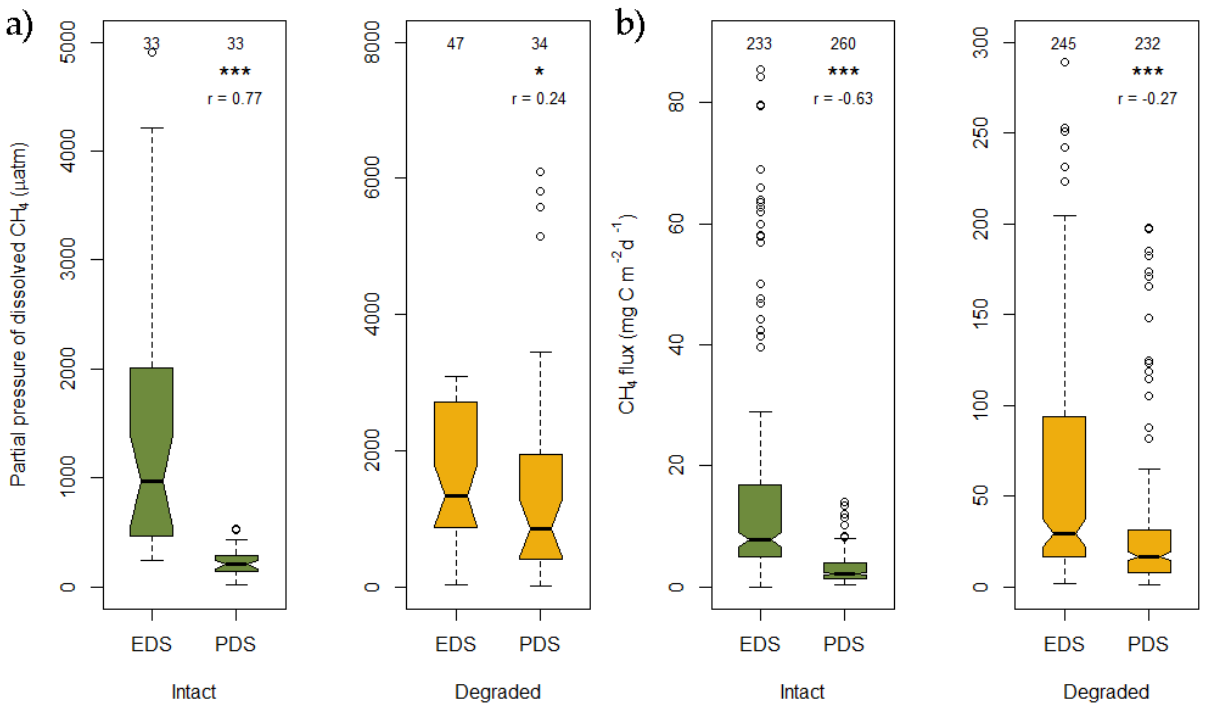

Figure 5.11: Partial pressures (a) and diffusive fluxes (b) of CH_4 measured from channels draining intact and degraded peat swamp forest, during the El Niño dry season (EDS) in 2015 and the post-El Niño dry season in 2016 (PDS), respectively. Note the different y-axis scales in both plots. Partial pressures of CH_4 were significantly higher in EDS with respect to PDS, at both the intact ($p = 4.22 \times 10^{-10}$) and degraded ($p = 0.03$) land classes, though the latter was far less statistically significant. Estimated fluxes of CH_4 were also significantly higher in EDS with respect to PDS, at both the intact ($p < 2.2 \times 10^{-16}$) and degraded ($p = 2.56 \times 10^{-9}$) land classes.

The median diffusive flux of CH_4 at the intact land class was 260 % higher during EDS than in PDS, when they measured 7.79 and 2.16 mg·CH_4-C·m^{-2}·d^{-1}, respectively. This difference was highly significantly different with a large effect size (Wilcoxon's rank sum test, W = 52,500, $p < 2.2 \times 10^{-16}$, r = -0.63).

At the degraded land class, the difference in median diffusive fluxes of CH_4 between the two dry seasons was less, with a lower effect size, but the difference was still statistically significant (W = 37,385, $p = 2.56 \times 10^{-9}$, r = -0.27). The median fluxes were 29.64 mg·CH_4-C·m^{-2}·d^{-1} during EDS, which was 76 % higher than the median flux of 16.83 mg·CH_4-C·m^{-2}·d^{-1} estimated for PDS.

5.3.6 CO_2 during and after the 2015 El Niño

Although differences were highly significant for both partial pressures and fluxes of CO_2, at both the intact and degraded land classes, the effect sizes were small to medium. As such, the El Niño does not appear to have a strong effect on dissolved partial pressures or emissions of CO_2, with respect to whether

a wet season falls within or outside of an El Niño. The largest cumulative effect observed for CO_2 was at degraded peat swamp forest, indicating it may be more easily perturbed by an El Niño, than intact peat swamp forest.

The observed differences may also have been due to the wet seasons being at different sides of the peak of the season; for instance EWS constitutes a potentially dry peat being re-wetted which can result in pulses of large quantities of labile DOC and CO_2 emissions (Fenner and Freeman, 2011).

For the dry seasons, the effect sizes at the intact land class for differences in dissolved CO_2 and fluxes of CO_2 were very near large, and those of the degraded sites were large. The effect sizes suggest that, during an El Niño event, it is during the dry season as opposed to the wet season that the greatest perturbations to dissolved CO_2 and CO_2 fluxes take place. Similar to wet season CO_2 dynamics, degraded peat swamp forest appears to be more easily perturbed than intact peat swamp forest, i.e. the effect sizes were larger for degraded peat swamp forest in both the wet and dry season comparisons.

Partial pressures and fluxes of CO_2 appeared to respond to the seasons and the changes in water table, whereby higher water tables at both land classes resulted in higher CO_2 partial pressures and emissions. This is likely due to a larger amount of wetted peat connected to the channels, and greater flows to the channels, delivering more degradable substrate and dissolved CO_2 from the catchment (see Chapter 3).

Overland flow is thought to dominate water flow as it moves from the centre of a tropical peat dome to its periphery, accounting for 84 % of total outward water flow (Baird et al., 2017). During wet seasons when overland flow occurs at the intact land class, the water can pick up labile C substrates from e.g. leaf litter or dissolved CO_2 from soil respiration. These solutes, respectively, can prime the channels for further in-stream degradation and/or raise the dissolved CO_2 concentration. Higher concentrations of dissolved CO_2 will cause CO_2 fluxes to increase, at the same gas exchange velocity.

The forest water table data (see Fig. 5.4) suggest there is less overland flow and more groundwater flow during dry seasons, when the water table drops below the surface. As such, less labile C or CO_2 reaches the intact channels, and fluxes correspondingly decrease.

A degraded tropical peat dome is thought to have water flow completely dominated by groundwater flow (Baird et al., 2017). Whilst this may be the dominant pathway at the centre of dome, the lower parts at a dome's periphery can flood for months at a time during a wet season (see Fig. 2.8 and Chapter

3). This could facilitate the movement of C substrates and CO_2 from the wider catchment to the channels, however, the C substrates could be more refractory (Moore, 2011). Without a metabolically active forest dominating the catchment, there will also be less C and CO_2 compared to an intact catchment. Reflecting this, the partial pressures of dissolved CO_2 and fluxes of CO_2 were generally less, particularly during the El Niño dry season.

Correspondingly, EDS had the lowest partial pressures and fluxes of CO_2 likely because the water table was so low and therefore a smaller volume of wetted peat is connected to the channels and delivery of C substrates and CO_2 was reduced. The wetted peat will also be composed of deeper peat layers where the C could be more refractory than that nearer the surface (Moore, 2011; Moore et al., 2013).

5.3.7 CH_4 during and after the 2015 El Niño

Similarly to CO_2, the effect sizes for the differences in wet season CH_4 partial pressures and fluxes were smaller for both the intact and degraded land classes, with respect to the dry season. Additionally the effect size was non-significant for the comparison between dissolved CH_4 at the degraded land class. Though differences were highly significant between the fluxes of CH_4 between the wet seasons, the differences may be within a range of natural variation (e.g. as a result of changing gas exchange velocities due to water flow/wind; see Chapter 3).

The higher partial pressures and fluxes of CH_4 during LWS, particularly at the intact site, may be an artefact of the wet season transitioning to the dry season earlier. An earlier dry season could mean that it was drier than a typical non-El Niño dry season, due to reduced rainfall associated with the El Niño. In other words, EWS might represent a more normal year.

The effect sizes for differences between dry season CH_4 partial pressures and fluxes were all larger than the equivalent wet season comparisons, and similarly to CO_2, the most anomalous CH_4 data were gathered during EDS, particularly for the intact land class, whereby the dissolved partial pressures and fluxes of CH_4 were much higher than all other sampling seasons; CH_4 dynamics during an El Niño dry season appear to change considerably from what seems to be an otherwise stable state.

It was during EDS that the intact land class underwent water table drawdown to the extent that it was in a range similar to that of the degraded land class in normal dry seasons, where it might be >1 m beneath the peat surface (e.g. Jauhiainen et al., 2008; Sundari et al., 2012). It was at this time (EDS) that

the intact land class also appeared to switch state, and CH_4 dynamics became similar to the degraded land class.

Another finding in this investigation was the (almost consistently) large differences in the partial pressures of CH_4 between the intact and degraded land classes; the degraded land class across all seasons except EDS, had much higher partial pressures of dissolved CH_4 than the intact land class. The quantity of dissolved CH_4 is proportional to the amount of CH_4 that can be emitted by the channel, therefore CH_4 emissions were consistently higher.

Being that a more normal, non-El Niño dry season such as PDS does not seem to significantly perturb the CH_4 dynamics of intact PSF, even though there is some water table drawdown, it suggests that there is a critical depth for the water table to reach before CH_4 cycling alters from a comparatively low to comparatively high CH_4 partial pressures and emissions.

If both land classes are responding to the same hydrological mechanism, then it appears that if the critical depth is reached, it induces a state shift, which may have been the case at the intact land class during EDS, but whereby the degraded land class appears to always be in that state, i.e. the channels consistently have high concentrations of dissolved CH_4 and are emitting comparatively large amounts of CH_4.

From Fig. 5.5 this critical limit appears to be at about $25-30$ cm below the peat surface. If the water table is much lower than 25 cm, as it was during EDS, then it is reasonable to assume that the vast majority of the rhizosphere is not connected to the water table (see Chapter 1). This could be relevant for CH_4 particularly as some CH_4 removal processes dependent on water may have been retarded by the low water table; there may have been less oxidation of CH_4 in the rhizosphere and/or less uptake by tree roots. If these processes were greatly limited it might explain why more CH_4 was found in the channels at the intact land class during EDS. As there are very few trees at the degraded land class, CH_4 may persist for longer as it could not be removed by rhizosphere oxidation or tree roots, which would be supported by the CH_4 data.

The much higher concentrations and emissions of CH_4 during EDS may also have been caused by water table dropping, causing CH_4 in peat pores to degas, some of which may dissolve in the water and get transported to the channels. As the overall volume of water in the peat would be much less in a very dry season such as EDS, it may cause the concentration of dissolved CH_4 to rise relative to a wetter dry

season, such as PDS. There was a significant drop in the water table at the intact land class during EDS and dissolved CH_4 did rise by 365 %, however, at the degraded land class where the water table would have been expected to drop more, dissolved CH_4 only rose by 56 % and therefore was not nearly of a similar magnitude. This may indicate that there is less CH_4 to degas from lower in the peat column at the degraded land class, or that CH_4 removal mechanisms dominate and were greatly inhibited during EDS. Favouring the latter possibility, PDS dissolved CH_4 at the degraded land class (when the water table was low, but not as low as EDS) did not demonstrate a significant increase with respect to a wet season, and actually had the lowest observed dissolved CH_4 of the four sampling seasons at eh degraded land class.

As these processes (CH_4 removal/degassing) were not measured, the processes can only be speculated about from a limited body of data, however, a broader set of potential mechanisms governing the partial pressures and fluxes of CH_4 will be explored in more detail in Chapter 6.

5.4 Conclusions

Partial pressures of dissolved CO_2 largely followed the results of Chapter 3; the intact land class generally had more CO_2 in its channels, and emitted more CO_2, than the degraded channels. Additionally partial pressures and emissions of CO_2 were higher during wet seasons, rather than dry seasons. The converse was true for CH_4; the degraded land class had higher channel concentrations and fluxes of CH_4 than the intact land class, and they were highest during the dry season.

The El Niño did not appear to exert a large impact on the wet season that fell within it, except that LWS was drier than an average wet season. The El Niño dry season produced the most significant departures from the average conditions encountered in the study. Intact peat swamp forest was the most stable of the two land classes in terms of CO_2 and CH_4 variability. However, intact peat swamp forest was impacted so greatly by the El Niño dry season that it temporarily behaved similarly to the degraded land class, producing comparable amounts of CH_4. This indicates that intact peat swamp forest may be made vulnerable to temporary state shifts during El Niño events. The greatest effects of El Niño events for both land classes appear to manifest during the dry season as opposed to the wet season. Those effects were the reduction of emissions of CO_2 and an enhancement of CH_4 emissions, with respect to a non-El Niño year.

The anomalous water table drawdown at the intact land class during the El Niño dry season caused CH_4 partial pressures and fluxes to rise to levels similar to those continually encountered at the degraded land class. This may have revealed some clues as to the mechanisms behind the state shift that peat swamp forest undergoes following degradation which results in a distinctly different behaviour with respect to CO_2, and particularly, CH_4 cycling.

Although concentrations of CH_4 were much higher during the El Niño dry season for both land classes, the water table was lower and aquatic surface areas were much reduced and confined to the channels. As the channels' surface area is much lower than, for instance, a floodplain in the wet season; the actual surface area of water emitting CO_2 and CH_4 to the atmosphere is much significantly smaller.

Intact peat swamp forest did appear to return to its former state (high CO_2 and low CH_4) following the El Niño dry season compared to degraded peat swamp forest, which demonstrated more stochasticity (more variable CO_2 and high CH_4). It is possible that such dry periods exacerbated by El Niños could induce permanent changes to C-cycling in intact peat swamp forest (e.g. Castro et al., 2010; Hueso et al., 2012). These changes may not be immediately observable but may manifest as 'lag effects', where anomalous partial pressures and emissions may indicate long-term changes to the microbial community in the peat (Davidson et al., 2008; Kwon et al., 2013; Nunes et al., 2015). Lag effects and longer-term changes to the microbial community structure of the soil, and ecosystem functioning, could alter the mix of greenhouse gases being emitted (Schimel and Gulledge, 1998). If changes are taking place to the microbial community it may make greenhouse gas emissions from peatlands harder to predict in the future.

Although strong El Niños are not that frequent (three events since 1950), it is believed that they could become more frequent in the future due to warming of the climate (Cai et al., 2014). As appeared to be the case in this study, the water table may have a very significant effect on dissolved CO_2 and CH_4 in the channels, and emissions of those gases to the atmosphere. In this sense, the geochemistry and fluxes from the channels can act as an indicator of the stability of a peat swamp forest carbon store (cf. Moore et al., 2013).

5.5 Author contributions

M.S.K., V.G., S.E.P. and C.D.E. conceived of the study. M.S.K., D.B., V.G., C.D.E. and S.E.P. devised the methods. M.S.K., H. and I. carried out the fieldwork. M.S.K. carried out the data analysis and wrote the manuscript. V.G., S.E.P. and C.D.E. provided comments on the manuscript.

Chapter 6

Thesis Synthesis

6.1 Introduction

In this thesis I have explored three major research questions that have shown: i) how emissions of channel CO_2 can change as a result of degradation of peat swamps (Chapter 3); b) how emissions of channel CH_4 can change as a result of degradation of peat swamps (Chapter 4); and c) how emissions of CO_2 and CH_4 can change from intact and degraded peat swamp forest as the result of an El Niño event (Chapter 5).

Here the findings of the three investigations are synthesised and discussed in a broader context together with their implications. Each research question has raised important issues and in combining them there will be a discussion of a) the general findings, b) the potential mechanisms that may have caused the intact land class to behave like the degraded land class during the El Niño, c) the greenhouse warming potential of the gases emitted by the channels and, finally, d) the channel fluxes upscaled to their respective landscapes, so that their contribution to landscape-scale emissions can be considered.

Suggestions for further work and a summary of the key findings will also be presented.

6.2 General reflection

Chapters 3 and 4 demonstrated that deforestation and drainage of peat swamp forest causes the cycling and emission of CO_2 and CH_4 to alter significantly. Degraded peat swamp forest channels were char-

acterised by lower emissions of CO_2, and much higher emissions of CH_4, relative to intact peat swamp forest channels. The land classes are known to be fundamentally different environments in terms of their vegetation and C-cycling, and further differences were found in terms of the channels draining the catchments. The deforestation and drainage of peat swamp forest was found to cause channel depth to oscillate between greater extremes, and the water was significantly warmer and more dissolved oxygen was present.

In terms of C mass loss, CO_2 was the dominant gas being evaded by channels in both land classes, by $2-3$ orders of magnitude and, therefore, CH_4 was a negligible term with regard to net ecosystem exchange of C. Even though channel CO_2 emissions were significantly higher at the intact land class, the forest ecosystem functions as a net C sink (Hirano et al., 2007) and the CO_2 in the channels was found to be of recent photosynthetic origin. At the degraded land class, the CO_2 in the channels was found to come from deep peats that could be millennia old, providing further evidence that the peatland is destabilising and losing previously stored carbon (cf. Moore et al., 2013). Further, the emission of CO_2 from degraded peat swamp forest channels represents an overwhelming loss of C from the ecosystem as there is negligible net primary productivity (Hirano et al., 2007). This study has shown that the emission of CO_2 and CH_4 from the channels add another pathway by which degraded peat swamp forest can lose C. The contribution of the channels to landscape-scale greenhouse gas emissions will be presented in Section 6.6.

Fluxes of CO_2 and CH_4 varied according to season whereby the dry season was characterised by significant reductions in CO_2 fluxes and increases in CH_4 fluxes, per unit channel area, compared to the wet season (see 6.1). Dry season greenhouse gas fluxes, however, are unlikely to make a big difference in terms of overall annual emissions as the duration of the dry season is only a third of the wet season, and channel area during the dry seasons is much reduced compared with the wet season. These differences coincided with water table drawdown during the drier seasons, which also significantly affects seasonal terrestrial greenhouse fluxes (Jauhiainen et al., 2005, 2008).

As reported in Chapter 5, the 2015 El Niño dry season caused the greatest deviation from the average fluxes across the study period, when the water table dropped to anomalous depths. This period produced the lowest CO_2 fluxes and the highest CH_4 fluxes measured throughout the entire study. For the only time in the study, the intact land class had dissolved CH_4 concentrations that were in the usual

Table 6.1: Summary of median CO_2 and CH_4 gas fluxes at the intact and degraded land classes, respectively, throughout the study period. The seasons are arranged chronologically. LWS = late wet season (April 2015 onwards), EDS = El Niño dry season (July 2015 onwards), PDS = Post-El Niño dry season (August 2016 onwards), and EWS = early wet season (October 2016 onwards). EDS emissions are highlighted in red to draw attention to the exceptional measurements made during this period.

	CO_2 ($g \cdot C \cdot m^{-2} \cdot d^{-1}$)				CH_4 ($mg \cdot C \cdot m^{-2} \cdot d^{-1}$)			
	El Niño		Post El Niño		El Niño		Post El Niño	
Land class	LWS	EDS	PDS	EWS	LWS	EDS	PDS	EWS
Intact	4.68	1.81	3.36	4.15	2.11	7.79	2.16	1.25
Degraded	2.49	1.07	2.58	3.13	13.81	29.64	16.83	9.48

range of the degraded land class, indicating a state shift in terms of CH_4 cycling. However, the intact forest demonstrated resilience and rebounded back to a normal state following the El Niño.

Drainage of peat swamp forest and El Niño events both enhance water table drawdown in the dry season and, therefore, this study has essentially been an investigation into the effects of water table depth on gas fluxes from two perspectives; land use change (degradation) and extreme climatic events. The impact of the El Niño on the intact land class, that caused it to behave like the degraded land class, may have provided some clues as to why the degraded land class appears to have shifted to a significantly different steady state which appears to particularly affect CH_4 cycling.

As CH_4, by mass, is a more powerful greenhouse gas than CO_2 in terms of its potential for warming the climate (Myhre et al., 2013; Neubauer and Megonigal, 2015), the effect that this has in terms of the greenhouse gases being emitted from the channels will be discussed in Section 6.7.

6.3 CO_2 dynamics in intact and degraded peat swamp forest

Chapters 3 and 5 reported that channel CO_2 emissions were consistently higher in intact rather than degraded PSF, and that this occurred due to two main reasons: a) the water level was consistently higher at the intact land class, and b) the presence of a metabolically active forest at the intact land class led to higher amounts of CO_2 and DOC being delivered to the channels (see 6.1). Further to point b) the DOC at the intact land class was more labile than at the degraded land class and hence could be more readily degraded in-stream.

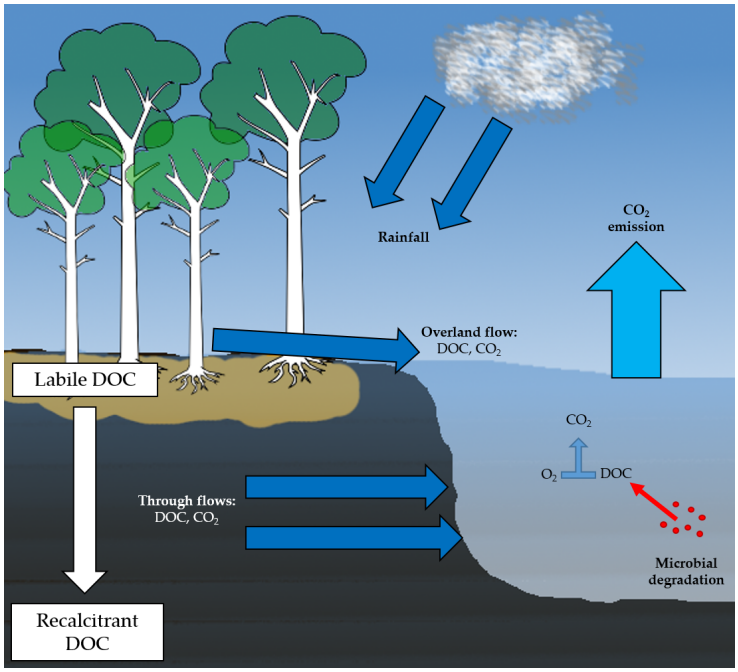

Figure 6.1: Schematic of major factors influencing abundance of dissolved CO_2 in the channels of intact PSF during a wet season. High rainfall during wet season months causes high water levels in the channel, a high water table in the peat and overland flows over the peat, each of which deliver dissolved CO_2 and more labile DOC from the upper peat profile. The surface and the upper layers of the peat are more biologically active, hence more dissolved CO_2 can be transported in water and through the peat matrix to the channels. As a result, CO_2 emissions tend to be high in the wet season compared to the dry season.

CO_2 fluxes responded seasonally at both land classes, with higher fluxes occurring during the wet seasons than the dry seasons. This was because delivery of DOC and CO_2 to the channels, as well as the potential for in-stream degradation of DOC, reduced (see 6.1). Further, CO_2 fluxes were lowest during the severe El Niño event in 2015 when channel water levels and the peat water table dropped to seemingly anomalous levels and some of the channels dried completely causing fieldwork to be abandoned.

CO_2 fluxes at the intact land class during the El Niño event (1.81 $g{\cdot}C{\cdot}m^{-2}{\cdot}d^{-1}$) dropped to levels usually associated with the degraded land class (1.07–3.13 $g{\cdot}C{\cdot}m^{-2}{\cdot}d^{-1}$), whereas they were otherwise the highest values in the study and were consistently higher than the degraded land class (intact = 3.36–4.68 $g{\cdot}C{\cdot}m^{-2}{\cdot}d^{-1}$). The extremely low water table during the El Niño event caused the low CO_2 fluxes at the intact land class and this indicates that the intact land class can behave like degraded PSF. Further, it provides quantifiable evidence that the digging of channels in peat, and the resultant loss in their ability to hydrologically regulate themselves, leads to peatlands degrading to a point where they function very differently to their intact analogues. After the El Niño event, when the water table returned to a range normally associated with intact PSF, the CO_2 fluxes there also rebounded.

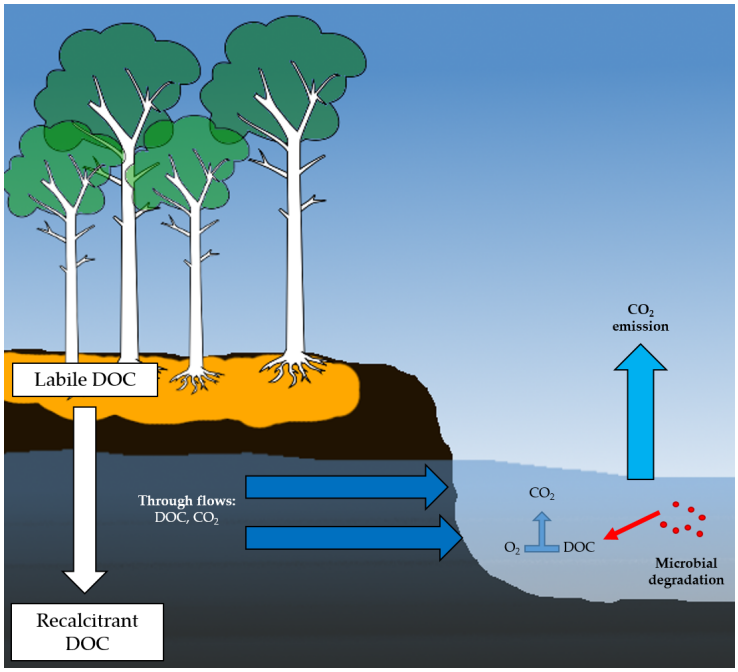

Figure 6.2: Schematic of major factors influencing abundance of dissolved CO_2 in the channels of intact PSF during a dry season. Rainfall drops significantly during the dry season causing channel water levels and the peat water table to drop. As a result the DOC being delivered to the channels is more recalcitrant in nature, which could reduce the amount of CO_2 produced by biodegradation. Overland and near-surface flows in the dry season are negligible with respect to the wet season and so a major source of dissolved CO_2 that is present in the wet season can become isolated from the channel. CO_2 emissions therefore tend to be lower in the dry season than in the wet season.

6.4 CO_2 emissions from peat swamp forest channels in the context of other southeast Asian fluvial systems

In the context of other southeast Asian fluvial systems, peat draining headwater channels produce similar amounts of CO_2 compared to non-peat draining rivers, but in some cases much less than peat-draining rivers (see Table 6.2 and left pane of Fig. 6.3); the average CO_2 fluxes for non-peat draining rivers, peat draining channels and peat draining rivers was 3.20, 3.18 and 7.30 $g{\cdot}C{\cdot}m^{-2}{\cdot}d^{-1}$, respectively. These data indicate that channels may not be hotspots of evasion with respect to lower stream orders in their catchments, the contrary of which has been reported for peat-draining headwaters in the Amazon (Richey et al., 2002; Mayorga et al., 2005) and in the temperate and boreal zones (Billett and Moore, 2008; Billett et al., 2015). The peat channels in this study had much higher quantities of dissolved CO_2 than the rivers (see Table 6.2 and right pane of Fig. 6.3). This therefore suggests that peat-draining channels

Table 6.2: Summary of dissolved CO_2 concentrations and CO_2 fluxes from southeast Asian rivers and channels.

Name in study	Stream type	Peat draining	Dissolved CO_2 (μatm)	CO_2 flux ($g \cdot C \cdot m^{-2} \cdot d^{-1}$)	Study
Lupar	River	No	1,274	2.0	Müller et al., 2016
Mekong	River	No	1,090	2.3	Li et al., 2013
Red	River	No	1,589	6.4	Le et al., 2018
Saribas	River	No	1,159	1.1	Müller et al., 2016
Xijiang	River	No	2,600	4.2	Yao et al., 2007
Batang Hari	River	Yes	2,400	0.9	Wit et al., 2015
Indragiri	River	Yes	5,777	10.2	Wit et al., 2015
Maludam	River	Yes	8,100	9.1	Müller et al., 2015
Musi	River	Yes	4,316	7.6	Wit et al., 2015
Rajang	River	Yes	2,445	1.9	Müller-Dam et al., 2019
Siak	River	Yes	8,555	14.1	Wit et al., 2015
Intact PSF	Channel	Yes	12,592	4.0	This study
Degraded PSF	Channel	Yes	13,496	3.0	This study
Kalimantan settled	Channel	Yes	No data	2.4	Jauhiainen and Silvenonnen, 2012
Kampar settled	Channel	Yes	No data	3.7	Jauhiainen and Silvenonnen, 2012
Kampar disturbed	Channel	Yes	No data	2.8	Jauhiainen and Silvenonnen, 2012

in southeast Asia have a significantly lower gas exchange velocity compared to rivers in southeast Asia and peat-draining channels in other parts of the world. Chapter 3 presented the gas exchange velocities of the channels in this study and showed that they were low compared to similar stream systems in the temperate region.

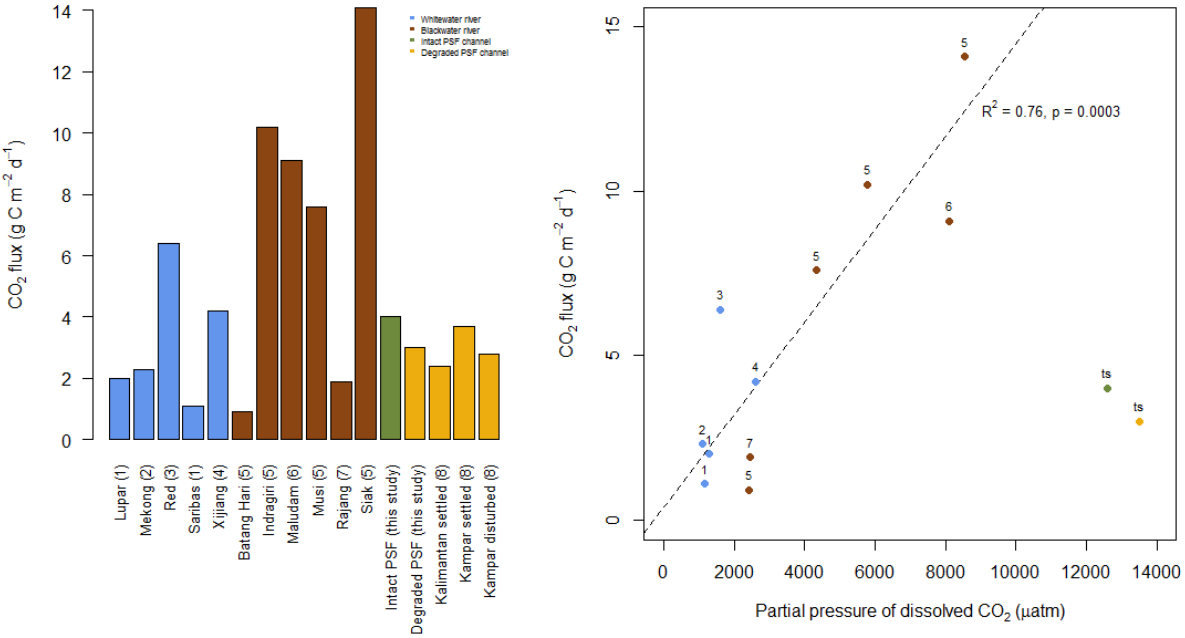

Figure 6.3: Left pane: Bar plot of average annual fluvial CO_2 fluxes ($g{\cdot}C{\cdot}m^{-2}{\cdot}d^{-1}$) from tropical rivers and channels in southeast Asia. Whitewater (non-peat draining) rivers, blackwater (peat draining) rivers, channels draining intact PSF, and channels draining degraded PSF are coloured blue, brown, green and yellow, respectively. Channels draining peat emit approximately the same amount of CO_2 as tropical whitewater rivers, but blackwater rivers appear to produce the greatest fluxes of CO_2 per unit area. References: (1) Müller et al., 2016; (2) Li et al., 2013; (3) Le et al., 2018; (4) Yao et al., 2007; (5) Wit et al., 2015, (6) Müller et al., 2015; (7) Müller-Dum et al., 2019; (8) Jauhiainen and Silvennonen, 2012. Average annual values for this study, (7) and (8) were calculated from their original seasonal emissions given a weighting of 9:3 wet season to dry season months. Right pane: Scatter plot of data in left pane correlated to the partial pressure of CO_2 given in the studies (numbers relate to those studies in the bar plot, as do the colours of the channel types). Data from study (8) could not be included as no partial pressure data were available. There was a positive correlation between river partial pressures and fluxes of CO_2 when the channel data in this study (ts) were excluded. The channels in this study had much higher quantites of dissolved CO_2 than those of the rivers, however the fluxes of CO_2 were comparatively low.

Headwater channels are often excluded from global-scale GHG emissions estimates, but in the case of peat draining channels in southeast Asia, they might act to reduce regional emissions estimates, whereas in catchments in other parts of the world they can act to increase them (Billett et al., 2015). If more measurements of CO_2 fluxes in channels draining peat were included in regional estimates, those estimates may be revised down. This is significant as recently revised CO_2 evasion estimates for southeast Asia by Lauerwald et al. (2015) and Wit et al. (2015) were, respectively, 25−37 % of those estimated by Raymond et al. (2013). Raymond et al. had significantly overestimated dissolved concentrations and the gas exchange velocity in southeast Asian rivers and consequently had overestimated fluxes by 7.9 to 10.0−times for Malaysia, and 2.7 to 4.4−times for Indonesia. Most of the studies included in Table 6.2 were published after the paper by Raymond et al., when little data were available, but it highlights the importance of obtaining more data by making bottom-up measurements, especially if those data are scarce and derived fluxes appear to have a significant effect of global CO_2 emissions estimates from fluvial systems.

This thesis adds data to a growing body of evidence that lotic CO_2 fluxes from southeast Asian peat-draining streams and rivers are moderate in size compared to those estimated by Raymond et al. (2013) (Müller et al., 2015; Wit et al., 2015; Müller-Dum et al., 2019).

6.5 CH_4 dynamics in intact and degraded peat swamp forest

Two questions that arise from the CH_4 data collected in this project are: a) Why is there significantly more dissolved CH_4 in −and hence higher CH_4 emissions from− the degraded land class channels?; and b) Why did the intact land class resemble the degraded land class in terms of elevated concentrations of dissolved CH_4 during the El Niño dry season?

CH_4 production or degradation processes were not measured in this study, nor were some of the relevant environmental variables that might drive those processes. However, from the data collected, there were some observations, trends, or lack of trends, that can be used infer potential dominant processes. Additionally, recent findings are demonstrating that the processes governing CH_4 dynamics can differ significantly in peat swamp forest as compared to boreal peatlands (Hoyt et al., 2016, 2017; Wong et al., 2018), and these need to be considered in order to better understand observations of CH_4 dynamics in peat swamp forest.

This section is not intended to be a description of the mechanisms that were responsible for the observed CH_4 fluctuations, but rather a discussion of the processes that could affect the abundance of CH_4 in the channels, and which of those may be dominant (it is likely that a multitude of processes is occurring simultaneously). The purpose of the discussion is to synthesise the data presented in this thesis with recent findings relating to CH_4 cycling, so that it may inform as to useful avenues of inquiry that future investigations may want to consider in the pursuit of better understanding CH_4 cycling in peat swamp forest.

6.5.1 Does the degraded land class produce more CH_4 than the intact land class?

Within channels, CH_4 is mostly produced in anoxic sediments in the stream bed. Sediment anoxia is mostly controlled by the oxygen content of the water and the flow velocity (Jones et al., 1995; Truax et al., 1995; Hondzo and Steinberger, 2008); methanogenesis requires sediments to be anoxic but these conditions become less likely when dissolved oxygen is higher and stream flows are faster. Dissolved oxygen concentrations were consistently and considerably higher at the degraded land class despite having higher concentrations of dissolved CH_4. Water flow at both land classes varied between flowing and near-still, yet there was no discernible response at a sub-season level that this affected dissolved CH_4. As such, sediment methanogenesis does not appear to be the dominant source of CH_4 in the channels.

Lowering water tables during the dry season may cause CH_4 concentrations in the channels to increase; as the water level drops, CH_4 may become more concentrated in the water as a result of the reduced water volume. Whilst dissolved CH_4 increased by 56 % at the degraded land class in the El Niño dry season, the following dry season had the lowest CH_4 concentrations of all the seasons even though water levels dropped significantly. CH_4 concentrations do not appear to be greatly affected by reduced water volumes.

Trees and other aerenchymatous plants can promote methanogenesis by providing fresh substrate via root exudates and leaf litter input to the soils (Ding and Cai, 2003; Koelbener et al., 2010; Girkin et al., 2018), however, the concentrations in the deeper intact peat swamp forest soils and the deforested degraded peat swamp forest soils indicate that bulk peat is also capable of producing significant quantities of CH_4, and very few trees are present at the degraded land class to produce CH_4 by this mechanism (see Fig. 6.4). Further, at KALA, there is very little plant cover to produce CH_4. Except for the upper 50 cm of intact peat swamp forest soils, the peat pore water CH_4 concentrations between the land classes are comparable. Methanogenesis in anoxic bulk peat is likely the main source of CH_4 in degraded peats, and it may also be a dominant source in intact peats.

The lower CH_4 concentrations in the upper peat at the intact land class may result from either tree-mediated transport whereby CH_4 enters roots and is channelled to the atmosphere, or CH_4 is oxidised in the rhizosphere, or a combination of both mechanisms. Hoyt et al. (2017) also found that high water flow rates at or near the surface suppress the build up of CH_4. Tree-mediated transport has been measured in intact peat swamp forest study area, whereas rhizosphere oxidation remains unknown. It is possible that the differences in peat pore water and channel CH_4 concentrations is due mostly to the two main removal mechanisms: tree-mediated transport and rhizosphere oxidation.

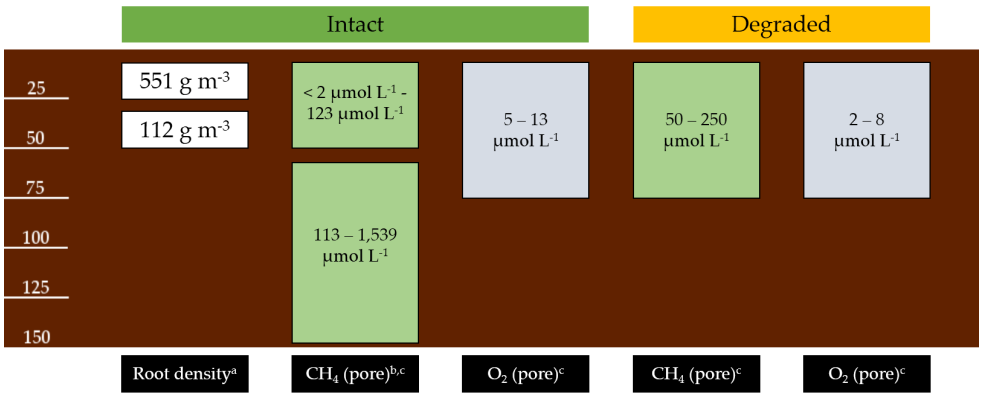

Figure 6.4: Root density and pore water CH_4 and O_2 data from studies of intact and degraded peat swamp forest soils. Ranges of values have been arranged according to the depth at which the measurements were made (depth indicated on the left, as centimetres below the peat surface). Data sourced from Sulistyanto (2005)[a], Pangala et al. (2013)[b] and Adji et al. (2014)[c]. No data have been collected for root density at the degraded land class.

6.5.2 Tree-mediated transport and rhizosphere oxidation of CH_4 in intact peat swamp forest

Tree-mediated transport and rhizosphere oxidation are both limited to the volume of peat adjacent to the roots. Root mass usually declines exponentially with soil depth (Jackson et al., 1996), and at the intact land class root density has found to be ˜5−times higher in the upper 25 cm of the peat than from 25 to 50 cm depth (Sulistyanto, 2005; see Fig. 6.4). This is because peat swamp forest soils are nutrient-poor and waterlogged at depth and, therefore, trees send their roots to scavenge for the most labile material located near the peat surface (Page et al., 1999). As such, the vast majority of total root mass is found in the top 25 cm (Jauhiainen et al., 2005).

Tree-mediated transport of CH_4 has been measured at the intact land class (Pangala et al., 2013), and although it has been shown to dominate terrestrial fluxes from peat swamp forest, the actual amount of CH_4 being emitted by trees is significantly lower than other forested tropical wetlands (Kirschke et al., 2013; Pangala et al., 2017). Additionally, the terrestrial fluxes of peat swamp forest appear to be approximately half those of boreal peatlands (Wong et al., 2018), which are not forested.

Oxidation is known to occur in tropical peats, and oxygen concentrations have been found to be higher in the peat of the intact land class than that of the degraded land class, as a result of tree-mediated transport from the atmosphere (Adji et al., 2014; see Fig. 6.4). Further, Adji et al. (2014) also found evidence that oxidation of CH_4 was occurring in the rhizosphere. It is likely that more oxidation occurs in the rhizosphere than the bulk soil because there will be more oxygen due to plant-mediated transport, and the rhizosphere can support much higher microbial biomass and activity (Nannipieri et al., 2007).

Hoyt et al. (2016) found that oxidation may remove large amounts of peat CH_4 before it reaches the atmosphere and that this was related to water table depth, and the amount of water flowing through the roots and the oxygen it transports to the peat.

During the wet season when the water table is near the surface, tree-mediated transport and rhizo-

sphere oxidation may remove CH_4 as water flows over land and through the soil to the channels (Baird et al., 2016; Hoyt et al., 2017), hence concentrations and fluxes of CH_4 could comparatively low, as was observed (see Fig. 6.5).

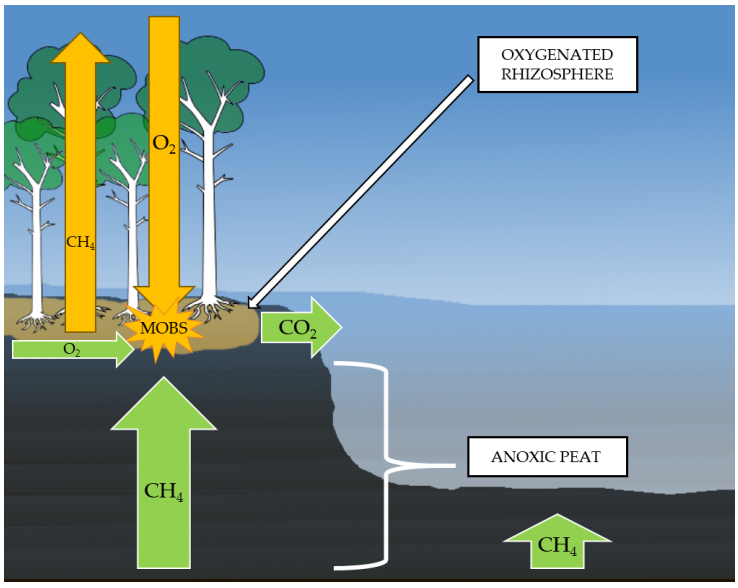

Figure 6.5: Schematic of the major processes governing dissolved CH_4 in the channels at the intact site, during a wet season. Tree-mediated processes are coloured yellow and passive gas transport through the soil coloured green. CH_4 is produced mainly in the deeper anoxic peats and can gradually diffuse upwards towards to surface, or into the channel. Trees provide conduits for oxygen ingress and CH_4 egress. Methane-oxidising bacteria (MOBS) in the rhizosphere may receive oxygen either via conducting plants or from pore water throughflow. This oxygen allows MOBS to metabolise CH_4 rising from deeper peats. This produces CO_2 that can be washed into the channels. If CH_4 reaches conducting plant roots before being oxidised, it can be translocated to the atmosphere. The figure is not to scale.

During the El Niño dry season the water table dropped below 50 cm for four months (see Chapter 5), and soil moisture in the upper layers of peat would have likely dropped significantly (e.g. Kwon et al., 2013). Water is necessary for the transport of dissolved CH_4 and O_2, and for CH_4 to enter tree roots (Brix et al., 1992; Whiting and Chanton, 1996). CH_4 being produced by the bulk peat in this time would have effectively been isolated from the rhizosphere and without significant removal processes acting on it could have led to CH_4 persisting, and its transport to the channels would have led to the observed, comparatively large concentrations and fluxes of CH_4 (see Fig. 6.6).

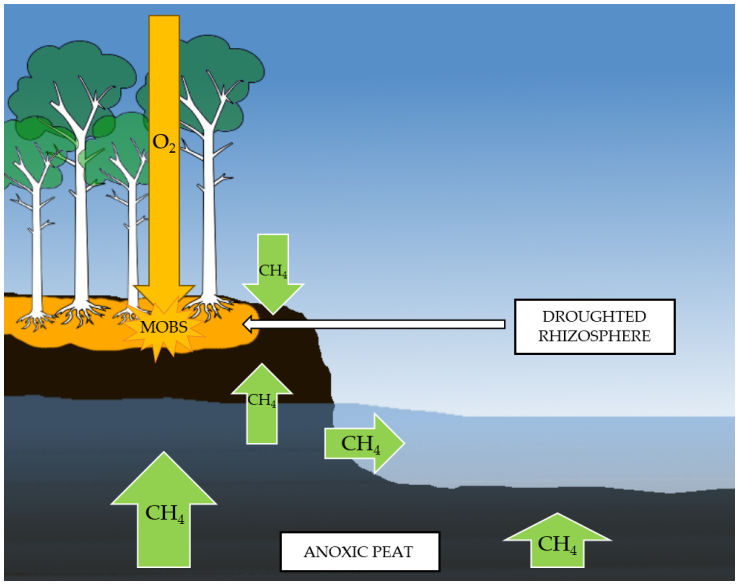

Figure 6.6: Schematic of the major processes governing dissolved CH_4 in the channels at the intact site, during an El Niño dry season. Tree-mediated processes are coloured yellow and passive gas transport through the soil coloured green. The diffusive potential of CH_4 rising from deeper, anoxic peats is much restricted by the much lower water table; the CH_4 is effectively isolated from the upper peat zone where it might a) reach plant roots and aerenchyma and be translocated to the atmosphere, and/or b) be oxidised by methane-oxidising bacteria (MOBS) in the rhizosphere. Some CH_4 may diffuse from the water into air spaces and get taken up by the soil sink, as atmospheric CH_4 can. The rest of the CH_4 may persist in the water and eventually be transported to the channel via soil throughflow. The figure is not to scale.

6.5.3 Methane dynamics at the degraded land class

The peats of the degraded land class can produce quantities of CH_4 comparable to the intact class, but it lacks vegetation and tree cover, thus oxidation in the rhizosphere and tree-mediated transport should also be negligible. Without those major CH_4 removal processes that operate at the intact land class, CH_4 may persist in the peats and pore water, and which may gradually be transported to the channels, similarly as was posited for the intact land class during the El Niño dry season. This may explain why this study found dissolved concentrations and fluxes of CH_4 were consistently and substantially higher.

Peat soil can act as a sink for atmospheric CH_4 (and CH_4 coming from below the peat surface) during dry seasons (Harriss et al., 1982), such as at the intact land class (Jauhiainen et al., 2005). But Jauhiainen et al. (2008) reported that even during the dry season (as well as the wet season) that peats at the degraded land class were a net-source of CH_4. This indicates that the peat CH_4 sink could be saturated due to CH_4 being evaded from belowground.

6.6 Upscaling fluxes for a landscape-scale perspective

6.6.1 The degraded land class

According to Rais and Ichsan (2008), the ex-Mega Rice Project covers 11,195 km^2 and has 4,470 km of drainage channels (see Fig. 6.7a). Very few data exist regarding the widths of the channels in the ex-Mega Rice Project area, making accurate areal estimates of total channel coverage challenging. Rais and Ichsan (2008) conducted a survey of a portion of the channel network in Block A, and the widths recorded in the study (n = 73; see Fig. 6.7b) were used to calculate a median channel width with which to upscale to the Mega Rice Project as a whole. Channel widths ranged from 3.2−20.3 m, giving a median width of 12.5 m and therefore the estimated total channel area was 55.9 km^2, or 0.5 % of the Mega Rice Project area.

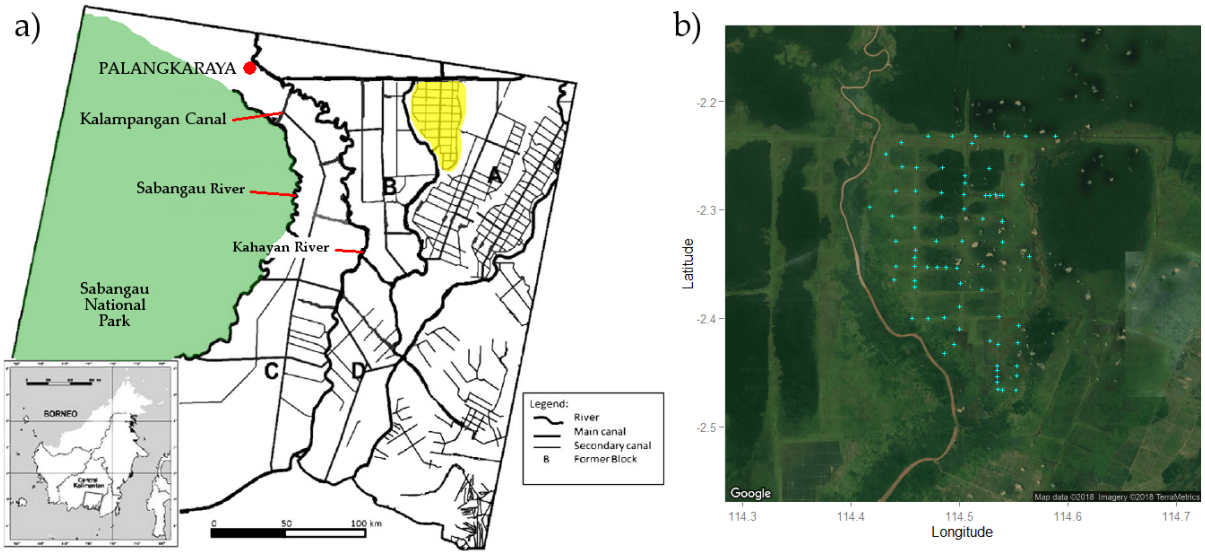

Figure 6.7: Map of the ex-Mega Rice Project adapted from Ritzema et al. (2014) showing the areas designated as Blocks A−D. An estimate of the channel surface area for the Mega Rice Project was made using channel width data from a survey by Rais and Ichsan (2008) conducted in Block A (highlighted in yellow in the left pane) with the individual survey points (n = 73) shown in the right pane (Source map © 2018 Google). Channel widths ranged from 3.2−20.3 m with the median width being 12.5 m.

To provide an estimate of gas emissions from the ex-Mega Rice Project channels during a non-El Niño year, CO_2 and CH_4 data from the non-El Niño dataset were used to calculate annual emissions (see Chapter 2). CO_2 emissions were estimated as 1,126 g·CO_2-C·m^{-2}·yr^{-1}, which is higher than the estimate for the 2015 El Niño year (779 g·CO_2-C·m^{-2} reported in Chapter 3). Non-El Niño channel CO_2 emissions therefore were the same order of magnitude, but somewhat exceeded, the peat surface emissions estimates of 823−1,014 g·CO_2-C·m^{-2}·yr^{-1} reported by Hirano et al. (2009).

Based on peat surface CO_2 emissions in Hirano et al. (2009), the ex-Mega Rice Project area is estimated to produce 9.21−11.35 Tg·CO_2-C·yr^{-1} from the peat surface. Upscaled channel CO_2 emissions were estimated to be 0.063 Tg·CO_2-C, or 0.6−0.7 %, of combined peat and channel surface emissions.

Jauhiainen et al. (2008) reported that degraded peat surfaces emit 0.147−0.206 g·CH_4-C·m^{-2}·yr^{-1} which, when upscaled to the ex-Mega Rice Project area, equates to 1.65−2.31 Gg·CH_4-C·yr^{-1}. The channels in this study are estimated to emit 0.23 Gg·CH_4-C·yr^{-1}, based on the annual emissions calculation described in Chapter 2.

With respect to total CH_4 emissions from channels and peat surfaces in the Mega Rice Project area, the proportion of CH_4 emitted from the channels was 9.1−12.3 %. The channels, therefore, make a much more significant contribution to landscape-scale emissions of CH_4 than CO_2. The CH_4 emissions in this study represent only the diffusive flux, and therefore it is possible that emissions from channels could exceed those from the land, if the ebullitive term were to be included.

The CH_4 flux data from a degraded channel near KALA reported by Jauhiainen and Silvennoinen (2012) very likely included the ebullitive term, even though they were reported as diffusive fluxes (see Chapter 4). The seasonal mean channel CH_4 fluxes in Jauhiainen and Silvennoinen (2012) were 4.5 and 224 g·CH_4-C·m^{-2}·d^{-1} for wet and dry seasons, respectively, which equates to 3.45 Gg·CH_4-C·yr^{-1}. This annual channel CH_4 emission estimate dominates the terrestrial flux, being 59.9−67.7 % of the total ex-Mega Rice Project CH_4 flux, based on the peat surface emissions reported in Jauhiainen et al. (2008). The channels, though covering only 0.5 % of ex-Mega Rice Project land, could be the dominant term in total CH_4 emissions at a landscape scale, and this may also apply to other areas of degraded peat swamp forest with drainage channels.

These upscaled CH_4 fluxes for the ex-Mega Rice Project involved assumptions in their calculation and therefore should be treated with caution because: a) the median channel width was estimated from a comparatively small portion of the ex-Mega Rice Project, and so it may not be representative; b) the CH_4 channel flux estimates were taken from only one channel, near KALA; c) the CH_4 peat soil flux measurements were taken from one site, near KALA; d) during the dry season the channels shrink, and therefore water may not fill the full width of the channels, and e) the channels can be subsumed in the wet season and form part of a wider floodplain, therefore the evading surface area may be much larger.

For the above reasons, it was decided that upscaling beyond the ex-Mega Rice Project (e.g. to

Borneo, Indonesia, or Southeast Asia) was not appropriate, due to the introduction of much greater degrees of uncertainty as a result of a scarcity of data. The only other data available regarding the fluxes of CO_2 and CH_4 from channels draining degraded peat swamp forest were reported by Jauhiainen and Silvenonnen (2012), who found that fluxes varied greatly between three areas of degraded peatland in Indonesia. One of these areas was Kalimantan and was used in this study and upscaling, and the other two were in Kampar, Riau Province. At Kampar, one similar and one different type of degraded peat swamp forest was investigated for greenhouse gas emissions and the results were significantly different from the data from Kalimantan (see Table 6.3).

Several factors could be responsible for the significant differences in the greenhouse gas fluxes

Table 6.3: Greenhouse gas fluxes reported by Jauhiainen and Silvenonnen (2012) for three degraded peatlands, one in Kalimantan and two in Kampar (Riau), using their descriptions of the status of the degradation (settled or disturbed). Percentage differences are in relation to Kalimantan.

Gas	Kalimantan (settled)	Kampar (settled)	(% difference)	Kampar (disturbed)	(% difference)
CO_2 ($mg{\cdot}m^{-2}{\cdot}d^{-1}$)	9,010	16,372	+81	10,982	+22
CH_4 ($mg{\cdot}m^{-2}{\cdot}d^{-1}$)	164	1,073	+554	89	-46
N_2O ($\mu g{\cdot}m^{-2}{\cdot}d^{-1}$)	0	2,785	(∞)	751	(∞)

observed by Jauhiainen and Silvenonnen (2012) between the three sites, however, the authors were not able to explain the variation in a way that greenhouse gas fluxes could be predicted, i.e. by gas exchange velocity, water flow rate, dissolved gas concentrations, etc. Given the degree of variation of greenhouse gas fluxes between the three sites (whereby two also have the same degradation status), as well as the unknowns of, for instance, channel area and land use type, for other degraded peatlands in Indonesia, it is clear that precise and meaningful estimates of gas fluxes would be difficult to produce.

6.6.2 The intact land class

Upscaling the intact land class channel fluxes to the Sabangau National Park involved some uncertainty. This is largely because the areal extent of the channels in the forest is unreported, and it is difficult to identify them using aerial photographs or satellite imagery. The best available channel data were obtained by the Borneo Nature Foundation. They provided all the channel lengths for the channels occurring in the LAHG research station area (400 km^2; Hamard, 2008) where there are 15 channels which range from

150 to 2,940 m, and one that is ~12 km long (Bernat Ripoll, personal communication; see Appendix Table 7.4).

As the channels in the forest were dug for light, selective logging, they were assumed to have a uniform width of 1.5 m, and the cumulative area was estimated to be 0.047 km^2. The proportion of the channel surface area to the LAHG research area was then applied to the Sabangau National Park (5,700 km^2) giving a total channel surface area of 0.67 km^2.

Jauhiainen et al. (2005) reported annual emissions of CO_2 and CH_4 from the peat surface. These were upscaled to the Sabangau National Park, giving totals of 5.43 Tg·CO_2-C·yr−1 and 5.80·Gg·CH_4-C yr−1. The channels were estimated to emit 2.65 Mg·CO_2-C·yr−1 and 0.99 kg·CH_4-C·yr−1, using the median fluxes of the respective gases scaled to a year, from the 2016 (non-El Niño) gas flux dataset. When the peat surface and channel fluxes were summed together, the channels emitted less than a millionth of both CO_2 and CH_4 than the peat surface emissions in the Sabangau National Park, thus channel fluxes of CO_2 and CH_4 appear insignificant with respect to the wider landscape. The main reasons for such small contributions to CO_2 and CH_4 evasion are because the channels were calculated to have such a small area with respect to the forest and also that the channels emitted only about 50 % more CO_2, and 50 % less CH_4, per unit area, than the peat surface.

There are some caveats with regards to the Sabangau National Park estimates: a) The areal extent of the channels may be different to the LAHG research station area, than in other parts of the forest and hence the channel extent may be significantly larger or smaller; b) There are several rivers that have sources within the Sabangau Forest (8 of which discharge into the Sabangau River and 4 that discharge into the Katingan River; Hamard, 2008), which constitute a significant aquatic surface area within the forest that could emit gases. However, there are no data on their lengths, widths or gas exchange velocities and they are also natural channels, not man-made; c) the area of the Sabangau National Park used in the calculation is the total area within the forest boundary and does not account for the areal extent of the rivers which, if accounted for, would reduce the peat surface area; d) the estimated CH_4 flux is diffusive only as there are no data on ebullition in the forest channels, however rates of ebullition may be low given the low concentrations of dissolved CH_4 in the channels; and e) significant portions of the channels can dry up during the dry season, and this was not accounted for.

6.7 Global warming potential

Greenhouse gases have differing potentials for absorbing infrared light (or heat) and they may persist for different lengths of time in the atmosphere, and as such they have differing potentials to warm the atmosphere and, if emitted in larger quantities than in nature, exacerbate global warming (Myhre et al., 2013). The global warming potential of CH_4 is considered to be 32 over a 100-year period. Global warming potential, however, is based on an instantaneous pulse of a greenhouse gas. The warming potential of a sustained greenhouse gas emission is greater than a pulse (except in the case of CO_2) and for methane the sustained global warming potential for a 100-year period is considered to be 45 (Neubauer and Megonigal, 2015).

In terms of global warming potential, CO_2 was the most important greenhouse gas being emitted from channels at both land classes, and this was consistently and overwhelmingly the case at the intact land class. However, the intact land class is a net-ecosystem CO_2 sink for (Hirano et al., 2007); although the fluxes were higher than the degraded land class, they are offset by terrestrial CO_2 sequestration (net C accumulation = 94 $g{\cdot}C{\cdot}m^{-2}{\cdot}yr^{-1}$; Moore et al., 2013), whereas at the degraded land class CO_2 sequestration is negligible and the ecosystem is a net-source (net C loss = 530 $g{\cdot}C{\cdot}m^{-2}{\cdot}yr^{-1}$; Moore et al., 2013), and the channels function as a further loss pathway for C. At the degraded land class during the dry seasons, CH_4 emissions from the channels were such that CO_2e fluxes were very near the same $-$or exceeded$-$ the CO_2e flux from channels at the intact land class (see Fig. 6.8, left pane), i.e. diffusive CH_4 emissions were sufficient to match the (more metabolically active) intact land class channel emissions in terms of CO_2e.

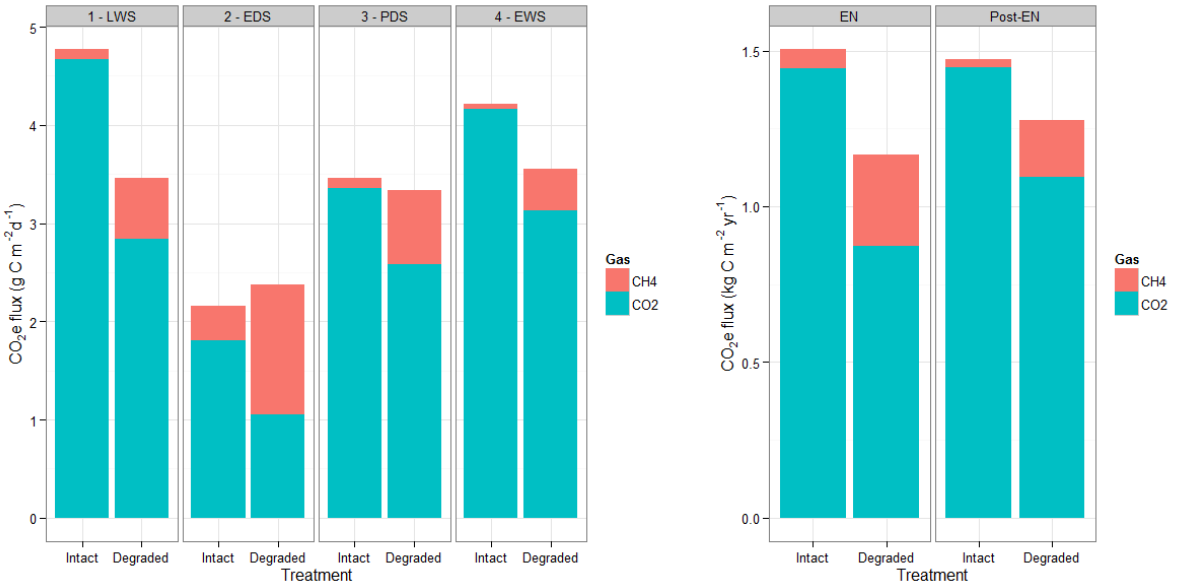

Figure 6.8: Diffusive CO_2e fluxes during the seasons (left pane) and as annual estimates during and after the 2015 El Nño (EN and Post-EN, respectively; right pane) per square metre of channel per day. CO_2e for methane was based on a sustained global warming potential of 45 (Neubauer and Megonigal, 2015). It is important to note that the intact land class, though having higher channel CO_2e fluxes, the ecosystem is a net-sink of C, whereas the degraded land class is a net source.

There was not much difference in the CO_2e channel emissions between the El Niño and post-El Niño years at the intact land class, both being $1.47-1.50$ kg·CO_2e-C·m^{-2}·yr^{-1} (see Fig. 6.8, right pane). CO_2e emissions at the degraded land class ($1.17-1.28$ kg·CO_2e-C·m^{-2}·yr^{-1}) were brought up significantly due to CH_4 and were about 80 % of the intact land class, which has a climate-cooling effect due to terrestrial C-sequestration. The degraded land class is a net source of CO_2 and CH_4 and the channel emissions represent a loss of carbon and has an overwhelming warming effect on the climate. Further, if CH_4 ebullition were included, this may make the degraded channels a more significant source of CO_2e emissions. Fig. 6.8 also shows the significant difference that degradation makes in terms of CH_4-CO_2e fluxes; the degraded land class consistently emits several times more than the intact land class.

6.8 Suggestions for further work

The fluxes in this study were measured exclusively in the daytime, and therefore it is not known whether and by how much fluxes may vary over a 24-hour period. Diel flux variability would be an important term to constrain in order to make accurate estimates of regional channel emissions; CH_4 fluxes can be more than twice as large during the daytime (Bastviken et al., 2004). Cooler temperatures during the

night may increase the solubility of CO_2 and CH_4 with respect to the daytime thus diffusive fluxes may reduce. Perhaps more significantly, rainfall could increase gas emissions from the channels (Ho et al., 1997).

Rain typically falls during the night and could cause CO_2 and CH_4 emissions to increase by a) increased delivery of those dissolved gases and DOC to the channels, b) causing water flows to increase, which may increase k, and c) increasing the rain itself, which can fall for several hours at a time and could further cause k to increase by disturbing the water surface. During the wet season, there is a possibility that emissions could be significantly higher in the night time, but floating chambers, which would shield the water surface from the disturbance caused by rain, would not be the most effective method for accurately quantifying emissions increases because the rain is likely a controlling variable.

A drawback of the floating chamber approach used in this study was that the bulk of the equipment limited the distance that could be travelled, limiting the number of sites that could be investigated. Acoustic Doppler velocimeters (see Chapter 2) could be installed along the breadth of the channel, near the banks and in the centre, to establish k and allow a more passive approach to estimating gas fluxes over a longer time period and over a greater spatial scale. If used in conjunction with other passive measurements of, for example, water depth and/or flow rate, it may for k and subsequently gas fluxes to be constrained in terms of changes to PSF hydrology during a year. Further, weather stations could be installed in degraded PSF so that the effect that wind has on k could be quantified. The weather station data could be used in conjunction with satellite data to estimate evasion from the seasonal floodplains that occur during the peak of the wet season at degraded PSF. Currently, data regarding k in tropical streams and channels are scarce compared their boreal equivalents. If k can be more accurately quantified by understanding its drivers, upscaling of gas fluxes can be done more effectively, provided dissolved gas concentrations are available (Raymond et al., 2013).

The degraded areas of peatland in Central Kalimantan continue to be developed to make the land more valuable. In my time there I saw that channels were still being dug and therefore this may increase the amount of greenhouse gases being emitted by channels, and also the rate at which C is being exported from degraded peats in the form of DOC. Estimation of C losses could be made by using the gas flux data in this study and the DOC data in Moore et al. (2013) in conjunction with satellite data that may elucidate the rate at which channel construction is occurring in degraded peatlands.

The sources of the greenhouse gases were not determined in this thesis: in situ, CO_2 can be produced within the channel as a result of biodegradation or photo-oxidation of DOC, and CH_4 can be produced in the channel sediments; however, CO_2 and CH_4 can be produced ex situ and be transported to the channel via lateral flows from the catchment soils. There are likely to be differences between intact and degraded PSF as, for example, DOC was found to be more aromatic and less bioavailable in degraded than intact PSF channels (Moore et al., 2013), and therefore may be more prone to photo-oxidation (Anesio et al., 2005; Stubbins et al., 2008). Further, degraded PSF has very little tree cover and therefore this maximises the amount of solar radiation that can reach the channels and drive photolysis of DOC.

Ebullition of CH_4 may be a significant term in total CH_4 flux in PSF channels and may exceed the diffusive flux by an order of magnitude (see Chapter 5). CH_4 ebullition could be measured by using bubble traps to catch gas bubbles rising from the channel sediment (Crawford et al., 2014). Using a comparatively large number of traps per unit area of channel would be preferable as ebullition is a spatially and temporally stochastic process, which is known to vary significantly in a 24-hour period (Bastviken et al., 2004).

Radiocarbon dating the C in dissolved CH_4 using a similar technique as in Chapter 3 could be employed to establish the source of the CH_4 (Garnett et al., 2013), i.e. whether it comes from modern sources such as the leachate from tree roots being deposited in the rhizosphere, or whether it comes from ancient layers of the peat column (cf. Moore et al., 2013). Gas collected from ebullition bubble traps could also be analysed for its ^{14}C content. Analysis of the CH_4 content of pore waters near the channel, at a range of depths, may also be used to determine the source of the dissolved CH_4 in the channel (cf. Hoyt et al., 2017).

In broader terms, the cycling of CH_4 in intact and degraded peat swamp forest is yet to be fully understood. In an intact peat swamp forest, there are numerous processes responsible for the production and degradation of CH_4; CH_4 can be produced in peat, the rhizosphere and by termites (Fraser et al., 1986), but emissions of CH_4 from peat swamp forest are comparatively low with respect to boreal peats (Wong et al., 2018) despite comparable CH_4 pore water concentrations. This suggests there are some significant removal processes at work, and simultaneous measurement of production and removal processes may shed light on the reasons why degraded peat swamp forest can become an overwhelming

CH_4 source.

The fates of the channel CO_2 and CH_4 were also not determined in this thesis. Channels such as the ones used in this study act as headwaters of large river systems than run 100s of kilometers to the sea. As such, there is potential for a significant quantity of CO_2 and CH_4 that originated in the PSF catchments to be evaded before it reaches the sea and therefore the rivers can act as another −and potentially significant− loss pathway for peatland C.

6.9 Conclusions

- The channels at intact land class emitted approximately twice the amount of CO_2 as the channels at the degraded land class. Carbon dioxide emissions in the wet season were more than twice that of the dry season for both land classes. Median emission rates during the wet season of 2015 were 4.67 and 2.84 g·C·m^{-2}·d^{-1}, and 1.81 and 1.05 g·C·m^{-2}·d^{-1} in the dry season, for the intact and degraded land classes, respectively. In terms of net ecosystem exchange, however, the intact land class channel emissions are offset by the C sink effect of the forest, whereas negligible net primary productivity occurs at the degraded land class and therefore the emissions add to other C losses from the peatland.

- Channels draining peat swamp forest emit moderate quantities of CO_2, and do not appear to be globally significant hotspots as was hypothesised in some high-impact publications earlier this decade. These findings support other recent CO_2 emission studies of rivers draining tropical peatlands. As such, transport of DOC by the channels remains the dominant term with regards fluvial carbon export out of tropical peatland catchments.

- Radiocarbon dating of dissolved CO_2 demonstrated that the CO_2 in the channels of the intact land class was highly ^{14}C-enriched and was of modern origin. At the degraded land class, the radiocarbon age of dissolved CO_2 was 341−1655 years BP, confirming that ancient peat layers and DOC are being degraded (cf. Moore et al., 2013).

- The degraded land class emitted considerably more CH_4 than the intact land class. Excluding the El Niño dry season, when the water table was anomalously low, the range of median CH_4 diffusive

fluxes in the other three seasons were 9.47−16.8 mg·C·m^{-2}·d^{-1}) at the degraded land class, 8 to 9−times larger than fluxes from the intact land class (1.25−2.16 mg·C·m^{-2}·d^{-1}).

- At a landscape scale, the channels of the intact Sabangau National Park may emit only a negligible amount of CO_2 and CH_4, with respect to the peat surface. In terms of the degraded ex-Mega Rice Project area, the channels emitted <1 % of the total CO_2 emitted from the landscape. However, the ex-Mega Rice Project channels may emit more CH_4 than the peat surface, despite covering only 0.5 % of the ex-Mega Rice Project area. Whereas diffusive fluxes amounted to 0.23 Gg·CH_4-C·yr^{-1} alone may account for 9.1−12.3 %, if ebullitive fluxes were included emissions could total 3.45 Gg·CH_4-C·yr^{-1} which may be 59.9−67.7 % of the total landscape flux of CH_4.

- The 2015 El Niño dry season had the lowest CO_2 and highest CH_4 fluxes of all of the sampling seasons, most likely as a result of extreme water table drawdown and reduced overland flow at the intact land class. A three-year water table dataset for the intact land class showed that the water table usually oscillated between being aboveground to ˜25 cm beneath the peat surface. During the El Niño the water table at the intact land class dropped lower than 50 cm for more than four months before rebounding back to normal levels.

- The El Niño event appeared to cause a dramatic change to CH_4 cycling at the intact land class; the median partial pressure of channel CH_4 did not exceed 170 μatm, however during the dry season it rose almost 6-times, to 968 μatm. The latter partial pressure was, for the only time in the study, within the range of dissolved CH_4 at the degraded land class (859−1,341 μatm). This indicated a potential state shift in that intact peat swamp forest may behave similarly to a drained, degraded peatland. CH_4 flux at the intact land class during the El Niño dry season increased 4−times, to 7.76 mg·C·m^{-2}·d^{-1}, from the 'normal' season median of 1.81 mg·C·m^{-2}·d^{-1}. At the degraded land class the El Niño CH_4 increase was only 56 % (to 29.6 mg·C·m^{-2}·d^{-1}). The intact land class did, however, display resilience in that it returned to its normal state, following the El Niño event.

- The primary driver of fluxes of CO_2 and CH_4 in peat swamp forest channels was their supersaturation in the channel water, rather than by the gas exchange velocity which was found to be low compared to many fluvial systems (median k_{600} did not exceed 1 m·d^{-1} at either land class). Dissolved CO_2 was found to be very high at the intact land class which, during the first wet season,

had a median value of ~13,500 μatm. This is one of the highest values to be reported for fluvial systems, globally, despite literature values often being reported as means (which can be less conservative). This is further confirmation that tropical blackwater streams and channels contain large amounts of dissolved C compared to the equivalent systems in the boreal zone.

- At both land class types, dry seasons caused CO_2 fluxes to decrease, and CH_4 fluxes to increase, with respect to the wet seasons. CO_2 was always the dominant gas to be emitted in terms of mass of C. The sustained global warming potential was also dominated by CO_2, except for the degraded land class during the El Niño dry season when the warming potential was dominated by CH_4.

Appendix

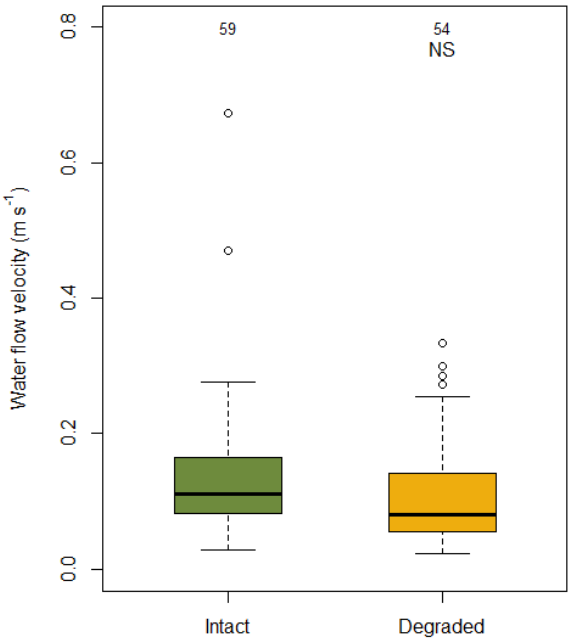

Figure 7.1: Channel water flow velocities measured with the impeller. There was no siginficant difference between the intact and degraded land classes (Two sample t-test, t = 1.02, df = 111, $p = 0.31$, means = 0.13 and 0.12 m·s^{-1}, respectively).

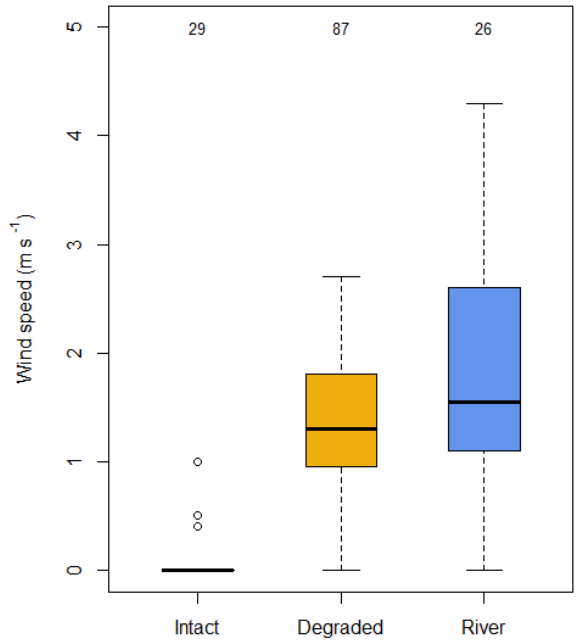

Figure 7.2: Wind speeds were measured with a handheld anemometer at the intact and degraded land classes, as well as on the Sabangau River. Only 3 of 29 measurements of wind speed at the intact land class were detectable. The median wind speeds at the degraded land class and the Sabangau River were 1.3 and 1.6 $m \cdot s^{-1}$, respectively.

Table 7.1: Bunsen coefficients used for calculating Henry's constant (K_H) for CO_2 and CH_4.

Gas	A_1	A_2	A_3	B_1	B_2	B_3	Source
CO_2	-58.0931	90.5069	22.2940	0.027766	-0.025888	0.0050578	Weiss, 1974
CH_4	-68.8862	101.4956	28.7314	-0.076146	0.043970	-0.006872	Weisenburg and Guinasso, 1979

Table 7.2: Coefficients used for calculating the Schmidt number (Sc) for CO_2 and CH_4.

Gas	A	B	C	D	E	Source
CO_2	1923.6	-125.06	4.3773	-0.085681	0.00070284	Wanninkhof, 2014
CH_4	1909.4	-120.78	4.1555	-0.080578	0.00065777	Wanninkhof, 2014

Table 7.3: Samples analysed for ^{14}C content by the NERC Radiocarbon Facility in East Kilbride. The RCL Code is the sample code used by the Facility.

RCL Code	Land Class	Site	^{14}C-Enrichment	Age (years BP$\pm 1\sigma$)
SUERC-65578	Intact	SAB1	103.75±0.45	N/A
SUERC-65579	Intact	SAB2	103.25±0.47	N/A
SUERC-65583	Intact	SAB3	103.72±0.48	N/A
SUERC-65584	Degraded	KALA	86.71±0.38	1,146±35
SUERC-65585	Degraded	TUN1	94.22±0.41	478±35
SUERC-65586	Degraded	TAR1	92.21±0.40	651±35
SUERC-72862	Degraded	KALA	81.38±0.37	1,655±36
SUERC-72863	Degraded	KALA	95.15±0.44	399±37
SUERC-72864	Degraded	TAR1	89.39±0.41	901±37
SUERC-72865	Degraded	TAR1	95.85±0.44	340±37
SUERC-72866	Degraded	TUN1	91.84±0.42	684±37
SUERC-72867	Degraded	TUN1	89.30±0.41	909±37

Table 7.4: Channel and channel branch lengths in the LAHG research station area. Data provided by Borneo Nature Foundation.

Channel Name	Length (m)
Adun	2,941
Agung	1,868
Alui	2,796
Ari	1,090
Bahkan	~12,000
Canal 1	1,995
Dodo	753
Erman	1,640
Jumri	1,267
Kartika	150
Ruslan	2,706
Udang	2,603
Ujau	1,123
Unyil	1,866
Unyil Cabang	276
Yali	1,211

References

Adji, F.F., Hamada, Y., Darung, U., Limin, S.H., Hatano, R., 2014. Effect of plant-mediated oxygen supply and drainage on greenhouse gas emission from a tropical peatland in Central Kalimantan, Indonesia. Soil Science and Plant Nutrition 60, 216-230.

Alin, S.R., de Fátima F.L. Rasera, M., Salimon, C.I., Richey, J.E., Holtgrieve, G.W., Krusche, A.V., Snidvongs, A., 2011. Physical controls on carbon dioxide transfer velocity and flux in low-gradient river systems and implications for regional carbon budgets. Biogeosciences 116, G01009.

Alkhatib, M., Jennerjahn, T.C., Samiaji, J., 2007. Biogeochemistry of the Dumai River estuary, Sumatra, Indonesia, a tropical blackwater river. Limnology and Oceanography 52, 2410-2417.

Anderson, Z.R., Kusters, K., Obidzinski, K., McCarthy, J., 2015. Growing the Economy: Oil palm and green growth in East Kalimantan, Indonesia. https://www.iss.nl/fileadmin/ASSETS/iss/Research_and_projects/Research_networks/BICAS/CMCP_20-_Anderson_et_al.pdf. Last accessed 06/12/17.

Anesio, A.M., Granéli, W., Aiken, G.R., Kieber, D.J., Mopper, K., 2005. Effect of humic substance photodegradation on bacterial growth and respiration in lake water. Applied and Environmental Microbiology 71(10), 6267-6275.

Arai, H., Hadi, A., Darung, U., Limin, S.H., Hatano, R., Inubushi, K., 2014. A methantrophic community in a tropical peatland is unaffected by drainage and forest fires in a tropical peat soil. Soil Science and Plant Nutrition 60, 577-585.

Aufdenkampe, A.K., Mayorga, E., Raymond, P.A., Melack, J.M., Doney, S.C., Alin, S.R., Aalto, R.E., Yoo, K., 2011. Riverine coupling of biogeochemical cycles between land, oceans, and atmosphere. Frontiers in Ecology and the Environment 9(1), 53-60.

Baer, D.S., Paul, J.B., Gupta, M., O'Keefe, A., 2002. Sensitive absorption measurements in the near-infrared region using off-axis integrated-cavity-output spectroscopy. Applied Physics B: Lasers and Optics 75(2), 261-265.

Baird, A.J., Low, R., Young, D., Swindles, G.T., Lopez, O.R., Page, S.E., 2017. High permeability explains the vulnerability of the carbon store in drained tropical peatlands. Geophysical Research Letters 44, 1333-1339.

Baird, A.J., Stamp, I., Heppell, C.M., Green, S.M., 2010. CH_4 flux from peatlands: a new measurement method. Ecohydrology 3(3), 360-367.

Barbier, E.B., 1993. Sustainable use of wetlands valuing tropical wetland benefits: economic methodologies and applications. Geographical Journal 159(1), 22-32.

Bartlett, K.B., Crill, P.M., Bonassi, J.A., Richey, J.E., Harriss, R.C., 1990. Methane Flux From the Amazon River Floodplain: Emissions During Rising Water. Journal of Geophysical Research 95(10), 16773-16788.

Bartlett, K.B., Crill, P.M., Sebacher, D.I., Harriss, R.C., Wilson, J.O., Melack, J.M., 1988. Methane Flux From the Central Amazonian Floodplain. Journal of Geophysical Research 93, 1571-82.

Bartlett, K.B., Harriss, R.C., 1993. Review and assessment of methane emissions from wetlands. Chemosphere 26, 261-320.

Bastviken, D., Cole, J., Pace, M., Tranvik, L., 2004. Methane emissions from lakes: Dependence of lake characteristics, two regional assessments, and a global estimate. Global Biogeochemical Cycles 18(4), GB4009, DOI:10.1029/2004GB002238

Bastviken, D., Sundgren, I., Natchimuthu, S., Reyier, H., Gålfalk, M., 2015. Cost-efficient approaches to measure carbon dioxide (CO_2) fluxes and concentrations in terrestrial and aquatic environments using mini loggers. Biogeosciences 12(12), 3849-3859.

Bastviken, D., Tranvik, L.J., Downing, J.A., Crill, P.M., Enrich-Prast, A., 2011. Freshwater methane emissions offset the continental carbon sink. Science 331, 50.

Battin, T.J., Kaplan, L.A., Findlay, S., Hopkinson, C.S., Marti, E., Packman, A.I., Newbold, J.D., Sabater, F., 2008. Biophysical controls on organic carbon fluxes in fluvial networks. Nature Geoscience 1, 95-100.

Battin, T.J., Luyssaert, S., Kaplan, L.A., Aufdenkampe, A.K., Richter, A., Tranvik, L.J., 2009. The boundless carbon cycle. Nature Geoscience 2, 598-600.

Baulch, H.M., Dillon, P.J., Maranger, R., Schiff, S.L., 2011. Diffusive and ebullitive transport of methane and nitrous oxide from streams: Are bubble-mediated fluxes important? Biogeosciences 116, G04028.

Baum, A., Rixen, T., Samiaji, J., 2007. Relevance of peat draining rivers in central Sumatra for the riverine input of dissolved organic carbon into the ocean. Estuarine, Coastal and Shelf Science 73, 563-570.

Belanger, T.V., Korzun, E.A., 1991. Critique of floating-dome technique for estimating reaeration rates. Journal of Environmental Engineering 117, 144-150.

Benson, B.B., Krause Jr., D., 1984. The concentration and isotopic fractionation of oxygen dissolved in freshwater and seawater in the equilibrium with the atmosphere. Limnology and Oceanography 29(3), 620-632.

Betts, R.A., Jones, C.D., Knight, J.R., Keeling, R.F., Kennedy, J.J., 2016. El Niño and a record CO_2 rise. Nature Climate Change 6, 806-810.

Billett, M.F., Dinsmore, K.J., Smart, R.P., Garnett, M.H., Holden, J., Chapman, P., Baird, A.J., Grayson, R., Stott, A.W., 2012. Variable source and age of different forms of carbon released from natural peatland pipes. Biogeosciences 117(G2), DOI:10.1029/2011JG001807

Billett, M.F., Garnett, M.H., Harvey, F., 2007. UK peatland streams release old carbon dioxide to the atmosphere and young dissolved organic carbon to rivers. Geophysical Research Letters 34(23), L23401, DOI:10.1029/2007GL031797

Billett, M.F., Garnett, M.H., Dinsmore, K.J., 2015. Should Aquatic CO_2 Evasion be Included in Contemporary Carbon Budgets for Peatland Ecosystems? Ecosystems 18, 474-480. DOI:10.1007/s10021-014-9838-5

Billett, M.H., Harvey, F.H., 2013. Measurements of CO_2 and CH_4 evasion from UK peatland headwater streams. Biogeochemistry 114, 165-181.

Billett, M.F., Moore, T.R., 2008. Supersaturation and evasion of CO_2 and CH_4 in surface waters at Mer Bleue peatland, Canada. Hydrological Processes 22(12), 2044-2054.

Bloom, A.A., Palmer, P.I., Fraser, A., Reay, D.S., 2012. Seasonal variability of tropical wetland CH_4 emissions: the role of the methanogen-available carbon pool. Biogeosciences 9, 2821-2830.

Boehm, H.D.V., Siegert, F., 2001. Ecological impact of the one million hectare rice project in Central Kalimantan, Indonesia, using remote sensing and GIS. In Paper presented at the 22nd Asian Conference on Remote Sensing (Vol. 5, p. 9).

Brix, H., Orr, P.T., 1992. Internal pressurization and convective gas flow in some emergent freshwater macrophytes. Limnology and Oceanography 37(7), 1420-1433.

Bubier, J.L., Moore, T.R., Bellisario, L., Comer, N.T., Crill, P.M., 1995. Ecological controls on methane emissions from a northern peatland complex in the zone of discontinuous permafrost, Manitoba, Canada. Global Biogeochemical Cycles 9(4), 455-470.

Butman, D., Raymond, P.A., 2011. Significant efflux of carbon dioxide from streams and rivers in the United States. Nature Geoscience 4(12), 839.

Butman, D.E., Wilson, H.F., Barnes, R.T., Xenopoulos, M.A., Raymond, P.A., 2015. Increased mobilization of aged carbon to rivers by human disturbance. Nature Geoscience 8(2), 112-116.

Cai, W., Borlace, S., Lengaigne, M., van Rensch, P., Collins, M., Vecchi, G., Timmermann, A., Santoso, A., McPhaden, M.J., Wu, L., England, M.H., Wang, G., Guilyardi, E., Jin, F-F., 2014. Increasing frequency of extreme El Niño events due to greenhouse warming. Nature Climate Change 4, 111-116.

Castro, H.F., Classen, A.T., Austin, E.E., Norby, R.J., Schadt, C.W., 2010. Soil microbial community responses to multiple experimental climate change drivers. Applied and Environmental Microbiology 76(4), 999-1007.

Chanton, J.P., Whiting, G.J., 1995. Trace gas exchange in freshwater and coastal marine environments: ebullition snf transport by plants. In Matson, P.A., Harriss, R.C. (eds), Biogenic Trace Gases: Measuring Emissions from Soil and Water. Blackwell Science, Oxford. 394 pp.

Cole, J.J., Bade, D.L., Bastviken, D., Pace, M.L., van de Bogert, M., 2010. Multiple approaches to estimating air-water gas exchange in small lakes. Limnology and Oceanography: Methods 8(6), 285-293.

Cole, J.J., Prairie, Y.T., Caraco, N.F., McDowell, W.H., Tranvik. L.J., Striegl. R.G., Duarte, C.M., Kortelainen, P., Downing, J.A., Middelburg, J.J., Melack, J., 2007. Plumbing the global carbon cycle: Integrating inland waters into the terrestrial carbon budget. Ecosystems 10, 171-184.

Cole, L.E.S., Bhagwat, S.A., Willis, K.J., 2015. Long-term disturbance and resilience of tropical peat swamp forests. Journal of Ecology 103, 16-30.

Cook, S., Peacock, M., Evans, C.D., Page, S.E., Whelan, M., Gauci, V., Khoon, K.I., 2016. Cold storage as a method for long-term preservation of tropical dissolved organic matter (DOC). Mires and Peat 18, 1-8.

Cooper, H.V., Vane, C.H., Evers, S., Alpin, P., Girkin, N.T., Sjögersten, S., 2019. From peat swamp forest to oil palm plantations: The stability of tropical peatland carbon. Geoderma 342, 109-117.

Couwenberg, J., Dommain, R., Joosten, H., 2010. Greenhouse gas fluxes from tropical peatlands in south-east Asia. Global Change Biology 16(6), 1715-1732.

Crawford, J.T., Stanley, E.H., Spawn, S.A., Finlay, J.C., Loken, L.C., Striegl, R.G., 2014. Ebullitive methane emissions from oxygenated wetland streams. Global Change Biology 20(11), 3408-3422.

Cuffney, T.F., 1988. Input, movement and exchange of organic matter within a subtropical coastal black-water river-floodplain system. Freshwater Biology 19, 305-320.

Dargie, G.C., Lewis, S.L., Lawson, I.T., Mitchard, E.T.A., Page, S.E., Bocko, Y.E., Ifo, S.A., 2017. Age, extent and carbon storage of the central Congo Basin peatland complex. Nature 542, 86-90.

Davidson, E.A., Nepstad, D.C., Ishida, F.Y., Brando, P.M., 2008. Effects of an experimental drought and recovery on soil emissions of carbon dioxide, methane, nitrous oxide, and nitric oxide in a moist tropical forest. Global Change Biology 14, 2582-2590.

Dawson, J.J., Billett, M.F., Hope, D., Palmer, S.M., Deacon, C.M., 2004. Sources and sinks of aquatic carbon in a peatland stream continuum. Biogeochemistry 70(1), 71-92.

de Angelis, M.A., Scranton, M.I., 1993. Fate of methane in the Hudson River and estuary. Global Biogeochemical Cycles 7, 509-523.

de Vries, F.T., 2003. Practical use of a hydrological model for peatlands in Borneo; modelling the Sungai Sebangau catchment in Central Kalimantan, Indonesia. Wageningen, Alterra, Green World Research. Alterra-rapport 1731.

Depetris, P.J., Kempe, S., 1990. The impact of the El Niño 1982 event on the Paraná River, its discharge and carbon transport. Global and Planetary Change 3(3), 239-244.

Devol, A.H., Quay, P.D., Richey, J.E., Martinelli, L.A., 1987. The role of gas exchange in the inorganic carbon, oxygen, and 222Rn budgets of the Amazon River. Limnology and Oceanography 32(1), 235-248.

Ding, W., Cai, Z., 2003. Effect of plants on methane production, oxidation and emission. The Journal of Applied Ecology 14(8), 1379-1384.

Dinsmore, K.J., Billett, M.F., Skiba, U.M., Rees, R.M., Drewer, J., Helfter, C., 2010. Role of the aquatic pathway in the carbon and greenhouse gas budgets of a peatland catchment. Global Change Biology 16(10), 2750-2762.

Dunfield, P., Knowles, R., Dumont, R., Moore, T.R., 1993. Methane production and consumption in temperate and subarctic peat soils: Response to temperature and pH. Soil Biology and Biochemistry 25(3), 321-326.

Evans, C., 2015. Biogeochemistry: Old carbon mobilized. Nature Geoscience 8(2), 85.

Evans, C.D., Page, S.E., Jones, T., Moore, S., Gauci, V., Laiho, R., Hruška, J., Allott, T.E., Billett, M.F., Tipping, E., Freeman, C., 2014. Contrasting vulnerability of drained tropical and high-latitude peatlands to fluvial loss of stored carbon. Global Biogeochemical Cycles 28(11), 1215-1234.

Evans, C.D., Williamson, J.M., Kacaribu, F., Irawan, D., Suardiwerianto, Y., Hidayat, M.F., Laurén, A., Page, S.E., 2019. Rates and spatial variability of peat subsidence in *Acacia* plantation and forest landscapes in Sumatra, Indonesia. Geoderma 338, 410-421.

Fenner, N., Freeman, C., 2011. Drought-induced carbon loss in peatlands. Nature Geoscience 4(12), 895-900.

Field, R.D., van der Werf, G.R., Fanin, T., Fetzer, E.J., Fuller, R., Jethva, H., Levy, R., Livesey, N.J., Luo, M., Torres, O., Worden, H.M., 2016. Indonesian fire activity and smoke pollution in 2015 show persistent nonlinear sensitivity to El Niño-induced drought. Proceedings of the National Academy of Sciences 113(33), 9204-9209.

Fraser, P.J., Rasmussen, R.A., Creffield, J.W., French, J.R., Khalil, M.A.K., 1986. Termites and global methane - another assessment. Journal of Atmospheric Chemistry 4(3), 295-310.

Freeman, C., Ostle, N., Kang, H., 2001. An enzymic 'latch' on a global carbon store. Nature 409, 149.

Gålfalk, M., Bastviken, D., Fredriksson, S., Arneborg, L., 2013. Determination of the piston velocity for water-air interfaces using flux chambers, acoustic Doppler velocimetry, and IR imaging of the water surface. Biogeosciences 118(2), 770-782.

Gandois, L., Teisserenc, R., Cobb, A.R., Chieng, H.I., Lim, L.B.L., Kamariah, A.S., Hoyt, A., Harvey, C.F., 2014. Origin, composition, and transformation of dissolved organic matter in tropical peatlands.

Geochimica et Cosmochimica Acta 137, 35-47.

Garnett, M.H., Dinsmore, K.J., Billett, M.F., 2012. Annual variability in the radiocarbon age and source of dissolved CO_2 in a peatland stream. Science of the Total Environment 427, 277-285.

Garnett, M.H., Hardie, S.M.L., Murray, C., Billett, M.F., 2013. Radiocarbon dating of methane and carbon dioxide evaded from a temperate peatland stream. Biogeochemistry 114, 213-223.

Gaveau, D.L., Kshatriya, M., Sheil, D., Sloan, S., Molidena, E., Wijaya, A., Wich, S., Ancrenaz, M., Hansen, M., Broich, M., Guariguata, M.R., 2013. Reconciling forest conservation and logging in Indonesian Borneo. PloS one 8(8), e69887.

Girkin, N.T., Turner, B.I., Ostle, N., Craigon, J., Sjögersten, S., 2018. Root exudate analogues accelerate CO_2 and CH_4 production in tropical peat. Soil Biology and Biochemistry 117, 48-55.

Goldenfum, J.A., 2011. GHG Measurement Guidelines for Freshwater Reservoirs, UNESCO/IHA, London, UK, 139 pp.

Gorham, E., 1991. Northern peatlands: Role in the carbon cycle and probable responses to climate warming. Ecological Applications 1, 182-195.

Gotsch, S.G., Crausbay, S.D., Giambelluca. T.W., Weintraub, A.E., Longman, R.J., Asbjornsen, H., Hotchkiss, S.C., Dawson, T.E., 2014. Water relations and microclimate around the upper limit of a cloud forest in Maui, Hawai'i. Tree Physiology 34(7), 766-777.

Guérin, F., Abril, G., Serça, Delon, C., Richard, S., Delmas, R., Tremblay, A., Varfalvy, L., 2007. Gas transfer velocities of CO_2 and CH_4 in a tropical reservoir and its river downstream. Journal of Marine Systems 66, 161-172.

Hamard, M., 2008. Vegetation correlates of gibbon density in the Sebangau National Park, Central Kalimantan, Indonesia. MSc thesis, Oxford Brookes University, Oxford, UK.

Haraguchi, A., Limin, S.H., Darung, U., 2007. Water chemistry of Sebangau River and Kahayan River in Central Kalimantan, Indonesia. Tropics 16(2), 123-130.

Harger, J.R.E., 1995. ENSO variations and drought occurrence in Indonesia and the Philippines. Atmospheric Environment 29(16), 1943-1955.

Harrison, M.E., Husson, S.J., D'Arcy, L.J., Morrogh-Bernard, H.C., Cheyne, S.M., van Noordwijk, M.A., van Schaik, C.P., 2010. The fruiting phenology of peat-swamp forest tree species at Sabangau and Tuanan, Central Kalimantan, Indonesia. The Kalimantan Forests and Climate Partnership, Palangka

Raya.

Helton, A.M., Wright, M.S., Bernhardt, E.S., Poole, G.C., Cory, R.M., Stanford, J.A., 2015. Dissolved organic carbon lability increases with water residence time in the alluvial aquifer of a river floodplain ecosystem. Biogeosciences 120(4), 693-706.

Hergoualc'h, K., Verchot, L.V., 2014. Greenhouse gas emission factors for land use and land-use change in Southeast Asian peatlands. Mitigation and Adaptation Strategies for Global Change 19(6), 789-807.

Hirano, T., Jauhiainen, J., Inoue, T., Takahashi, H., 2009. Controls on the carbon balance of tropical peatlands. Ecosystems 12(6), 873-887.

Hirano, T., Segah, H., Harada, T., Limin, S., June, T., Hirata, R., Osaki, M., 2007. Carbon dioxide balance of a tropical peat swamp forest in Kalimantan, Indonesia. Global Change Biology 13(2), 412-425.

Hirano, T., Segah, H., Kusin, K., Limin, S., Takahashi, H., Osaki, M., 2012. Effects of disturbances on the carbon balance of tropical peat swamp forests. Global Change Biology 13, 3410-3422.

Ho, D.T., Bliven, L.F., Wanninkhof, R., Schlosser, P., 1997. The effect of rain on air-water gas exchange. Tellus B 49(2), 149-158.

Hodson, E.L., Poulter, B., Zimmermann, N.E., Prigent, C., Kaplan, J.O., 2011. The El Niño-Southern Oscillation and wetland methane interannual variability. Geophysical Research Letters 38(8), DOI:10.1029/2011GL046861

Holmes, M.E., Chanton, J.P., Tfaily, M.M., Ogram, A., 2015. CO_2 and CH_4 isotope compositions and production pathways in a tropical peatland. Global Biogeochemical Cycles 19, 1-18. DOI:10.1002/2014GB004951

Hooijer, A., Silvius, M., Wösten, H., Page, S., 2006. PEAT-CO2, Assessment of CO_2 emissions from drained peatlands in SE Asia. Delft Hydraulics Report Q3943, Delft, The Netherlands.

Hooijer, A., van der Vat, M., Prinsen, G., Vernimmen, R., Brinkman, J.J., Zijl, F., 2008. Hydrology of the EMRP Area - Water Management Implications for Peatlands, Technical Report Number 2 of the Master Plan for the Rehabilitation and Revitalisation of the Ex-Mega Rice Project Area in Central Kalimantan. Euroconsult Mott McDonald and Deltares Delft Hydraulics.

Hondzo, M., Steinberger, N., 2008. Sediment Oxygen Demand (SOD) in Rivers, Lakes, and Estuaries. In García, M.H. (ed), Sedimentation Engineering - Processes, Measurements, Modeling, and Practice.

American Society of Civil Engineers. 1132 pp.

Hope, D., Billett, M.F., Cresser, M.S., 1994. A review of the export of carbon in river water: fluxes and processes. Environmental Pollution 84, 301-324.

Hope, D., Palmer, S.M., Billett, M.F., Dawson, J.J.C., 2001. Carbon dioxide and methane evasion from a temperate peatland stream. Limnology and Oceanography 46(4), 847-857.

Hosciło, A., Page, S.E., Tansey, K.J., Rieley, J.O., 2011. Effect of repeated fires on land-cover change on peatland in southern Central Kalimantan, Indonesia, from 1973 to 2005. International Journal of Wildland Fire 20(4), 578-588.

Hoyt, A., Corbett, J.E., Gandois, L., Cobb, A., Pangala, S.R., Gauci, V., Harvey, C.F., 2017. Global trends in peatland methane production. AGU Fall Meeting Abstracts, B41M-07.

Hoyt, A., Pangala, S.R., Gandois, L., Cobb, A., Gauci, V., Harvey, C.F., 2016. Methane oxidation in a tropical peatland. AGU Fall Meeting Abstracts, B21L-06.

Huang, T.H., Fu, Y.H., Pan, P.Y., Chen, C.T.A., 2012. Fluvial carbon fluxes in tropical rivers. Current Opinion in Environmental Sustainability 4(2), 162-169.

Hudson, J.J., Dillon, P.J., Somers, K.M., 2003. Long-term patterns in dissolved organic carbon in boreal lakes: the role of incident radiation, precipitation, air temperature, southern oscillation and acid deposition. Hydrology and Earth System Sciences Discussions 7(3), 390-398.

Hueso, S., García, C., Hernández, T., 2012. Severe drought conditions modify the microbial community structure, size and activity in amended and unamended soils. Soil Biology and Biochemistry 50, 167-173.

Huijnen, V., Wooster, M.J., Kaiser, J.W., Gaveau, D.L.A., Flemming, J., Parrington, M., Inness, A., Murdiyarso, D., Main, B., van Weele, M., 2016. Fire carbon emissions over maritime southeast Asia in 2015 largest since 1997. Scientific Reports 6, DOI:10.1038/srep26886

Huttunen, J.T., Alm, J., Liikanen, A., Juutinen, S., Larmola, T., Hammar, T., Silvola, J., Martikainen, P.J., 2003. Fluxes of methane, carbon dioxide and nitrous oxide in boreal lakes and potential anthropogenic effects on the aquatic greenhouse gas emissions. Chemosphere 52, 609-621.

Ilina, S.M., Drozdova, O.Y., Lapitskiy, S.A., Alekhin, Y.V., Demin, V.V., Zavgorodnyaya, Y.A., Shirokova, L.S., Viers, J., Pokrovsky, O.S., 2014. Size fractionation and optical properties of dissolved organic matter in the continuum soil solution-bog-river and terminal lake of a boreal watershed. Organic

Geochemistry 66, 14-24.

Inubushi, K., Furukawa, Y., Hadi, A., Purnomo, E., Tsuruta, H., 2003. Seasonal changes of CO_2, CH_4 and N_2O fluxes in relation to land-use change in tropical peatlands located in coastal area of South Kalimantan. Chemosphere 52(3), 603-608.

Inubushi, K., Otake, S., Furukawa, Y., Shibasaki, N., Ali, N., Itang, A.M., Tsuruta, H., 2005. Factors influencing methane emission from peat soils: Comparison of tropical and temperate wetlands. Nutrient Cycling in Agroecosystems 71, 93-99.

Ito, A., Inatomi, M., 2012. Use of a process-based model for assessing the methane budgets of global terrestrial ecosystems and evaluation of uncertainty. Biogeosciences 9(2), 759-773.

Jackson, R.B., Canadell, J., Ehleringer, J.R., Mooney, H.A., Sala, E.O., Schulze, E.D., 1996. A global analysis of root distributions for terrestrial biomes. Oecologia 108, 389-411.

Jähne, B., Haussecker, H., 1998. Air-water gas exchange. Annual Review of Fluid Mechanics 30(1), 443-468.

Jauhiainen, J., Limin, S., Silvennoinen, H., Vasander, H., 2008. Carbon Dioxide and Methane Fluxes in Drained Tropical Peat Before and After Hydrological Restoration. Ecology 89, 35033514. DOI:10.1890/07-2038.1

Jauhiainen, J., Silvennoinen, H., 2012. Diffusion GHG fluxes at tropical peatland drainage canal water surfaces. Suo 63, 93-105.

Jauhiainen, J., Takahashi, H., Heikkinen, J.E.P., Martikainen, P.J., Vasander, H., 2005. Carbon fluxes from a tropical peat swamp forest floor. Global Change Biology 11, 1788-1797.

Jiménez-Muñoz, J.C., Mattar, C., Barichivich, J., Santamaría-Artigas, A., Takahashi, K., Malhi, Y., Sobrino, J.A., van der Schrier, G., 2016. Record-breaking warming and extreme drought in the Amazon rainforest during the course of El Niño 20152016. Scientific Reports 6, DOI:10.1083/srep33130

Johnson, M.S., Lehmann, J., Riha, S.J., Krusche, A.V., Richey, J.E., Ometto, J.P.H.B., Couto, E.G., 2008. CO_2 efflux from Amazonian headwater streams represents a significant fate for deep soil respiration. Geophysical Research Letters 35, L17401, DOI:10.1029/2008GL034619

Jones, C.D., Collins, M., Cox, P.M., Spall, S.A., 2001. The carbon cycle response to ENSO: A coupled climate-carbon cycle model study. Journal of Climate 14(21), 4113-4129.

Jones, J.B., Holmes, R.M., Fisher, S.G., Grimm, N.B., Greene, D.M., 1995. Methanogenesis in Arizona, USA dryland streams. Biogeochemistry 31(3), 155-173.

Jones, B.J., Mullholland, P.J., 1998. Methane input and evasion in a hardwood forest stream: Effects of subsurface flow from shallow and deep pathways. Limnology and Oceanography 43, 1243-1250.

Junk, W.J., An, S., Finlayson, C.M., Gopal, B., Květ, J., Mitchell, S.A., Mitsch, W.J., Robarts, R.D., 2013. Current state of knowledge regarding the worlds wetlands and their future under global climate change: a synthesis. Aquatic Sciences 75(1), 151-167.

Kashino, Y., España, N., Syamsudin, F., Richards, K.J., Jensen, T., Dutrieux, P., Ishida, A., 2009. Observations of the North Equatorial current, Mindanao current, and Kuroshio current system during the 2006/07 El Niño and 2007/08 La Niña. Journal of Oceanography 65(3), 325-333.

Keeling, C.D., Whorf, T.P., Whalen, M., van der Plicht, J., 1995. Interannual extremes in the rate of rise of atmospheric carbon dioxide since 1980. Nature 375, 666-670.

Keil, A., Zeller, M., Wida, A., Sanim, B., Birner, R., 2008. What determines farmers' resilience towards ENSO-related drought? An empirical assessment in Central Sulawesi, Indonesia. Climatic Change 8, 291-307.

Kirschke, S., Bousquet, P., Ciais, P., Saunois, M., Canadell, J.G., Dlugokencky, E.J., Bergamaschi, P, Bergmann, D., Blake, D.R., Bruhwiler, L., Cameron-Smith, P, Castaldi, S., Chevallier, F., Feng, L., Fraser, A., Heimann, M., Hodson, E.L., Houweling, S., Josse, B., Fraser, P.J., Krummel, P.B., Lamarque, J-F., Langenfelds, R.L., Le Qur, C., Naik, V., O'Doherty, S., Palmer, P.I., Pison, I., Plummer, D., Poulter, B., Prinn, R.G., Rigby, M., Ringeval, B., Santini, M., Schmidt, M., Shindell, D.T., Simpson, I.J., Spahni, R., Steele, L.P., Strode, S.A., Sudo, K., Szopa, S., van der Werf, G.R., Voulgarakis, A., van Weele, M., Weiss, R.F., Williams, J.E., Zeng, G., 2013. Three decades of global methane sources and sinks. Nature Geoscience 6, 813-823.

Köchy, M., Hiederer, R., Freibauer, A., 2015. Global distribution of soil organic carbon Part 1: Masses and frequency distributions of SOC stocks for the tropics, permafrost regions, wetlands, and the world. Soil 1, 351-365.

Koelbener, A., Ström, L., Edwards, P.J., Venterink, H.O., 2010. Plant species from mesotrophic wetlands cause relatively high methane emissions from peat soil. Plant and Soil 326(1-2), 147-158.

Koh, L.P., Miettinen, J., Liew, S.C., Ghazoul, J., 2011. Remotely sensed evidence of tropical peatland conversion to oil palm. Proceedings of the National Academy of Sciences 108(12), 5127-5132.

Koplitz, S.N., Mickley, L.J., Marlier, M.E., Buonocore, J.J., Kim, P.S., Liu, T., Sulprizio, M.P., DeFries, R.S., Jacob, D.J., Schwartz, J., Pongsiri, M., 2016. Public health impacts of the severe haze in Equatorial Asia in SeptemberOctober 2015: demonstration of a new framework for informing fire management strategies to reduce downwind smoke exposure. Environmental Research Letters 11(9), 094023

Koprivnjak, J.F., Dillon, P.J., Molot, L.A., 2010. Importance of CO_2 evasion from small boreal streams. Global Biogeochemical Cycles 24(4).

Kozlowski, T.T., 1997. Responses of woody plants to flooding and salinity. Tree physiology 17(7), 490.

Kremer, J.N., Nixon, S.W., Buckley, B., Roques, P., 2003. Conditions for using the floating chamber method to estimate air-water gas exchange. Estuaries 26(4), 985-990.

Kutzbach, L., Schneider, J., Sachs, T., Giebels, M., Nykänen, H., Shurpali, N.J., Martikainen, P.J., Alm, J., Wilmking, M., 2007. CO_2 flux determination by closed-chamber methods can be seriously biased by inappropriate application of linear regression. Biogeosciences 4(6), 1005-1025.

Kwon, M.J., Haraguchi, A., Kang, H., 2013. Long-term water regime differentiates changes in decomposition and microbial properties in tropical peat soils exposed to the short-term drought. Soil Biology and Biochemistry 60, 33-44.

Laanbroek, H.J., 2010. Methane emissions from natural wetlands: interplay between emergent macrophytes and soil microbial processes. A mini-review. Annals of Botany 105, 141-153.

Lapierre, J-F., Guillemette, F., Berggren, M., del Giorgio, P.A., 2013. Increases in terrestrially derived carbon stimulate organic carbon processing and CO_2 emissions in boreal aquatic ecosystems. Nature Communications 4, DOI:10.1038/ncomms397

Lauerwald, R., Laruelle, G.G., Hartmann, J., Ciais, P., Regnier, P.A.G., 2015. Spatial patterns in CO_2 evasion from the global river network. Global Biogeochemical Cycles 29, 1-21.

Le, T.P.Q., Marchand,C., Ho, C.T., Le, N.D., Duong, T.T.,Lu, X., Doan, P.K., Nguyen, T.K., Nguyen, T.M.H., Vu, D.A., 2018. CO_2 partial pressure and CO_2 emission along the lower Red River (Vietnam). Biogeosciences 15, 47994814.

Leopold L.B., Wolman, M.G., Miller, J.P., 1964. Fluvial processes in geomorphology. New York, Dover Publishers, 522 pp.

L'Heureux, M.L., Takahashi, K., Watkins, A.B., Barnston, A.G., Becker, E.J., di Liberto, T.E., Gamble, F., Gottschalck, J., Halpert, M.S., Huang, B., Mosquera-Vásquez, K., 2017. Observing and predicting the 2015-16 El Niño. Bulletin of the American Meteorological Society, DOI:10.1175/BAMS-D-16-0009

Li, S., Lu, X.X., Bush, R.T., 2013. CO_2 partial pressure and CO_2 emission in the Lower Mekong River. Journal of Hydrology 504, 40-56.

Lilley, M.D., de Angelis, M.A., Olson, E.J., 1996. Methane concentrations and estimated fluxes from Pacific Northwest rivers. Internationale Vereinigung für Theoretische und Angewandte Limnologie: Mitteilungen 25(1), 187-196.

Limpens, J., Berendse, F., Blodau, C., Canadell, J.G., Freeman, C., Holden, J., Roulet, N., Rydin, H., Schaepman-Strub, G., 2008. Peatlands and the carbon cycle: from local processes to global implications a synthesis. Biogeosciences 5(5), 1475-1491.

Lohberger, S., Stängel, M., Atwood, E.C., Siegert, F., 2017. Spatial evaluation of Indonesia's 2015 fire affected area and estimated carbon emissions using Sentinel-1. Global Change Biology 24(2), 644-654.

Lorke, A., Bodmer, P., Noss, C., Alshboul, Z., Koschorreck, M., Somlai, C., Bastviken, D., Flury, S., McGinnis, D.F., Maeck, A., Müller, D., Premke, K., 2015. Drifting vs. anchored flux chambers for measuring greenhouse gas emissions from running waters. Biogeosciences Discussions 12(17), 14619-14645.

MacIntyre, S., Wanninkhof, R., Chanton, J.P., 1995. Trace gas exchange across the air-water interface in freshwater and coastal marine environments. In Matson, P.A., Harriss, R.C. (eds), Biogenic Trace Gases: Measuring Emissions from Soil and Water. Blackwell Science, Oxford. 394 pp.

Maeck, A., Hofmann, H., Lorke, A., 2014. Pumping methane out of aquatic sediments: ebullition forcing mechanisms in an impounded river. Biogeosciences 11, 2925-2938.

Manahan, S.E., 2010. Environmental Chemistry 9e. Boca Raton, Florida, CRC Press, 754 pp.

Marwanto, S., Agus, F., 2014. Is CO_2 flux from oil palm plantations on peatland controlled by soil moisture and/or soil and air temperatures? Mitigation and Adaptation Strategies for Global Change 19, 809-819.

Materić, D., Peacock, M., Kent, M., Cook, S., Gauci, V., Röckmann, T., Holzinger, R., 2017. Characterisation of the semi-volatile component of Dissolved Organic Matter by Thermal Desorption - Proton Transfer Reaction - Mass Spectrometry. Scientific Reports 7:15936, DOI:10.1038/s41598-017-16256-x

Matthews, C.J., St. Louis, V.L., Hesslein, R.H., 2003. Comparison of three techniques used to measure diffusive gas exchange from sheltered aquatic surfaces. Environmental Science and Technology 37(4), 772-780.

Mayorga, E., Aufdenkampe, A.K., Masiello, C.A., Krusche, A.V., Hedges, J.I., Quay, P.D., Richey, J.E., Brown, T.A., 2005. Young organic matter as a source of carbon dioxide outgassing from Amazonian rivers. Nature 436, 538-541.

McAlpine, C.A., Johnson, A., Salazar, A., Syktus, J.I., Wilson, K., Meijaard, E., Seabrook, L.M., Dargusch, P., Nordin, H., Sheil, D., 2018. Forest loss and Borneo's climate. Environmental Research Letters, DOI:10.1088/1748-9326/aaa4ff

McClain, M.E., Boyer, E.W., Dent, C.L., Gergel, S.E., Grimm, N.B., Groffman, P.M., Hart, S.C., Harvey, J.W., Johnston, C.A., Mayorga, E., McDowell, W.H., Pinay, G., 2003. Biogeochemical hot spots and hot moments at the interface of terrestrial and aquatic ecosystems. Ecosystems 6(4), 301-312.

McGill, R., Tukey, J.W., Larsen, W.A., 1978. Variations of Box Plots. The American Statistician 32(1), 12-16.

Megonigal, J.P., Day, F.P., 1992. Effects of flooding on root and shoot production of bald cypress in large experimental enclosures. Ecology 73(4), 1182-1193.

Meijaard, E., Abram, N.K., Wells, J.A., Pellier, A.S., Ancrenaz, M., Gaveau, D.L., Runting, R.K., Mengersen, K., 2013. Peoples perceptions about the importance of forests on Borneo. PloS one 8(9), e73008.

Meybeck, M., Vörösmarty, C., 1999. Global transfer of carbon by rivers. Global Change Newsletter 37, 18-19.

Meyer, J.L., Edwards, R.T., 1990. Ecosystem Metabolism and Turnover of Organic Carbon along a Blackwater River Continuum. Ecology 71(2), 668-677.

Miettinen, J., Hooijer, A., Shi, C., Tollenaar, D., Vernimmen, R., Liew, S.C., Malins, C., Page, S.E., 2012. Extent of industrial plantations on Southeast Asian peatlands in 2010 with analysis of historical expansion and future projections. Global Change Biology: Bioenergy 4, 908-918.

Miettinen, J., Hooijer, A., Vernimmen, R., Liew, S.C., Page, S.E., 2017. From carbon sink to carbon source: extensive peat oxidation in insular Southeast Asia since 1990. Environmental Research Letters 12(2), 024014.

Miettinen, J., Shi, C., Liew, S.C., 2011. Deforestation rates in insular Southeast Asia between 2000 and 2010. Global Change Biology 17(7), 2261-2270.

Miettinen, J., Shi, C., Liew, S.C., 2016. Land cover distribution in the peatlands of Peninsular Malaysia, Sumatra and Borneo in 2015 with changes since 1990. Global Ecology and Conservation 6, 67-78.

Molles Jr, M.C., Dahm, C.N., 1990. A perspective on El Niño and La Niña: global implications for stream ecology. Journal of the North American Benthological Society 9(1), 68-76.

Moore, S., 2011. Effects of ecosystem disturbance on fluvial carbon losses from tropical peat swamp forest. PhD thesis, Open University, Milton Keynes, UK.

Moore, S., Evans, C.D., Page, S.E., Garnett, M.H., Jones, T.G., Freeman, C., Hooijer, A., Wiltshire, A.J., Limin, S.H., Gauci, V., 2013. Deep instability of deforested tropical peatlands revealed by fluvial carbon fluxes. Nature 493, 660-664.

Moore, S., Gauci, V., Evans, C.D., Page, S.E., 2011. Fluvial organic carbon losses from a Bornean black-water river. Biogeosciences 8, 901-909.

Müller, D., Warneke, T., Rixen, T., Müller, M., Jamahari, S., Denis, N., Mujahid, A., Notholt, J., 2015. Lateral carbon fluxes and CO_2 outgassing from a tropical peat-draining river. Biogeosciences 12(20), 5967-5979.

Müller, D., Warnecke, T., Rixen, T., Müller, M., Mujahid, A., Bange, H.W., Northolt, J., 2016. Fate of terrestrial organic carbon and associated CO_2 and CO emissions from two Southeast Asian estuaries. Biogeosciences 13, 691-705.

Müller-Dum, D., Warnecke, T., Rixen, T., Müller, M., Baum, A., Christodoulou, A., Oakes, J., Eyre, B.D., Notholt, J., 2019. Impact of peatlands on carbon dioxide (CO_2) emissions from the Rajang River and Estuary, Malaysia. Biogeosciences Discussions, DOI:10.5194/bg-2018-391

Myhre, G., Shindell, D., Bréon, F.M., Collins, W., Fuglestvedt, J., Huang, J., Koch, D., Lamarque, J.F., Lee, D., Mendoza, B., Nakajima, T., 2013. Anthropogenic and Natural Radiative Forcing. In Stocker, T.F.D., Qin, G-K., Plattner, M., Tignor, S.K., Allen, J., Baschung, A., Nauels, Y., Xia, Y., Bex, V., Midgley, P.M. (eds) Climate Change 2013: The Physical Science Basis. Contribution of Working Group I to the Fifth Assessment Report of the Intergovernmental Panel on Climate Change, 658-740 (Cambridge University Press, Cambridge, United Kingdom and New York, NY, USA, 2013)

Nannipieri, P., Ascher, J., Ceccherini, M.T., Landi, L., Pietramellara, G., Renella, G., Valori, F., 2007. Microbial diversity and microbial activity in the rhizosphere. Ciencia del suelo 25(1), 89-97.

Neubauer, S.C., Megonigal, J.P., 2015. Moving beyond global warming potentials to quantify the climatic role of ecosystems. Ecosystems 18(6), 1000-1013.

Nunes, F.L.D., Aquilina, L., de Ridder, J., Francez, A-J., Quaiser, A., Caudal, J-P., Vandenkoornhuyse, P., Dufresne, A., 2015. Time-scales of hydrological forcing on the geochemistry and bacterial community structure of temperate peat soils. Scientific Reports 5, DOI:10.1038/srep14612

O'Brien, J.M., Warburton, H.J., Graham, S.E., Franklin, H.M., Febria, C.M., Hogsden, K.L., Harding, J.S., McIntosh, A.R., 2017. Leaf litter additions enhance stream metabolism, denitrification, and restoration prospects for agricultural catchments. Ecosphere 8(11), DOI:10.1002/ecs2.2018

Page, S., Hosciło, A., Langner, A., Tansey, K., Siegert, F., Limin, S., Rieley, J., Cochrane, M.A., 2009a. Tropical peatland fires in Southeast Asia. Tropical Fire Ecology, 263-287. DOI:10.1007/978-3-540-77381-8-9

Page, S., Hosciło, A., Wösten, H., Jauhiainen, J., Silvius, M., Rieley, J., Ritzema, H., Tansey, K., Graham, L., Vasander, H., Limin, S., 2009b. Restoration ecology of lowland tropical peatlands in Southeast Asia: Current knowledge and future research directions. Ecosystems 12, 888-905.

Page, S.E., Baird, A.J., 2016. Peatlands and global change: Response and resilience. Annual Review of Environment and Resources 41, 35-57.

Page, S.E., Rieley, J.O., Banks, C.J., 2011. Global and regional importance of the tropical peatland carbon pool. Global Change Biology 17, 798-818.

Page, S.E., Rieley, J.O., Shotyk, Ø.W., Weiss, D., 1999. Interdependence of peat and vegetation in a tropical peat swamp forest. Philosophical Transactions of the Royal Society B: Biological Sciences 354(1391), 161-173.

Page, S.E., Siegert, F., Rieley, J.O., Boehm, H-D.V., Jaya, A., Limin, S., 2002. The amount of carbon released from peat and forest fires in Indonesia during 1997. Nature 420, 61-65.

Page, S.E., Wüst, R.A.J., Weiss, D., Rieley, J.O., Shotyk, Ø.W., Limin, S.H., 2004. A record of Late Pleistocene and Holocene carbon accumulation and climate change from an equatorial peat bog (Kalimantan, Indonesia): implications for past, present and future carbon dynamics. Journal of Quaternary Science 19(7), 625-635.

Pandey, S., Houweling, S., Krol, M., Aben, I., Monteil, G., Nechita-Banda, N., Dlugokencky, E.J., Detmers, R., Hasekamp, O., Xu, X., Riley, W.J., Poulter, B., Zhang, Z., McDonald, K.C., White, J.W.C., Bousquet, P., Röckmann, T., 2017. Enhanced methane emissions from tropical wetlands during the 2011 La Niña. Scientific Reports 7, DOI:10.1038/srep45759

Pangala, S.R., Enrich-Prast, A., Basso, L.S., Peixoto, R.B., Bastviken, D., Hornibrook, E.R., Gatti, L.V., Marotta, H., Calazans, L.S.B., Sakuragui, C.M., Bastos, W.R., Malm, O, Gloor, E., Miller, J.B., Gauci, V., 2017. Large emissions from floodplain trees close the Amazon methane budget. Nature 552, 230.

Pangala, S.R., Moore, S., Hornibrook, E.R., Gauci, V., 2013. Trees are major conduits for methane egress from tropical forested wetlands. New Phytologist 197(2), 524-531.

Peacock, M., Freeman, C., Gauci, V., Lebron, I., Evans, C.D., 2015. Investigations of freezing and cold storage for the analysis of peatland dissolved organic carbon (DOC) and absorbance properties. Environmental Science: Processes and Impacts 17, 1290-1301.

Posa, M.R.C., Wijedasa, L.S., Corlett, R.T., 2011. Biodiversity and conservation of tropical peat swamp forests. BioScience 61(1), 49-57.

Price, J., Rochefort, L., Quinty, F., 1998. Energy and moisture considerations on cutover peatlands: Surface microtopography, mulch cover and Sphagnum regeneration. Ecological Engineering 10, 293-312.

R Development Core Team., 2013. R: A Language and Environment for Statistical Computing. R Foundation for Statistical Computing, Vienna, Austria.

Rais, D.S., Ichsan, N., 2008. Water Management (Hydrological) Assessment of the Block A North In Ex-Mega Rice Project Central Kalimantan. Wetlands International Indonesia Programme. Bogor.

Raymond, P.A., Hartmann, J., Lauerwald, R., Sobek, S., McDonald, C., Hoover, M., Dutman, D., Streigl, R., Mayorga, E., Humborg, C., Kortelainen, P., Dürr, H., Meybeck, M., Ciais, P., Huth, P., 2013. Global carbon dioxide emissions from inland waters. Nature 503, 355-359.

Raymond, P.A., Zappa, C.J., Butman, D., Bott, T.L., Potter, J., Mulholland, P., Laursen, A.E., McDowell, W.H., Newbold, D., 2012. Scaling the gas transfer velocity and hydraulic geometry in streams and small rivers. Limnology and Oceanography: Fluids and Environments 2, 41-53.

Regnier, P., Friedlingstein, P., Ciais, P., Mackenzie, F.T., Gruber, N., Janssens, I.A., Laruelle, G.G., Lauerwald, R., Luyssaert, S., Andersson, A.J., Arndt, S., 2013. Anthropogenic perturbation of the carbon

fluxes from land to ocean. Nature Geoscience 6(8), 597.

Richey, J.E., Melack, J.M., Aufdenkampe, A.K., Ballester, V.M., Hess, L.L., 2002. Outgassing from Amazonian rivers and wetlands as a large tropical source of atmospheric CO_2. Nature 416, 617-620.

Ritzema, H., Limin, S., Kusin, K., Jauhiainen, J., Wösten, 2014. Canal blocking strategies for hydrological restoration of degraded peatlands in Central Kalimantan, Indonesia. Catena 114, 11-20.

Rixen, T., Baum, A., Pohlmann, T., Balzer, W., Samiaji, J., Jose, C., 2008. The Siak, a tropical black water river in central Sumatra on the verge of anoxia. Biogeochemistry 90, 129-140.

Rosenthal, R., 1991. Meta-analytic procedures for social research 2e. Newbury Park, CA: Sage.

Rosnow, R.L., Rosenthal, R., 2005. Beginning behavioural research: A conceptual primer 5e. Upper Saddle River, NJ: Pearson/Prentice Hall.

Roulet, N., Moore, T., Bubier, J., Lafleur, P., 1992. Northern fens: methane flux and climatic change. Tellus B 44(2), 100-105.

Rydin, H., Jeglum, J.K., 2006. The Biology of Peatlands. Oxford, Oxford University Press, 344 pp.

Schimel, J.P., Gulledge, J.A.Y., 1998. Microbial community structure and global trace gases. Global Change Biology 4(7), 745-758.

Schlesinger, W.H., Bernhardt, E.S., 2013. Biogeochemistry: an analysis of global change 3e. Waltham, Massachusetts, Academic Press, 673 pp.

Segers, R., 1998. Methane production and methane consumption: a review of processes underlying wetland methane fluxes. Biogeochemistry 41, 23-51.

SenseAir, 2018. SenseAir ABC-Algorithm. `https://senseair.com/knowledge/sensor-technology/technology/senseair-abc-algorithm/`. Last accessed 20/03/18.

Siegert, F., Ruecker, G., Hinrichs, A., Hoffmann, A.A., 2001. Increased damage from fires in logged forests during droughts caused by El Niño. Nature 414, 437-440.

Sioli, H., 1975. Tropical rivers as expressions of their terrestrial environments. In Tropical Ecological Systems: Trends in Terrestrial and Aquatic Research, Eds, Golley, F.B., Medina, E. Berlin, Springer.

St. John, T.V., Anderson, A.B., 1982. A re-examination of plant phenolics as a source of tropical black water rivers. Tropical Ecology 23, 151-154.

Stubbins, A., Hubbard, V., Uher, G., Law, C.S., Upstill-Goddard, R.C., Aiken, G.R., Mopper, K., 2008. Relating carbon monoxide photoproduction to dissolved organic matter functionality. Environmental

Science and Technology 42(9), 3271-3276.

Sulistyanto, Y., 2005. Nutrient dynamics in different sub-types of peat swamp forest in Central Kalimantan, Indonesia. PhD thesis, University of Nottingham, Nottingham, UK.

Sundari, S., Hirano, T., Yamada, H., Kusin, K., Limin, S., 2012. Effect of groundwater level on soil respiration in tropical peat swamp forests. Journal of Agricultural Meteorology 68(2), 121-134.

Sundh, I., Nilsson, M., Granberg, G., Svensson, B.H., 1994. Depth Distribution of Microbial Production and Oxidation of Methane in Northern Boreal Peatlands. Microbial Ecology 27(3), 253-265.

Sundquist, E.T., 1993. The global carbon budget. Science 259, 934-941.

Svensson, B.H., 1984. Different temperature optima for methane formation when enrichments from acid peat are supplemented with acetate or hydrogen. Applied and Environmental Microbiology 48, 389-394.

Takahashi, H., Usup, A., Hayasaka, H., Limin, S.H., 2003. Estimation of ground water levels in a peat swamp forest as an index of peat/forest fire. Proceedings of the International Symposium on Land Management and Biodiversity in Southeast Asia. Bali, Indonesia, 17-20 September 2002. Hokkaido University, Japan and Indonesian Institute of Sciences, Bogor, Indonesia, pp. 311314.

Thornton, S.A., Dudin, Page, S.E., Upton, C., Harrison, M.E., 2018. Peatland fish of Sabangau, Borneo: diversity, monitoring and conservation. Mires and Peat 4, 1-25.

Tonks, A.J., Aplin, P., Beriro, D.J., Cooper, H., Evers, S., Vane, C.H., Sjögersten, S., 2017. Impacts of conversion of tropical peat swamp forest to oil palm plantation on peat organic chemistry, physical properties and carbon stocks. Geoderma 289, 36-45.

Truax, D.D., Shindala, A., Sartain, H., 1995. Comparison of two sediment oxygen demand measurement techniques. Journal of Environmental Engineering 121(9), 619-624.

Turetsky, M.R., Kotowska, A., Bubier, J., Dise, N.B., Crill, P., Hornibrook, E.R., Minkkinen, K., Moore, T.R., Myers-Smith, I.H., Nykänen, H. and Olefeldt, D., 2014. A synthesis of methane emissions from 71 northern, temperate, and subtropical wetlands. Global Change Biology 20(7), 2183-2197.

Ueda, S., Go, C-S.U., Yoshioka, T., Yoshida, N., Wada, E., Miyajima, T., Sugimoto, A., Boontanon, N., Vijarnsorn, P., Boonprakub, S., 2000. Dynamics of dissolved O_2, CO_2, CH_4, and N_2O in a tropical coastal swamp in southern Thailand. Biogeochemistry 49, 191-215.

Vachon, D., Prairie, Y.T., 2013. The ecosystem size and shape dependence of gas transfer velocity versus wind speed relationships in lakes. Canadian Journal of Fisheries and Aquatic Sciences 70(12), 1757-1764.

Vachon, D., Prairie, Y.T., Cole, J.J., 2010. The relationship between near-surface turbulence and gas transfer velocity in freshwater systems and its implications for floating chamber measurements of gas exchange. Limnology and Oceanography 55, 1723-1732.

Wang, X., Piao, S., Ciais, P., Friedlingstein, P., Myneni, R.B., Cox, P., Heimann, M., Miller, J., Peng, S., Wang, T., Yang, H., 2014. A two-fold increase of carbon cycle sensitivity to tropical temperature variations. Nature 506, 212-215.

Wanninkhof, R., 2014. Relationship between wind speed and gas exchange over the ocean revisited. Limnology and Oceanography: Methods 12(6), 351-362.

Wanninkhof, R., Asher, W.E., Ho, D.T., Sweeney, C., McGillis, W.R., 2009. Advances in Quantifying Air-Sea Gas Exchange and Environmental Forcing. Annual Review of Marine Science 1, 213-244.

Warren, M., Frolking, S., Dai, Z., Kurnianto, S., 2017. Impacts of land use, restoration, and climate change on tropical peat carbon stocks in the twenty-first century: implications for climate mitigation. Mitigation and Adaptation Strategies for Global Change 22, 1041-1061.

Weisenburg, D.A., Guinasso, Jr, N.L., 1979. Equilibrium Solubilities of Methane, Carbon Monoxide, and Hydrogen in Water and Sea Water. Journal of Chemical and Engineering Data 24(4), 356-360.

Weishaar, J.L., Aiken, G.R., Bergamaschi, B.A., Fram, M.S., Fuji, R., Mopper, K., 2003. Evaluation of specific ultraviolet absorbance as an indicator of the chemical composition and reactivity of dissolved organic carbon. Environmental Science and Technology 37, 4702-4708.

Weiss, R., 1974. Carbon dioxide in water and seawater: the solubility of a non-ideal gas. Marine Chemistry 2(3), 203-215.

Wells, J.A., Wilson, K.A., Abram, N.K., Nunn, M., Gaveau, D.L., Runting, R.K., Tarniati, N., Mengersen, K.L., Meijaard, E., 2016. Rising floodwaters: mapping impacts and perceptions of flooding in Indonesian Borneo. Environmental Research Letters 11(6), 064016.

Whiting, G.J., Chanton, J.P., 1996. Control of the diurnal pattern of methane emission from emergent aquatic macrophytes by gas transport mechanisms. Aquatic Botany 54(2-3), 237-253.

Wit, F., Müller, D., Baum, A., Warnecke, T., Pranowo, W.S., Müller, M., Rixen, T. 2015. The impact of disturbed peatlands on river outgassing in Southeast Asia. Nature Communications 6:10155, DOI:10.1038/ncomms10155

Wolter, K., Timlin, M.S., 2011. El Niño/Southern Oscillation behaviour since 1871 as diagnosed in an extended multivariate ENSO index (MEI.ext). International Journal of Climatology 31(7), 1074-1087.

Wong, G.X., Hirata, R., Hirano, T., Kiew, F., Aeries, E.B., Musin, K.K., Waili, J.W., San Lo, K., Melling, L., 2018. Micrometeorological measurement of methane flux above a tropical peat swamp forest. Agricultural and Forest Meteorology 256, 353-361.

Worrall, F., Burt, T., Adamson, J., 2005. Fluxes of dissolved carbon dioxide and inorganic carbon from an upland peat catchment: implications for soil respiration. Biogeochemistry 73(3), 515-539.

Worrall, F., Burt, T.P., Adamson, J., 2006. The rate of and control upon DOC loss in a peat catchment. Journal of Hydrology 321, 311-325.

Wulffraat, A., Greenwood, C., Faisal, K.F., Sucipto, D., 2017. The Environmental Status of Borneo. Jakarta/Petaling Jaya, WWF Heart of Borneo Programme, 198 pp.

Yao, G., Gao, Q., Wang, Z., Huang, X., He, T., Zhang, Y., Jiao, S., Ding, J., 2007. Dynamics of CO_2 partial pressure and CO_2 out-gassing in the lower reaches of the Xijiang River, a subtropical monsoon river in China. Science of the Total Environment 376, 255266.

Yu, Z., Beilman, D.W., Frolking, S., MacDonald, G.M., Roulet, N.T., Camill, P., Charman, D.J., 2011. Peatlands and their role in the global carbon cycle. Eos 92(12), 97-98.

Yu, Z., Loisel, J., Brosseau, D.P., Beilman, D.W., Hunt, S.J., 2010. Global peatland dynamics since the Last Glacial Maximum. Geophysical Research Letters 37(13), DOI:10.1029/2010GL043584

Yu, Z.C., 2012. Northern peatland carbon stocks and dynamics: a review. Biogeosciences 9(10), 4071.

Yule, C.M., 2010. Loss of biodiversity and ecosystem functioning in Indo-Malayan peat swamp forests. Biodiversity and Conservation 19(2), 393-409.

Zhang, Z., Zimmermann, N.E., Stenke, A., Li, X., Hodson, E.L., Zhu, G., Huang, C., Poulter, B., 2017. Emerging role of wetland methane emissions in driving 21st century climate change. Proceedings of the National Academy of Sciences 114(36), 9647-9652.

Zhu, Q., Peng, C., Ciais, P., Jiang, H., Liu, J., Bousquet, P., Li, S., Chang, J., Fang, X., Zhou, X., Chen, H., Liu, S., Lin, G., Gong, P., Wang, M., Wang, H., Xiang, W., Chen, J., 2017. Interannual Variation

in Methane Emissions from Tropical Wetlands Triggered by Repeated El Niño Southern Oscillation. Global Change Biology 00:1-11. DOI:10.1111/gcb.13726